THE EXTENT OF BURIAL OF THE *RENA* OIL SPILL WITHIN BAY OF PLENTY COASTAL SEDIMENTS

A thesis

submitted in partial fulfilment

of the requirements for the degree

of

Masters of Earth and Ocean Sciences

at

The University of Waikato

by

Neeltje P.H.M. de Groot

THE UNIVERSITY OF
WAIKATO
Te Whare Wānanga o Waikato

2014

ABSTRACT

The grounding of the MV Rena on October 5th, 2011 caused 350-400 tons of heavy fuel oil to spill into the ocean. A significant portion of the oil reached the Bay of Plenty coastline six days later. This thesis investigated the effectiveness of oil clean-up operations that involved spill response crew and some eight thousand volunteers. Previous oil spill studies discussed in literature, have established that spilled oil can mix with sediment beneath the beach surface. 26 Sediment cores averaging ~80cm in length were retrieved ~one year after the Rena oil spill at 12 locations between Waihi and Maketu and were chemically analysed to a depth of 40 cm (0-20 cm and 20-40 cm). GC/MS quantitative results concluded that polycyclic aromatic hydrocarbons (PAHs) were present in the sediment. However, only 7 of the 52 samples contained 4 of the 5 fingerprinted PAHs; phenanthrene, pyrene, benzo(a)anthracene and chrysene, that characterise the Rena oil, with naphthalene undetected in all of the 52 samples. Naphthalene degrades quickly due to its low molecular weight and commonly evaporates from the marine environment within the first few weeks of exposure. Therefore, the absence of naphthalene was anticipated. Variations of phenanthrene and pyrene were detected 27 other sediment samples at low, mid and high tide locations, in both surface 0-20 cm samples and the deeper 20-40 cm samples. Due to the absence of the most resilient PAHs benzo(a)anthracene and chrysene in the 27 samples characterise Rena oil, is likely that phenanthrene and pyrene have come from other hydrocarbon sources such as stormwater outfalls. Laboratory settling flask experiments demonstrated that heavy fuel oil formed droplets and would bind to sediment of both siliciclastic and bioclastic origin. Oil droplets would sink, float or stay suspended in the water column due to oil droplet density variations. Oil that bound to sand grains tended to sink and join the bottom sediments, and oil droplets that contained bubbles of water or air tended to float to the surface of the water column. Storms that occurred in the weeks after the initial Rena spill hindered oil clean-up operations and increased wave activity which potentially enabled oil to mix further into coastal sediments. The maximum depth of disturbance was recorded at Pukehina Beach at 28 cm during storm conditions

which established that chemical analysis to a depth of 40 cm encompassed the maximum depth that oil could be mixed into the beach sediment in the intertidal zone. This study has set the foundations on understanding the geotechnical effects of spilled oil and coastal sediment interactions in the Bay of Plenty. The region would benefit from further depth of disturbance studies to assist in more efficient remediation of possible oil spills in the future.

ACKNOWLEDGEMENTS

TABLE OF CONTENTS

LIST OF FIGURES

LIST OF TABLES

CHAPTER ONE: INTRODUCTION

1.1 THE *RENA* DISASTER

The Bay of Plenty region contains some of the most visited beaches in New Zealand, and is a popular summer holiday destination for many New Zealanders. On October 5th, 2011, the MV *Rena* cargo ship ran aground on the Astrolabe Reef situated ~12 nautical miles (22 km) off the coast of Tauranga (Figure 1.1). In the days that followed, up to 400 tonnes of heavy fuel oil (HFO 380) spilt into the ocean.

The first of the *Rena* oil arrived at Mount Maunganui on the 10th of October, almost a week after the grounding. A storm on the night of the 11th of October caused the wreck to shift, resulting in additional oil being spilled into the sea. 1,733 tonnes of heavy fuel oil was on board the *Rena* when it grounded. However, ~1,300 tonnes was able to be recovered through direct fuel removal operations on-board (Maritime.govt.nz, 2013) resulting in ~350 to 400 tonnes of oil estimated to have been spilled into the ocean in the first six days (Maritime.govt.nz, 2013). The spill is considered New Zealand's most significant maritime disaster to date. The spill initiated the highest level of response. Maritime response crew were called to immediate action (*Rena*recovery.org.nz).

Heavy fuel oil is a high viscosity residual oil and when spilled on water can spread as thick slicks (NOAA, 2013), coat sand grains, and can clump into smaller patches and tar-balls (Delvigne, 2002). All of these forms of oil washed up onto the Bay of Plenty coast in the days following the *Rena* grounding. Oil reached the inner Tauranga Harbour and estuary, the northwest open coast at Waihi Beach, Pukehina in the south east as illustrated in Figure 1.1. Oil also reached Waihau Bay and Cape Runaway to the north east. However, most of the coast between Pukehina and Waihau Bay was largely unaffected (BoPDHB, 2011).
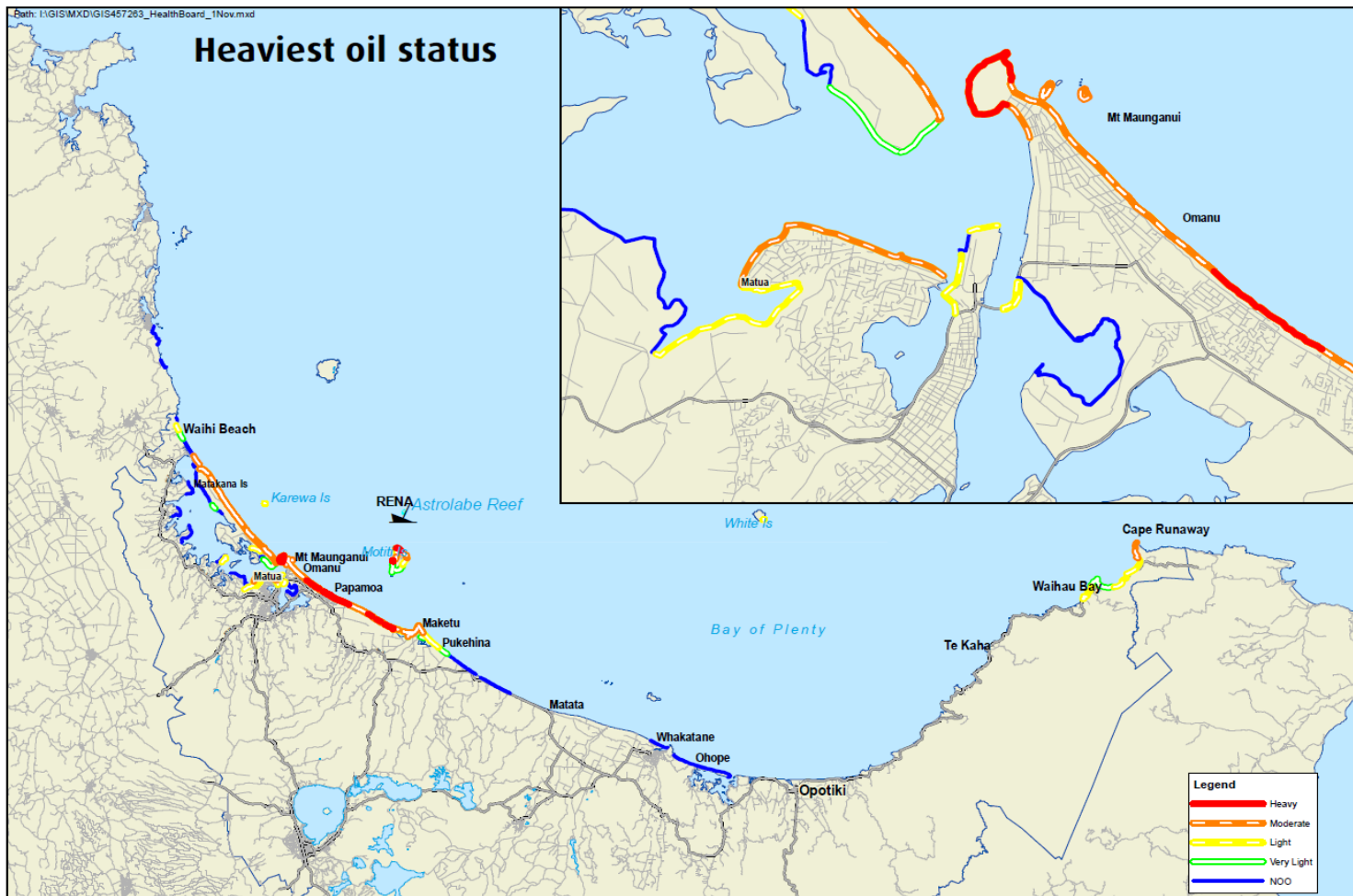
Figure 1.1: Heaviest oiling on the Bay of Plenty coast after the *Rena* oil spill in October, 2011 (Source: BoPDHB.govt.nz, 2011).

On the 11th of October, 2011 six days after the MV *Rena* grounded, storms affected the region's coastline not only halting salvaging operations but, also releasing more oil and debris from the wreck. Storm conditions can induce strong onshore winds and high energy waves with increased significant wave height. These physical factors can cause a change the beach slope profile and increase mixing depth of sediment in the intertidal zone and allow oil to be mixed into the beach sediments (NRC, 2003).

During the large scale clean-up of the *Rena* oil spill that involved ~8,000 volunteers and oil response personnel, a variety of different forms of oil were seen along the Bay of Plenty coastline. Oil sheets illustrated in Figure 1.2 were common on beaches that were affected by larger volumes of oil such as Papamoa Beach at Omanu Surf Club and further west along the beach towards Mount Maunganui. Oil coated sand and tarballs (Figure 1.3) were also common occurrence where there were moderate amounts of oil present.

Figure 1.2: Oil sheets on Papamoa Beach, 13th of October, 2011. (Source: msn.news.co.nz).

Figure 1.3: Tar Balls on Mount Maunganui Beach 11th of October, 2011. (Source: www.abc.net.au).

Tarballs washed up onto the beaches for many months after the grounding. Some of these tarballs may have been re-released from the ocean floor sediment during periods of increased turbulence where they then washed up on shore. However, some may have come directly from the *Rena* wreck that was in the process of being dismantled for more than two years after the grounding.

Oil spilled from the *Rena* onto the coastline affected a range of environments from low energy estuaries, sandy intermediate state beaches, to rocky headlands and islands. The diversity of surroundings that were affected led to the use of different clean up techniques depending on the substrate type and fragility of the area. On the beaches, clean up mainly consisted of manual removal of the sand by oil response personnel and volunteers. Sand sifting, shovelling (Figure 1.4) *Beach Tech* sweepers, and vacuums with attached collection drums were used to remove tarballs from sand (Maritimenz.govt.nz, 2013).

Figure 1.4: NZ Army troops shovelling spilled oil on Papamoa Beach October, 2011. (Source: www.theaustralian.com.au).

Surf washing was also carried out on Papamoa Beach where oil contaminated sand was moved into the intertidal zone to be picked up by waves where it either dispersed, or form larger balls that could more easily be collected (Maritimenz.govt.nz, 2013). Hot water blasting and the use of organic fibres and polypropylene to absorb chemicals were used on the hard substrate. Most methods were thought to be effective at removing oil, however some methods were considered more successful than others. The use of natural fibres to mop up oil from the rocky coast was considered the most effective method with the least amount of damage to the rocky shore ecosystem.

1.2 AIMS AND OBJECTIVES

The main aim of this study was to assess the effectiveness of the oil recovery operations by determining if detectable levels of oil remain buried in affected beaches, and to assess the mixing depth and influence that oil has on the geotechnical properties of the beach sediment. The specific objectives for the first aim were:

1. Obtain short cores from the affected beaches between Matakana Island and Matata from the intertidal flats of Maketu Estuary and from the shallows of Centre Bank, Tauranga Harbour.
2. Describe the sedimentology of each core, identify and characterise any visual indicators of the presence of residual oil.
3. Sub-sample selected cores based on the outcome of objective 2 for laboratory analysis of the vertical distribution of Total Petroleum Hydrocarbons (TPH).

Due to oil recovery procedures and the time elapsed since the oil spill in October 2011 it was considered that little may oil remain within the beach profiles. Therefore, depth of disturbance measurements was taken at some beaches over a semi diurnal tidal cycle and oil sediment mixtures were created in the laboratory. The specific objectives for the second aim were:

4. The impact of varying oil concentrations on sediment behaviour and settling were assessed on oil-sediment mixtures in the laboratory using sediments and seawater from the field.
5. Depth of sediment disturbance in the intertidal was determined for the Bay of Plenty beaches and compared to previous studies conducted overseas. The applicability of these for predicting the depth to which oil spills will be mixed was assessed.

1.3 THESIS OUTLINE

Following on from this introductory chapter; the following chapters are described:

Chapter Two: Literature review of previous oil spill research, oil behaviour in the coastal environment and past literature that has looked at depth of sediment disturbance in the intertidal zone.

This thesis is then divided into three main topics:

Chapter Three: Chemistry of *Rena* oil, and its presence within sediments of the coastal environment.

Chapter Four: Laboratory experiments on oil/sand/seawater mixtures.

Chapter Five: Depth of disturbance studies in the intertidal on sandy beaches of the Bay of Plenty and hence the potential burial depth of oil.

Each chapter of the three main topics will be subdivided into three sections: the methodology, results and discussion.

Chapters Six and Seven: Summary and conclusions as well as recommendations for future research.

CHAPTER TWO: LITERATURE REVIEW

Crude oil is the basis for all hydrocarbon products and is a fossil fuel produced from the remains of predominantly marine but also lacustrine or terrestrial microorganisms. There are many varieties of crude oil and other petroleum products carried by ships. Each oil varies in composition, viscosity and density and have a variety of uses.

Crude oil is a complex mixture of natural products with components that range over a large molecular weight from 16 (methane) to 20,000 (NRC, 2003) and is generally made up of 97 % hydrogen and carbon with the remaining 3 % consisting of nitrogen, oxygen, sulphur, metals and salts (Table 2.1).

Table 2.1: Average chemical composition of crude oil (Speight 1999).

Element (Symbol)	Percentage Range (%)
Carbon (C)	80-87
Hydrogen (H)	10-14
Sulphur (S)	0.05-6.0
Nitrogen (N)	0.1-2.0
Oxygen (O)	0.05-1.5
Metals	< 0.1%
Salts	< 0.1%

The variation in oil mixtures comes from the hydrocarbon origin; the depth, pressure and temperature to which the oil-bearing rock is exposed. The blend of various hydrocarbons will also influence colour (black to yellow) and viscosity (light to heavy and nearly solid). The type and abundance of hydrocarbons present can indicate the origin of the crude oil (Hyne, 2001).

The American Petroleum Institute (API) quantified the method used for measuring the density of petroleum based on the following formula at 15.6°C;

API gravity = (141.5/specific gravity) +131.5   (API, 1992).

Giving the following definitions;

- Light oil – °API > 31.1 (less than 870 kg/m^3)

- Medium oil – °API between 22.3 and 31.1 (870 to 920 kg/m^3)
- Heavy oil– °API < 22.3 (920 to 1000 kg/m^3)
- Extra Heavy oil – °API < 10.0 (greater than 1000 kg/m^3)

The behaviour of oil once spilled into a marine environment is dependent on the oil's viscosity and density, and the degradation rate is determined by the oil's composition and the volume of oil spilled, as well as the nature of the environment it resides in. The MV *Rena* was carrying Bunker C heavy fuel oil (HFO 380) at the time of the grounding. Due to turbulence and heavy fuel oil's specific gravity, Bunker C oil can be suspended within the water column or float on the surface as illustrated in Figure 2.1 (Sterling, et al., 2003; NOAA, 2013).
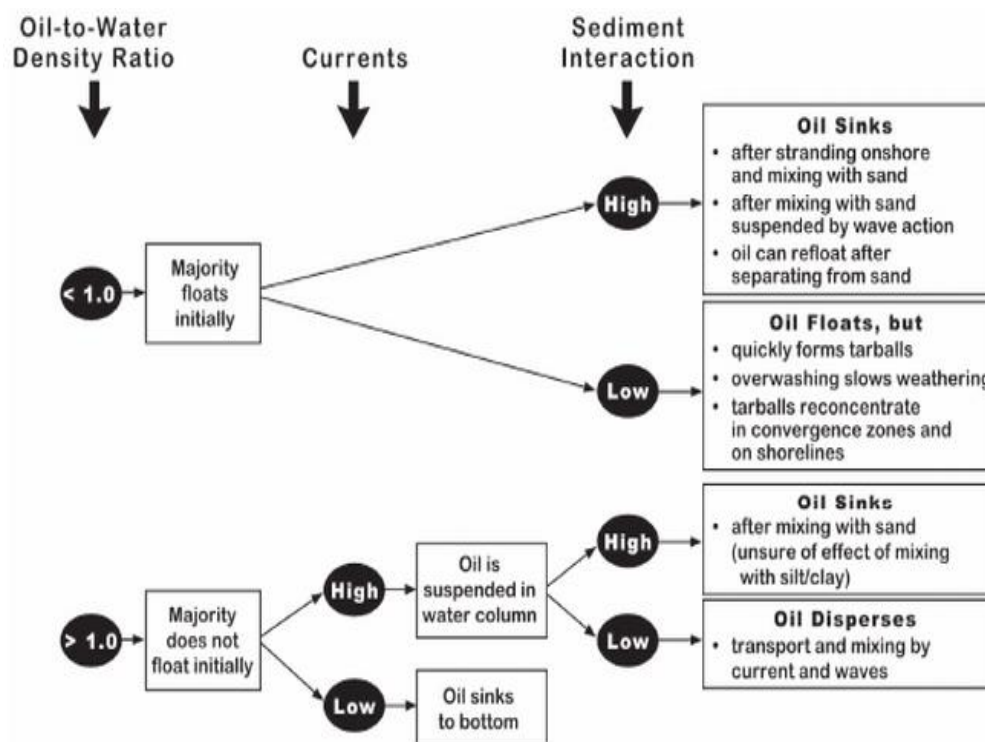
Figure 2.1: Factors determining sediment and oil interaction and whether oil will sink or float in the ocean (Source: NRC, 2003).

Oil spilled from the *Rena* and was transported to shore by advection, dispersion and entrainment (NRC, 2002), as a result of several different mechanisms, including: surface jets, oscillations, bottom currents and surface stress, which can together be described as turbulence (Sterling, et al., 2003).

Frequently, tarballs and oil sheets washed up onto Tauranga beaches for many weeks after the initial grounding. Changes in the physical form of oil as a result of weathering in the marine environment has been the subject of research (Delvigne, 2002; NRC, 2003; Bernabeu et al., 2006; Wang and Roberts, 2013) which has established that tarballs and oil coated grains in a high sediment environment could potentially get mixed into the sediment at the coast (Figure 2.1) and can persist in the environment for many years (NRC, 2003; NOAA, 2013).

A contradiction to the general consensus is found in a paper by Santas and Santas (2000) that states that due to oil's viscosity and adhesiveness, it does not penetrate the surface sediments under the influence of wave action in calm conditions.

2.1 HYDROCARBON CHEMISTRY AND FINGERPRINTING

Hydrocarbons not only enter the coastal environment through point source discharges, such as oil spills, pipeline breaks and ballast water; they can also enter as a non-point source such as urban runoff, wastewater discharge and aerosols.

All crude oil and petroleum products have varying chemical compositions from dissimilarities in source and refinery processes (Wang, et al., 1999). Being able to identify the source of oil is an important tool resolving questions of environmental impact and legal liability (Wang, et al., 1999).

Oil composition reflects the chemistry of its source materials and the process of distinguishing compositional features of hydrocarbons and linking them to their original source is called fingerprinting (Ehrhardt & Blumer, 1972).

Ehrhardt & Blumer, (1972) developed the basic method for identifying oils in the marine environment using gas chromatography (GC). In order for fingerprinting to work, oil from different sources must have; (1) characteristic compositional differences resulting from different refining processes; (2) the differences need to persist in the marine environment for at least a few days; and (3) be able to distinguish oil pollution from the natural hydrocarbon background (Ehrhardt & Blumer, 1972).

This fingerprinting method is now widely used and accepted as a technique for identifying petroleum products and their sources. Chemical fingerprinting contributed to research carried out on the *Exxon Valdez* oil spill (Table 2.3) of 1989 (Boehm, et al., 1997) and later, the *Prestige* oil spill described in Table 2.3 (Díez et al., 2007).

Four different types of hydrocarbon molecules are present in crude oil. The relative percentage of each varies from oil to oil (Hyne, 2001).

Table 2.2: Composition by weight of hydrocarbon types in oils (Source: Hyne, 2001).

Hydrocarbon	Average	Range
Alkanes (paraffins)	30 %	15 to 60 %
Naphthenes	49 %	30 to 60 %
Aromatics	15 %	3 to 30 %
Asphaltics	6 %	remainder

Heavy oil is characterized by a high ratio of aromatics and naphthenes to alkanes. Polycyclic aromatic hydrocarbons (PAHs) are the often the most abundant and persistent in the marine environment making them good indicators for hydrocarbon source fingerprinting. Also, out of all hydrocarbons, PAHs appear to pose the greatest toxicity to the environment (NRC, 2003).

PAHs are organic compounds consisting of two of more fused aromatic rings in angular, linear or clustered arrangements containing carbon and hydrogen. PAHs may contain up to seven member rings, those with five or six rings are the most common (Figure 2.2). PAHs are solids, many with low volatility at ambient air temperature and are lipophilic (mix more easily to oil than water), and most can be photo-oxidized and degraded to simpler substances (NRC, 2003).

PAHs are easily and rapidly absorbed by organisms and can accumulate in an organism or be passed on through the food web (Nasher, et al., 2013). PAHs include compounds that are known to cause toxic effects in some marine organisms.

The United States Environmental Protection Agency (US EPA) has classified 16 priority PAHs known for their carcinogenic, mutagenic, and teratogenic properties. These are:

- naphthalene,
- acenaphthylene,
- acenaphthene,
- fluorene
- phenanthrene,
- anthracene,
- fluoranthene,
- pyrene,
- benz[a]anthracene,
- chrysene,
- benzo[b]fluoranthene,
- benzo[k]fluoranthene,
- benzo[a]pyrene,
- dibenz[a,h]anthracene,
- benzo[ghi]perylene, and
- indeno[1,2,3-cd]pyrene

Their ring structure is illustrated in Figure 2.2. Some four to six ring PAHs (pyrene/fluoranthene through to coronene) are carcinogens and are usually present at low or trace concentrations within a crude oil (NRC, 2003).

Stability of a PAH compound in the environment is determined by the ring arrangement. Linear structures are the least stable and fused rings in step are the most stable. PAH's solubility and volatility generally decreases with an increasing number of fused rings (Wilson & Jones, 1993).

PAHs are only slightly soluble in water and their solubility decreases as the molecular weight increases. For example, anthracene is less soluble than phenanthrene, and benzo(g,h,i)perylene is less soluble than chrysene or benz[a]anthracene. However, a rise in temperature from 5 to 30 °C increases the solubility of PAHs three- to four-fold (Moore & Ramamoorthy, 1984).

PAHs are present in heavy fuel oils in varying types and abundances; consequentially individual oils have their own PAH fingerprint. Once a fingerprint for a specific oil is identified, it is possible to track spilled oil back to its original source. Due to some PAHs having low volatility, they can persist in

the marine environment for many years. The previously determined PAH fingerprint of the *Rena* oil (Wilkins, 2013) and its degradation products was utilised in this study to identify any oil found within the cores was a result of the spill.

1. Naphthalene   2. Acenaphthene   3. Acenaphthylene   4. Fluorene

5. Phenanthrene   6. Anthracene   7. Fluoranthene   8. Pyrene

9. Benzo(*a*)anthracene   10. Crysene   11. Benzo(*b*)fluoranthene   12. Benzo(*k*)fluoranthene

13. Benzo(*a*)pyrene   14. Dibenzo(*a,h*)anthracene   15. Benzo(*g,h,i*)perylene   16. Indeno(*1,2,3-c,d*)pyrene
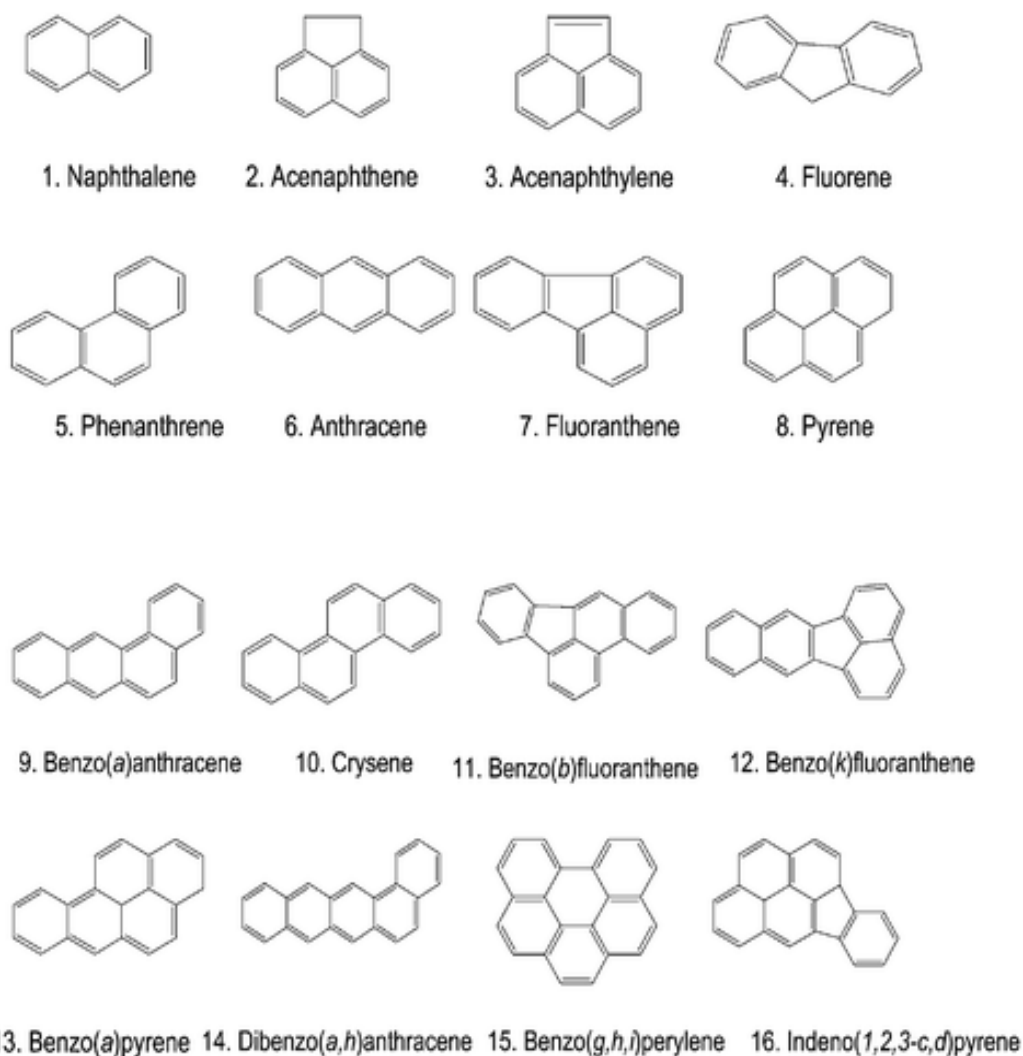
Figure 2.2: The molecular structure of the 16 EPA priority PAHs (Source: Bruzzoniti, et al., 2009).

The University of Waikato's Chemistry department identified the parent PAHs by comparing retention times and the total ion chromatogram (TIC) mode mass spectral fragmentation patterns to those determined for the *Rena* oil fingerprint from 16 genuine specimens of EPA priority PAHs purchased from Sigma Aldrich (Wilkins, 2013).

The GC/MS fingerprinting method carried out qualitatively determines the presence of PAHs and alkylated equivalents of parent PAHs in subsamples of the mixed oil and sand. Fingerprint profiles for eight groups of hydrocarbon compounds were derived: (1) Hydrocarbons (2) naphthalenes, (3) phenanthrenes, (4) pyrenes, (5) Benzo[a]anthracenes and chrysenes, (6) pentacyclic and hexacyclic PAHs (7) dibenzothiophenes and tribenzothiophenes and (8) hopanoids (Wilkins, 2013).

Three *Rena* tank oil samples, tarballs and oiled sand samples were analysed. The tarballs were collected from various Tauranga beaches days after the initial grounding, between 10th and 27th of October, 2011. The sand samples were collected a few months later, between 23rd of January and the 10th of February, 2012 from Katikati, Matakana Island, Mt Maunganui, Leisure Island and Maketu Estuary (Wilkins, 2013).

The heavy fuel oil tarball characteristics are dominated by branched chain hydrocarbons (alkanes), PAHs and alkylated analogues of PAHs and low levels of petroleum biomarker compounds (C_{27}-C_{35}). Hopanoids are also detectable (Wilkins, 2013).

2.1.1 OIL WEATHERING AND BIODEGRADATION

Oil spilled onto water undergoes a series of weathering processes that occurs at different rates depending on the environment and the type of oil (NRC, 2003). Many weathering processes are temperature dependent, with colder temperatures slowing processes down. However, oil viscosity, density and solubility are generally more important factors than environmental conditions (NRC, 2003).

The fastest rate of weathering occurs immediately after the oil is spilt into the environment when evaporation takes place. The primary factors controlling evaporation rate are type of oil (Figure 2.3), surface area of a slick, temperature and wind speed (Wolfe, et al., 1994). Evaporation of volatile oil components can remove more toxic low-molecular weight compounds such as benzene and smaller *n*-alkanes (Venosa & Zhu, 2003). C_{5-6} benzenes, C_{11}-C_{13} alkanes, and methyl naphthalenes are most likely to evaporate in natural conditions where they then

13

rapidly oxidise to photolysis products (Wolfe, et al., 1994). Figure 2.3 illustrates the amount of evaporation that occurs in the first few days in different petroleum products.
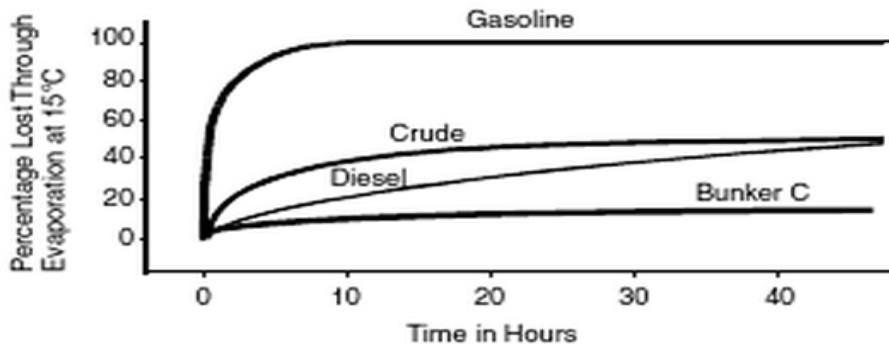
Figure 2.3: Evaporation rates of different types of oil at 15°C (Source: NRC, 2003).

Rena Bunker C oil was a persistent oil with only 5 % to 10 % likely to evaporate within the first hours of exposure. Bunker C oil showed evaporative mass loss of 0.1 % after 24 hours in a fume hood in a study carried out by Wang, et al., 1998.

Both physical and chemical processes are responsible for the denudation of oil in the marine environment. Figure 2.4 demonstrates the different mechanisms that are involved in the dispersal and removal of oil over time from an oiled shoreline.
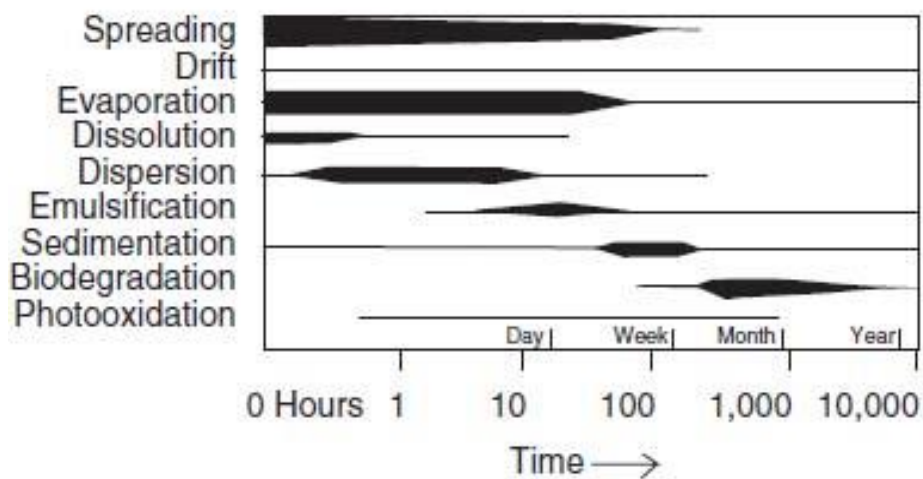
Figure 2.4: Temporal changes and processes acting on an oil slick following a spill. The line thickness indicates the relative magnitude of each process (Reproduced from Swan, et al., 1994).

The mixing of oil in the marine environment by waves affects the nature of an oil spill, both chemically and physically (Santas & Santas, 2000). These effects

14

include (a) breaking up of an oil slick by creating bands and streaks allowing spreading of oil over a greater surface area, (b) greater evaporation by waves breaking, (c) oil droplet dispersion, and (d) oil and water emulsion (mousse) (Santas & Santas, 2000). Some spilled oils become mostly mousse over time with relatively high viscosity and specific gravity, which tends to adhere to shoreline surfaces and is not easily entrained by tidal, wave or wind action (Wolfe, et al., 1994). However, oil behaviour is dependent on oil viscosity and therefore, oil type. Emulsions are not easily formed in Bunker C heavy fuel oil and there was no report of the presence of oil mousse emulsion at sea or arriving at the coast resulting from the *Rena* spill.

Experiments and modelling of the *Exxon Valdez* spill (Table 2.3) concluded that the rate of weathering of PAHs is strongly affected by the ratio of the surface area to volume of hydrocarbons in the environment. Weathering causes changes in PAH distribution based on the relative solubility of individual compounds (Short & Heintz, 1997). The relative removal of PAH groups as spilled oil weathers is in the order of: naphthalene > fluorenes > phenanthrenes and pyrenes > chrysenes (Wang & Stout 2006).

Major compositional changes in spilled oil into the marine environment include a rapid loss of volatile aromatics and an intense decrease in naphthalenes in relation to other alkaylated PAHs (Wang, et al., 1999). Weathering enriches chrysene relative to other PAHs and results in a substantial decrease in the naphthalene, phenanthrene, dibenzothiophenes, and fluorenes to chrysenes relative ratios (Wang, et al., 1999).

PAHs are degraded through the process of photo-oxidation from exposure to the sun (Harayama, et al., 2004). However, they differ in their sensitivity. Photodegradation studies (Nagata & Kondo, 1977) of several PAH compounds were mixed in acetone-water or carbon tetrachloride (CC_{l4}) - water solvents that concluded that anthracene, phenanthrene, and benz[a]anthracene were the most sensitive PAHs to photodegradation. Whereas, chrysene, fluorene, pyrene, and benzo[a]pyrene were relatively resistant to photodegradation (Nagpal, 1993). The effects of photodegradation causes the aromatic fraction in oil to decrease (Harayama, et al., 2004).

PAHs bound to particles are more susceptible to photolysis than those PAHs solely in the water column. The oxidation pathways also vary for PAHs attached to particulates. For example, anthracene is oxidized to anthraquinone when adsorbed to alumina or silica gel in the presence of light. Benzo[a]pyrene studies determined that degradation rates increased with increasing dissolved oxygen as well as temperature and light intensity (Moore & Ramamoorthy, 1984).

Biodegradation is considered one of the most important processes in oil denudation and the main process affecting PAH persistence in the environment (Hadibarata, et al., 2009). Biodegradation patterns of hydrocarbons in Alberta Sweet Mixed Blend oil has shown to be significantly different from the pattern produced from physical weathering in freshwater studies (Wang, et al., 1998).

The percentage of hydrocarbon utilizing microorganisms can significantly increase in an oil polluted environment where they can constitute up to 100 % of the microbial community in comparison to less than 0.01 % in an uncontaminated ecosystem (Venosa & Zhu, 2003).

The growth of oil degraders occurs almost solely at the oil/water interface. Therefore, surface area plays an important role in biodegradation rate. Different oil forms may also affect biodegradation rates. Tar-balls reduce the surface area, which limits access and restricts biodegradation (Venosa & Zhu, 2003). Biodegradation rates are also thought to decrease with increasing depth since the number of degraders decreases with depth (Acosta-González, et al., 2013).

 Individual components of petroleum pass into marine organisms at different rates depending on their physical and chemical properties. Once inside an organism, there are many different reactions depending on the magnitude and type of hydrocarbon ingested (Venosa & Zhu, 2003).

Light oils biodegrade faster than heavy fuel oils. Biodegradation is also influenced by the concentration of oil constituents. High concentrations may cause toxicity and low concentrations may result in weak ineffective microbial reactions (Venosa & Zhu, 2003).

Many organisms metabolise and excrete hydrocarbons, although the result may create more toxic intermediates (NRC, 2003). Biodegradation of crude oil generally involves a range of microbes working in succession, not one single microorganism can degrade all types of hydrocarbon components (Venosa & Zhu, 2003). Certain organisms may utilise the primary petroleum product, which then results in intermediate compounds, that a different subset of microbes are able to exploit (Venosa & Zhu, 2003).

The fastest biodegradation occurs in saturated petroleum hydrocarbons, involving terminal oxidation (the last step in aerobic respiration) followed by light aromatics and then high-molecular weight aromatics (Wolfe et al., 1994; Venosa & Zhu, 2003). Molecular weights between C_{10} and C_{26} are the more commonly used by microbes. However, biodegradation can occur with weights up to C_{44}. Aromatics are generally more resistant to biodegradation than saturates (Venosa & Zhu, 2003).

Branched alkanes resist microbial attack. Therefore, they are less degradable in comparison to *n*-alkanes. Highly branched isoprenoid alkanes (phytane and pristine) are easily biodegraded, unlike cycloalkanes which are resistant to biodegradation, and complex alicyclic compounds (hopanes and steranes) are among the most persistent compounds. The rates at which certain alkyl PAHs degrade, can determine that rate at which biodegradation of an oil spill is occurring (Venosa & Zhu, 2003).

Studies have determined that biodegradation decreases with the increase of alkylation. Therefore, alkylated aromatics are degraded less rapidly than their parent compounds. (Wolfe, et al., 1994; Wang, et al., 1998; Venosa & Zhu, 2003). PAHs with five or more rings do not generally biodegrade, but co-oxidation has been observed (Wolfe et al., 1994).

Many PAHs are susceptible to fungal and bacterial degradation (Peng, et al., 2008), including those that make up the *Rena* fingerprint; naphthalene, phenanthrene, pyrene, chrysene and benzo(a)anthracene.

Naphthanlene is the most easily degradable, followed by dibenzothiophene, fluorene and then phenanthrene (Wang, et al., 1998). Several *Pseudomonas* species and *Bacillus thermoleovorans* can degrade naphthalene (Eaton & Chapman, 1992). A white rot fungi called *Ganoderma lucidum* has proven to successfully remove pyrene and phenanthrene from Taiwanese river sediments (Ting, et al., 2011). However, rates were dependent on environmental conditions such as pH and temperature, with an optimum temperature of 30°C and pH of 4 (Ting, et al., 2011). *Pseudomonas aeruginosa*, completely removed phenanthrene from a heavily polluted stream over 30 days and *Mycobacterium spp.*, strain KR2 removed up to 60 % pyrene within 8 days at 20°C in terrestrial polluted soil (Haritash & Kaushik, 2009).

From marine sediments, different microbes are utilised to degrade PAHs. The loss of pyrene from marine beach sediments was studied. In the control, loss of pyrene after 63 days was 66.6 % and application of fertilizer (osmocote and chitosan) increased the amount removed to 98.2 % (Li, et al., 2006). *Cycloclasticus* strains grow on specific aromatic hydrocarbons, naphthalene, phenanthrene and anthracene, and other marine bacteria; *Vibrio, Pseudoalteromonas, Marinomonas* and *Halomonas* have been isolated as being capable of degrading phenanthrene or chrysene (Harayama, et al., 2004).

Resins and asphaltenes are complex structures and not as well studied as aromatics and saturates, so less is known about their biodegradation. However, there is evidence that asphaltene degrades through co-metabolism relying on a primary compound for simultaneous degradation (Venosa & Zhu, 2003).

Biodegradation is aided by evaporation of volatile oil components removing more toxic low-molecular-weight components, such as benzene and smaller *n*-alkanes. At lower temperatures evaporation rate is reduced and oil viscosity increases affecting the volatility of PAHs, which then also delays biodegradation (Venosa & Zhu, 2003).

Biodegradation may be also limited by oxygen or nutrient availability. Aerobic conditions are generally needed for degradation of spilled oil, since aromatics and saturates involve oxygenases (Venosa & Zhu, 2003). However, some studies have

discussed that anaerobic metabolism occurs in certain conditions (Head & Swannell, 1999). PAHs, specifically naphthalene and phenanthrene, have shown to degrade under sulphate reducing conditions in marine sediment studies (Coates, et al., 1997). Under further investigation, methylnaphthalene, fluorene, and fluoranthene oxidized anaerobically, but pyrene and benzo[a]pyrene did not (Coates, et al., 1997). Anaerobic conditions more readily occur in low energy environments e.g. estuaries, where nutrient levels are more persistent than high energy environments such as beaches (Venosa & Zhu, 2003).

Ideally, 150 mg of nitrogen and 30 mg of phosphorus is needed by an organism to convert 1 g of hydrocarbon (Redfield ratio) into cell materials. An increase of carbon via an oil spill may cause nitrogen and phosphorus to become limited (Venosa & Zhu, 2003).

The pH of sea water is marginally alkaline and studies have shown that optimum biodegradation occurs in slightly alkaline conditions (7-9). High energy shorelines require a constant or frequent nutrient supply and have a lower carrying capacity than low energy (estuarine) environments which are more likely to become anoxic or anaerobic (Venosa & Zhu, 2003).

Salinity studies on biodegradation of PAH components of spilled crude oil in sediments determined that various NaCl amounts reduced different hydrocarbons. In 1 % NaCl, phenanthrene, anthracene and pyrene reductions were higher, while fluoranthene and chrysene reductions were higher in 0 % NaCl (Minai-Tehrani, et al., 2009).

Overall, the environmental impact of spilled oil depends on the amount and the physical and chemical characteristics of oil spilled, as well as the environmental conditions, and the retention during weathering of specific biologically derived oil components (Blumer, et al., 1973).

2.2 PREVIOUS OIL SPILL RESEARCH

A range of oil spills that have been previously studied is discussed, considering particularly the effectiveness of the clean-up processes, hydrocarbon source

identification, the processes of natural degradation of oil, and its effects on the environment.

Table 2.3: A summary of previous oil spills that are discussed in the text showing some of the characteristics of the oil spill that occurred.

Vessel name	Year	Location	Oil type	Amount spilled (metric tons)	Clean up (metric tons)
Florida barge	1969	Buzzards Bay, Massachusetts, US	No.2	600	NA
Arrow	1970	Chedabucto Bay, Nova Scotia	No.6- Bunker C	1,000	100-600
TSESIS	1977	Baltic Sea, Sweden	No. 5	1,000	~700
Ixtoc 1 rig	1979	Bay of Campeche, Mexico	Crude oil	480,000	NA
Nestucca	1988	Washington, US	No.6- Bunker C	1,100	NA
Odyssey	1988	Nova Scotia, Canada	North Sea crude oil	132,000	NA
Exxon Valdez	1989	Prince William Sound, Alaska	North Slope crude oil	35,500	3,000
Gulf War	1991	Persian Gulf	Crude oil	1,300,000	120,000
Erika	1999	Brittany, France	Heavy fuel oil	31,000	NA
Prestige	2002	Galicia, Spain	No.6- Bunker C	77,000	53,000
Bouchard	2003	Buzzards Bay, Massachusetts, US	No.6- Bunker C	3,750	
Deepwater Horizon	2010	Gulf of Mexico	No.6- Bunker C	560,000-585,000	NA

Due to the close proximity of the *Rena* wreck to the shore (12 nautical miles), the concentration of oil on certain parts of the Bay of Plenty coast resemble abundances seen in much larger spills worldwide. The extent of degradation of spilled oil in coastal areas is thought to depend largely on environmental conditions (Rashid, 1974). Short cores were taken more than a year after the *Rena* grounding from a variety of coastal environments including beaches, estuarine tidal flats and sand banks to determine if there is any variance in presence of oil in the sediment cores retrieved from different environments. Therefore, persistence is an important aspect to consider.

Bulmer, et al., (1973) looked at the fate of two light no. 2 crude oils stranded in Massachusetts and Bermuda. The study found over the course of 13-16 months

that oil persisted and remained as crude oils. Only evaporation of the more volatile hydrocarbons and minor microbial degradation occurred over the research period. Bermuda alkanes degraded slower than at Massachusetts, which had a nutrient rich substrate where decaying seaweed was present. The higher molecular weight *n*-alkanes were utilized only after the lower homologues had disappeared (Bulmer, et al., 1973).

Some years later, the *Bouchard* oil spill (Table 2.3) was the subject of research using a new GC x GC technique. The results also showed that there was a significant loss of *n*-alkanes from evaporation and biodegradation as well as naphthalene, the most volatile PAH. Table 2.4 shows that PAH loss nearly equalled the losses of the alkane group (Nelson, et al., 2006).

Table 2.4: The distribution of chemical classes of the *Bouchard* 120 oil spill after day 12 and 179 (From Nelson, et al., 2006).

Compound class	Day 12 9 May 2003 % of total	Day 179 23 Nov.2003 % of total	% change from day 12 to day 179
alkanes and cycloalkanes	35.9	34.5	−3.9
alkylbenzenes	4.4	4.2	−4.5
PAHs	52.1	46.5	−10.7
steranes	2.3	4.1	+78
hopanes	1.4	2.5	+79
Other Compounds	3.9	8.3	+113

Nutrient load plays a role in the degradation process of oil that is spilled into the environment, affecting biodegradation rates. Two fjords in Norway were the site for an oiling and nutrient affects experiment (Berge, et al., 1987). Large quantities (resembling heavy pollution), of North Sea crude oil was mixed into sediment and placed in boxes in the subtidal zone in one oligotrophic fjord and one eutrophic fjord. The eutrophic fjord showed no signs of depuration or biodegradation of hydrocarbons within the sediment 3 months after exposure. After 13 months of exposure in the oligotrophic fjord, 33% of the oil still remained in the sediment and most soluble components (naphthalene and

methylnaphthalene) were reduced by two orders of magnitude and less soluble components such as phenanthrene and methylphenanthrene by one order of magnitude. Reduction was more prominent in the surface sediments (Berge, et al., 1987). Oxygen levels were also affected, with redox potential reduced after 9 and 13 months. Biodegradation occurred after an initial lag period. The results found that the addition of oil resembles the effect of eutrophication suggesting that bioturbation and re-suspension rates are responsible for the reducing conditions (Berge, et al., 1987).

During advection in the Prince William Sound, *Exxon Valdez* oil (Table 2.3) was dispersed and underwent biodegradation within the water column without significant nutrient and oxygen limitations. Toluene (methylbenzene) biodegradation potential was elevated in coastal water samples taken 12 days after the spill. Elevated degradation rates also occurred for C_{14} naphthalene and C_{14} hexadecane oiled shoreline samples (Wolfe, et al., 1994).

The *Exxon Valdez* spill of 1989 (Table 2.3) underwent bioremediation. With the addition of fertilizer, biodegradation was not limited by nutrients during this time and was estimated at about 2.2 g oil/kg sediment/year for surficial sediments and dropped to almost half that at a depth of 30 cm (Wolfe, et al., 1994).

Previous research has shown that at varying depths within the beach profile, biodegradation rates vary. Five sediment cores from original locations were sampled twenty years after the 1969 Buzzards Bay spill (Table 2.3). Three cores showed no evidence of oil, one core taken from the subtidal zone contained traces of biodegraded fuel at 10-15 cm depth in the sediment and another contained weathered and biodegraded fuel oil at 0-15 cm with varying degrees of concentration (Teal, et al., 1992).

However, not all research is in agreement. Deliberate oil spills studies were carried out in low energy environments comprised of mangroves and salt marshes in Gladstone, Australia to determine whether bioremediation affected the rate of penetration and retention of Bunker C oil and a medium range crude oil (Burns, et al., 2000). Sediment core GC results concluded that bioremediation did not

significantly impact its rate of loss in the salt marsh sediments, and no difference was found in the mangrove sediments (Burns, et al., 2000).

The bioremediation of the *Prestige* oil spill (Table 2.3) at Sorrizo Beach, Spain determined that the addition of nutrients and microorganisms did not increase the removal rate of oil from sand deposits at any depth (Fernández-Álvareza, et al., 2006). The system may not have been nutrient deprived before the addition of fertilizer.

There are also contradictory results in past studies on the processes responsible for the rate of removal of PAH compounds in soils (Wilson & Jones, 1993). In various soil types, field and laboratory studies have determined that abiotic processes are more important than biological processes whereas, other research has found that micro-organisms play a more important role in oil denudation than that of physical processes. Biodegradability of two and three ring PAHs has been shown to be extensive, and for four to six ring PAHs it is noticeably less substantial (Wilson & Jones, 1993).

Values in previous literature for the half lives of PAHs in sediment are in the order of two months for biphenyl, eight months for indan to trimethyl napthtalenes, two years for acenapnthalenes to anthracene and six years for pyrene to dibenzanthracene (Wolfe, et al., 1994).

Studies on the *Exxon Valdez* spill (Table 2.3) found that low molecular weight PAHs half-lives in sediment are in the order of two months for in the upper intertidal sediment to 3.8 months in the lower intertidal zone with physical removal processes playing a more important role than biodegradation (Wolfe, et al., 1994). In a sandy soils experiment, two ring PAHs had a half-life of two days; anthracene and phenanthrene (three ring PAHs) had half-lives of 16 and 134 days respectively and higher ringed PAHs' half-lives exceeded 200 days (Wilson & Jones, 1993).

British field studies of buried oil to a depth of 20 cm in dune sand revealed that decomposition rates varied due to the presence of water (Rowland, et al., 2000). Using Forties light crude oil, the results showed that decomposition was strongly related to temperature in the oiled sand layer and rainfall. A difference in

microbial activity was dependent on site location and varied considerably also. The decomposition seemed to stop when sand became saturated and began again when the sand dried out. It was also thought that larger particle size and more calcium content could be factors governing the rate of decomposition (Rowland, et al., 2000).

Not only does the presence of nutrients and water affect the rate of oil depuration from an environment but sediment particle size and composition is also thought to have an effect. A study on the concentrations of 16 US EPA priority PAHs were analysed in Boston Harbour sediments in four sediment size fractions in three sediments (Wang, et al., 2001). Total PAH concentrations varied greatly amongst the four sizes (<62, 62-125, 125-250, and >250 μm). The highest PAH concentrations were associated with the largest grain size decreased with grain size. The sediments, regardless of size were dominated by PAHs with three or more rings and displayed similar patterns. The study also concluded that the quantity and quality of organic matter present in the sediment could act as a source and adsorb matrices of the heavier PAHs in the larger sediment size fraction (Wang, et al., 2001).

Total PAH concentrations were significantly correlated with sedimentary total organic compounds (TOC) in a Spanish study on the continental shelf associated with a busy shipping channel (Viñas, et al., 2010). However, this study concluded that total PAH concentrations were greater in the deeper sediment of finer mud size grains, contradicting the results from Wang, et al., 2001. The correlation decreased slightly for coastal sediments due to different content of sands and the organic carbon within the sediment being both biogenic and anthropogenic (Viñas, et al., 2010).

Gas chromatograph results from a Canadian study showed that oils that spilled onto high energy environments lost the *n*-alkanes more rapidly than those in lower energy environments. The loss of *n*-alkanes altered the residual oil, which became more viscous and adhered to coastal sediment and reduced the mobility of the oil (Rashid, 1974). The samples were obtained three and a half years after the grounding of the 1970 *Arrow* (Rashid, 1974) of which only a minimum of 10% was removed during clean up (Lee, et al., 2003).

The 1970 *Arrow* spill (Table 2.3) has been subject to long term study of oil weathering. Biomarker compounds were used to match and identify the oil source, since most saturated and PAH constituents would have been lost 22 years after the *Arrow* spill (Wang, et al., 1994). The aromatic compounds were too degraded and altered (Wang, et al., 1999). The results from the GC/MS analysis of 11 sediment samples identified 47 triterpanes and steranes. C_{29}/C_{30} hopanes were especially apparent and used to clearly identify the source of the oil as being the *Arrow*. This study also documents that, apart from a few minor locations, the 260 km of coastline oiled by Bunker C oil has self-cleaned through natural weathering processes over the past 22 years. Where the oil remains it is usually as a thin stain on coarse sediments or bedrock (Wang, et al., 1994).

Certain hydrocarbons can be present in benthic species for much longer than is present in the contaminated sediment. A long term impact study in a sheltered lagoon concluded that the oil had undergone substantial biodegradation and the sediment had the ability to degrade hexadecane, octacosane and naphthalene (Lee, et al., 2003). There was no toxicity detected from the residual oil in the interstitial water or in all of the species tested (Lee, et al., 2003).

Data suggests that depuration of the spilled oil during the first month after the *TSESIS* spill (Table 2.3) was rapid and nearly complete at all but the most heavily oiled sites. However, as investigated by Boehm, et al., 1981, petroleum hydrocarbons can reside in benthic communities for extended periods of time.

There are many similarities between the *Nestucca* (Table 2.3) and *Rena* disasters. Both spilled Bunker C oil only a few miles from the shore. This allowed for the clean-up of freshly spilled oil along the coast to occur promptly. Timely clean-up of the *Nestucca* spill situated only 3 km from the coast is thought to have been a major contribution to the rapid removal of hydrocarbons from the coast (Strand, et al., 1992). A monitoring program was carried out researching the fate of oil in selected intertidal and shallow subtidal environments involving beach surveys 7, 10 and 13 months after the *Nestucca* spill at eight coastal sites. Only trace amounts of oil were found in the first 15 cm of the sediment 13 months after oiling which suggests that depuration of oil occurred rapidly within the environment. Contributions may be due to the efficient clean up, as well as the

type of beach that was affected and the cold, settled weather allowing oil to congeal before stranding (Strand, et al., 1992). However, the weather conditions were contrasting for the *Rena*, with a succession of storms intermittently affecting the coastline for some weeks after the initial grounding.

Tarball and oiled sand samples were retrieved from various beaches around the Bay of Plenty. A large amount of variation was present in the tarballs and oiled sand samples fingerprints with regards to the low molecular weight PAHs (Wilkins, 2013). The loss of the more volatile alkanes such as naphthalene and to a lesser extent phenanthrene in the October 2011 tarballs is primarily a result of weathering from evaporation. Hydrocarbon depletion in the January-February 2012 oiled sand samples was more extensive, and evaporation cannot solely be responsible for (Wilkins, 2013).

A notable consistency in the fingerprint patterns and ratio of peaks was detected for the *Rena* samples for parent and alkylated phenanthrenes, alkylated dibenzothiophenes, tetracyclic, pentacylic, and hexacyclic PAHs (such as fluoranthrene, pyrene, chrysene, benzo[a]anthracene, di- and trtribenzothiophenes) and C_{27}-C_{35} hopanoid petroleum biomarker compounds due to their resistance to weathering (Wilkins, 2013).

2.2.1 DEPTH OF OIL BURIAL ON BEACHES

Many studies in the past have only focused on the oil contamination in the surface sediments of the intertidal zone of beaches (Miller & Mudge, 1997; Rowland et al., 2000; Pereira & Mudge, 2004), as well as real cases (Teal et al.,1978; Strain, 1986; Hayes, et al., 1993; Kingston, et al., 2003; Lee, et al., 2003;). However, studies, such as the *Prestige* spill of 2002, have shown that oil can penetrate past surface sediments depending on oil viscosity, sediment porosity, the height of the water table, wave conditions and beach morphology (Bernabeu, et al., 2006). Sediment can be transported in calm conditions from the subtidal up to the intertidal section of the beach. Due to the sediment re-working and transportation, oil can become buried in the sediment. During storm conditions, the depth to which sediment and also oil, is reworked in the intertidal zone increases in depth due to increased wave energy (Bernabeu, et al., 2006).

Previous studies have shown that many factors determine the rate at which hydrocarbons disperse from a marine environment. It is believed that temporal impacts of spilled oil in a marine environment become more prolonged when oil is mixed into the sediment (Boehm, et al., 1981). Aromatic and saturated hydrocarbons can persist in sediment for substantial periods of time (years) as indicated by studies carried out in the 1970s by Blumer and Sass (1972b); Teal, et al., (1978), Keizer, et al., (1978) and Mayo, et al., (1978).

Persistence of oil in lower energy environments such as salt marshes and estuaries has been researched in Buzzards Bay, Massachusetts after contamination by 600 tons of No. 2 fuel oil spilled in 1969 (Blumer & Sass, 1972a). Two years later, fuel oil hydrocarbons were still persistent in the marsh and offshore sediments. The study revealed that oil degradation was slow, especially below the surface sediments (Blumer & Sass, 1972a).

The depth to which oil is buried into sediments affects the rate of evaporation. An experimental study was carried out in the 1980s on a sandy pocket beach in Nova Scotia, Canada (Strain, 1986). After four months, evaporation of light crude oil was significantly lower in the upper intertidal zone surface sands with C_8 hydrocarbons still present after 3 months. However, at depths of 5-10 cm and the surface in the mid-intertidal zone there was no loss of volatiles over the first 6 months. Preferential dissolution was significant in these zones however but, neither was as rapid nor extensive as in the upper intertidal zone surface sands (Strain, 1986).

Very light crude oil is less viscous and more volatile than heavy fuel oil, such as Bunker C *Rena* oil. Therefore, more hydrocarbons readily evaporate from the oil. Strain (1986) concluded that light crude oil can reside at depth within the intertidal zone over a long period of time (years).

The March 1989, *Exxon Valdez* spill (Table 2.3) was spread by winds and currents, reaching the coast of Alaska, up to 750 km from the source (Wolfe, et al., 1994). Approximately 45% of the spilled oil was washed onto the shoreline in Prince William Sound and Peninsula within two months. Oil was found as deep as the depth of activation of 25 cm on the central platform of beaches. 90 % or more

of the oil was removed from these beaches during the 1989-1990 winter storms. Both biodegradation and physical processes are thought to be the main contributing factors of removing PAHs and other hydrocarbons in the upper intertidal sediments two to four months post the *Exxon Valdez* spill. In more protected environments of fine sediments underlying mussel beds, oil persisted until 1992 (Wolfe, et al., 1994).

The sinking of the *Prestige* (Table 2.3) ~48 km off the coast of Spain in 2002 resulted in 77,000 metric tonnes of Bunker C oil spilled. 53,000 tonnes was removed in a major open sea operation, with the remaining oil reaching the Spanish and French coastline (Albaigés, et al., 2006). This event is probably the most scientifically researched and published oil spill to date. The following is a review of some of the research that has been undertaken on the *Prestige* oil spill in the past decade.

It was found that n-C_{18}/phytane, and methylnaphthalene ratios were useful in indicating the rates of evaporation, biodegradation and dissolution processes in over 200 oil samples that were retrieved from the Spanish coast beginning a month after the *Prestige* oil spill and continued on for one year (Díez, et al., 2007). Results showed a gradual decrease of the n-alkanes in the $<n$-C_{20} range over time. The data showed that n-alkanes biodegraded quicker than isoprenoids. However, there was a delay of ~2 months before degradation of n-alkanes became apparent. Dibenzothiophene and chrysene/benzo[*a*]anthracene PAH compounds were found to be useful indicators of oil weathering in sediments. Advanced degradation such as photo-oxidation had low influence on natural weathering of oil a year after the spill (Díez, et al., 2007).

It is thought that the morphodynamic behaviour of the beach as well as wave conditions determine the burial of oil with sediment. A study on 20 cores taken from Nemiña and O Rostro Beaches in Spain by Bernabeu, et al., 2006, identified that *Prestige* oil was present in the beach sediment up to a depth of 2.38 m (maximum length of the core). O Rostro and Nemiña Beach are both intermediate bayed beaches. However, O Rostro is more exposed than Nemiña and is therefore subject to intense and variable waves. At the time of the oil spill, the coast line

28

was experiencing intense storms with a maximum wave height of 9.34 m and 15.5 s wave period.

Gonzalez, et al., 2009 extended the study for three years on O Rostro Beach confirming the previous study that oil was able to be buried into the sand matrix 2-3 m deep. Based on the field observation made after four years, the deep buried oil had degraded rapidly (Gonzalez, et al., 2009).

Storms also affected the Bay of Plenty coast six days after the *Rena* ran aground although wave heights were significantly smaller than those seen at O Rostro and Nemiña Beaches. Increased wave action increased sediment activation depth within the intertidal zone but, also released more oil into the ocean and hindered clean up.

A model was formulated for the *Prestige* oil spill to predict the burial and subsequent evolution of the oil and sediment in the intertidal zone of a beach (Figure 2.5).

Bernabeu, et al., 2006 identified four different physical forms of oil with specific size ranges; (1) tar balls (cm), (2) particles (mm), (3) oil coatings on grains and, (4) oil/water emulsions, which vary with distribution depending on wave exposure. Oil particles were observed in the field to adhere preferentially to bioclastic sediment over siliciclastic. Further research has shown that different forms of oil result in a variation of weathering rates (Bernabeu, et al., 2010). A degradation sequence of buried oil from tar balls to oil coated sediment revealed that biodegradation was occurring even though the oil was buried but, only as a secondary process. Increased water flow velocity and low salinity decreased the break down rate of the tarball into oil coatings. However, the presence of water is thought to be the main contributing factor to tarball degradation (Bernabeu, et al., 2010).
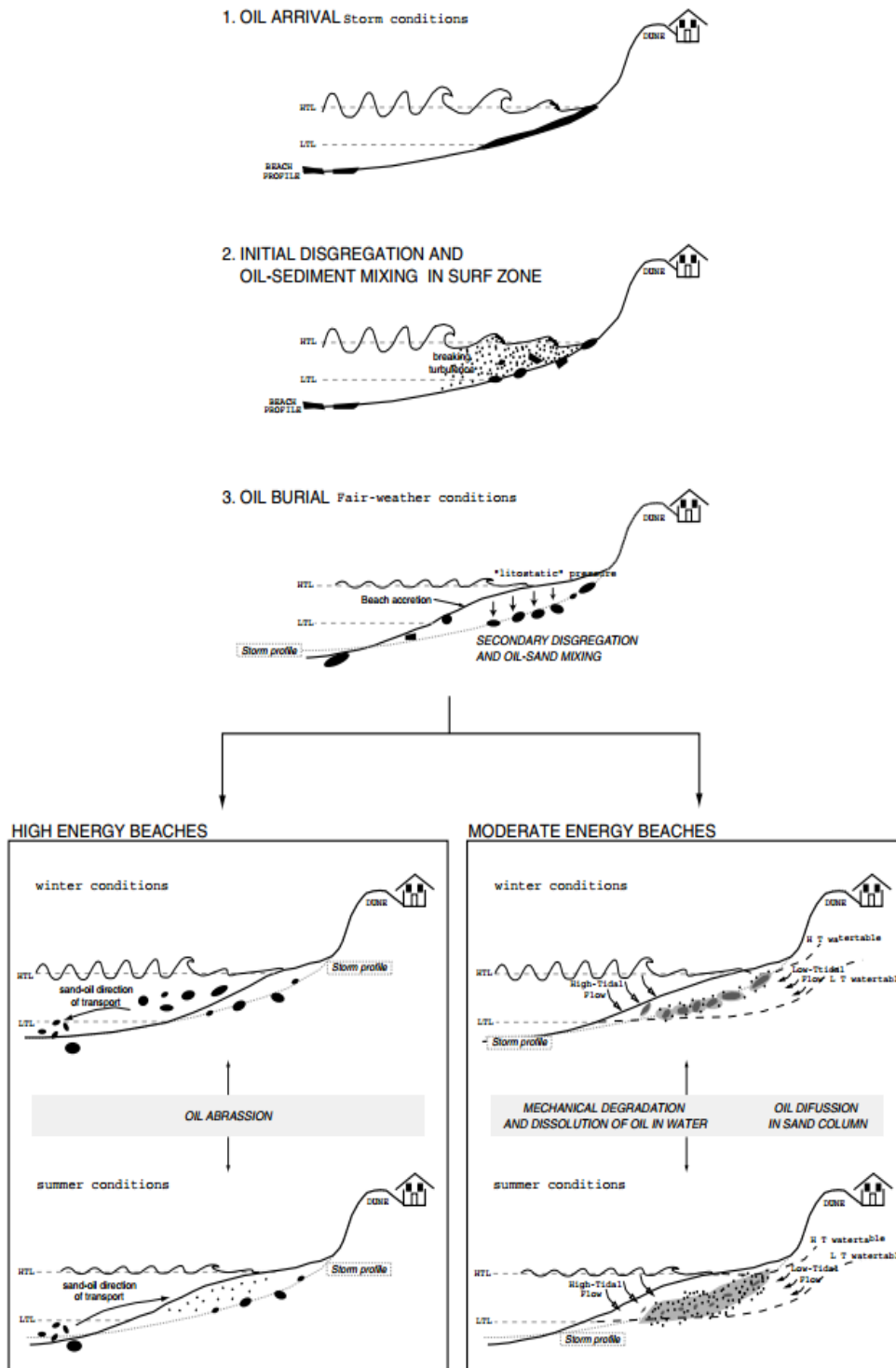
Figure 2.5: Oil and sediment evolution in the intertidal zone of a beach (Bernabeu, et al., 2006).

Experiments on tar balls were carried out and found that degradation of the buried oil follows a series of processes. Emulsification acts on the tar ball surface, diffusion and advection of oil particles by water flow and adsorption on the sediment grains. It is thought that equilibrium between advection and adsorption

probably depends on the concentration of oil. On beaches with high seasonal sand mobility, oil coating formation will not occur since the buried oil would be exhumed before the degradative process could begin (Bernabeu, et al., 2010).

During a severe storm in December 1999, the *Erika* tanker (Table 2.3) broke in two about 40 miles off the coast of Brittany, France. The tanker was carrying over 31,000 tonnes of heavy fuel oil that spilled into the ocean and reached the coast of France. Using GC/MS, a quantitative and qualitative study was carried out on PAH contamination in beach sediment as well as contamination of water, suspended particulate matter and intertidal molluscs (Tronczyński, et al., 2004). Using pre-spill and post-spill samples (July, 2000) from the French Biscay coast, the fingerprint of the *Erika* PAHs was determined. The results show that the compositional pattern of PAHs after the *Erika* spill included alkyl-substituted phenanthrenes, pyrenes, chrysenes and sulphur heterocycle compounds in higher relative abundances than those in the pre-spill samples of these compartments. Also contamination was confined to shallow and intertidal sediments and heavily oiled shorelines (Tronczyński, et al., 2004).

GC/MS results of 13 sediment samples from the Niger Delta, a busy shipping region found that of the 16 PAHs analysed, 5 and 6 ring PAHs (benzo(b)flouranthene, benzo(k)flouranthene, benzo(a)pyrene, dibenz(a,h)anthracene) were present in higher concentrations than all the other compounds indicating their resistance to microbial degradation (Anyakora, et al., 2005).

The intentional oil spill of the 1991 Gulf War is the largest to date (Adriana, et al., 2010). 12 years after the spill, shoreline sediments around Saudi Arabia contained PAH concentrations that were above acceptable levels for benthic fauna ($ESBTU_{FCV,43}$). Sediments from 0-30 cm depth from low energy tidal flats and 30-60 cm heavily oiled mangroves contained a large amount of high risk samples (PAHs above acceptable levels). Other studies on the same spill around Saudi Arabia, state that impacts of the oil contamination along the coast will take many more decades to recover. It is thought that the geomorphology of the affected area is largely responsible for the long retention time of hydrocarbons present in the system (Adriana, et al., 2010).

In 2010, the Gulf of Mexico was affected by an oil spill from the failed *Deepwater Horizon* (Table 2.3) well that involved approximately 7×10^5 m^3 of oil over the course of 84 days. Beach oiling resulted in a cross shore distribution of both surface and buried oil. Five different types of oil contamination were classified following the spill by Wang and Roberts (2013); (1) tar balls, (2) tar patties, (3) tar cakes, (4) oil sheets and (5) stained sand.

Tarballs were by far the most abundant, which are described as accumulations of oil and sand mixtures <10 cm in diameter. Tar patties are >10 cm in diameter and tar cakes are more than 3 cm thick. Oil sheets are laterally extensive thin layers covering 5 m or more of the beach surface. Oil stains are described as a thin veneer of oil that coats sediment and stains quartz to a brown colour (Wang & Roberts, 2013). Deposition of oil, specifically, tar balls and oil stain locations were associated with individual wave run-up termini. Buried oil was found beneath the berm crest as deep as 50 cm. Oil burial depth decreased both landward and seaward. The study concluded that different forms of contamination occurred in different beach zones. Oil was found in all forms along the entire 200 km coast of Alabama, both on the surface and at depth and was concentrated at the berm crest (Wang & Roberts, 2013).

An international workshop held in Canada in 2000, identified research priorities for oil particle interactions in aquatic environments, which included, (1) the mechanism of oil-particle interaction, (2) the persistence of oil in the environment with respect to oil-particle interaction, and (3) the application of countermeasures to oil spills (Lee, 2002). Numerous past studies have shown the oil-particle interaction controls the physical transport of spilled oil from the sea surface to the ocean floor. Oil-particle interaction includes adsorption of hydrocarbons, with both organics and inorganics and the binding of < 2 μm particles with oil (agglomeration) causing sedimentation. Gordon, et al. (1973) predicted that up to 98% of oil may end up in particulate form (Lee, 2002). Boehm (1987) suggested greater potential for sequestering oil at sediment particulate matter concentrations greater than 100 mg/L. Mesocosm experiments suggested that up to 50% of the insoluble hydrocarbon fraction dispersed in the water column can be removed by adsorption and agglomeration on oil and sediments (Lee, 2002). A mass balance

calculation estimated that 10-15% of the 300 tons of *TSESIS* oil spilled was removed by adsorption to sediment (Johansson, et al., 1980). Studies in the 1940s on mineral type and oil interaction reported that kaolinite was an efficient mineral for sedimenting oil. Not until the early 2000s did research on the *Exxon Valdez* spill by Bragg and Owens (1994) determine that clay-oil flocculation was responsible for the removal of oil from low energy environments (Lee, 2002).

Large oil sheets, oil coated sediment, oil droplets and patches were observed along the Bay of Plenty coastline for many days after the *Rena* spill. Although removal of the beached oil was prompt, storms that affected the coast a week after the spill increased turbulence and wave action which curbed clean-up operations and assisted the mixing of oil into the beach sediments.

2.2.2 OIL AND BEACH SEDIMENT EXPERIMENTS

In the past 20 years there has been a growing interest in the interaction of oil and sediments in the marine environment due to particle influence on residual oil persistence (Lee, 2002). The formation of oil-mineral aggregates (OMA) has proven to be particularly important in low energy environments such as estuaries where these aggregates self-clean by reducing oil adhesion. Smaller particles < 2 µm in size have reported to facilitate oil sedimentation through agglomeration (Lee, 2002).

PAHs entering the marine environment have a high affinity for suspended particulates in the water column, due to their hydrophobic nature. PAHs tend to sorb to these particles, they eventually settle onto the bottom sediments and out of the water column. Therefore, the PAH concentrations in water are generally low in relation to the concentrations in the bottom sediments (Moore & Ramamoorthy, 1984). The behaviour of PAHs includes processes such as coagulation, sedimentation, flocculation and filtration with sand or activated carbon.

Interaction between oil droplets and minerals was first reported in experiments by Delvigne, et al., (1987), and Payne, et al., (1989) proposed that the amount of oil binding to sediment was influenced by the oil viscosity and composition, the type of sediment, the amount of turbulent energy and water salinity. To validate the

interactions and evaluate the possible use of fine particles in oil spill remediation OMA have been subject to laboratory studies (Lee, 2002).

Three types of oil contaminated sediment were investigated in an oil-sediment contamination study, (1) natural harbour sediment from Rotterdam Petroleum Harbour, (2) laboratory samples simulating the natural oil and sediment interaction and (3) sediment prepared by direct mixing of large volumes of oil and sediment (Delvigne, 2002). Observations under a microscope during the laboratory study showed three possible oil forms in sediment: (1) droplets, (2) coatings and (3) patches. Patches are larger than spherical oil droplets and do not have a uniform shape. The forms were dependent on oil concentration, oil type and the sediment interaction processes (Delvigne, 2002). This separate study compares well with the joint studies carried out by Khelifa, et al., (2002); Lee, et al., (2002); Le Floch, et al., (2002); Omotoso, et al., (2002); Owens & Lee, (2002); and Stoffyn-Egli and Lee, (2002).

Stoffyn-Egli and Lee (2002) also identified three forms of OMA; (1) droplets, (2) solid aggregates and (3) flake aggregates. Like Delvigne, et al. (1987) and Payne, et al. (1989) this study concluded that factors determining OMA type, size and amount were; mineral properties, viscosity, oil type and the oil/mineral ratio (Stoffyn-Egli & Lee, 2002).

Once formed, OMAs are very stable structures and are on average less dense than mineral aggregates and therefore are more buoyant. OMAs act as a surfactant and they can increase the surface volume of spilled oil which intensifies weathering processes such as biodegradation, photo-oxidation and evaporation (Stoffyn-Egli & Lee, 2002). A further study on the salinity effects on the formation of OMAs concluded that there is a linear decrease in the oil incorporated into OMAs with reducing salinity (Le Floch, et al., 2002).

Omotoso, et al., (2002) also agreed that oil-mineral formation is dependent on mineral composition, oil viscosity and water chemistry. Mineral surface area is a more important marker for OMA formation than particle size. Oil droplet size varied between 2 and 50 µm. The addition of high viscosity oils such as Bunker C slows down the settling rate of sediment. Two types of microstructures were

observed during the study; (1) oil continuous areas with entrained minerals at the oil-water interface and, (2) minerals stabilising oil droplets in a water continuous phase.

In further experiments with relatively low mineral concentrations of 100 mg/L, oil mineral aggregates formed readily with several types of oils. The study found that oil droplet shape and size did not relate to oil viscosity. Oil droplets tended to be spherical in all eight oil types experimented on. However, the number of oil droplets strongly correlated to viscosity and temperature (Khelifa, et al., 2002).

Quartz and kaolinite were shown to interact more readily with low-viscosity oils whereas calcite interacted readily with oil all types of oil irrespective of viscosity (Lee, 2002).

Owens and Lee (2002) looked at the application of OMA as a natural cleaning process for low energy shorelines in the colder regions of Canada and North America and found that it was successful at a number of oiled sites. Sediment relocation of oiled sand to intertidal zone on sandy beaches enabled surf washing from waves and tidal activity to remove residual oil from beaches.

Further research at experimental plots confirmed that sediment relocation treatments reduced the amount of oil located on two mixed sediment beaches over the five day trial period (Lee, et al., 2003). One site contained 50 % clay particles and the other 33 % clay with quartz and feldspars accounting for the rest of the minerals. OMA occurred naturally on the oiled beaches at both locations and a significant proportion of the oil dispersed into the nearshore region where OMAs then biodegraded (Lee, et al., 2003).

2.3   DEPTH OF SEDIMENT DISTURBANCE

Calculating the depth of sediment disturbance or activation depth in the surf and swash zone along a beach profile (Figure 2.6) gives a better understanding of nearshore processes, such as beach replenishment and morphodynamics (Ciavola, et al., 2013). Sediment disturbance depth is important for determining the depth to which oil and other contaminants may have been mixed into the beach and where it may reside for many years.
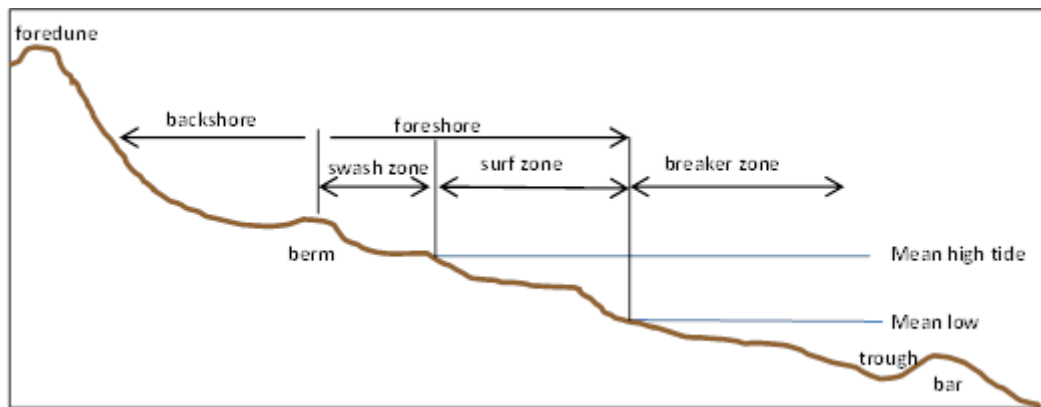
Figure 2.6: A typical beach profile (Adapted from fhwa.dot.gov).

Despite the small number of published studies that have carried out research on beach sediment mixing depth in the intertidal zone, many different methods and terminologies have been utilized. The depth of sediments affected by hydrodynamic processes is generally termed activation depth but, specifically referred to as mixing depth or disturbance depth (Anfuso, 2005). Mixing depth values are short term and a fixed point in time whereas, disturbance depth is generally over a single tidal cycle. However, these terms are not consistent and due to terminology differences used by various researchers, comparisons are conceptually difficult to make (Anfuso, 2005).

Sediment disturbance depth is a result of waves, and/or currents (Sunamura & Kraus, 1985). Sand is placed and kept in suspension by turbulence created by waves and currents and transported by advection of the suspended load as well as saltation on the stationary bed as bedload. The swash zone strongly affects beach sediments as it is the area of convergence of both swash uprush and backwash (Williams, 1971).

Depth of disturbance is strongly influenced by breaking wave characteristics and breaking wave height (Voulgaris & Collins, 2000; Anfuso, 2005; Ciavola, et al., 2013). Depth of disturbance values differ depending on the cross-shore position on the beach (Komar, 1983) and the beach slope profile. Disturbance depth studies reveal that disturbance is greater in the low tide zone and near the breaker zone during high-water still stand (Jackson & Nordstorm, 1993).

36

The surf similarity index also known as the Irribarren number (ξ) predicts the type of breaking wave;

$$\xi o = \frac{\tan \alpha}{\sqrt{H_0/L_0}}$$

Where H is the breaking wave height, *tan α* is beach slope and L is the deepwater wave length (Battjes, 1974). Surging breakers $=\xi > 2$, plunging breakers $=0.4 < \xi < 2$ and spilling breakers $=\xi < 0.4$.

Wright and Short (1984) studied beach and surf zone dynamics over three years at 26 different beaches around Australia in order to clarify a classification system of morphodynamic beach states. Beach state can be distinguished on the basis of the surf scaling parameter:

$$\xi = a_b \, w^2/(g \, \tan^2\beta)$$

Where a_b is breaker amplitude, w is incident wave radian frequency, g is acceleration due to gravity, and β is beach slope. If $\xi < 2.5$ the beach is reflective and if greater than $\xi = 30$ it is dissipative with ranges in-between defining intermediate beaches. Beach state has been recognized in previous studies to affect the depth to which sediment is mixed in the intertidal zone (Anfuso, 2005).

A reflective beach is a steep beach with small subaqueous sand storage and coarse grained to pebbly and has the greatest depth of mixing in the intertidal zone. A dissipative beach is flat, fine grained and shallow with relatively large subaqueous sand storage with the smallest depth of sediment disturbance at the shore. Four different intermediate beaches are classified their morphological features; (1) longshore bar-trough, (2) rhythmic bar and beach, (3) tranverse bar and rip, and (4) ridge-runnel and have mixing depths that are generally shallower than reflective beaches and deeper than dissipative beaches (Wright and Short, 1984).

Different formulas can be used to determine beach state, such as Dean's Parameter; $\Omega = \frac{H_b}{wT_p}$

Where H_b is the significant breaking wave height, w is the settling velocity and T_p is the incident wave period (Lisi, et al., 2011). The morphodynamic classification

for beaches is $\Omega > 6$ for dissipative, $1< \Omega > 6$ for intermediate, and $\Omega < 1$ for reflective beaches.

2.3.1 DEPTH OF DISTURBANCE MEASUREMENTS

Depth of disturbance has been studied using different empirical methods; (1) fluorescent tracers added into the beach profile, (2) small-scale pipe pro-filing to monitor beach step migration over tidal cycles (Nordstrom & Jackson, 1990), (3) dyed sand in plug holes and (4) disturbance rods, with or without washers (Ferreira, et al., 2000).

Each method has its advantages and disadvantages; fluorescent tracers and dyes show horizontal displacement as well as vertical, and are less likely to be disrupted by other factors such as curious beach goers and wind. However, they also require resource consent (RMA, 1991). The disturbance rod and washer method is the simplest and most cost effective method giving reasonably reliable results of depth of disturbance, which has been used in past studies by Jackson and Nordstrom (1993); Sherman, et al. (1994); Ferreira, et al. (2000); Anfuso, et al. (2003) and Balouin, et al. (2012).

More recently, a new technique of freezing coloured sand cores while in place after the tidal cycle has been considered (Brook, 2010).

One of the first disturbance depth studies was conducted by King (1951) using dyed sand at four different locations around the English coast. At low tide the dyed sand was placed into a dug out hole on the beach face to approximately 5-10 cm deep and then filled in. After a tidal cycle, the depth at which the dyed sand was found determined the disturbance depth. The results concluded that under normal (fair weather) conditions on a fine sand beach, the disturbance depth was approximately 30 % of breaking wave height at breaking point (King, 1951). The relationship was shown to be nearly linear, therefore it was assumed that it can be extrapolated over a range of breaking wave heights. It was also found that depth of disturbance (DoD) was deeper as the sand became coarser (King, 1951).

A study on three beaches in Hong Kong by Williams (1971) also used marked sand, and concluded that breaker wave height is the dominant process on DoD by

waves in beach sediment in the mid tide and possibly also low tide zones. The results from over 150 samples indicated that 82 % of the factors affecting DoD at the mid tide zone could be attributed to beach gradient, wave period and breaker height whereas, at high tide marks, the influence of disturbance by these factors was considerably less (Williams, 1971).

Mixing depth was measured on a typical dissipative (ξ= 30) Pacific Ocean beach in Mexico with ~ 2 m tidal range using 20-50 kg of fluorescent sand tracer grains injected into the mid surf position during an ebbing tide by Gaughan (1978). A coring device was employed during wave action so that depth of vertical mixing of tracers could be accurately measured. Using tracer concentrations, the study results showed that over the autumn/winter period the concentration was highest at the bed surface shoreward of the release site and 0.4 cm to 1.2 cm below the bed surface seaward of the release site. The winter study resulted in a mean of 1.1 cm and 0.5 cm standard deviation in depth of disturbance whereas the summer study showed a mean of 0.5 cm and standard deviation of 0.5 cm (Gaughan, 1978).

A Canadian study using disturbance rods on a multiple barred, medium to fine grained (0.43-0.13 mm mean diameter) beach at Georgian Bay was carried out during a storm (Greenwood & Sherman, 1986). The wave height exceeded 2 m (H_s) and maximum wave period was 5 s. Sediment disturbance was recorded at 0.14 m. Orbital velocities were greater than the threshold of motion needed to entrain the mean grain size present (Greenwood & Sherman, 1986).

A predictive model for the average depth of mixing of sediment in the surf zone was formulated by Sunamura and Kraus (1984).

Z/D = 8.14 (Ψb-Ψc)

Where *Z* is the average depth of mixing in the surf zone, *D* is grain size, Ψb is the Shield's parameter at the wave breaking point and Ψc is the critical Shield's number for oscillatory flow (Sunamura & Kraus, 1985). The mixing depth is predicted to increase with breaking wave height up to about 1.5 m in a reasonably linear fashion. This linear relationship was observed by Ciavola, et al. (1997) on steep beaches in Portugal.

A Delaware Bay study on medium sand in a low energy estuarine environment by Jackson and Nordstrom (1993) was carried out over a semi diurnal tidal cycle to determine activation depth. The significant wave heights ranged from 0.06 m to 0.52 m. The mean grain size at mid foreshore was 0.46 mm. The results support previous studies that sediment activation is greater on steeper beach profiles and the ratio of depth of activation to wave height is also comparable to results from other studies provided that beach slope is measured in the breaking wave height calculation (Jackson & Nordstrom, 1993).

Reflective beaches studies had quite different values for average mixing depth. Sherman, et al. (1994) observed a mixing depth over the entire surf zone at 22 % (ranging between 16-30 %) of the significant wave height which ranged between 0.09 m to 0.13 m with maximum given at the breaker line with wave periods of 2.1 sec to 2.2 sec. For three field experiments containing 192 tube cores, the recorded DoDs averaged to 25 mm, 27 mm, and 28 mm with beach slopes of up to 8°. Whereas, Ciavola, et al. (1997) obtained values at 27 % of the average significant breaking wave height on beaches with comparative slopes to the studies of Sherman, et al. (1994) wave heights (0.34–0.80 m), wave periods (5.1–7.0 s) and mean grain sizes (0.26 and 0.38 mm). The study also concluded that DoD is a function to wave period but, not of mean grain size.

Anfuso, et al. (2000) achieved similar disturbance values at 16 % significant breaking wave height although the beaches observed during the study were smoother than those in the two previous cases. As with King (1951), a good linear regression allows the formula to be extrapolated over a wide range of beach states from dissipative to reflective beaches.

Ferreira, et al. (2000) undertook seven field experiments on the coast of Portugal to obtain mixing depths that related to a range of wave heights on steep beaches (tan β > 0.8). Disturbance rod and plug hole techniques were used. The results showed similar outcomes with previous studies on steep beaches with a correlation between significant breaking wave height (H_{bs}) and mean sediment activation depth ($Z0$). The relationship can be expressed as sediment activation depth being equal to 0.23 H_{bs} but is about eight times larger than observed on

gentler beach slopes reviewed in this study. Through analysis of gentle and steep beaches as well as beach slope (β), the following relationship was obtained;

$Z0 = 1.85\ H_s\ tan\beta$ (Ferreira, et al., 2000).

Mixing depth experiments carried out on a dissipative beach were found to reach maximum values of about 0.15 m using the Ferreira, et al. (2000) formula. The formula generally worked well for both averaged and non-averaged approach to breaking wave height. However, the non-averaged approach had better results in the low tide zone and the standard deviation of the difference between calculated and observed values was much larger (Gonzalez, et al., 2004).

Beach profile changes at intra-tidal time scales have been subject to little study however their importance is indisputable. Large scale morphodynamic changes can result in permanent migration of the surf zone especially on reflective meso and macro tidal beaches (Taborda, et al., 2006). These morphological changes can be linked with the time average geometry of the active sediment layer. Pressure transducers were used to measure morphological changes on Faro beach in Portugal over a tidal cycle. Mixing depth was measured using disturbance rods with washers, and marked sand. Faro beach is meso-tidal and classified as a reflective beach comprised of a low tide terrace and rips. During the experiment the semi diurnal tidal range was 2.5 m, low energy swells with significant wave heights (H_s) ranging from 0.25 m to 0.32 m. (Taborda, et al., 2006). The analysis confirms the role of tides in profile evolution and that profile variation was strongly related to the development and migration of a beach step at the base of the beach face. Beach step variations dominate the cross shore mixing depth signal in this study therefore understanding step dynamics is essential to comprehend the mixing depth behaviour on beaches with these characteristics (Taborda, et al., 2006).

Activation depth measurements taken at two contrasting beaches in France produced good results for the high energy St Trojan beach between field measurements and predictions. However, the low energy Arcay Sandspit was underestimated for sediment disturbance by 40-60 % (Bertin, et al., 2008). The differences are suggested to be from the influence of wave obliquity on sediment

disturbance depths. Bertin, et al. (2008) derived a new formula for sediment activation depths which takes into account the significant wave height the slope of the beach slope (β) and the wave angle at breaking (α);

$$Z0 = 1.6 tan\ (\beta)\ H_{bs}\ 0.5\sqrt{1 + sin\ (2\alpha)}$$

This can be applied to a wide variety of beach gradients wave heights and wave incidence (Bertin, et al., 2008).

Sainia, et al. (2009) evaluated sediment disturbance of an estuarine beach to determine whether activation depth is less in pebbles than sand. Rods with washers on three beach plots with different sediments were monitored over 27 days. Significant wave heights ranged from 0.18-0.40 m and sediment activation depths between 0.02 and 0.12 m. Activation depth for the pebble plot were less for similar wave heights than for sand and granules and mixed grain plots. However, once waves had reworked the sediment, there was little difference in activation depths for all sediment types (Sainia, et al., 2009).

The same method is utilised in the current study for determining disturbance depth as Sainia, et al., (2009). However, the sampling period and type of environment is different as it is being conducted over a single tidal cycle and along various intermediate sloped beaches around the Bay of Plenty region.

On dissipative beaches with spilling breakers and wide surf zones, investigations were carried out showed that swash processes tended to be the dominant mixing factor rather than surf processes. Fluorescent tracers were injected at low tide in the foreshore and used to investigate depth of disturbance over an entire tidal cycle at medium sand composite, intermediate to reflective beach in south west Spain (Bellido, et al., 2011). Cores taken from the beach after the fluorescent deposition tidal cycle showed mean disturbance depths of 3.3 and 4.3 cm. Where plunging and surging breakers prevail in the foreshore, disturbance depths of 10 cm were recorded (Bellido, et al., 2011).

Grosser Wellen Kanal in Hanover was the location for a sediment mixing experiment to determine the effects of a buried drainage system on the beach face (Ciavola, et al., 2013). During the test the wave energy varied from *Hs* 0.59 m to

0.83 m. Values of sediment activation varied between 2% and 6% of the breaking wave height. The drained area showed slightly lower levels of sediment mixing in drained conditions however not significant enough to trigger beach stabilisation (Ciavola, et al., 2013).

Table 2.5 summarizes previous DoD that have been recorded during various studies in the past ~ 30 years. Beaches are classified using the Wright and Short beach state model (1984) based on both Dean's Parameter (Ω) and Irribarren Number (ξ).

Table 2.5: Beach profile data as well as Wright and Short (1984) beach classification using Dean's Parameter(Ω) and Irribarren Number (ξ) (Adapted from Anfuso, 2005).

Authors	Place	Year	H_{bs} (m)	Tz (s)	Beach slope (°)	Dean's Parameter Ω	Wright and Short (1984) beach state based on Ω	Intermed-iate state	Irribarren Number ξ	Wright and Short (1984) beach state based on ξ	Measured activation depth (mm)	1.86 H_{bs} tan β (Ferreria et al. (1998)	Activation depth / H_s
Greenwood & Hale 1980		1976	2	6.5	-						70	-	0.35
Sunamura & Kraus 1985	Ajiguara	1978	1	9	0.6	122.70	Dissipative		0.12	Dissipative	38	19	0.04
	Ajiguara	1979	1.1	6.5	0.6	122.70	Dissipative		0.08	Dissipative	29	21	0.03
	Shimokita	1979	0.6	4.9	1.2	30.67	Dissipative		0.17	Dissipative	23	23	0.04
	Hirono	1980	1.6	8.7	5.7	1.35	Intermediate	low tide terrace	0.86	Intermediate	37	297	0.02
	Hirono	1980	1	8.4	5.7	1.35	Intermediate	low tide terrace	1.05	Intermediate	30	186	0.03
	Orai	1980	1	10.2	0.6	122.70	Dissipative		0.13	Dissipative	28	19	0.03
	Orai	1981	1.11	6.1	0.6	122.70	Dissipative		0.08	Dissipative	23	22	0.02
	Orai	1982	0.8	75	1.2	30.67	Dissipative		2.19	Reflective	19	31	0.02
Sherman, et al., 1994	Fire Island	1992	1.22	-	-						27	-	0.22
Ciavola, et al., 1997	Culata	1993	0.37	5.8	6.3	1.10	Intermediate	low tide terrace	1.31	Reflective	106	76	0.29
	Culata	1993	0.34	5.1	6.3	1.10	Intermediate	low tide terrace	1.21	Reflective	106	70	0.31
	Culata	1993	0.37	5.1	6.3	1.10	Intermediate	low tide terrace	1.16	Reflective	106	76	0.29
	Garrao	1993	0.49	5.4	5.7	1.35	Intermediate	low tide terrace	0.96	Intermediate	103	91	0.21
	Faro	1996	0.8	7	7.9	0.70	Reflective		1.36	Reflective	220	206	0.28
Ferreria, et al., 1998	Quarteira	1996	0.49	-	6.3	1.10	Intermediate	low tide terrace			107	101	0.22
	Quarteira	1997	0.6	-	5.7	1.35	Intermediate	low tide			160	111	0.27

Reference	Location	Year					State	Beach type		State			
								terrace					
	Quarteira	1997	0.81	-	5.7	1.35	Intermediate	low tide terrace			153	150	0.19
	Quarteira	1997	0.61	-	6.8	0.95	Reflective				144	135	0.24
	Faro	1997	0.85	-	7.9	0.70	Reflective				162	219	0.19
Anfuso, et al., 2000	Rota	1996	0.52	10	3.4	3.81	Intermediate	rhythmic bar & beach	1.03	Intermediate	85	57	0.16
	Rota	1997	0.58	11	3.4	3.81	Intermediate	rhythmic bar & beach	1.07	Intermediate	75	64	0.13
	La Ballena	1997	0.35	4.5	2.3	8.34	Dissipative		0.38	Intermediate	44	26	0.13
	Tres Piedras	1997	0.7	10	1.2	30.67	Dissipative		0.31	Dissipative	30	27	0.04
	Tres Piedras	1997	0.45	10	1.2	30.67	Dissipative		0.39	Intermediate	18	18	0.04
	Tres Piedras	1997	0.8	12	2.8	5.63	Intermediate	longshore bar & trough	0.82	Intermediate	40	31	0.05
Anfuso, et al., 2003	Aguadulce	1997	0.9	12	1.7	15.28	Dissipative		0.47	Intermediate	60	82	0.07
	La Barrosa	1997	0.5	9	1.2	30.67	Dissipative		0.33	Dissipative	30	28	0.06
Anfuso & Ruiz 2004	Faro	2002	0.5	4							30	19	0.06
	Faro	2002	0.5	4	6.3	1.10	Intermediate	low tide terrace	0.78	Intermediate	90	103	0.18
Ciavola, et al., 2005	Beach models & wave flumes	2004	2.5	6.5	1.1	36.50	Dissipative		0.10	Dissipative	45-101	-	0.2
			4	9	3	4.90	Intermediate	longshore bar & trough	0.29	Dissipative			
Sainia, et al., 2009	Delaware	2006	0.4	-	9	0.54	Reflective				110	118	0.22
Brook, 2010	Southport	2005	0.7	4.3	4.3	2.38	Intermediate	low tide terrace	0.48	Intermediate	98	98	0.14

2.4 SUMMARY

The *Rena* oil spill of October, 2011 affected a significant portion of the Bay of Plenty coastline. The disaster prompted a large scale clean up involving thousands of volunteers and response crew.

Previous oil spill studies at various locations around the World have determined that PAHs present in oil can reside in the coastal environment for many years. Generally as the weight and the ring number of the PAH increases, so does it's resistance to weathering.

Biodegradation is considered an important process in the removal of hydrocarbons including PAHs from spilled oil in the environment. Biodegradation is a complex process involving a succession of microbes working together. However, the work of micro-organisms may not follow the same oil degradation pattern as weathering. Largely, the lighter molecular weight PAHs biodegrade much quicker than heavier PAHs, which is also seen in weathering profiles. But, when biodegradation is occurring in three and four ring PAHs, microbes favour specific PAHs depending on the environmental conditions. However, three and four ring PAHs will still biodegrade before the heavier five and six ringed PAHs.

In some studies, oil tended to be more resistant to weathering and biodegradation when buried in beach sediments. However, other studies implied increased weathering and biodegradation.

Mixing of oil in the intertidal zone on beaches occurs through various hydrodynamic processes together described as turbulence. A number of studies have researched the depth of sediment disturbance (DoD) in the intertidal zone but, only a few have applied this to oil burial.

DoD disturbance equations have been derived by various authors in the past 30 years utilizing significant wave height and beach slope as variables to determine the maximum depth of mixing. A variety of different DoDs have been determined at various beach locations with diverse beach slopes and wave conditions.

The efficacy of the *Rena* oil clean-up and natural weathering of PAHs is tested in this report, by retrieving sediment cores from various beach locations in the Tauranga area and analysing them. DoD is also measured using the disturbance rod and washer technique and the results compared to those obtained in earlier studies.

CHAPTER THREE: *RENA* OIL ON THE SANDY COASTS

3.1 FIELD METHODS

3.1.1 VIBROCORING

Beach sediment cores were obtained by vibrocoring. The vibrocorer consists of an eccentric cam in a head unit linked to a drive motor by a flexible mechanical linkage (Figure 3.1). The head unit transfers the vibrating motion produced by the motor to the attached core. The vibrocorer head was clamped to an aluminium core tube; 2.5m in length, 75 mm outer diameter, and 1.6 mm wall thickness. Aluminium cores were used to avoid the introduction of hydrocarbon contaminants.

Figure 3.1: Vibrocoring on Matakana Island, 25th of January, 2013.

Figure 3.2: the core barrel being winched up on Matakana Island 25th of January, 2013.

A core catcher was attached to the bottom of the aluminium tube to prevent the loss of sediment when the core barrel was recovered from the beach. The tube was manually placed vertically in the chosen location along the beach profile. The

motor was then switched on and the vibration began. The core tube penetrated the sand while vibrating. The core barrel would usually cease penetration at about 1 m depth, when the friction of the surrounding sediment exceeded the driving force provided by the vibrocorer head.

A plumber's plug was placed on the top end of the core tube to create suction and the vibrocorer clamp was removed. A clamp with a handle was attached to the core allowing the tripod mounted hand winch to extract the core from the beach (Figure 3.2).

Before the core cleared the beach surface, the sediment depth was measured to determine compaction during vibrating and the excess core barrel sawn off, capped and taped to remove any free space and keep sediment structure. The core was then manually removed from the beach surface and inverted to remove the core catcher. The excess space created by removing the core catcher, was also sawn off the tube overall, capped and taped. The core was labelled (

Figure 3.3) and then transported horizontally to the laboratory. The GPS co-ordinates of each core site were recorded using a Garmin 60CS x.

Figure 3.3: Photo of a core cut, capped and taped, ready for transport.

A total of 26 cores at 12 different locations around the Bay of Plenty sandy beaches were retrieved.

Back at the University, the cores barrels were placed in a wooden brace that also acted as a cutter guide. An angle grinder was used to cut approximately 5 mm depth along the length of the aluminium core barrel and repeated on the opposite side. The cap ends and sediment were then cut through with a knife, and the core was carefully opened to give two essentially even sediment halves.

3.1.2 SHEAR STRENGTH

Shear strength was measured using a hand held shear vane at each of the core locations. To ensure an undisturbed soil surface, a small hole was dug into the beach approximately 20-30 cm deep and a flat surface created by scraping the spade along the base of the hole. A hand held shear vane with a standard size 19 mm diameter by 29 mm high vane blade was held perpendicular to the surface and pushed into the sand so the vane blade was completely enclosed. The vane head was rotated manually at a slow and uniform rate. The sand would shear when the device released the torsion and the pointer registered the maximum deflection to which the spring was subjected. At each site, the shear test was replicated five times. Using the BS1377 calculation on shear vane results gives the vane shear strength reported to the nearest kPa (NZGS, 2001). Shear strength is usually conducted on cohesive soil and very sandy or brittle soils are considered unsuitable (NZGS, 2001). However, it was considered that residual oil would provide cohesion that may be measured via this technique. The results from the shear vane were then compared to the calibration sheet for the shear vane and shear strength was derived.

3.2 LABORATORY ANALYSIS

A series of various analyses were conducted on the sediment cores. Visual analysis, grain size analysis and qualitative GC/MS chemical analysis were undertaken at the University of Waikato in various laboratories. Further quantitative GC/MS analysis on selected sediment samples was carried out by Hill's Laboratories in Hamilton.

3.2.1 VISUAL ANALYSIS

The sediment cores were photographed and described on a core log sheet in accordance with the New Zealand Soil and Rock Field Description Guidelines (NZGS, 2005). Decisions were made with regards to presence and depth of oil,

sediment colour using the Munsell Colour System, sediment texture (Folk, 1954), organics and shell fragment content. Major structural features, boundaries and contacts were also recorded. Figure 3.4 shows a halved core from Matakana Island, Tank Road mid tide that underwent visual analysis.
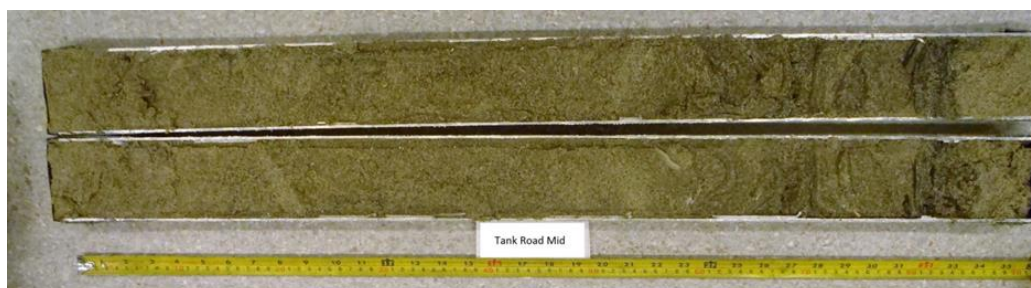

Figure 3.4: Core taken from Matakana Island Tank Road mid mean water level, 90cm in length.

3.2.2 GRAIN SIZE ANALYSIS

A Malvern Particle Laser Sizer (Mastersizer 2000) was utilised to determine grain size and sorting of the sediment through the cores. Approximately two teaspoons of sediment at 5 cm intervals throughout the length of each core was placed into a glass vial with ~ 30 ml of 10 % hydrogen peroxide solution and left for two to three days to dissolve organic matter. The subsamples were then sieved through a 2 mm mesh sieve to remove shell fragments and analysed in the laser sizer. The results were studied to determine if there was any pattern in grain size variations in relationship to depth changes and beach location as well as, beach state and distance from sediment source.

3.2.3 CHEMICAL ANALYSIS

Using gas chromatography mass spectrometry (GC/MS) the University of Waikato's Chemistry department identified the parent petroleum aromatic hydrocarbons (PAHs) by comparing retention times and the total ion chromatogram (TIC) (Figure 3.5) mode mass spectral fragmentation patterns to those determined for the *Rena* oil fingerprint from 16 genuine specimens of Environmental Protection Agency priority PAHs purchased from Sigma Aldrich (Wilkins, 2013).

One half of each of the cores were sub-sectioned for extraction of any oil present in the pores or adhered to sediment grains. Since it was difficult to predict what levels could be present, the procedure started with the cores considered most likely to contain oil, from the Omanu Beach high tide location (Figure 3.7), and use the smallest sample size that could provide enough material to analyse. Initially, the sediment from one half of the cores from Omanu Beach was sub-sectioned into 5 cm increments down to 40 cm, and transferred to separate glass containers in preparation for analysis.
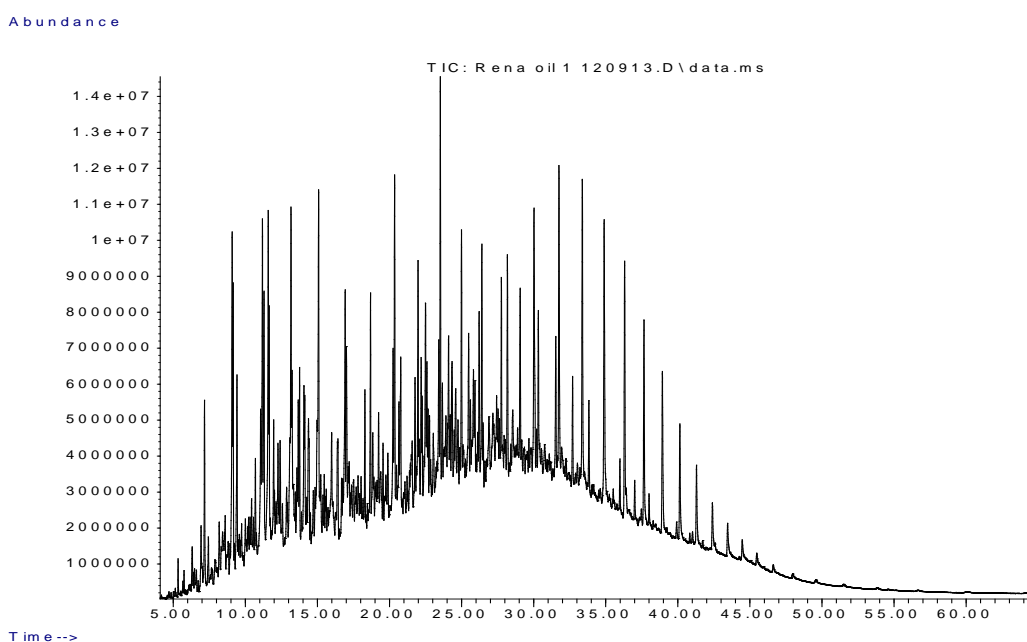

Figure 3.5: Total ion chromatogram of un-degraded *Rena* oil from tanker samples.

No fingerprint of *Rena* oil petroleum aromatic hydrocarbons (PAHs) was found in any of the eight samples. Therefore, to increase the potential concentration of extracted oil, subsequent extractions were based on 20 cm increments for the top 40 cm of each core resulting in two samples from each core. A total of 58 samples were chemically analysed using the following method.

Dichloromethane was added to the sediment sample, left to soak for ten minutes. The solution decanted filtered through a Pasteur pipette containing cotton wool, and repeated. The solution was then concentrated down to approximately 5 ml using a rotary evaporator. The solution was decanted off into a GC/MS vial. The correct amount of phen-d10 into the solvent soaked sample GC/MS vials. The samples were put into the GC/MS and run in batches with a *Rena* oil vial at the

start, the batch of samples, and a response factor standard last. The response factor mix is diluted down with dichloromethane to a similar peak height as the samples ($10^{-5}gL^{-1}$) and is used to check the detection levels, retention times and peak shapes.

The eight 5 cm Omanu high tide samples, as well as, a random selection of 11 other 20 cm size samples were analysed by GC/MS using a qualitative method. The remaining 39 samples were analysed with the same GC/MS. It then became apparent that the first 19 samples had been affected by a GC/MS column blockage. The elutriates of these were re-analysed on the same GC/MS apart from the smaller Omanu 5 cm samples, instead the other half of the Omanu high tide core was used to obtain two 20 cm samples for analysis. The re-analysed samples are considered to be more accurate and have therefore been used as the key results.

Each sample produced a total ion chromatogram trace (Figure 3.5) and an extracted ion chromatogram (Figure 3.6), in descending order naphthalene 128, phenanthrene 178, pyrene 202 and benzo(a)anthracene and chrysene 228. These five PAHs have approximate retention times of naphthalene at 7-8 minutes, phenanthrene at 18-19 minutes, pyrene at 24 minutes and benzo(a)anthracene and chrysene at 27-28 minutes (2 peaks).

18 samples were selected for further analysis based on their qualitative results. The other half of the core sediment was utilised to derive 20 cm samples for quantitative analysis. The samples analysed were: (1) the first eleven 20 cm size samples that were affected by the column blockage (except the 5 cm size Omanu Beach samples), (2) the two 20 cm Omanu Beach samples and, (3) five from the last 39 samples that were qualitatively analysed, where the extracted chromatograms contained some PAHs of interest. Selected samples were analysed by Hill's Laboratories also using GC/MS to determine the presence of 16 specific EPA priority PAHs. Although this method can give the abundance of the selected 16 PAHs, it is not as sensitive as the qualitative method.
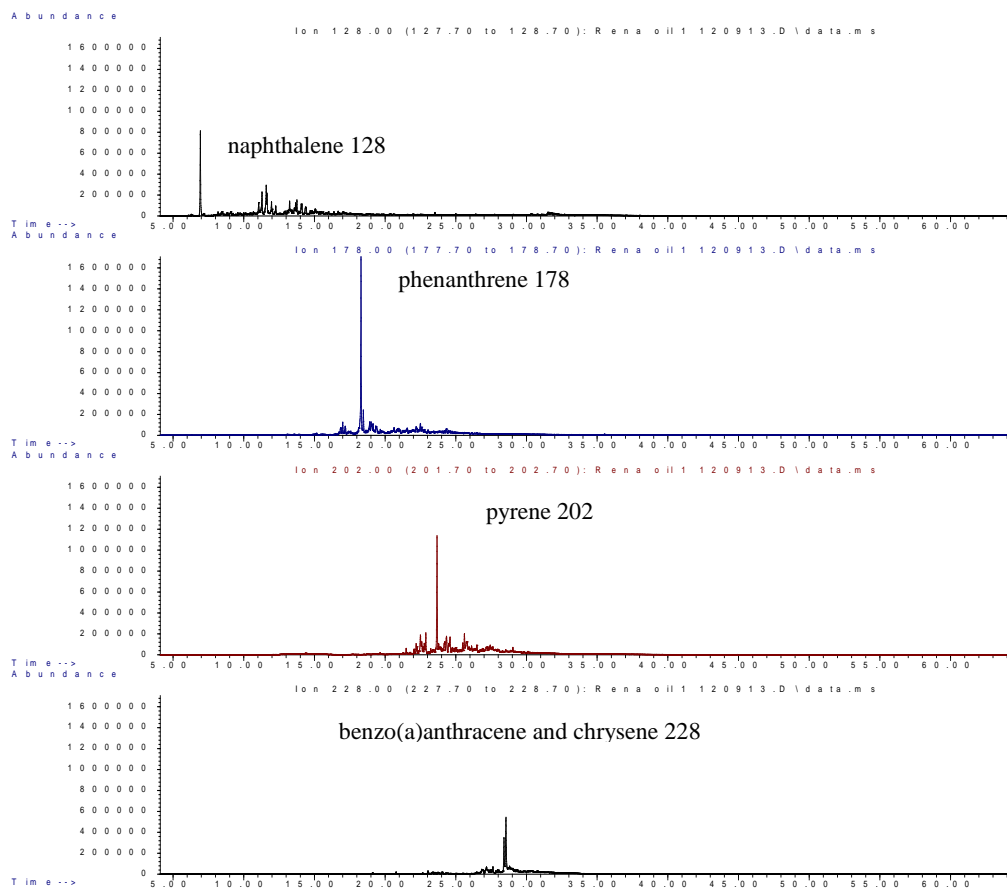
Figure 3.6: Extracted ion chromatogram for *Rena* oil showing the key PAHs. These are; naphthalene 128 (black); phenanthrene 178 (blue); pyrene 202 (red); and benzo(a)anthracene and chrysene 228 (black) at the bottom (Source: Wilkins, 2103).

After Maketu Spit, Estuary and Matakana Island core sediments were analysed, the sand was returned to their respective sampling locations as requested by relevant iwi or their representatives.

3.3 RESULTS

3.3.1 VISUAL CORE DESCRIPTIONS

A total of 26 cores were retrieved from 12 beach and intertidal locations affected by the *Rena* oil spill in the Bay of Plenty. The sedimentology of each core was described and identification and characterisation any visual indicators of the presence of residual oil (Figure 3.7). Individual visual descriptions written as core logs with photos are given in Appendix I. Core site locations as well as, core lengths, compaction and summary statistics are specified in Table 3.1.

Based on visual inspection, there was no residual oil identified throughout any of the cores. Black bands of various thicknesses within the beach profile at several site locations had been reported as being oil deposits. However, upon further inspection, it was found that these black bands were titanomagnetite placer deposits (Appendix I).

Table 3.1: Core site locations with GPS co-ordinates, individual core length and compaction. Summary statistics are also given.

Site	Location	date	WGS 1984 GPS co-ordinates	distance between cores (m)	length of core (m)	Compaction (m)	Compaction %
1	Waihi- Surf club mid	10/01 /2013	S 37 23.749 E 175 56.297	high to mid: 43.3	0.61	0.02	3.17
1	Waihi- Surf club high	10/01 /2013	S 37 23.747 E 175 56.326		0.65	0.17	20.73
2	Waihi- Bowentown mid	10/01 /2013	S 37 23.772 E 175 56.336	high to mid: 28.52	1.02	0.165	13.92
2	Waihi- Bowentown high	10/01 /2013	S 37 23.783 E 175 56.323		1.14	0.5	42.01
3	Matakana Tank Rd mid	26/01 /2013	S 37 35.546 E 176 06.591	high to mid: 18.45	0.9	0.17	15.88
3	Matakana Tank Rd high	26/01 /2013	S 37 35.554 E 176 06 583		0.69	0.35	33.65
4	Matakana Panepane mid	26/01 /2013	S 37 38.154 E 176 09.675	high to mid: 27.5	1	0.46	31.51
4	Matakana Panepane high	26/01 /2013	S 37 38.165 E 176 09.662		0.84	0.29	25.66
5	Centre Bank	12/12 /2012	S 37 38.583 E176 10.425		0.71	0.5	41.32
6	Mt Maunganui low	6/12/ 2012	S 37 37.840 E 176 10.689	low to mid: 11.42	0.72	0.25	25.77
6	Mt Maunganui mid	6/12/ 2012	S 37 37.844 E 176 10.686		0.76	0.11	12.64
6	Mt Maunganui high	6/12/ 2012	S 37 37.510 E 176 10.406		0.82	0.3	26.79
7	Omanu Beach mid	7/12/ 2012	S 37 39.508 E 176 12.953	mid to high: 14.3	0.87	0.11	11.22
7	Omanu Beach high	7/12/ 2012	S 37 39.514 E 176 12.944		1.21	0.13	9.70
8	Harrison's low	3/12/ 2012	S 37 41.412 E 176 16.436	low to mid: 8.72	1.43	0.2	12.27
8	Harrison's mid	3/12/ 2012	S 37 41.416 E 176 16.430	mid to high: 13.3	1.2	0.57	32.20
8	Harrison's high	3/12/ 2012	S 37 41.442 E 176 16.425		1.14	0.2	14.92

9	Taylor's low	4/12/2012	S 37 42.371 E 176 19.391		0.84	0.3	26.32
9	Taylor's mid	4/12/2012	S 37 42.603 E 176 19.636	low to mid: 8.24	0.64	0.2	31.25
9	Taylor's high	7/12/2012	S 37 42.620 E 176 19.653		0.86	0.17	16.50
10	Maketu Ford Rd-mid	24/01/2013	S 37 44.860 E 176 24.975	high to mid: 11.3	0.82	0.5	37.88
10	Maketu Ford Rd-high	8/01/2013	S 37 44.866 E 176 24.975		0.69	0.42	37.83
11	Maketu Spit mid	6/12/2012	S 37 45.263 E 176 26.985	low to mid: 13.48	0.95	0.2	17.39
11	Maketu Spit high	6/12/2012	S 37 45.271 E 176 26.985		0.9	0.35	28.00
12	Maketu Estuary 1	8/01/2013	S 37 45.428 E 176 27.088	estuary	0.65	0.74	53.24
12	Maketu Estuary 2	8/01/2013	S 37 45.412 E 176 27.053	estuary	0.71	0.47	39.83
				Total (m)	22.77	7.84	
				Average (m)	0.88	0.30	25.42
				Min (m)	0.61	0.02	
				Max (m)	1.43	0.74	
				SD (m)	0.21	0.18	

The average length for the cores was 88 cm. The shortest core of 61 cm was retrieved from Waihi Beach at the surf club in the mid tide zone. The longest core at 1.44 m came from Harrison's Cut on Papamoa Beach from the low tide zone. The standard deviation for core length was 21 cm.

Every core was affected by compaction from the settling of sand grains caused by vibration during viborcoring. Compaction was measured as the difference between beach height to the surface of the core, before the core was extracted from the beach profile, plus core length and given as both a percentage of total core length, as well as the measured depth to the core surface.

Compaction is thought to occur in the top most surface portion of the beach where the sediment is regularly activated and aerated by hydrodynamic processes. This affects chemistry sub sample sizing where 20 cm increments of each core to a depth of 40 cm were analysed for PAHs with regards to the *Rena* fingerprint. The compaction affect not only makes the actual depth of oil in the environment in the

20 cm sub samples difficult to determine but it also means that in some cases, chemistry analysis went much deeper than 40 cm.

Maximum compaction occurred at Maketu Estuary in core 1 at 74 cm (53.24%) where the sediment compacted over half the length of the core retrieved. Minimum compaction was at Waihi Surf club with only 2 cm (3.17%) compaction in the mid tide core. In average of 30 cm (25.42 %) compaction with a standard deviation of 18 cm was recorded.

There was no trend in length of cores or compaction with regards to beach location. However, the most compacted sites tended to be in lower energy environments with high water tables. This was seen in the two Maketu Estuary cores and the Centre Bank core.
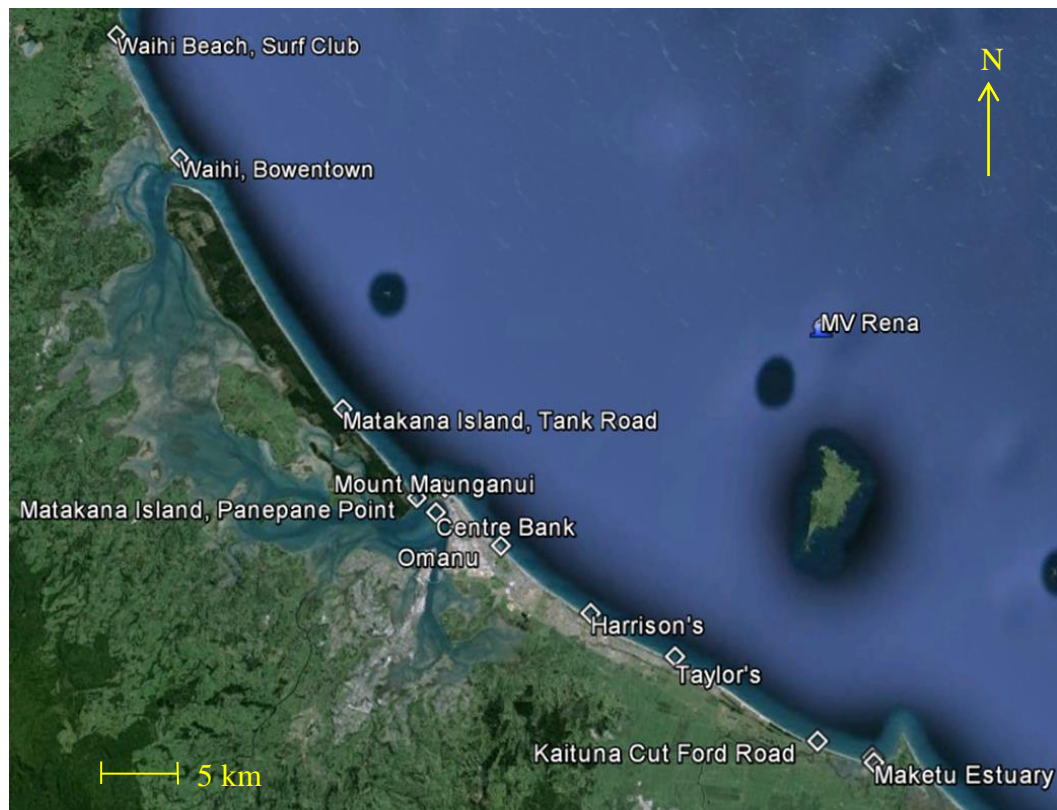
Figure 3.7: Map of the Bay of Plenty Region illustrating the 12 locations where 26 cores were retrieved during the summer of 2012/13, a year after the *Rena* grounded in October 2011.

3.3.2 LASER SIZING RESULTS

Samples were taken in 5 cm increments throughout the length of each core and processed utilising the University's Malvern Particle Laser Sizer for grain size analysis. The methodology is described in the previous section and the results are given in Appendix II.

There are conflicting results in previous research on grain size and PAH concentrations. Viñas, et al., (2010) determined that finer clay size sediments contained higher concentrations of PAHs than larger particles. In contrast, Boston Harbour sediment results concluded that larger grain sizes of > 250 μm contained a greater fraction of PAHs then the three smaller size fractions of < 62, 62-125, and 125-250 μm (Wang, et al., 2001). However, it is agreed that once oil is bound to particles, flocculation and sedimentation occur, making PAHs more susceptible to photolysis (Moore & Ramamoorthy, 1984).

Utilising the Wentworth Scale for grain size analysis, all of the 26 cores are predictably comprised of a substantial proportion of sand sized sediment (Table 3.2). Mean grain sizes ranged from 150 μm (fine sand) to 939 μm (coarse sand). Overall, no strong trends were evident in the depth profile of the cores.

Table 3.2: Summary of grain size analysis from the 26 cores retrieved for this study. Wright and Short (1984) beach classification is also given.

Site	location	Core length (m)	Mean grain size range (μm)	Grain size standard deviation (μm)	Wentworth Scale size class for the mean grain size (After Wentworth, 1922)	Estimated beach classification (Wright & Short, 1984)
1	Waihi- Surf club mid	0.61	234 –466	95 – 291	Fine-medium SAND	Intermediate/ dissipative
1	Waihi- Surf club high	0.65	230 –300	85 - 132	Fine-medium SAND	Intermediate/ dissipative
2	Waihi- Bowentown mid	1.02	298 - 428	99 - 174	Medium SAND	Intermediate/ dissipative
2	Waihi- Bowentown high	1.14	272 - 473	78 - 224	Medium SAND	Intermediate/ dissipative
3	Matakana Tank Rd mid	0.9	360 - 541	114 - 236	Medium-coarse SAND	Intermediate
3	Matakana	0.69	395 - 602	152 - 252	Medium-coarse	Intermediate

					SAND	
	Tank Rd high				SAND	
4	Matakana Panepane mid	1	560 - 731	188 - 286	Coarse SAND	Intermediate/ spit
4	Matakana Panepane high	0.84	402 - 607	149- 283	Medium-coarse SAND	Intermediate/ spit
5	Centre Bank	0.71	150-736	135 - 425	Fine-coarse SAND	Bank
6	Mt Maunganui low	0.72	299- 638	143 - 415	Medium- coarse SAND	Intermediate
6	Mt Maunganui mid	0.76	591 - 955	324 - 390	Coarse- very coarse SAND	Intermediate
6	Mt Maunganui high	0.82	546 - 780	206 - 344	Coarse SAND	Intermediate
7	Omanu mid	0.87	371 - 549	153 - 281	Medium-coarse SAND	Intermediate
7	Omanu high	1.21	294 - 406	96 - 172	Medium SAND	Intermediate
8	Harrison's low	1.43	341- 648	146 - 319	Medium-coarse SAND	Intermediate
8	Harrison's mid	1.2	389 -801	148 – 453	Medium-coarse SAND	Intermediate
8	Harrison's high	1.14	303– 603	109 – 445	Medium-coarse SAND	Intermediate
9	Taylor's low	0.84	460 - 886	285– 409	Medium-coarse SAND	Intermediate
9	Taylor's mid	0.64	413 - 691	187 - 383	Medium-coarse SAND	Intermediate
9	Taylor's high	0.86	426 - 622	183 - 317	Medium- coarse SAND	Intermediate
10	Maketu Ford Rd-mid	0.82	680 - 939	251 - 346	Coarse SAND	Intermediate
10	Maketu Ford Rd-high	0.69	424 - 728	203 - 362	Medium-coarse SAND	Intermediate
11	Maketu Spit mid	0.95	314 - 741	130 - 367	Medium-coarse SAND	Intermediate
11	Maketu Spit high	0.9	310 - 686	117 - 341	Medium-coarse SAND	Intermediate
12	Maketu Estuary 1	0.65	249 - 704	129 - 402	Fine-coarse SAND	Estuary
12	Maketu Estuary 2	0.71	244 - 817	126 - 480	Fine- coarse SAND	Estuary
		Mean	368 - 657	155 - 328		
		Min.	150	78		
		Max.	955	480		

The smallest grain sizes were found in the lower energy environments from the Centre Bank core, and two cores from Maketu Estuary (refer to Table 3.1 for GPS locations). These three sediment cores were comprised of minor amounts of silt and clay fractions at certain depths. However, their mean grain size still ranged from fine to coarse sand giving them some of the largest standard deviations amongst all of the cores (up to 480 µm). Centre Bank had the smallest mean grain size with a range of 150 µm to 736 µm (standard deviation of 135-425 µm).

The cores that were taken from beaches with a slightly steeper profile and closer to a sediment source contained coarser grains. All three of the Mt Maunganui cores were largely coarse grained. However, the largest mean grain size was present in the mid tide core ranging from coarse (591 µm) very coarse sand (955 µm) SD 324 - 390 µm. The Ford Road mid tide core at Kaituna Cut contained a narrower range of coarse grains similar to the Mt Maunganui mid tide core.

The Waihi Surf Club high tide core contained the most uniform grain size of all of the cores, with a standard deviation of only 85-132 µm consisting of fine to medium size sand grains. Bowentown mid tide and Omanu high tide, comprising of medium sands also showed reasonably consistent grain sizes throughout each core, with standard deviations of 99-174 µm and 96-172 µm respectively. Tank Road high tide also indicated a reasonably uniform grain size with a standard deviation of 152-252 µm and mean grain size results ranged in the medium to coarse sand on the Wentworth Scale.

Most cores show no trends with depth, fluctuating every 5 cm from coarser to finer grain sizes throughout. However, Mt Maunganui mid tide core (70 cm) has a well-defined trend of increasing grain size with depth. Both Panepane Point and Taylor's Beach mid tide, as well as Maketu Spit high tide, and Maketu Estuary 2 cores also show grain size increasing with depth yet, not as distinct as the Mt Maunganui mid tide core. No cores display a defined trend of decreasing in grain size with depth. However, some cores generally decrease in grain size with depth such as Harrison's Cut low tide, mid tide cores at Omanu Surf Club, and Ford Road.

Generally, grain size displayed no common trends amongst the cores in relationship to depth, with some cores coarsening and others fining in grain size with depth. Most cores showed no trend, though commonly the grain size change was gradual with progressive increases and/or decreases throughout the cores. Due to the large variation in grain size in each sample, there are no statistically significant trends in the results.

3.3.2.1 GRAIN SIZE AND GRAIN COMPOSITION TRENDS

Grain composition was visually determined and described in the core logs which are provided in Appendix I. From the visual analysis on the cores some conclusions were made on grain size composition.

The grain size is commonly coarser, in sections where shell hash or large shell fragments dominate, For example, the three Mt Maunganui cores have sections of up to 50 % shell hash and/or shell fragments (most of which was sieved out before lazer sizing as they exceeded the size limit of 2 mm) and showed the largest grain size overall. Shells were more abundant within the cores that were taken from high energy environments.

Titanomagnetite placer deposits were easily determined due to the black colour of mineral contrasting the paler colours of quartz dominated sand. Titanomagnetite is mainly comprised of magnetite generally a finer grained deposit. Due to its density, titanomagnetite needs higher energy environment for transportation and therefore, forms as a placer deposit. Bands of titanomagnetite within the cores did not vary greatly in grain size in relationship to the surrounding sand grains. Sand and titanomagnetite seemed homogenous in size with smooth transitions between titanomagnetite bands and the paler, more quartz dominated sands.

3.3.1 CHEMISTRY RESULTS

There are three sets of chemistry results obtained using two separate GC/MS instruments. The methods used are outlined in the previous section (3.2.3) All 26 cores were divided into 20 cm batches to a depth of 40 cm utilising one half of the core resulting in 52 samples. These samples are the key chemistry results given in Appendix III. The 52 samples retrieved from the beach sediment cores in this

study, were run through the GC/MS to compare the results to the previously determined *Rena* oil PAH fingerprint.

A further selected 18 samples were taken using the remaining half of the cores also to 40 cm depth based on the abundance of PAHs present from the first analysis and were analysed by Hills Laboratories using a quantitative method (Appendix IV). A final set of results are given in Appendix V are from the original analysis, where it was later discovered that the GC/MS may have been affected by a column blockage. The elutriates of these samples were re-analysed and are used as the key results in Appendix III.

3.3.1.1 QUALITATIVE ANALYSIS

The selected ion chromatograms of Appendix III are summarised in Table 3.3.

Table 3.3: Summary table of Appendix III qualitative chemistry results showing possible PAHs found during GC/MS analysis in selected ion chromatograms.

#	Location/depth	Sample date	Analysis date	Possible PAHs
1	Waihi- Surf club mid 0-20 cm	10/01/2013	09/07/2013	pyrene 202, phenanthrene 178
2	Waihi- Surf club mid 20-40 cm	10/01/2013	08/07/2013	pyrene 202, phenanthrene 178
3	Waihi- Surf club high 0-20 cm	10/01/2013	27/08/2013	No PAHs
4	Waihi- Surf club high 20-40 cm	10/01/2013	27/08/2013	No PAHs
5	Waihi- Bowentown mid 0-20 cm	10/01/2013	09/07/2013	pyrene 202, phenanthrene 178 and benz(a)anthracene/ chrysene 228.
6	Waihi- Bowentown mid 20-40 cm	10/01/2013	16/08/2013	No PAHs
7	Waihi-Bowentown high 0-20 cm	10/01/2013	27/08/2013	No PAHs
8	Waihi- Bowentown high 20-40 cm	10/01/2013	27/08/2013	No PAHs
9	Matakana Tank Rd mid 0-20 cm	26/01/2013	09/07/2013	pyrene 202, phenanthrene 178
10	Matakana Tank Rd mid 20-40 cm	26/01/2013	08/07/2013	pyrene 202, phenanthrene 178
11	Matakana Tank Rd high 0-20 cm	26/01/2013	16/08/2013	No PAHs
12	Matakana Tank Rd high 20-40 cm	26/01/2013	27/08/2013	No PAHs
13	Matakana Panepane mid 0-20 cm	26/01/2013	16/08/2013	No PAHs
14	Matakana Panepane mid 20-40 cm	26/01/2013	08/07/2013	phenanthrene 178
15	Matakana Panepane high	26/01/2013	27/08/2013	No PAHs

	0-20 cm			
16	Matakana Panepane high 20-40 cm	26/01/2013	27/08/2013	No PAHs
17	Centre Bank 0-20 cm	12/12/2012	27/08/2013	No PAHs
18	Centre Bank 20-40 cm	12/12/2012	27/08/2013	No PAHs
19	Mt Maunganui low 0-20 cm	6/12/2012	28/06/2013	phenanthrene 178
20	Mt Maunganui low 20-40 cm	6/12/2012	28/06/2013	pyrene 202, phenanthrene 178 and benz(a)anthracene/ chrysene 228
21	Mt Maunganui mid 0-20 cm	6/12/2012	11/07/2013	phenanthrene 178
22	Mt Maunganui mid 20-40 cm	6/12/2012	28/06/2013	No PAHs
23	Mt Maunganui high 0-20 cm	6/12/2012	28/06/2013	phenanthrene 178
24	Mt Maunganui high 20-40 cm	6/12/2012	28/06/2013	phenanthrene 178
25	Omanu mid 0-20 cm	7/12/2012	16/08/2013	phenanthrene 178 and pyrene 202
26	Omanu mid 20-40 cm	7/12/2012	16/08/2013	phenanthrene 178 and pyrene 202
27	Omanu high 0-20 cm	7/12/2012	27/08/2013	phenanthrene 178 and pyrene 202
28	Omanu high 20-40 cm	7/12/2012	27/08/2013	No PAHs
29	Harrison's Cut low 0-20 cm	3/12/2012	16/08/2013	No PAHs
30	Harrison's Cut low 20-40 cm	3/12/2012	03/06/2013	pyrene 202, phenanthrene 178, benz(a)anthracene/ chrysene 228
31	Harrison's Cut mid 0-20 cm	3/12/2012	03/06/2013	pyrene 202 and phenanthrene 178
32	Harrison's Cut mid 20-40 cm	3/12/2012	03/06/2013	pyrene 202 and phenanthrene 178
33	Harrison's Cut high 0-20 cm	3/12/2012	04/06/2013	pyrene 202 and phenanthrene 178
34	Harrison's Cut high 20-40 cm	3/12/2012	04/06/2013	pyrene 202
35	Taylor's Reserve low 0-20 cm	4/12/2012	03/06/2013	pyrene 202, phenanthrene 178 and benz(a)anthracene/ chrysene 228
36	Taylor's Reserve low 20-40 cm	4/12/2012	03/06/2013	pyrene 202 and phenanthrene 178
37	Taylor's Reserve mid 0-20 cm	4/12/2012	04/06/2013	pyrene 202 and phenanthrene 178
38	Taylor's Reserve mid 20-40 cm	4/12/2012	04/06/2013	pyrene 202
39	Taylor's Reserve high 0-20 cm	7/12/2012	16/08/2013	No PAHs
40	Taylor's Reserve high 20-40 cm	7/12/2012	04/06/2013	pyrene 202 and phenanthrene 178
41	Kaituna Cut- Ford Rd mid 0-20 cm	24/01/2013	11/07/2013	phenanthrene 178

42	Kaituna Cut-Ford Rd mid 20-40 cm	24/01/2013	11/07/2013	phenanthrene 178
43	Kaituna Cut-Ford Rd high 0-20 cm	8/01/2013	11/07/2013	pyrene 202
44	Kaituna Cut-Ford Rd high 20-40 cm	8/01/2013	11/07/2013	pyrene 202
45	Maketu Spit mid 0-20 cm	6/12/2012	08/07/2013	phenanthrene 178
46	Maketu Spit mid 20-40 cm	6/12/2012	09/07/2013	pyrene 202, phenanthrene 178 and benz(a)anthracene/ chrysene 228
47	Maketu Spit high 0-20 cm	6/12/2012	27/08/2013	No PAHs
48	Maketu Spit high 20-40 cm	6/12/2012	27/08/2013	No PAHs
49	Maketu Estuary 1 0-20 cm	8/01/2013	08/07/2013	pyrene 202, phenanthrene 178 and benz(a)anthracene/ chrysene 228
50	Maketu Estuary 1 20-40 cm	8/01/2013	08/07/2013	pyrene 202, phenanthrene 178 and benz(a)anthracene/ chrysene 228
51	Maketu Estuary 2 0-20 cm	8/01/2013	08/07/2013	pyrene 202, phenanthrene 178
52	Maketu Estuary 2 20-40 cm	8/01/2013	08/07/2013	pyrene 202, phenanthrene 178

The qualitative analysis results display that seven samples contain four of the five peaks in the selected ion chromatogram that are present in the *Rena* PAH fingerprint chromatogram, which is most likely due to naphthalene having high volatility and being the first to degrade (Table 3.4).

Table 3.4: locations where 4 of 5 PAHs were present in the sediment samples qualitatively analysed by GC/MS. The four PAHs being: (1) pyrene 202, (2) phenanthrene 178 and (3) benz(a)anthracene 228 (4) and chrysene 228.

location	depth
Waihi- Bowentown mid	0-20 cm
Mt Maunganui low	20-40 cm
Harrison's Cut low	20-40 cm
Taylor's Reserve low	0-20 cm
Maketu Spit mid	20-40 cm
Maketu Estuary 1	0-20 cm
Maketu Estuary 1	20-40 cm

An example of the selected ion chromatogram that was attained for all 52 chemistry samples is given in Figure 3.8. Many of the chromatograms contained peaks at various times and abundances that did not coincide with the key PAHs that characterise the *Rena* fingerprint. For example, a peak was regularly seen at 22-23 minutes (Figure 3.8) which the GC/MS library has fit with cyclic octaatomic sulphur. Sulphur is derived naturally from volcanoes as well as being a common ingredient in fertiliser. Therefore, these peaks that do not distinguish *Rena* PAHs are not considered further in this study.
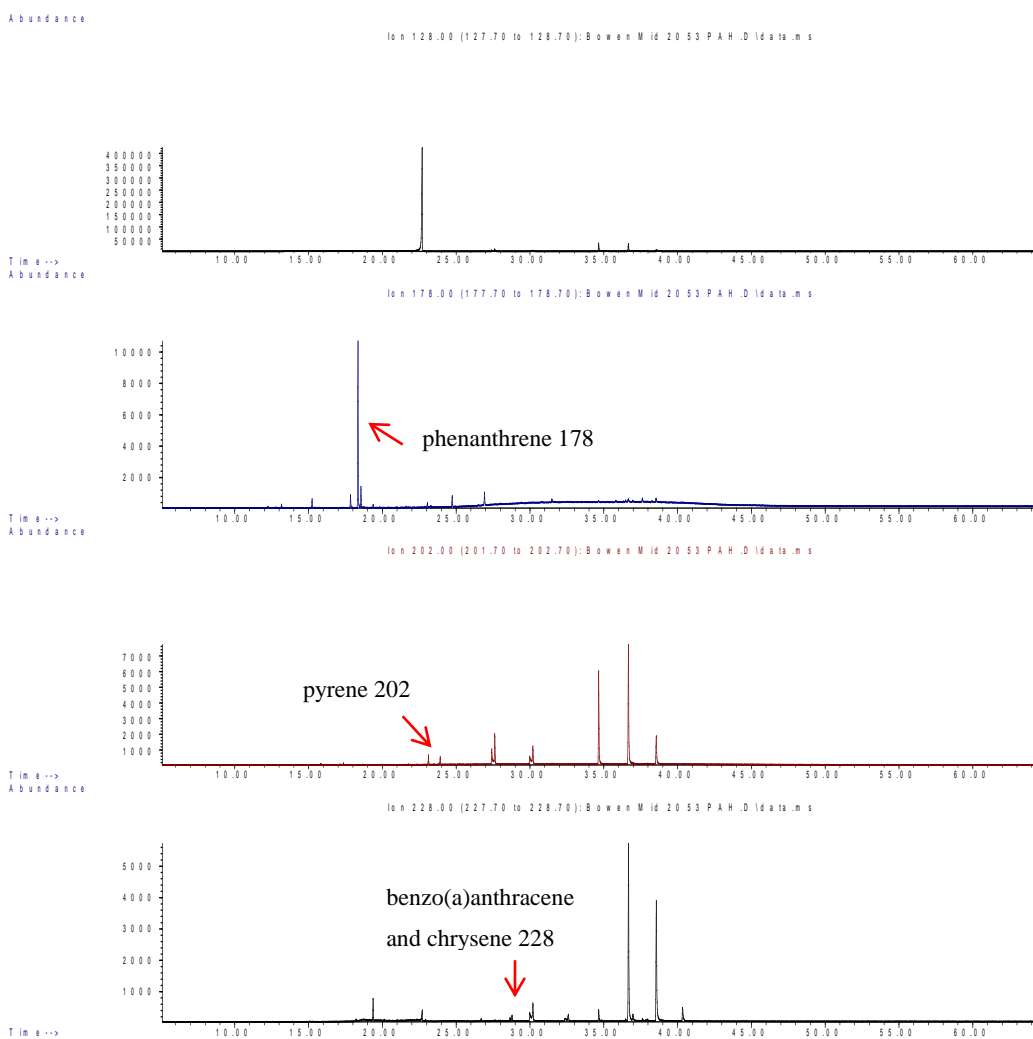
Figure 3.8: Site 2, Bowentown mid tide core for sediment 0-20 cm deep. GC/MS chromatograph results from *Rena* PAH fingerprint analysis for naphthalene 128 (top), phenanthrene 178 (second), pyrene 202 (third) and benzo(a)anthracene and chrysene 228 at the bottom.

Each of the seven samples contain phenanthrene 178, pyrene 202 and benzo(a)anthracene 228 and chrysene 228 peaks. Not only are naphthalene peaks

not present in any of the samples containing the other four relevant PAHs, but naphthalene is not present in any of the 52 samples qualitatively analysed, which is most likely due to naphthalene having high volatility and being the first to degrade.

Four PAHs are present in three of the six low tide samples at varying depths. Three low tide cores were retrieved at three locations along Papamoa Beach in Tauranga (refer to Figure 3.7) with each of these containing pyrene, phenanthrene and benzo(a)anthracene and chrysene at varying depths. Both Harrison's Cut and Mount Maunganui low tide cores contain the four PAHs at 20-40 cm deep. Taylor's Reserve low 20-40 cm is comprised of only pyrene and phenanthrene but, at the surface to 20 cm depth, the sample contains four the PAHs characterising the *Rena* fingerprint. Harrison's Cut mid and high tide cores have pyrene and phenanthrene present throughout. However there are no PAHs detected in the 20-40 cm low tide sample.

Two cores were retrieved from Maketu Estuary totalling in four sediment samples for chemistry analysis. The Estuary 1 core was located approximately 100 m further into the estuary than the Estuary 2 core. The two samples from Estuary 1 both contained pyrene, phenanthrene and benzo(a)anthracene/chrysene, whereas, the Estuary 2 samples only consists of pyrene and phenanthrene hydrocarbons. Maketu Spit mid in the 20-40 cm sediment sample consists of the four PAHs of interest. However, only phenanthrene is present in the shallower 0-20 cm sample at this site and, the high tide core at Maketu Spit does not contain any PAHs of concern.

The last of the seven samples that contain pyrene, phenanthrene and benzo(a)anthracene/chrysene is from Waihi at Bowentown, in the mid tide core, 0-20 cm deep. However, none of the two Bowentown high tide samples or the deeper mid tide sample (20-40 cm) contains any relevant PAHs. On the opposite side of Waihi Beach near the surf club, only the mid tide core consists of both pyrene and phenanthrene throughout, but no hydrocarbons are detected in the high tide core samples.

66

On Matakana Island, four cores were retrieved. No relevant hydrocarbons were identified in either the Panepane Point or the Tank Road high tide cores. Tank Road mid tide core contains phenanthrene and pyrene throughout the two samples, and a phenanthrene peak is evident in the Panepane Point mid tide core at 20-40 cm and Tank Road.

A total of 18 samples do not contain any PAHs that match with the *Rena* fingerprint (Table 3.5). Among these is Centre Bank, the only site where a single core was obtained and also the only site within Tauranga Harbour. 12 of these samples were located in the high tide zone, two samples are from the mid tide and only one in the low tide intertidal zone.

Table 3.5: The samples that do not contain PAHs from qualitative GC/MS analysis.

location	depth
Waihi- Surf club high	0-20 cm
Waihi- Surf club high	20-40 cm
Waihi- Bowentown mid	20-40 cm
Waihi-Bowentown high	0-20 cm
Waihi-Bowentown high	20-40 cm
Matakana Tank Rd high	0-20 cm
Matakana Tank Rd high	20-40 cm
Matakana Panepane mid	0-20 cm
Matakana Panepane high	0-20 cm
Matakana Panepane high	20-40 cm
Centre Bank	0-20 cm
Centre Bank	20-40 cm
Mt Maunganui mid	20-40 cm
Omanu Beach high	20-40 cm
Harrison's Cut low	0-20 cm
Taylor's Reserve high	0-20 cm
Maketu Spit high	0-20 cm
Maketu Spit high	20-40 cm

The remaining 27 samples contain pyrene, phenanthrene or both (Table 3.6). Benzo(a)anthracene/chrysene peaks are not present in any of the 20 high tide samples. In the three Mount Maunganui cores (high, mid and low), phenanthrene is the only hydrocarbon present in any of the surface samples (0-20 cm) or the 20-40 cm high tide sample. The mid tide sample at (20-40 cm) did not contain any PAHs and the low tide 20-40 cm sample was one of the seven that displays peaks for pyrene, phenanthrene and benz(a)anthracene and chrysene. Pyrene and

67

phenanthrene peaks appear in three of the four samples taken at Omanu Beach; the Omanu high tide 20-40 cm sample is void of any relevant PAHs.

At Kaituna Cut near Maketu the Ford Road mid tide core has only pyrene present throughout and the high tide core contains only phenanthrene.

Table 3.6: Samples from quantitative GC/MS analysis containing pyrene, phenanthrene or both.

location	depth	pyrene	phenanthrene
Waihi- Surf club mid	0-20 cm	yes	yes
Waihi- Surf club mid	20-40 cm	yes	yes
Matakana Tank Rd mid	0-20 cm	yes	yes
Matakana Tank Rd mid	20-40 cm	yes	yes
Matakana Panepane mid	20-40 cm		yes
Mt Maunganui low	0-20 cm		yes
Mt Maunganui mid	0-20 cm		yes
Mt Maunganui high	0-20 cm		yes
Mt Maunganui high	20-40 cm		yes
Harrison's Cut mid	0-20 cm	yes	yes
Harrison's Cut mid	20-40 cm	yes	yes
Harrison's Cut high	0-20 cm	yes	yes
Harrison's Cut high	20-40 cm	yes	yes
Omanu mid	0-20 cm	yes	yes
Omanu mid	20-40 cm	yes	yes
Omanu high	0-20 cm	yes	yes
Taylor's Reserve low	20-40 cm	yes	yes
Taylor's Reserve mid	0-20 cm	yes	yes
Taylor's Reserve mid	20-40 cm	yes	
Taylor's Reserve high	20-40 cm	yes	yes
Kaituna Cut Ford Rd mid	0-20 cm		yes
Kaituna Cut Ford Rd mid	20-40 cm		yes
Kaituna Cut Ford Rd high	0-20 cm	yes	
Kaituna Cut Ford Rd high	20-40 cm	yes	
Maketu Spit mid	0-20 cm		yes
Maketu Estuary 2	0-20 cm	yes	yes
Maketu Estuary 2	20-40 cm	yes	yes

There did not seem to be a pattern in the amount of oiling and PAH detection. The main beach from Mount Maunganui to northwest of Kaituna Cut (refer to Figure

1.1) received the heaviest oiling status. A total of 11 cores were taken from the main beach area, giving a total of 22 subsamples. Three of the six low tide samples contained four fingerprinted PAHs. 15 samples contained phenanthrene, pyrene or both with no PAHs detected in the remaining four samples.

50 % of the low tide samples and 10 % in the mid tide consisted of 4 out of 5 PAHs.

The mid tide samples displayed less consistency. 15 of the total 20 mid tide samples contained phenanthrene and/ or pyrene, three samples did not contain any PAHs and two contained phenanthrene, pyrene, benzo(a)anthracene and chrysene. Phenanthrene was the most commonly occurring PAH in the mid tide samples (16 out of 20). When looking solely at the mid tide samples taken at the Main beach between Mt Maunganui and Taylor's reserve all but one of the eight samples contained phenanthrene and/ or pyrene but, no other selected PAHs.

52 samples were analysed by GC/MS using a qualitative method, seven samples contain four PAHs that characterise the *Rena* fingerprint, those being pyrene, phenanthrene and benzo(a)anthracene and chrysene. Three of these samples were obtained from the low tide zone on the main beach at Tauranga at different locations, two samples came from the same core retrieved from Maketu Estuary, one from the mid tide zone at Maketu Spit and the last from Waihi at Bowentown, also in the mid tide core. 18 samples analysed do not contain any selected PAHs of which 12 samples came from the high tide zone at various beaches. The final 27 samples consist of a variation of the hydrocarbons; pyrene and phenanthrene. An obvious trend is not visible with regards to depth and hydrocarbon presence. The depth to which relevant PAHs are located or absent varies at each location.

3.3.1.2 QUANTITATIVE ANALYSIS

The results of 18 samples analysed by Hill's Laboratories using quantitative method of 16 priority EPA PAHs are given in Appendix IV. The samples included (1) 5 of the 7 samples that showed pyrene, phenanthrene and benzo(a)anthracene and chrysene peaks in the qualitative analysis and, (2) 13 samples thought to be affected by a GC column blockage. These 13 samples were quantitatively analysed in order to ensure that reliable results were achieved.

The other side of the stored core was used to obtain the 20 cm samples of sediment and analysed on the 26th of August, 2013, 9-10 months after the cores were retrieved from their respective locations.

Omanu high tide 0-20 cm sample was the only sample that contained above detection levels of PAHs in the quantitative analysis. Minor amounts of phenanthrene (0.008 mg/kg dry wt.) and 0.002 mg/kg dry wt. of pyrene were present as well as acenaphthene and fluorine.

3.3.2 SHEAR STRENGTH RESULTS

Shear strength using a hand held shear vane was taken at all core locations except Matakana Island at Panepane Point. A summary of the shear vane results is given in Table 3.7.

Table 3.7: Shear strength summary statistics from hand held shear vane field records taken during vibrocoring around the Bay of Plenty, 2012/2013.

Location	date	WGS 1984 GPS co-ordinates	mean shear vane (kPa)	Minimum shear vane (kPa)	Maximum shear vane (kPa)	standard deviation (kPa)
Waihi- Surf club mid	10/01/2013	S 37 23.749 E 175 56.297	135	117	159	10.1
Waihi- Surf club high	10/01/2013	S 37 23.747 E 175 56.326	150.6	133	169	8.3
Waihi- Bowentown mid	10/01/2013	S 37 23.772 E 175 56.336	149.6	113	194	29.4
Waihi- Bowentown high	10/01/2013	S 37 23.783 E 175 56.323	112.6	87	165	31.3
Matakana Tank Rd mid	26/01/2013	S 37 35.546 E 176 06.591	100	84	122	14.2
Matakana Tank Rd high	26/01/2013	S 37 35.554 E 176 06 583	68.2	52	84	12.2
Centre Bank	12/12/2012	S 37 38.583 E176 10.425	80.6	66	107	15.9
Mt Maunganui low	6/12/2012	S 37 37.840 E 176 10.689	36.8	32	45	3.3
Mt Maunganui mid	6/12/2012	S 37 37.844 E 176 10.686	52.8	29	68	15.1

Mt Maunganui high	6/12/2012	S 37 37.510 E 176 10.406	71.2	45	97	15.5
Omanu Beach mid	7/12/2012	S 37 39.508 E 176 12.953	126.8	99	156	13.4
Omanu Beach high	7/12/2012	S 37 39.514 E 176 12.944	127.4	113	144	6.8
Harrison's low	3/12/2012	S 37 39.514 E 176 16.436	26.4	23	34	4.5
Harrison's mid	3/12/2012	S 37 41.416 E 176 16.430	110.8	91	144	26.8
Harrison's high	3/12/2012	S 37 41.442 E 176 16.425	77.0	52	117	25.5
Taylor's low	4/12/2012	S 37 42.371 E 176 19.391	68.2	16	104	37.7
Taylor's mid	4/12/2012	S 37 42.603 E 176 19.636	72.5	62	92	13.4
Taylor's high	7/12/2012	S 37 42.620 E 176 19.653	80.25	55	130	33.7
Maketu Ford Rd-mid	24/01/2013	S 37 44.860 E 176 24.975	46.2	29	62	13.6
Maketu Ford Rd-high	8/01/2013	S 37 44.866 E 176 24.975	64.8	41	87	20.3
Maketu Spit mid	6/12/2012	S 37 45.263 E 176 26.985	65.6	52	78	11.7
Maketu Spit high	6/12/2012	S 37 45.271 E 176 26.985	70	58	83	11.1
Maketu Estuary 1	8/01/2013	S 37 45.428 E 176 27.088	32.2	26	36	4.5
Maketu Estuary 2	8/01/2013	S 37 45.412 E 176 27.053	19.8	16	22	17.4

The results for the shear strength were not utilised for further research in this study.

3.4   DISCUSSION: *RENA* OIL AND SOFT SEDIMENT COASTS

The grounding of the *MV Rena* resulted in ~350 tonnes of heavy fuel oil being spilled into the ocean and a proportion of this washing up on the nearby shores of the Bay of Plenty region. The disaster prompted a response involving official clean-up crew and some eight thousand volunteers. In order to evaluate the efficacy of the clean-up, as well as the state of the residual oil, an analysis was carried out on short cores retrieved from the sandy beaches around Tauranga one year after the spill.

Heavy fuel oil is lipophilic and mixes more easily with lipids than water, so tends to resist mixing into the water column, and some polycyclic aromatic hydrocarbons (PAHs) in oil are resistant to dissolution by water (NRC, 2003). These characteristics, along with heavy fuel oil's specific gravity, allow for easy transportation of oil spilled into the ocean onto the coast, without significant loss of the PAHs present in the original oil (Sterling, et al., 2003; NOAA, 2013). Oil binds easily to sediments (Refer to Chapter 4) producing tarballs, oil patches and oil coated sand grains at the coast and on the sea floor. All of these forms of oil were observed on the Bay of Plenty coastline for weeks, and even months after the *Rena* spill.

On visual inspection of the cores, no oil was observed indicating that the clean-up and natural weathering of *Rena* oil on the beaches was effective at removing the residual oil left by the response clean-up. In addition to the cores, there was no visible presence of oil observed on or within the beaches during field work.

Qualitative GC/MS analysis on 52 sediment sub-samples taken from the cores down to 40 cm depth was used determine if some residual oil was dispersed within the sediment at concentrations too low to be visible. Five specific petroleum aromatic hydrocarbons (PAHs) that characterise the *Rena* PAH fingerprint (Wilkins, 2013) were targeted. The presence of all of the five specific PAHs; (1) naphthalene 128, (2) phenanthrene 178, (3) pyrene 202 and (4) benzo(a)anthracene and (5) chrysene 228 were considered an indication of the possible presence of *Rena* oil (Wilkins, 2013). One of the key PAHs, naphthalene

was not detected in all 52 samples. In order to conclude that this indicates that total absence of *Rena* oil, it is necessary to consider the impacts of degradation on the *Rena* PAH fingerprint.

Wilkins' (2013) analysis of tarballs collected only a few days after the initial spill, from the same Tauranga beaches showed that, although there was great variation in the presence of the more volatile PAHs, there was a loss of naphthalene and in some cases also phenanthrene. Primary degradation is thought to be solely from evaporation (Wilkins, 2013). However, tarballs and oiled sand collected later, about 2-3 months after the initial spill were also analysed and the results showed that degradation of *Rena* oil over 2 months is not solely from evaporation. Processes such as photo-oxidation, and biodegradation may also contribute to denudation of oil from the beach sediments over time (Wilkins, 2013).

In previous oil spill studies, the loss of naphthalene in the marine environment has also occurred in the first few weeks (Wolfe, et al., 1994; Venosa & Zhu, 2003, Nelson et al., 2006). Evaporation removes PAHs in a general order based on molecular weight, evaporating light molecular weight two ring naphthalenes first and then fluorenes, thirdly, phenanthrenes and pyrenes and then, chrysenes (Wang & Stout, 2006). Therefore, the absence of the naphthalene fingerprint PAH is not a sufficient indicator of the absence of *Rena* oil, but it does mean that it is difficult to conclusively demonstrate that any oil present did originate from the *Rena* oil spill.

With this in mind, the remaining four fingerprint PAHs of phenanthrene, pyrene, benzo(a)anthracene and chrysene were detected in seven of the 52 sediment samples that underwent qualitative analysis. Six cores contained the seven fingerprinted samples and were scattered across the various sites, with no obvious relationship to the reported amount of oiling that occurred (Figure 3.9).
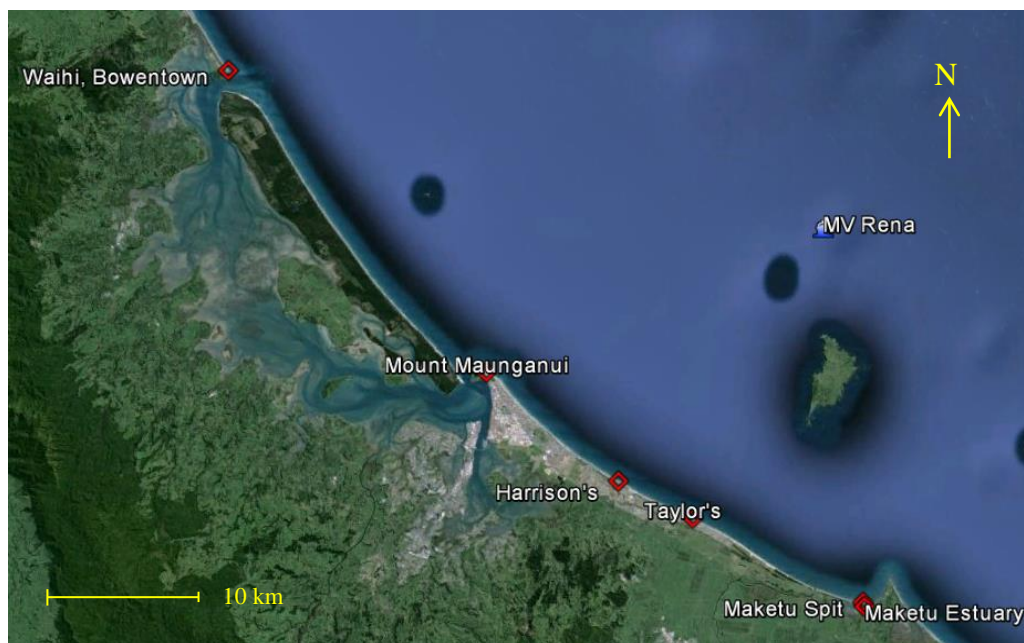
Figure 3.9: The six locations that had sub samples from qualitative analysis containing four of the five PAHs characterising the *Rena*: phenanthrene 178, pyrene 202 and benzo(a)anthracene and chrysene 228.

The dispersed distribution of the most contaminated cores could be due to a number of factors;

- clean up was more effective at certain sites more than others,
- oil had naturally degraded quicker at some locations due to differing physical processes,
- and, core extraction from some locations may have missed the oiled area since surface oiling was not visible during coring field work.

However, the intertidal core location within intertidal zone did appear to influence the presence of fingerprint PAHs. Three of the six contaminated cores came from the low tide along the heaviest oiled area along the main beach (Figure 1.1). The sites include, Mt Maunganui (20-40 cm), Harrison's (20-40 cm) and Taylor's Reserve (0-20 cm) with no low tide core retrieved from Omanu Beach, which is also located at the main beach.

Low tide contamination may be explained by several factors. Firstly, the low tide intertidal zone spends less time exposed to the atmosphere, slowing physical weathering such as photodegradation (Nagata & Kondo, 1977). However, all PAHs vary in sensitivity to photodegradation, with some PAHs being more

resistant than others. Secondly, exposure only during low tide limited clean-up to a smaller time frame than oil in the mid and high tide zones and may also allow for more oiling, which is being transported by the sea. Thirdly, rapid mixing of oil into beach sediment below the surface in the low tide zone may have made residual oil undetectable to the clean-up response crew. Oil and sediment mixing is discussed in more detail in Chapters 4 and 5.

This pattern is reinforced by the high tide samples, of which 60 % (12 of 20) were without PAHs above GC/MS detection levels. The remaining eight of the total high tide samples contained only phenanthrene and/or pyrene.

More variation was seen in the mid tide samples. Three samples contained no PAHs, and two samples contained the four selected PAHs. Phenanthrene was detected in 16 of the 20 (80 %) mid tide samples. Phenanthrene is considered the least soluble PAH in water (Jonkers, et al., 2006) and is more resistant to surf washing and other hydrodynamic processes that may dominate the removal of hydrocarbons from the beach environment.

Pyrene, a four ringed PAH (Figure 3.11), was also a common occurrence in the mid tide samples. Four ring PAHs are less volatile than two ring PAHs such as naphthalene, and are more resistant to biodegradation processes (Venosa & Zhu, 2003; Wolfe et al., 1994). However, some microorganisms target specific PAHs. Marine microbes such as *Vibrio, Pseudoalteromonas, Marinomonas* and *Halomonas* target and utilise phenanthrene and chrysene (Harayama, et al., 2004). Phenanthrene can also be biodegraded by *Cycloclasticus* strains, as well as being able to degrade naphthalene (Harayama, et al., 2004).

Biodegradation by specific microorganisms was not researched in this particular study, as a separate microbial project was planned to examine the cores. This did not occur and, hence, no data are available on microbial effects on *Rena* oil. Therefore, it was not possible to determine biodegradative species and the rate at which biodegradation occurred.

Previous studies agreed that PAH persistence in the environment increases with increasing numbers of benzene rings. Also, as the molecular weight of PAH increases, it becomes less likely to degrade. However, this degradation pattern

was not seen the majority of the samples, instead an altered succession of PAHs was detected in the current study.

Chrysene and benzo(a)anthracene, two four ringed PAHs (Figure 3.11), are the heaviest and most persistent PAHs that were seldom detected in the sediment samples; occurring in only 7 of the 52 samples equivalent to 13 %. Yet, pyrene (four ringed but, lower molecular weight) and more commonly phenanthrene (three ringed) were frequently observed at 48.1 % and 55.8 % of the 52 samples respectively.

Reasons for this anomaly may be due to;

- the detected phenanthrene and pyrene came from another contamination source or sources;
- microorganisms in the Bay of Plenty targeted the other PAHs chrysene and benzo(a)anthracene before phenanthrene and pyrene, (*viz.* Harayama, et al., 2004);
- pyrene and phenanthrene are the most stable of the alkylated phenanthrenes and rate of removal of these PAHs converges when the total mass loss approaches 60 % (Wang & Stout, 2006); and/or
- surf washing was a major contributor in removing oil from the beaches and was more effective at removing chrysene and benz(a)anthracene than the less soluble PAH, phenanthrene (Moore & Ramamoorthy, 1984; Jonkers, et al., 2006).

It could then be inferred that; (1) much of the *Rena* oil was effectively removed from the beach sediment during clean-up, (2) weathering has degraded any residual oil in the year between the spill and sample collection, (3) chrysene and benz(a)anthracene were in such minor abundances that they fell below GC/MS detection levels, or (4) contamination from the *Rena* never occurred at some sites.

Further analysis using Hill's Laboratories quantitative method for 18 sediment samples concluded that PAH levels were below detection levels for 17 of the 18 samples. However, this method is less sensitive than the qualitative analysis.

The Omanu high tide core at 0-20 cm was the only sample that had PAHs above detection levels. These PAHs were phenanthrene, pyrene, acenaphthene, and fluorene which were all detected at very low quantities (at or below 0.008 mg/kg dry wt.). Qualitatively phenanthrene and pyrene were also detected in the Omanu high tide sample.

PAHs can occur both naturally and anthropogenically in the environment (EPA.gov, 2013). The most common PAH sources into the marine environment are dyes, plastics and pesticides, stormwater runoff, recreational motor boats, shipping activities and aerosols from incomplete combustion of fuels such as vehicle exhausts (EPA.gov, 2013).

A report by Park 2009 discussed coastal sediment contamination results from three monitoring programmes in the Bay of Plenty carried out from 2006-2008, three years before the *Rena* spill. The three surveys were: baseline monitoring of contaminants at 31 sites within Tauranga Harbour; an ecological survey with benthic and macrofauna sampling; and a stormwater outfall survey around Tauranga City.

The stormwater outfall survey results show elevated concentrations of PAHs and heavy metals, with fluorene and phenanthrene concentrations (0.037 and 0.28 mg/kg dry weight) exceeding the Australian and New Zealand guidelines for sediment quality (low level - 0.019 and 0.24) (ANZECC, 2000). Sources for phenanthrene and fluorene are commonly coal tar, asphalt and engine exhaust and can be carried into the coastal environment via stormwater pipelines and streams (Park, 2009).

The PAH levels in the 2009 survey were higher than any PAH levels recorded in the current 2012 *Rena* contamination study. The sample sites varied between the two studies although, some of the core sites were situated less than 20 m from stormwater outfalls and stream discharges. These sites are Waihi at the surf club, Omanu, Harrison's Cut, and Maketu at Ford Road (Kaituna Cut). Therefore, contamination of these cores may have come from stormwater runoff from the nearby stormwater outlets (Figure 3.10).
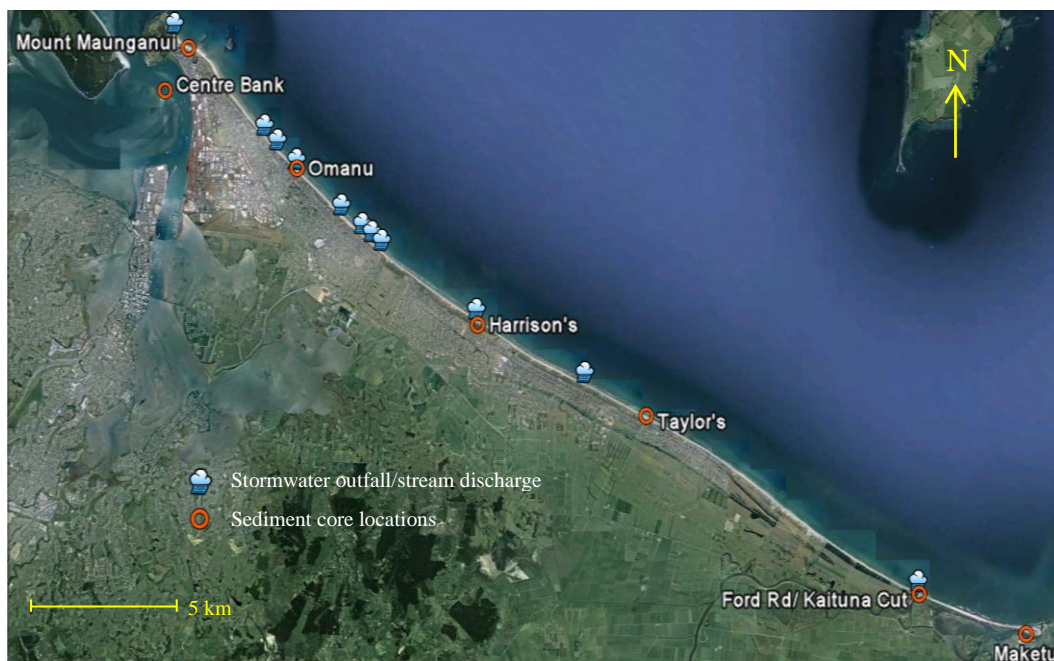
Figure 3.10: Locations along the main beach of Tauranga of stormwater outfalls and stream discharge points in conjunction to sediment core locations utilised for this study.

This study also assessed the depth of mixing that occurs along the beach in the intertidal zone from wave and tidal action (Chapter 5). The depth of disturbance (DoD) was measured during storm conditions in order to determine the maximum depth to which oil may possibly be buried in beach sediments. These data were needed to assess if the coring analysis went deep enough to detect *Rena* oil, and secondly to guide any future clean-up operations. The results from this analysis are discussed in Chapter 5.2.

Papamoa, Omanu, Waihi and Pukehina were the locations for DoD measurements. Although no cores were retrieved at Pukehina Beach since it was not thought to be heavily affected by *Rena* oiling, it was chosen for DoD analysis because it is a relatively steep beach with a slope of 4.9 ° that contrasts with the flatter beaches cored. A steeper beach should increase the depth of sediment disturbance due to plunging and surging waves. The maximum DoD recorded at Pukehina was 28 cm, confirming that chemistry sampling depth to 40 cm would have encompassed *Rena* oil if present.

Large bands of titanomagnetite deposits were present in some of the core samples (Appendix I) at depths between 40 and 80 cm, which are thought to have been

deposited during large storms in the 1970s. Storms of this magnitude have not occurred since the grounding of the *Rena* in 2011. Therefore, it is assumed that the DoD during and subsequent to the *Rena* oil spill did not extend deeper than these thick titanomagnetite placer deposits.

3.4.1 COMPARISON TO PREVIOUS OIL SPILLS

Spills such as the *TSESIS* spill of 1977, the 1988 *Nestucca, Exxon Valdez* of 1989, and *Bouchard* oil spill of 2003 all show similar results in the degradation of low molecular weight naphthalene occurring in the first few months after each spill (Boehm, et al. 1981; Strand, et al., 1992; Wolfe, et al., 1994; Nelson et al., 2006).

The *Bouchard* oil spill showed significant degradation from evaporation and biodegradation of alkanes and PAHs in the first six months (Nelson, et al., 2006).

Furthermore, this study agrees well with the *Exxon Valdez* oil spill results where rates of PAH removal was faster in the upper intertidal (high tide zone) than the lower intertidal (Wolfe, et al., 1994).

Previous contaminated sediment experiments confirm the resistance to weathering of higher ringed PAHs (Figure 3.11) (Wilson & Jones, 1993).

Two ring PAHs (naphthalene) have half-lives of a couple of days, phenanthrene had half-life of just under 5 months. 4+ ringed PAHs such as benzo(a)anthracene and chrysene have half-lives greater than 6 months (Wilson & Jones, 1993). Pyrene can reside in sediments for up to six years (Wolfe, et al., 1994).

Although the lack of naphthalene in the current study's samples is in agreement with previous research, the greater occurrence of phenanthrene than higher ringed PAHs is conflicting, since, the more resistant PAHs benzo(a)anthracene and chrysene are undetected in 45 of the 52 samples. It is likely that the more commonly occurring PAHs phenanthrene and pyrene in beach sediment come from another contamination source such as stormwater runoff and shipping activities, and hence may not indicate the presence of residual *Rena* oil.
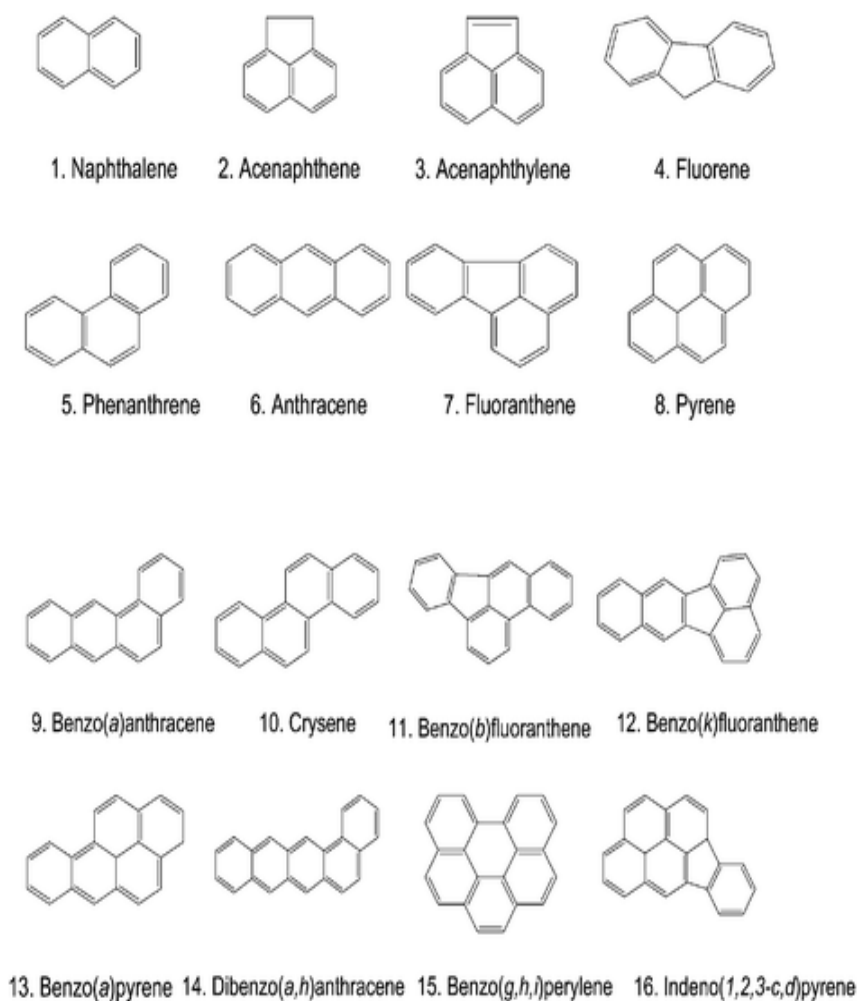
Figure 3.11: The molecular structure of the 16 EPA priority PAHs (Source: Bruzzoniti, et al., 2009).

3.4.2 COMPACTION EFFECTS ON SAMPLES

Although compaction in itself is not a problem, it would have an effect on the chemistry sample volume. The depth to which chemistry sampling occurred was assumed to cover at least 40 cm (2 x 20 cm) within each core. However, due to compaction in 99 % of cores, sediment samples probably encompass more depth than the top 40 cm of the beach profile, and, hence, represent a larger total volume of the undisturbed beach sediment. This affects the results when considering what depth oil may have been mixed to since the 20 cm cut off line between the two sediment samples taken from each core would by no means be exact. Further, the concentrations of PAHs determined by Hills Laboratories are likely to over-estimate the actual concentrations in the undisturbed sediment.

80

Table 3.8 shows effect of compaction on the seven samples that contained phenanthrene, pyrene, benzo(a)anthracene and chrysene. Compaction was less than 30 % for five of the cores.

Table 3.8: The compaction effects on the seven most contaminated sediment samples.

Location	Depth (cm)	Core length (m)	Core compaction (m)	Compaction %
Waihi- Bowentown mid	0-20 cm	1.02	0.165	13.92
Mt Maunganui low	20-40 cm	0.72	0.25	25.77
Harrison's low	20-40 cm	1.43	0.2	12.27
Taylor's low	0-20 cm	0.84	0.3	26.32
Maketu Spit mid	20-40 cm	0.95	0.2	17.39
Maketu Estuary 1	0-20 cm	0.65	0.74	53.24
Maketu Estuary 1	20-40 cm	0.65	0.74	53.24

Maketu Estuary 1 core is the only core that contained the four PAHs in both 20 cm samples and was also most affected by compaction. Compaction was half of the entire core length (53.24 %) so, the 20 cm sediment samples utilised for chemistry analysis may cover an extra 10 cm or more of the beach profile, possibly down to a depth of 60 cm rather than 40 cm.

3.4.3 THE EFFECTS OF SEDIMENT SIZE ON PAH PRESENCE

Previous studies on the relationship between sediment grain size and PAH concentrations have produced contradicting hypotheses, which were compared with the results from this study. Spanish studies by Viñas, et al., (2010) concluded that finer clay size sediments contained a higher fraction of PAHs than larger sediments. In contrast, Boston Harbour sediment results showed that sand grain sizes > 250 μm contained higher PAH concentrations than three smaller size fractions (Wang, et al., 2001).

A study of Otago Harbour sediment studies found elevated levels of PAHs and other contaminants in the fine sediment of the upper harbour, where fine sediment

naturally deposits (Hickey, 2011). Re-suspension of the contaminated fine sediment is thought to transport the sediment to the lower harbour, where it accumulates. PAH contamination sources for the Otago Harbour are similar to those that are present at Tauranga Harbour and include bilge discharges and other shipping operations, as well as industrial run off and stormwater inputs (Hickey, 2011). The results of the study showed slightly higher levels of naphthalene in the silty sand sediment samples compared to the sand samples. However, in 16 of the 18 samples, all other PAHs were below detection levels (Hickey, 2011).

The Centre Bank core was the only sample taken in this study from inside the Tauranga Harbour. Previous monitoring of Tauranga Harbour sediments in 2008, observed high levels of total PAH concentrations in sediment around stormwater impacted sites (Park, 2009). At some locations within the Harbour, PAH levels exceeded the low level sediment quality guidelines of 4 mg/kg dry wt. Centre Bank is a small bank exposed at low tide, bordering the north west side of the dredged shipping channel. The grain size on Centre Bank ranged from fine to coarse sand (150-736 μm). Potential contamination sources of PAHs within the harbour include shipping activities, industrial runoff and stormwater discharges (Park, 2009). Two 20 cm samples obtained from the Centre Bank core were analysed qualitatively and quantitatively for the present study. However, no PAHs were detected during analysis in either of the two 20 cm samples. Due to the close proximity of Centre Bank to the fast flowing shipping channel, contaminated fine sediment may not be able to settle on the channel edge. Although *Rena* oil was observed to have entered the Tauranga Harbour during the initial spill, the volume was considered minor and may not have reached the harbour edges before the ebbing tide transported the suspended oil back out the harbour entrance.

Grain size variation for all cores ranged between an average minimum of 150 μm and a maximum of 955 μm. When looking solely at the six most contaminated cores, grain size varied between averages of 244 μm and 886 μm. Since there was substantial variation in sediment particle size amongst the contaminated cores, it is thought that grain size did not have an effect on *Rena* oil PAH concentrations in sediment.

3.4.4 LIMITATIONS

The production of the heaviest oiling status map (Figure 1.1) produced subsequent to the spill is subjective. Oiling was not measured or quantified, but assessed qualitatively, based on various people's observations.

Core sites were chosen to give a good representation of each beach location since core results are extrapolated over a wider beach area. However, core sediments and chemistry may not be a true representative of the greater environment.

Biodegradation of the PAHs may have also occurred during storage of the cores since there was an eight month period between the initial analysis and the more detailed analysis. The cores were cut in half lengthways, wrapped in aluminium foil (plastic wrap may have caused cross contamination of PAHs) and stored at room temperature in the basement of the University's science block.

CHAPTER FOUR: LABORATORY EXPERIMENTS

4.1 **METHODOLOGY**

Three class A+ 1lt glass mixing cylinders were utilised to carry out settling experiments (Figure 4.1). Beach sand taken from Omanu Beach (294 – 406 μm, medium sand) in Papamoa was used to fill the base of each cylinder to the 150 ml mark. Each cylinder was then topped up with seawater with an average initial temperature of approximately 16°C to the 1 lt mark.
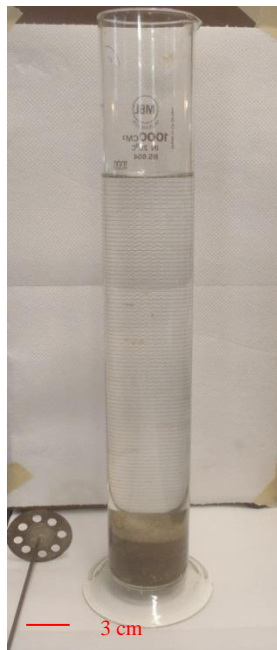
Figure 4.1: The stirrer (bottom left) and settling column used for laboratory experiments.

One cylinder was left 'clean' with no oil added which acted as a control, 10 ml of heavy bunker fuel oil (HBFO 380) was added to the second cylinder and 20 ml of HBFO 380 was added to the third cylinder.

All of the cylinders were mixed vigorously using a metal stirrer to mimic turbulence caused by waves in the intertidal zone. Mixing took approximately 30 seconds to ensure that the entire mixture was amalgamated. From the moment that mixing ceased and the stirrer removed from the columns, settling behaviour

and the time it took for each mixture to settle after mixing had ceased was recorded. The experiment was repeated five times for the various mixtures and averaged.

Photos were taken every 5 seconds after mixing to capture settling velocity and the nature of settling with particular interest in the effects of differing volumes of oil. Both the 10 ml and 20 ml were also visually recorded to allow for repeated viewing giving a more accurate account of settling behaviour.

Samples were taken from each column and placed on glass petri dishes to be examined under an Olympus petrographic microscope. Two samples of approximately 10 ml were taken from each of the following locations; the water surface, top, middle and bottom section of the water column as well as from the sediments at the base of the cylinder using disposable Pasteur pipettes. Magnification was 5 x.

4.2 **RESULTS**

4.2.1 SETTLING FLASK OBSERVATIONS

Settling flask experiments were designed to simulate processes of an oil spill on sandy beaches to gain an understanding of sediment-oil interactions under turbulent conditions caused by waves in the intertidal zone.

Using one litre settling flasks containing sand and seawater and various ratios of heavy bunker fuel oil (HBFO), mixtures were observed during settling for oil behaviour and its effects on total settling velocity of sand in seawater, and the changes in settling behaviour with the addition of 10 ml and 20 ml of oil (resembling heavy oiling). The experiment was repeated five times for each mixture.

The behaviour of a clean control flask without oil was used as a baseline for settling time and behaviour of a non-oiled site to compare to the oiled mixtures. The percentage of settling is not quantified but, solely based on observations.

- After 5 seconds, ~ 30 % of grains settled,

- 10 seconds, ~ 50 % of sand sized grains settled,
- 15 seconds, ~ 75 % of sand sized grains settled (Figure 4.2),
- 20 seconds, ~ 95 % of sand sized grains settled.

The total settling velocity of the sand portion after mixing ceased in the control averaged 23 s (Table 4.1).

Table 4.1: Sand settling velocities for all three settling flask experiments with varying amounts of oil.

experiment	clean sand settling (s)	10 ml HBFO settling (s)	20 ml HBFO settling (s)
1	21.96	23.6	23.33
2	23.17	23.3	24.19
3	23.44	24.77	23.28
4	22.16	24.32	24.6
5	24.25	24.51	25.46
average	23.0	24.1	24.2

The seawater remained cloudy > 4 days after mixing ceased from the minor fraction of clay and impurities present in the sand, which was present as a foam at the surface of the column before mixing.

With the addition of 10 ml and 20 ml of HBFO, the settling times for sand grains were on average one second slower than the control, taking 24 seconds in both mixtures (Table 4.1). Figure 4.3 and Figure 4.4 illustrate the sand settling velocities in the 10 ml and 20 ml mixtures at 15 seconds are almost identical to that of the control (Figure 4.2). However, oil droplets remained suspended after sediment had settled in both the 10 ml and 20 ml oil mixtures.

The two oiled mixtures behaved similar to each other regardless of volume of oil and are discussed collectively.

The mixed oil formed droplets that were almost perfectly spherical. Oil droplet size varied between ~ 5 mm and < 1 mm. To the naked eye, sediment-oil interactions were not detectable. The larger droplets have been described as small tarballs or oil patches in previous literature.

Figure 4.2: the control flask without the addition of oil 15 *s* after mixing had ceased showing ~30 of sediment had settled.

Figure 4.3: The 10 ml HBFO 380 mixture at 15 *s* showing ~ 70% of sediment had settled.

Figure 4.4: The 20 ml HBFO 380 mixture at 15 *s* showing ~70 % of the sediment had settled.

Some droplets settled during the first 30 seconds and settled at various depths within the sediment (Figure 4.5). However, a larger fraction of oil settled on the sediment surface after the sand had settled. Oil droplets were present throughout the entire sediment portion but, more abundant in the upper section towards the sediment-water interface.

After 30 seconds, ~ 85 % of oil settled out of the water column. Movement of the oil droplets slowed considerably as the water column was settling.

After 1 minute, ~ 90 % of oil settled. Droplets smaller than 2 mm would either slowly rise to the surface or sink to the sediment water interface regardless of initial position within the water column. A large proportion of the small oil droplets (< 2 mm in size) that stayed in the water column remained motionless.

After 1 minute and 30 seconds, ~ 95 % of oil settled out of the water column. Movement either up or down the water column of > 2 mm size droplets was very slow. Most of the oil droplets stayed relatively stationary.
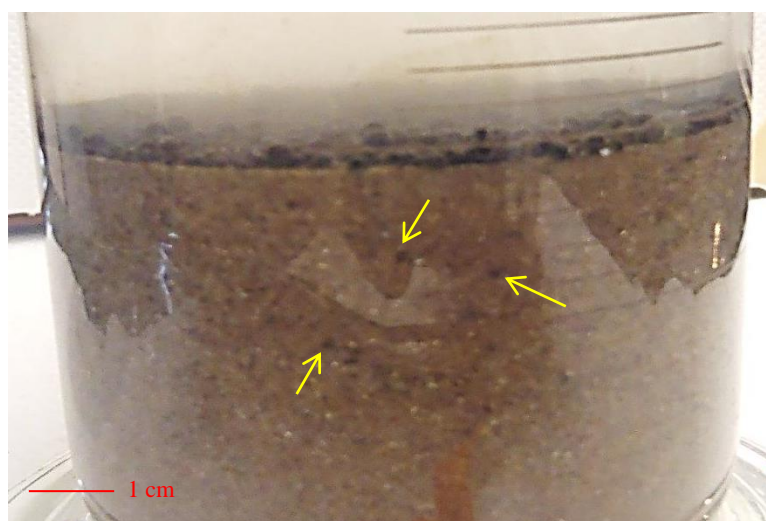
Figure 4.5: the bottom sediments of the settling flask with 10 ml oil added showing an accumulation of oil droplets at the water-sediment interface. A minor portion of droplets are situated in the sediment at depth (arrows).

After 2 minutes, no more settling occurred. The water column was almost stationary. Approximately 5 % of the oil remained suspended as small droplets in the water column.

Total settling for the 10 ml HBFO was on average 126.2 s and 124.6 s for the 20 ml oil mixture (Table 4.2).

Table 4.2: Oil settling velocities in the 10ml and 20 ml oil settling flask experiments.

experiment	10 ml HBFO settling (s)	20 ml HBFO settling (s)
1	121.8	136.8
2	134.4	120
3	121.2	122.4
4	132	121.2
5	121.8	122.4
average	126.2	124.6

The < 2 mm oil droplets still present in the water column stayed suspended. There was very little movement of oil droplets.

Oil droplets in both mixtures were rising and falling at differing speeds although, During settling, a larger proportion of settled oil floated (70 %) to the surface and minor amounts (30 %) sunk to settle at the sediment/water interface. On average

movement of oil was slower than sand settling velocity. The direction to which the oil droplets travelled was regardless of position in the water column and oil droplet size.

Oil droplets situated at the base of the surface oil tended to stay as separate droplets, not binding together (Figure 4.6). Occasionally, these oil droplets that had settled at the surface oil would dislodge and slowly descend through the water column where they came to rest in the bottom sediments (Figure 4.5). The same segregated oil droplets were also present on top of the bottom sediments.

Figure 4.6: The surface portion of oil floating on the seawater surface showing segregated oil droplets situated on the underside.

If the settling flask was disturbed, a large droplet (> 10 mm) would break off from the surface portion of settled oil and sink to the bottom of the water column.

Unlike the control, both the 10 ml and 20 ml HBFO saw the water column clear almost completely within a few days. Although, a minor portion of < 1 mm size oil droplets remained suspended, the water seemed to contain less suspended particles in the two oiled flasks, than the control flask.

4.2.2 MICROSCOPE OBSERVATIONS

Two sub-samples of the settling flask mixtures were taken from five different locations within the flasks and then placed onto petri dishes for viewing under microscope. The sand grains from Omanu Beach used for the settling flask experiments were identified as quartz, feldspars, shell fragments, pumice and volcaniclastics as well as a minor portion of titanomagnetite and other opaques.

Aside from there being a larger proportion of oil present in the 20 ml HBFO380 samples compared to the 10 ml HBFO380 samples, there did not appear to be a difference in sediment and oil particle interaction.

Approximately 70 % of the oil in both 10 ml and 20 ml mixtures floated on the seawater surface. Under compound microscope, the large oil droplets at the surface attracted sediment grains which adhered to the edges (Figure 4.7). Due to the oil's viscosity, the microscopic light was unable to penetrate the oil droplets, and therefore it was difficult to determine if sediment grains were incorporated within the droplets. However, in some microscope images such as Figure 4.8 almost complete amalgamation of some sediment grains on the edges of the oil was observed.

Small round droplets coalesced together; once merged they formed larger spheres. Oil droplets larger than 10 mm did not stay strictly spherical taking on many forms yet, still stayed intact. The non-spherical, larger droplets that contain some sediment are referred to as oil patches in previous experiments (Delvigne, 2002). To a lesser degree, minute air or water bubbles became trapped within oil droplets and exhibited themselves as spherical voids within an oil droplet (Figure 3.7).
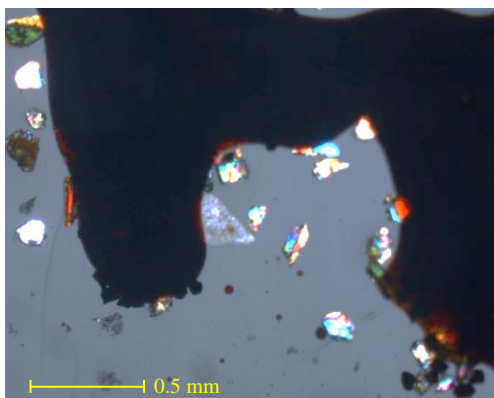
Figure 4.7: Surface section of the settling column showing a large oil patch with sediment grains adhering to the edges.
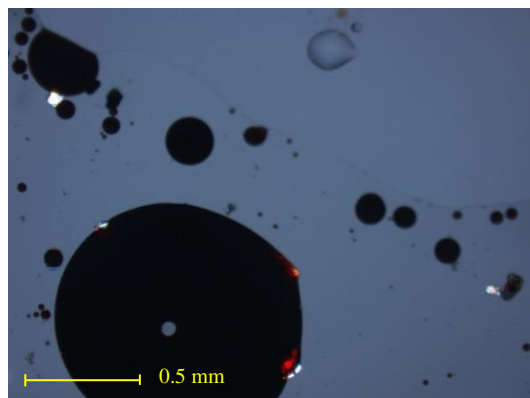
Figure 4.8: Surface section of settling column showing three grains almost completely incorporated into an oil patch. The oil patch contains a small void of possibly air or water in its centre.

Two samples were obtained from three sections within the water column; at the top, middle and bottom where a minor fraction of small oil particles remained

suspended. There was no obvious variation between the three water column samples of differing heights when viewed under microscope (Figure 4.9 and Figure 4.10).

All three locations, as with the surface samples, contained air or water bubbles within the oil droplets. No sediment grains were present within the oil droplets left in suspension in the water column under inspection. The oil droplets appeared to be less viscous in all of the water column samples, taking on a paler brown colour rather than the dark brown to almost black droplets present in the surface section. The samples contained similar sized oil particles suspended within the water column with no pattern present with regards to location within the water column and droplet size.
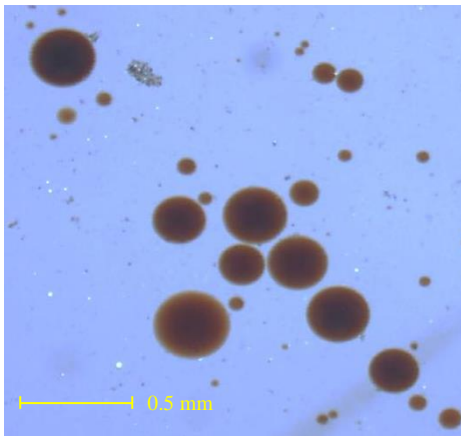
Figure 4.9: The top portion of the water column showing oil droplets of various sizes.
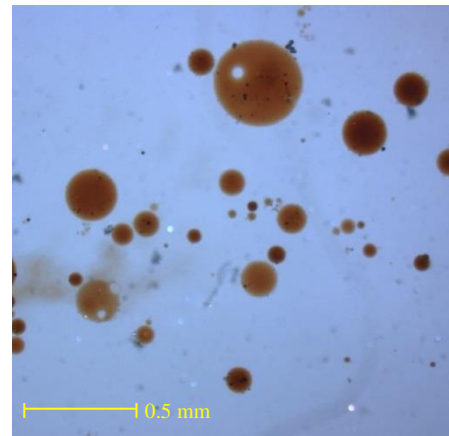
Figure 4.10: The bottom section of the water column showing oil droplets of various sizes.

Some suspended particles are also visible in the microscope images, present as miniscule black marks in Figure 4.9 and Figure 4.10.

The sediment/water interface sub samples under microscope illustrated various oil, seawater and particle interactions.

- Oil droplets stayed spherical irrespective of sediment presence (Figure 4.11).
- Some oil droplets appeared to hover over the sediment rather than adhere to it.
- Oil droplets appeared to be attracted to the seawater edge (Figure 4.12).

91
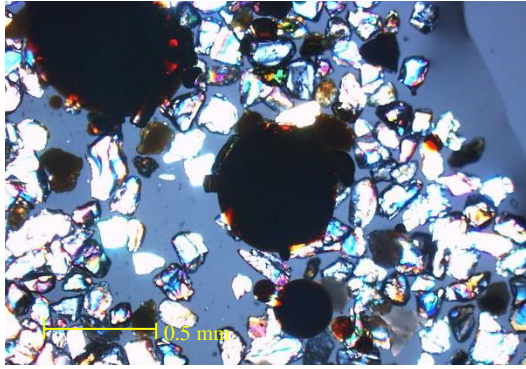
Figure 4.11: The sediment water interface section of the settling flask. Oil droplets, oil patches and sediment.
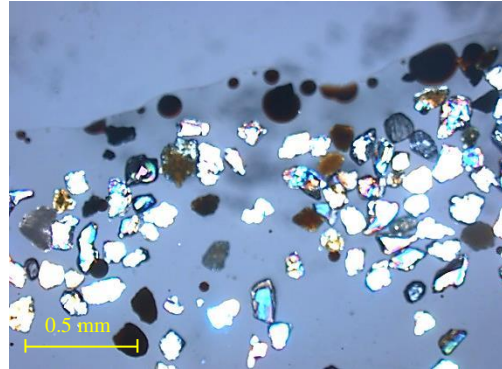
Figure 4.12: The sediment water interface section of the settling flask. Oil droplets and sediment.

4.3 DISCUSSION: SEDIMENT AND OIL INTERACTIONS

The *Rena* disaster raised some questions regarding the effects of oil on Bay of Plenty beach sediment behaviour. Due to effective clean up and natural weathering of oil, oiling effects were not able to be observed in the field during this study, a year after the spill. Therefore, laboratory experiments were carried out to observe settling behaviour of sand and oil mixtures mimicking the turbulence caused by waves in the intertidal zone.

Settling columns consisting of seawater and sand (294-406 μm) collected from the field, and various quantities of heavy bunker fuel oil (HBFO) were mixed. Their settling times and behaviour were observed. The methodology is outlined in 4.1.

Omotoso, et al. (2002) observed that high viscosity oils such as Bunker C slowed down the settling rate of sediment. However, with the addition of oil, sand settling times did not significantly increase in comparison to the control in the present study. The addition of 10 ml and 20 ml HBFO did not greatly alter the sand settling velocities slowing sand settling by 1 s from 23 s to 24 s for both mixtures. However, due to HBFO's specific gravity, oil droplets settled much slower than the sand grains.

Average settling times for oil in the 10 ml mixture was 126.2 s and 124.2 s for the 20 ml mixture. Oil was observed to float, sink or stay suspended in the water

column. About 5 % of the oil stayed suspended in the water column after turbulence had ceased due to the oil droplets having the same density as the surrounding seawater.

The direction in which oil travelled was independent of oil droplet size and initial position in the water column after mixing ceased. The direction of travel was probably determined by the amount of sediment or air bound within the oil droplets and the resulting density of the oil droplet.

Previous studies have determined that oil in the marine environment has a high affinity for suspended solids within water due to its hydrophobic nature (Moore & Ramamoorthy, 1984). Although the sand encompassed in the oil could not be seen with the naked eye, it was viewed under microscope later in the study. Oil droplets that adhered to or encased sand grains sank due to increased density. Sand settling that occurred after oil droplets had sunk, resulted in burial of oil droplets underneath the sediment surface. Oil droplets containing air bubbles floated to the surface.

Some droplets would initially float to the surface and then slowly sink to join the bottom sediments. Initial rising followed by the sinking of oil droplets may be a result of;

- trapped air bubbles within the droplet which burst or escaped allowing the droplet to sink , or,
- turbulent mixing produces vertical currents that cause droplets with almost neutral buoyancy to rise, and once turbulence has ceased the oil droplets are able to sink due to their specific gravity.

Previous studies have focused mainly on smaller sediment sizes of < 2 μm which have proven to readily bind with oil in the coastal environment forming oil mineral aggregates (OMAs). Once oil is bound to a mineral it is more easily transported out of a low energy environment (Lee, 2002). OMA formation is considered to be more prominent in low energy environments such as estuaries where naturally sediment grain size is smaller (Lee, 2002). OMA formation and removal may be partially responsible for the removal of residual oil from the Centre Bank and Maketu Estuary. OMAs are more buoyant than sediment,

therefore are more likely to be removed from the environment by currents and OMAs are more easily degraded by photo-oxidation (Stoffyn-Egli & Lee, 2002).

After four days of settling, the clean appearance of the water column in the oiled flasks in comparison to the cloudy unoiled flask, may also be due to the formation of OMAs by coagulation, sedimentation, flocculation and filtration (Moore & Ramamoorthy, 1984). In the current experiment, the un-oiled settling flask the fine particles within the sand stayed suspended in the water column for over four days and the water remained cloudy during this time. The addition of oil to the settling experiments aided in removing other suspended solids from the water column. Oil and suspended sediments smaller than 2 µm bind together and then settle onto the bottom sediments (Moore & Ramamoorthy, 1984). Both the 10 ml and 20 ml HBFO mixtures cleared within 48 hours after mixing had ceased.

4.3.1 MICROSCOPE OBSERVATIONS

Determining the size and distribution habits of OMAs and oil droplets is of interest for future oil spill response techniques (Ma, et al., 2008). A better understanding of oil in the marine environment at microscopic scale can provide better data for computer modelling helping understand the fate and transport of oil (Ma, et al., 2008). For a better understanding of oil and sediment interactions in the current study, samples were taken throughout the settling period at different locations within the settling flasks for inspection under microscope.

Previous experiments carried out on OMAs found that different forms of oil were a result of oil concentration, oil type, sediment interaction and water salinity (Delvigne et al., 1987: Payne et al., 1989; Delvigne, 2002). As with the experiment carried out by Delvigne, 2002, oil droplets, oil coatings and oil patches were also observed in the current study. Patches are described as larger, non-spherical oilings with some sediment incorporated (Delvigne, 2002). The presence of sediment is thought to be what causes the oil patch to become non-spherical in shape (Delvigne, 2002).

Under the microscope, oil was observed to bind to sediment in the surface and the bottom sediment sections of the settling tube. The addition of sediment increases

the density of the oil droplet enabling it to sink, resulting in more oil coated sediment located in the bottom sediments. Air bubbles incorporated in the oil were only present in the water column and surface samples, confirming that air trapped in oil may increase oil buoyancy.

No sediment was incorporated into the suspended oil droplets within the water column. These droplets were similar in diameter to those in the bottom sediment and the surface sections, but tended to be paler in colour. The suspended droplets are therefore assumed to be thinner making them a similar density to the surrounding seawater, which allows them to stay suspended in the water column.

The *Exxon Valdez* (Table 2.3) spilled 35,500 metric tons of North Slope crude oil into Alaskan waters. As with the current study, research on the *Exxon Valdez* spill concluded that larger oil droplets initially rose to the surface waters and only smaller oil droplets that did not contain sediments remained dispersed within the water column (Wolfe, et al., 1994). However, this oil behaviour was observed at sea, where no particle interaction with sediment occurred.

Over 24 hours, the suspended oil droplets may have adhered to the remaining suspended particles where they bound together, and descended to join the bottom sediments which cleared the water column of suspended particles (Moore & Ramamoorthy, 1984).

Monitoring of sandy beaches in Spain after the *Prestige* oil spill revealed thick layers (>1 m thick) of oil coated sand that was found buried under sand within the beach profile (Bernabeu, et al., 2010). Burial was sometimes up to 3 m below the surface. The burial was largely due to significant sediment accretion of the beach that occurred after the spill. It was thought that tarballs became incorporated into beach sediment and then evolved under the pressure of the sand mass above and water table interactions (Bernabeu, et al., 2006) into oil coated sand grains.

This behaviour was not seen during field work on Bay of Plenty beaches, due to the efficient clean-up and natural removal of residual oil that occurred in the year between the initial spill and field work, resulting in a lack of oil present. However, the oil coated sand grains were observed under microscope during the laboratory

experiments. Further, small tarballs, called oil patches, were observed to be incorporated in bottom sediments in the settling flask experiments.

Laboratory experiments by Bernabeu, et al. (2010) consisted of six sand columns and filtered seawater similar to the current study but, much larger volumes of sediment were used (approximately 20 cm deep). The experiment involved burying tarballs down to 10-12 cm depth and observing them over the course of 130 days at various salinities, and flow rates.

After three weeks, sand surrounding the tarballs was stained a grey colour in 5 of the 6 samples. Staining continued and increased throughout the length of the study (130 days). The remaining column that did not stain the sand surrounding the tarball had constant flow rates. It is therefore assumed that the constant flowing seawater allowed for natural cleaning of the sediment (Bernabeu, et al., 2010).

Although tarballs were observed incorporated into beach sediment by residents in the Bay of Plenty; the staining effects were not observed during the settling experiments due to the shorter time frame that the experiment was conducted under. It is possible that if the sediment and oil mix had been left over some weeks that the same oil staining would have been observed in the oil sediment mix in the bottom sediments of the settling flasks. However, no staining effects were observed in the core samples.

The sediment used in the settling flask experiments was observed to contain siliciclastics, volcaniclastics and bioclastics. Siliciclastics comprised mainly of quartz and feldspars and a minor portion of volcaniclastics such as pumice. Shell fragments made up the majority of the bioclastic portion of the sediment.

A study by Lee (2002) found that quartz bound more readily to low-viscosity oils, whereas, shell fragments had a high affinity for oil regardless of the viscosity. In the present study, oil patches in the bottom sediments seemed to have a high affinity for shell fragments. However, oil patches also incorporated quartz grains (Figure 4.13).
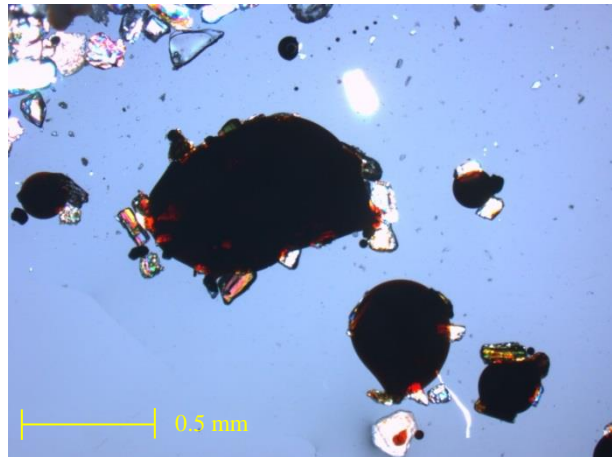
Figure 4.13: the bottom sediments from the 10 ml oil settling flask showing oil patches adhering to sand grains.

Bernabeu, et al. (2006) also found during sampling of Spanish beaches affected by the *Prestige* oil spill (Table 2.3), that oil droplets of similar dimensions to the sand grain size accumulated principally on the layered bioclastic portion of sediment.

It was difficult to determine whether the *Rena* oil patches preferentially adhered to bioclastics over siliciclastics since the proportions were unevenly distributed. Siliciclastics of mainly quartz comprised of approximately 80 % of the total sediment grains. Had there been a higher fraction of shell fragments and other bioclastics, the relationship variations between sediment grains may have been more obvious.

4.3.2 LIMITATIONS

Observations are based on one observer and may be affected by observer bias. A stopwatch was used to record the time therefore, exact times were difficult to obtain.

CHAPTER FIVE: DEPTH OF DISTURBANCE

5.1 **METHODOLOGY**

Four beach locations were chosen to analyse sediment activation depth (Figure 5.3). Six stainless steel rods 1.5 m long, and 10 mm in diameter were placed along two transects at low, mid, high tide locations. The two transects were placed approximately 10-15 metres apart (Figure 5.1). The rods were driven into the beach sediment at a marked 50 cm. A 5 cm^2 lead washer was placed over each of the rods, which settled on the beach sediment surface. The rods were exposed to a full semi diurnal tidal cycle (low tide to low tide) during a storm event with above average significant wave heights. The depth the washer was mixed into the beach sediment was recorded as well as any change in beach elevation using the 50 cm mark on the disturbance rods.

Figure 5.1: Placement of two disturbance depth transects at Pukehina Beach before a storm at low tide.

A Garmin 60CSx handheld GPS was used to record the locations of the rods and a beach profile survey of the intertidal zone was also obtained at each activation depth site using a Nikon DTM-322 Total Station. The survey extended from beginning of the foreshore and to the backshore region of the beach, as illustrated in Figure 5.2. Coordinates were measured approximately every metre (a step

forward) beginning at the low tide zone and moving toward the foredune area. The wave conditions were estimated from wave data presented by Swellmap.co.nz.
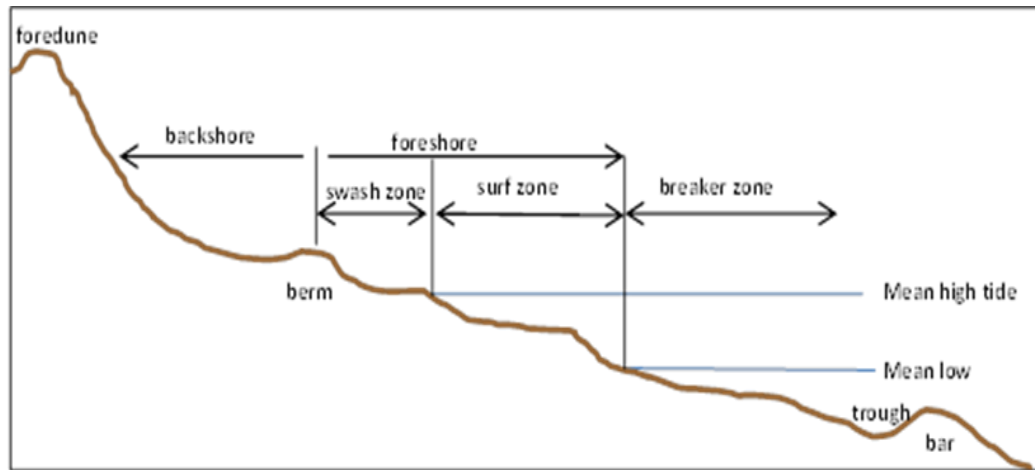
Figure 5.2: A typical beach profile diagram (adapted from fhwa.dot.gov).

5.2 RESULTS

It is thought that the depth of oil burial affects the rate at which oil degrades in the marine environment (Strain, 1986; Wolfe, et al., 1994; Díez, et al., 2007; Gonzalez, et al., 2009; Bernabeu, et al., 2010). Therefore, determining depth to which spilled oil can be mixed into the beach profile is vital to fully understand the fate of oil. Oil burial in the intertidal zone of sandy beaches can be determined by the depth of disturbance (DoD).

Disturbance rods and washers were set in two transects located at high, mid and low tide locations at various beach locations around the Bay of Plenty (Figure 5.3).

The depth to which the washer fitted over the rod was mixed into the sand was recorded as depth of disturbance. Table 5.1 summarises the locations where DoD was obtained as well as the beach profile changes over a semi diurnal tidal cycle.

Figure 5.3: The beach sites for depth of disturbance (DoD) studies carried out during this study.

Table 5.1: Summary of depth of disturbance (DoD) and beach profile changes during a single tidal cycle, taken at various locations around the Bay of Plenty.

location	GPS location	date	transect A	DoD (cm)	profile change (cm)	distance between rods (m)
Papamoa	S 37 41.727	23/05/2013	High A	0	3.5	10
	E 176 17.113		Mid A	10.9	0	
			Low A	6.3	-10	10
			High B	0.4	5	
			Mid B	4.2	0	
			Low B	10.7	6	
Waihi	S 37 23.746	1/06/2013	High A	2.5	0	20
	E 176 56.357		Mid A	8	0	
			Low A	2.5	1	20
			High B	2.7	0	
			Mid B	3.8	0	
			Low B	4.8	1	
Pukehina	S 37 45 37.07 E 176 29 04.05	4/06/2013	High A	4.5	2	10
			Mid A	10	9.5	
			Low A	14.1	3.2	10
			High B	10.7	9	
			Mid B	4.7	0	
			Low B	28.1	4	
Omanu	S 37 39.536	3/08/2013	High A	4	0	17
	E 176 12.970		Mid A	3.7	5.8	
			Low A	6.8	4	23

100

High B	1.8	-2.4
Mid B	6	2.8
Low B	7.6	17.8

The sea and weather conditions during disturbance studies are given in Table 5.2 which was extracted from Swellmap.com on the day of the field experiments. Swellmap.com retrieves its data from a series of wave buoys located around Tauranga and the rest of New Zealand.

Both Pukehina and Omanu disturbance depth data were retrieved during storm conditions. Papamoa and Waihi Beach disturbance depth data was taken during fair-weather conditions. Since Papamoa wind and wave data was also not obtained, the DoD results are not discussed any further.

Table 5.2: Wave and wind data for locations and dates during depth of disturbance data studies. (Source:swellmap.com).

location	date	Swell (m)	Wave (m)	set face (m)	period (s)	swell direction	wind (kts)	gusts (kts)
Waihi	1/06/2013	0	0.1	0.1	16	SW	W:9	12
Pukehina	4/06/2013	1.7	2.6	2.6	12	NE	N/NE:22	27
Omanu	3/08/2013	3	3.6	3.6	11	NE	SE:29	38

The deepest mixing in the intertidal at all three beach sites occurred in the low tide zone regardless of weather conditions. The general trend was then followed by the mid tide and lastly high tide with the shallowest depths recorded.

Full beach slope data and wave conditions were collected at Pukehina and Omanu Beaches and can be compared to results from prior DoD studies. However, beach slope profile was not recorded at Waihi or Papamoa making comparisons with other studies difficult.

Although no cores were retrieved at Pukehina Beach for visual and chemical analysis with regards to *Rena* oiling, the beach was chosen due to its close proximity to the wave buoy and the beach steepness. DoD increases with beach steepness.

Pukehina Beach recorded the greatest DoD overall in the intertidal zone and the waves were approximated to be 2.6 m. Transect A was placed on a ridge and Transect B in a runnel. The low tide rods displayed the greatest DoD. Transect B recorded a DoD of 28.1 cm and Transect A to 14.1 cm deep. The mid tide and high tide DoDs alternated with depth between the two transects (Figure 5.4) varying between 4.5 cm and 10.7 cm.

Omanu Beach had the largest waves during DoD studies, approximated to be 3.6 m breaking wave height (H_{bs} or set face in Table 2.5). Omanu Beach is slightly flatter than Pukehina and also had shallower DoD recorded at low tide transect A as 6.8 cm and transect B as 7.6 cm. mid and high tide DoD varied between 1.8 cm and 6 cm.
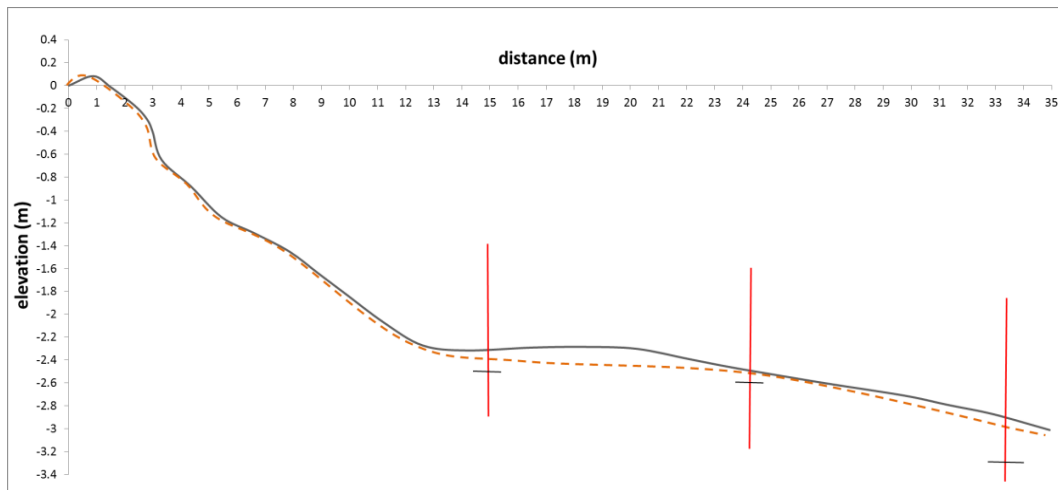
Figure 5.4: The beach profile at Pukehina on June 4th 2013, before the storm (solid black line) and after the storm (dashed orange line) based on results from transect B. Red vertical lines mark the rod position and small black horizontal lines mark the washer location or DoD.

Average beach slope for Pukehina Beach was 4.9°. Using the Wright and Short beach classification system and applying the Dean's Parameter calculation or the Irribarren Number to beach conditions, Pukehina is categorized as an intermediate beach (Table 5.3). Omanu Beach had a gentler slope at 3.2° and was also classified as an intermediate beach with both Dean's parameter and the Irribarren number.

Table 5.3: Wright and Short (1984) beach state based on Dean's Parameter and the Irribarren Number as well as recorded DoD.

	H_{bs} (m)	Tz (s)	Beach slope (˚)	Dean's parameter Ω	Wright & Short (1984) beach state	Irribarren Number	Wright & Short (1984) beach state	Mean activation depth (mm)
Pukehina	2.6	12	4.9	1.83	Intermediate	0.80	Intermediate	120
Omanu	3.6	11	3.2	4.3	Intermediate	0.40	Intermediate	49

Beach slope profiles are very dynamic and can vary over a single tidal cycle. This is illustrated in Figure 5.4 showing Pukehina Beach slope smoothing out after a storm (dashed orange line) in comparison the profile before the storm (solid black line). Similar results in a change in profile were also recorded for Omanu Beach. Omanu Beach has a gentler slope than Pukehina and is illustrated in Figure 5.5.
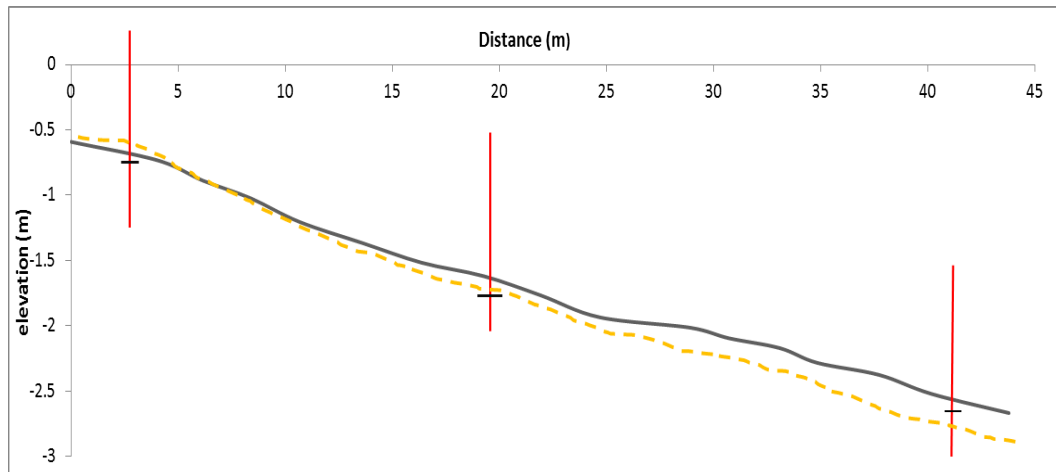
Figure 5.5: The beach profile at Omanu Beach on August the 3rd, 2013, before the storm (solid black line) and after the storm (dashed orange line) based on results from transect B. Red vertical lines mark the rod position and small black horizontal lines mark the washer location or DoD.

A collection of previous DoD results from various studies between 1980 (Greenwood & Hale 1980) and 2005 (Brook, 2010) for various beach states is summarised in Table 2.5. Summary statistics in Table 5.4 show a maximum DoD recorded previously for intermediate beaches using the Irribarren number calculation is at an average of 58 mm. Dean's parameter formula gives a slightly higher DoD for intermediate beaches with an average of 92 mm. Omanu Beach had a recorded mixing depth of 49 mm which is comparative to summary

statistics of previous studies using both Dean's parameter and Irribarren number. Omanu's beach slope of 3.2 ° places it on the flatter end of intermediate beaches closer to a dissipative beach slope.

Pukehina is also classified as an intermediate beach, but, substantially steeper at 4.9 °, which is comparative to a greater mixing depth of an average of 120 mm.

Table 5.4: Previous DoD studies summary statistics for the different Wright and Short (1984) beach states using Dean's Parameter and Irribarren Number.

Dissipative beach	Dean's parameter (Ω)	Activation depth (mm)	Irribarren number (ξ)	DoD (mm)
Average	58.69	31	0.18	29
Maximum	122.70	60	0.33	38
Minimum	8.34	18	0.08	23
Standard deviation	47.89	12	0.10	5
Intermediate Beach Average	2.19	92	0.75	58
Maximum	5.63	160	1.07	103
Minimum	1.10	30	0.38	18
Standard deviation	1.56	40	0.27	29
Reflective Beach Average	0.72	109	1.45	111
Maximum	0.95	220	2.19	220
Minimum	0.54	27	1.16	19
Standard deviation	0.17	72	0.43	71

5.3 DISCUSSION: DEPTH OF DISTURBANCE

Oil reached the shoreline six days after the initial grounding of the *Rena*, and presented itself in various forms depending on oil abundance and shoreline type. The primary spill formed sheets, blanketing entire sections of shoreline. A large proportion of beached oil was removed by means of traditional cleaning techniques described in Chapter 1.1. However, the oil that remained or was

released from the wreck during the storm events that followed was subjected to the action of waves breaking in the intertidal zone.

The movement of waves breaking creates turbulence that is very efficient in stirring sediment at the sediment/water interface (*viz.* Bernabeu, et al., 2006). Santas and Santas (2000) described the initial fragmentation of oil on beaches is due to this mechanism. This way, oil can form tarballs or oil patches, be mixed with beach sands and buried into the beach profile.

It is understood that temporal impacts of spilled oil in a marine environment become more prolonged when oil is mixed into the sediment (Boehm, et al., 1981). Aromatic and saturated hydrocarbons can persist in sediment for substantial periods of time (years) as indicated by studies carried out in the 1970s by Teal, et al. (1978), Keizer, et al. (1978) and Mayo, et al. (1978).

Beaches are dynamic and cycle between storm and fair weather profiles. Storms bring stronger wave conditions with increased significant wave height (H_{bs}) which flattens the intertidal zone due to sediment re-working and transportation (Bernabeu, et al., 2006). During calm conditions, depending on beach slope, the intertidal zone forms berms, troughs and rips where there is more complex wave activity occurring. This cyclic activity has been described in past literature by Wright and Short, (1984). The beach slopes for both Pukehina and Omanu were measured at low tide, before the storm waves were able to flatten the beach profile.

The disturbance rod and washer technique was utilised in this study to determine the possible depth to which oil may be buried into beach sediment. The methodology used is outlined in Chapter 5.1. The results can be used in the future for a more efficient clean-up of beached oil if such events were to occur in the future.

At Pukehina Beach and Omanu Beach, depth of disturbance (DoD) was recorded over a single semi-diurnal tidal cycle during a storm. The average DoD for Pukehina during the survey was 120 mm and 49 mm for Omanu Beach (Table 5.1).

Waihi and Papamoa Beach were also measured for DoD as trials but, the measurements were not carried out during storm conditions. Papamoa DoD averaged at 54 mm. Due to the calm conditions and dissipative beach state of Waihi Beach had a shallower DoD, which averaged at 37 mm. However, beach slope was not measured for Waihi, so comparisons with other dissipative beaches are difficult to make.

On dissipative beaches, DoD is smoother and more likely to show a linear relationship with changing wave height since a flatter beach slope results in spilling breakers, which do not greatly disturb bottom sediments (Anfuso, 2005).

Both Pukehina and Omanu are intermediate beaches when classified using the Dean's Parameter or the Irribarren number calculation to determine the Wright and Short (1984) beach state. However, Omanu is more dissipative than Pukehina (4.9 °) with a slope of 3.2 ° and this is reflected in the shallower DoD that would be expected for gently sloping intermediate beach.

Previous DoDs measured at various beaches in the Northern Hemisphere (Table 2.5) varied depending on beach slope and wave conditions. The DoD is compared from this study (Table 5.3) to summary statistics of previous studies' results, also with an intermediate beach state (Table 5.4).

Beach state derived by either Dean's parameter or Irribarren number showed that Omanu DoD of 49 mm compared well with previous measured DoDs for intermediate state beaches with an average of 92 mm and 58 mm utilising either Dean's parameter or the Irribarren number respectively. However, Pukehina's DoD measured average was 120 mm which is comparative with intermediate beach state using Dean's parameter but, it exceeds the maximum DoD of 103 mm when beach state is determined with the Irribarren number.

Pukehina Beach is on the more reflective side of intermediate beaches, due to its steep beach face averaging 4.9°. Breaking wave heights (H_{bs}) were approximated at 2.6 m (Swellmap.com, 2013) which is greater than any recorded wave height during previous DoD studies in Table 2.5. Ciavola, et al., 2005 recorded similar H_{bs} to that of Pukehina at 2.5 m. The measured DoDs were between 45-101 mm. However, the study was carried out on a dissipative beach with a gentler slope of

1.1°. Therefore, DoDs would be expected to be less than the steeper sloping beach of Pukehina. The large H_{bs} and the beach slope steepness is most likely the cause for greater DoDs at Pukehina than previously recorded in other studies.

Several processes are responsible for sediment mixing in the intertidal zone. King (1951) and Williams (1971) both concluded that breaking wave height (H_{bs}) is the most dominant factor in determining DoD. King, (1951) calculated from four beach studies conducted in the United Kingdom that DoD was 30 % of H_{bs} with a near linear relationship at varying wave heights.

Variations of the formula derived by King (1951) have been established by other studies since then. Sherman, et al. (1994), and Ciavola, et al. (1997) looked solely at reflective beaches. However, each study varied in how their measurements were recorded giving two very different results. Sherman, et al. (1994) observed DoD at the breaker line only and determined that DoD was 22 % of H_{bs}. Whereas, Ciavola, et al. (1997) recorded DoD values that correspond to 27 % of H_{bs} calculated by averaging the maximum DoD during the breaking line migration. Anfuso, et al. (2000) on slightly flatter beaches, obtained a DoD of 16 % H_{bs}.

Ferreira, et al. (2000) derived a formula for reflective beaches similar to Sherman, et al. (1994) using 23 % of H_{bs}. However, this overestimated DoD on intermediate and dissipative beaches where DoD was about eight times larger than the observed DoD. Ferreira, et al. (2000) then derived a formula suitable for a variety of beach slopes where DoD was equal to 1.85 H_{bs} *tan β*. Using this formula in experiments determined that maximum DoD was 150 mm and tended to work better for the low tide zone on dissipative beaches. This formula would give a maximum DoD at Pukehina of 412 mm and 372 mm at Omanu which is more than 3 x greater than the maximum DoD recorded at Pukehina almost 8 x greater than the Omanu recorded DoD. Bertin, et al. (2008) calculated a new formula by taking into consideration breaking wave angle;

Z0=1.6tan (β*) H_{bs} 0.5$\sqrt{1 + sin\ (2\alpha)}$ (Bertin, et al., 2008)

This can be applied to a wide variety of beach gradients wave heights and wave incidence (Bertin, et al., 2008) and may be a factor in the variation of recorded

DoDs for this study in comparison to other studies. However, it cannot be compared to the current study since wave angle was not measured.

More recent investigations by Ciavola, et al. (2013) concluded that DoD averaged between 2-6 % H_{bs} for wave heights (H_s) 0.61 m to 0.83 m wave conditions in a drained system.

Ciavola, et al. (1997) DoD was published in Anfuso, 2005 as being 0.39 % H_{bs}. However, after researching the original paper by Ciavola, et al. (1997), it appears that the value may have been an error. DoD was calculated at 27 % H_{bs} by Ciavola, et al. (1997) but, the average grain size is recorded as being 0.39 mm.

These various formulas by King (1951), Sherman, et al. (1994), Ciavola, et al. (1997) and Anfuso, et al. (2000) that have been utilised to determine DoD in past studies during fair weather conditions, were compared to the measured DoD results obtained in the current study. However, the present study was performed during storm conditions, which causes an increase in H_{bs}.

Four formulas overestimated the DoD at both Pukehina and Omanu with expected DoDs up to 22 x greater than recorded (Table 5.5). However, the Ciavola et al. (2013) 2-6 % H_{bs} calculation compared well for Pukehina beach with the measured DoD 120 mm agreeing well with the range of 52-156 mm. Although Omanu Beach's measured DoD of 49 mm was less than the calculated range of 72-216 mm, the formula by Ciavola, et al., 2013 was more accurate than the other H_{bs} calculations.

Table 5.5: A summary of the various significant wave height formulas that have been used in previous studies as a measure of DoD and applying them to the current study's results.

Pukehina Beach	2.6 H_{bs}				
Author	King, 1951	Sherman, et al., 1994	Ciavola, et al., 1997	Anfuso, et al., 2000	Ciavola, et al., 2013
Formula	0.30 H_{bs}	0.22 H_{bs}	0.27 H_{bs}	0.16 H_{bs}	0.02-0.06 H_{bs}
Predicted DoD (mm)	780	572	702	416	52-156
Measured DoD (mm)	120	120	120	120	120
Omanu Beach	3.6 H_{bs}				
Author	King, 1951	Sherman, et al., 1994	Ciavola, et al., 1997	Anfuso, et al., 2000	Ciavola, et al., 2013
Formula	0.30 H_{bs}	0.22 H_{bs}	0.27 H_{bs}	0.16 H_{bs}	0.02-0.06 H_{bs}

Predicted (mm)	DoD	1080	792	972	576	72-216
Measured (mm)	DoD	49	49	49	49	49

Variations in wave height recording and may have caused the discrepancy in DoD formula results compared to measured results in the current study. H_{bs} was calculated from wave height data that was retrieved from Swellmap.com using wave bouy data. Therefore, the H_{bs} may not be as accurate as recording breaking wave height directly at the beach. King (1951) and Anfuso, et al. (2000) used predicted and observed wave and tide height using metric rule. Whereas, Sherman, et al. (1994) and Ciavola, et al. (1997) used pressure transducers to measure surface water elevations.

Variations in field measuring could give differences in surveyed beach slope values and DoD values. Therefore, DoD results are not necessarily comparable with each other or the current study (Anfuso, 2005).

5.3.1 THE EFFECT OF DEPTH OF DISTURBANCE ON OIL DEGRADATION

Oil stranded onto a beach, can be mixed into the sediments. The depth to which oil can be buried is dependent on oil and sediment characteristics as well as the elevation of the water table, wave conditions and beach morphology (Bernabeu, et al., 2006). The morphodynamic behaviour of beaches not only affects DoD depths but, also the subsequent degradation and evolution of oil (Bernabeu, et al., 2006).

The *Exxon Valdez* spill of 1989 (Table 2.3) was spread by winds and currents reaching the coast of Alaska (Wolfe, et al., 1994). Approximately 45% of the spilled oil was washed onto the shoreline in Prince William Sound and Peninsula within two months. Oil was found as deep as the depth of activation of 25 cm on the central platform of beaches (Wolfe, et al., 1994).

Many processes are at work to remove oil from the beach and it is thought that some processes are slowed or become inactive when oil is mixed into sediment

(Blumer & Sass, 1972b). Therefore, understanding oil burial processes can aid in more efficient clean-up practices.

Keizer, et al., (1978), Mayo, et al., (1978), and Teal, et al., (1978) concluded that aromatic and saturated hydrocarbons, components of oil, can persist in beach sediments for years. Oil evaporation and photo-oxidation rate is dependent on the depth that oil is buried into sediments (Strain, 1986). Strain (1986) determined from an experiment using light crude oil, that there was no loss of volatiles in oil buried 5-10 cm deep and in the mid intertidal surface sediments in the first six months. Also, biodegradation rates are slowed when oil becomes buried (Bernabeu, et al., 2006) but, does not cease completely (Bernabeu, et al., 2010).

The *Prestige* oil spill of 2002, involved 77,000 tons of Bunker C heavy fuel oil affecting the coasts of Spain and France and also led to a variety of scientific research programs investigating the effects of oil on the marine environment. Bernabeu, et al. (2006) concluded from their studies based on the *Prestige* spill, that the morphodynamic behaviour of beaches is a strong controlling factor in the burial of oil. Reflective beaches can bury oil deeper and more efficiently than a dissipative beach depending on weather conditions during and after oil reaches the coast. To put it simply, the greater the H_{bs}, the deeper the DoD.

Chemical analysis of sediment cores retrieved from 12 locations around the Bay of Plenty, a year after the *Rena* oil spill, investigated the presence of key PAHs in beach sediment to 40 cm depth. The GC/MS analysis was looking specifically for PAHs that matched the previously determined *Rena* oil fingerprint (Wilkins, 2013). As previously mentioned, PAHs are thought to degrade at a slower rate once buried under the beach surface. However, the results for the present study did not confirm slower degradation of oil constituents at depth.

Samples 20-40 cm deep did not contain more PAHs than those samples that were 0-20 cm deep. However, if the sample size had been smaller than 20 cm increments, such as 5 cm increments, variations in the surface portion of sediment to deeper sediment may have become apparent. Omanu's high tide core was initially sampled at 5 cm increments down to 40 cm. But, GC/MS analysis was unable to detect PAHs because of the low abundance of oil present. Therefore, it

was necessary to increase the sub-sample thickness in order to provide a larger volume of sediment for elutriation to extract the PAHs. Due to the 20 cm sample size, the analysis is limited in sensitivity by only being able to determine the difference between residual oil buried deeper than 20 cm or shallower than 20 cm.

5.3.2 LIMITATIONS

It is important to remember the morphodynamic behaviour of beaches, especially when referring to beach state. Beach slope can change over a single tidal cycle. The beach slope for both Omanu and Pukehina were taken before the storm waves affected the beach face and resulted in flattening the beach slope profile. Variations in beach slope profile measurements and different techniques utilised for DoD may cause discrepancies in results and make comparisons difficult.

SUMMARY AND CONCLUSIONS

Approximately one year after the *Rena* oil spill contaminated the Bay of Plenty coastline, 26 cores were retrieved from 12 beach locations between Waihi and Maketu to determine levels of residual *Rena* oil and beach sediment interactions. The cores underwent visual and chemical analysis using both quantitative and qualitative GC/MS techniques to determine the presence and nature of residual *Rena* oil in beach sediments.

No oil was visually observed in any of the cores. A separate study had identified the key PAHs comprising a fingerprint of the *Rena* oil (Wilkins, 2013), which could be used to assess if *Rena* oil was present a low concentrations that could not be detected visually. Sensitive qualitative GC/MS analysis identified 7 of the 52 samples (two 20 cm samples from each core) that contained 4 of the 5 *Rena* fingerprinted PAHs of pyrene, phenanthrene, benzo(a)anthracene and chrysene, with naphthalene missing in all 52 samples. Previous studies have determined that naphthalene evaporates from the environment within the first few weeks due to its low volatility (Boehm, et al., 1981; Strand, et al., 1992; Wolfe, et al., 1994; Nelson, et al., 2006), so the absence of naphthalene was expected.

34 out of 52 samples that underwent GC/MS quantitative analysis contained one or more PAHs. However, 27 of these did not consist of the more resilient, higher ringed PAHs benzo(a)anthracene and chrysene that make up a portion of the *Rena* fingerprint, which were expected to remain the longest within beach sediment. There could be are a variety of reasons for this anomaly. However, it is most likely that the PAHs, phenanthrene and pyrene, in the 27 samples are derived from other sources of contamination present along the Bay of Plenty coast. This is consistent with previous studies carried out around Tauranga Harbour, three years before the *Rena* spill. These detected PAH levels near stormwater outfall pipes along the coast, that were higher than any PAH levels detected in the current study (Park, 2009).

Further chemical analysis confirmed that although four PAHs; pyrene, phenanthrene, benzo(a)anthracene and chrysene were present in 6 of the 26 cores,

they are at very low abundances, falling below the detection levels when tested quantitatively. Only the 0-20 cm subsample of the Omanu high tide core contained four PAHs above detection levels in the quantitative analysis. Only two of these PAHs; phenanthrene and pyrene are characteristic of the *Rena* fingerprint.

Of the six most contaminated cores, three were from low tide locations on the main beach in Tauranga. The PAHs at this elevation may have had less exposure to photodegradation, and oil clean-up in the low tide zone would have been restricted.

Previous oil spill studies have found oil buried at depth on beaches (Wolfe, et al., 1994). The depth to which oil can be buried relies of the depth of sediment disturbance in the intertidal zone, and the amount of vertical accretion following initial burial. Chemical analysis established that PAHs were present in both the surface 0-20 cm samples and the deeper 20-40 cm samples, but the PAH species distributions were not consistent with degradation of buried *Rena* oil.

Depth of disturbance (DoD) by tides and wave action is considered the main contributing factors in the mixing of oil into beach sediment in the intertidal zone over the year that elapsed since the *Rena* oil spill. Disturbance rods and washers were used in this study to determine the DoD on Pukehina and Omanu Beaches, during storm conditions, over a semi diurnal tidal cycle.

Using the slope profile data, both Pukehina and Omanu were classified as intermediate state beaches, applying the Wright and Short (1984) beach classification system.

Papamoa and Waihi Beach DoD was also measured but, during fair-weather conditions. Beach slope profile was also not obtained at either of these beaches making comparisons with previous DoD difficult.

Pukehina recorded an average DoD of 120 mm and Omanu at 49 mm depth. Omanu Beach DoD results agree well with the previous studies of DoD on intermediate state beaches in the Northern Hemisphere. However, Pukehina Beach average DoD exceeded the previous recorded DoD based on the Irribarren number

formula. This anomaly may be due to the significant wave height (H_{bs}) of 2.6 m being greater than those reported for other intermediate beaches in the literature.

A maximum DoD of 280 mm was recorded at Pukehina Beach during storms with similar wave heights to the storms that were seen a week after the initial *Rena* oil spill on October the 11th, 2011. Without taking into account compaction, chemical analysis covered a depth of 400 mm, comfortably encompassing the maximum the *Rena* oil, if present, may have been buried in the intertidal zone. This is also supported by the presence of titanomagnetite placer deposits often found in sediment cores between the depths of 40 and 80 cm. The placer deposits are thought to have formed during extremely large storms during the 1970s, and indicate that there has not been significant accretion since the *Rena* oil spill, or extensive disturbance of the beach sediment.

The current study's DoD results were compared with theoretical approaches for determining DoD over a range of beach slopes and significant wave heights. All four methods determine DoD of the intertidal zone as a fixed percentage of the breaking significant wave height (H_{bs}). Every method greatly overestimated the DoD for both Omanu and Pukehina, ranging from 4 x to 22 x greater than the recorded DoDs. Again, the H_{bs} at both beaches were greater than those previously reported for intermediate beaches due to storm conditions at the time of the investigation. However, the H_{bs} used in this study was not directly recorded at the beach during the field investigation but, estimated from Swellmap.com where H_{bs} is extrapolated from wave buoy data.

Laboratory settling flask experiments were designed to simulate the effect of spilled oil in the intertidal zone on beaches. The settling flask experiments observed at the rate of sediment settling and the effect that heavy bunker fuel oil (HBFO) may have on settling velocities as well as observing sediment and oil interaction.

The experiments found that the addition of 10 ml or 20 ml HBFO did not have a great effect on sand settling velocity. Average settling velocity decreased from 23 s to 24 s for both oiled samples in comparison to the control. However, the oil

settled at much slower rates than the sand. Average settling times for oil was 126.2 s for the 10 ml mixture and 124.2 s for 20 ml.

Oil was observed to float, sink or stay suspended in the water column. After turbulence had ceased, about 5 % of the oil stayed suspended in the water column due to oil being the same density as the seawater in the flask. Field observations from the *Exxon Valdez* saw similar behaviour with only smaller droplets of spilled oil remaining suspended in seawater (Wolfe, et al., 1994).

In order to better understand oil and sediment interactions, samples from the settling tube experiments were viewed under microscope.

Oil was observed to readily bind to sediment, increasing the density, causing a larger proportion of oil to sink to the bottom of the settling tube. Oil was incorporated into the bottom sediments at depth due to sand settling on top of oil that had sunk prior to the settling sand. The direction of oil droplet travel was probably determined by the amount of sediment or air bound within the oil droplets which causes a change in oil droplet density. Oil droplets bound to sediment would sink, and oil droplets that contained bubbles of air or water would float to the surface.

The sand used for the settling flask experiment was obtained from high tide zone at Omanu Beach. Various studies have observed oil binding more readily to the bioclastic portion of sediment than siliciclastic sediment (Lee, 2002; Bernabeu, et al., 2006). This preference for bioclastic sediment was difficult to observe due to the large proportion of siliciclastic sediment (~ 80 %) present in the sand.

In conclusion, the six sediment core locations where four PAHs characterising the *Rena* PAH fingerprint were detected using sensitive analysis may have been a result of the *Rena* oil spill. However, abundances were so low that less sensitive qualitative analysis did not detect any PAHs in these samples above detection levels. The chemistry results determine that although various PAHs were present in 34 samples, contamination may have come from other sources such as stormwater runoff.

The DoD studies confirmed that the chemical analysis covered sufficient depth of sediment to encompass *Rena* oil that may have been buried underneath surface sediments during storms.

Overall, the results in this study confirm that *Rena* clean-up operations and natural degradation of oil over a year was effective at removing the *Rena* oil from sediments around the Bay of Plenty. The remaining PAHs are very low levels and may represent ongoing contamination from local sources, rather than a residual deposit from the *Rena*.

LIMITATIONS AND RECOMMENDATIONS FOR FUTURE RESEARCH

To better understand the nature and behaviour of spilled oil in the coastal environment of the Bay of Plenty, a more detailed analysis is needed on all aspects of this foundation study. Due to time restraints, field work began approximately a year after the initial *Rena* oil spill occurred. Ideally, sediment cores would have been retrieved 3, 6, 9 and 12 months after the initial spill in order to compare degradation rates of the residual oil.

Chemical analysis was restricted by financial restraints. With more funding, all of the 52 sediment samples that were qualitatively GC/MS analysed for PAHs would also have been analysed for alkanes, hopanes and heavy metals. In addition, all 52 samples would have undergone quantitative analysis by Hill's Laboratories on in order to confirm primary qualitative GC/MS analysis.

The laboratory studies would have benefited from more accurate recording of settling velocities. This would have allowed for more significant results comparable to other oil and sediment studies. Less time restrictions would have allowed for extension of lab experiments over three months or more to observe the long term effects of tarballs buried in sediment.

Since depth of disturbance research was focused predominately on the maximum depth to which oil could be mixed into the beach, storms with large significant wave heights were necessary for achieving accurate results. However, the mild winter in the Bay of Plenty over the research period resulted in relatively minor storms affecting the coast and only two storms were able to be measured for disturbance depth. Had there been less time constraints, possibly over a few winters, more locations over a variety of beach slopes could have been measured. Wave recorders deployed at each site would have given more accurate results specific to the beach rather than extrapolating from wave buoy data.

REFERENCES

Adriana, C.B., and Michel, J. (2010). Large-scale risk assessment of polycyclic aromatic hydrocarbons in shoreline sediments from Saudi Arabia: Environmental legacy after twelve years of the Gulf war oil spill. *Environmental Pollution.* Vol. 158, pp.1561–1569.

Agency for Toxic Substances and Disease Registry (ATSDR) (2013). Toxic Substances - *Polycyclic Aromatic Hydrocarbons. What Are Polycyclic Aromatic Hydrocarbons (PAHs)?* Retrieved on 14th of May, 2013, from: http://www.atsdr.cdc.gov.

Albaiges, J., Morales, B., and Vilas. .F. (2006). *The Prestige oil spill: a scientific response.* Marine Pollution Bulletin. Vol. 53, pp. 205–207.

Anfuso, G., Gracia, F.J., Andre´s, J., Sa´nchez, F., Del Rı´o, L., and Lo´pez, F. (2000). Depth of disturbance in mesotidal beaches during a single tidal cycle. *Journal of Coastal Research.* Vol 16, pp. 446–457.

Anfuso, G., Benavente, J., Del Rı´o, L., Castiglione, E., and Ventorre, M. (2003). Sand transport and disturbance depth during a single tidal cycle in a dissipative beach: La Barrosa (SW Spain). Proc. 3rd IAHR Symp. *River, Coastal and Estuarine Morphodynamics.* Vol. 2, pp.1176–1186.

Anfuso, G., and Ruiz, N. (2004). Morphodynamic of a mesotidal, low tide terrace exposed beach (Faro, South Portugal). *Cienc. Mar.* Vol. 30, pp.575–584.

Anfuso, G. (2005). Sediment-activation depth values for gentle and steep beaches. *Marine Geology.* Vol. 220, pp.101-112.

Anyakora , C., Ogbeche, A., Palmer, P., Coker, H., Ukpo, G., and Ogah C. (2005). GC/MS analysis of polynuclear aromatic hydrocarbons in sediment samples from the Niger Delta region. *Chemosphere.* Vol. 60, pp. 990-997.

ANZECC (2000). *Australian and New Zealand guidelines for fresh and marine water quality.* Vol. 1 and 2. Australian and New Zealand Environment and Conservation Council, Canberra, ACT, Australia.

API scale (1992). In Academic Press *Dictionary of Science and Technology.* Retrieved on November 20th, 2013, from: http://ezproxy.waikato.ac.nz/login?qurl=http%3A%2F%2Fwww.credorefe rence.com/entry/apdst/api_scale

Acosta-González, A., Rosselló-Móra, R., and Marqués, S. (2013).Characterization of the anaerobic microbial community in oil‐polluted subtidal sediments: aromatic biodegradation potential after the Prestige oil spill. *Environmental Microbiology.* Vol.15, pp. 77- 92.

Balouin, Y., Ciavola, P., Anfuso, G., Armaroli, C., Corbau, C., and Tessari, U. (2012). Morphodynamics of intertidal sand bars: field studies in the Northern Adriatic, NE Italy. *Geomorphology.* Vol. 143-144 pp. 69-80.

Battjes (1974). Surf Similarity. Proc. *14th International Conference Coastal Engineering, ASCE*, pp. 466–480.

Bellido, C., Anfuso, G., Plomaritis, T.A., and Rangel-Buitrago, N. (2011). Morphodynamic behaviour, disturbance depth and longshore transport at Camposoto Beach (Cadiz, SW Spain). *Journal of Coastal Research*,

(Proceedings of the 11th International Coastal Symposium). SI 64, pp.35-39.

Bernabeu, A.M., Rey, D. Lago, A., and Vilas F. (2010). Simulating the influence of physicochemical parameters on subsurface oil on beaches: Preliminary results. *Marine Pollution Bulletin*. Vol. 60, pp. 1170–1174.

Bernabeu, A.M., Nuez de la Fuente, M., Rey, D., Rubio, B., Vilas, F., Medina, R., and Gonzalez, M. (2006). Beach morphodynamics forcements in oiled shorelines: coupled physical and chemical processes during and after fuel burial. *Marine Pollution Bulletin*. Vol. 52, pp. 1156-1168.

Berge, J.A., Lichtenthaler, R.G., and Oreld, F. (1987). Hydrocarbon depuration and abiotic changes in artificially oil contaminated sediment in the subtidal. *Estuarine, Coastal and Shelf Science*. Vol. 24, pp. 567-583.

Bertin, X., Castell, B., Anfuso, G., and Ferreira, O. (2008). Improvement of sand activation depth prediction under conditions of oblique wave breaking. *Geo-Marine Letters*. Vol.28, pp.65–75.

Blumer, M., and Sass, J. (1972a). Oil pollution: Persistence and degradation of spilled fuel oil. *Science*. Vol. 176, pp. 1120–1122.

Blumer, M and Sass, J. (1972b). Indigenous and petroleum-derived hydrocarbons in a polluted sediment. *Marine Pollution Bulletin*. Vol. 3, pp. 92-94.

Blumer, M., Ehrhardt, M., and Jones, J.H. (1973). The environmental fate of stranded crude oil. *Deep Sea Research*. Vol. 20, pp.239-259.

Boehm P.D., Barak, J.E., Fiest, D.L., and Elskus, A.A. (1981). A chemical investigation of the transport and fate of petroleum hydrocarbons in littoral and benthic environments: The TSESIS Oil Spill. *Marine Environmental Research*. Vol. 6, pp.157-188.

Boehm, P.D., (1987). *Transport and transformation processes regarding hydrocarbon and metal pollutants in offshore sedimentary environments*. In: Boesch, D.F. and Rabalais, N.N. (Eds.), Long-Term Environmental Effects of Offshore Oil and Gas Development, Elsevier Applied Science, London and New York. pp. 233–287.

Boehm, P.D., Douglas, G.S. Burns, W.A. Mankiewicz, P.J., Page, D.S., and Bence A.E. (1997). Application of petroleum hydrocarbon chemical fingerprinting and allocation techniques after the Exxon Valdez oil spill. *Marine Pollution Bulletin,* Vol. 34, pp.599-613.

Bragg, J.R., and Owens, E.H. (1994). Clay–oil flocculation as a natural cleansing process following oil spills: part 1 – studies of shoreline sediments and residues from past spills. In: *Proceedings of the 17th Arctic and Marine Oil Spill Program (AMOP) Technical Seminar*. Environment Canada, Ottawa, Ontario, pp. 1–23.

Brook, A., and Lemckert, C. (2010). A new technique for measuring depth of disturbance in the swash zone. Coastal Conference, Australia, 2011.

Bruzzoniti, M. C., Fungi, M., and Sarzaninia, C. (2009). Determination of EPA's priority pollutant polycyclic aromatic hydrocarbons in drinking waters by solid phase extraction-HPLC. *Analytical Methods*, Vol. 2 pp. 739-745.

Burns, K. A., Codi., S., and Duke, N.C. (2000). Gladstone, Australia Field Studies: Weathering and Degradation of Hydrocarbons in oiled mangrove and salt marsh sediments with and without the application of and experimental bioremediation protocol. *Marine Pollution Bulletin*. Vol. 41, pp. 392-402.

Coates, J.D., Woodward, J., Allen, J., Philip, P., and Lovley, D.R. (1997). Anaerobic degradation of polycyclic hydrocarbons and alkanes in petroleum-contaminated marine harbour sediments. *Applied Environmental Microbiology.* Vol. 63, pp. 3589–3593.

Ciavola P., Taborda, R., Ferreira, O., and Dias, J.A.(1997). Field observations of sand-mixing depths on steep beaches. *Marine Geology.* Vol. 141, pp. 147–156.

Ciavola, P., Contestabile, P., Aristodemo, F., and Vicinanza, D. (2013). Beach sediment mixing under drained and undrained conditions. In: Conley, D.C., Masselink, G., Russell, P.E., and O'Hare, T.J. (eds.), Proceedings 12th International Coastal Symposium (Plymouth, England), *Journal of Coastal Research.* Special Issue No. 65, pp. 1503-1508.

Delvigne, G.A., van der Stel, J.A., and Sweeney, C.E. (1987). Measurement of vertical turbulent dispersion and diffusion of oil droplets and oiled particles. *Final report: OCS Study MMS 87-111.* US Department of the Interior, Minerals Management Service, Anchorage AK, pp.501.

Delvigne, G.A.L. (2002). Physical appearance of oil in oil-contaminated sediment. *Spill Science & Technology Bulletin.* Vol. 8, pp. 55–63.

Díez, S., Jover, E., Bayona, J.M., and Albaigés, J. (2007). Prestige oil spill. Fate of heavy oil in the marine environment. *Environmental Science and Technology.* Vol. 41, pp. 3075–3082.

Eaton R.W., and Chapman P.J. (1992). Bacterial metabolism of naphthalene: construction and use of recombinant bacteria to study ring cleavage of 1,2-dihydroxynaphthalene and subsequent reactions. *Journal of Bacteriology.* Vol. 174, pp. 7542-7554.

Ehrhardt, M., and Blumer, M. (1972). The Source Identification of Marine Hydrocarbons by Gas Chromatography and Spectrometry. *Environmental Pollution.* Vol. 3, pp. 179-194.

Fernández-Álvarez, P., Vila, J., Garrido-Fernández, J.M., Grifoll, M., and Lema, J.M. (2006).Trials of bioremediation on a beach affected by the heavy oil spill of the Prestige. *Journal of Hazardous Materials.* Vol. 137, pp. 1523–1531.

Ferreira, Ó., Ciavola, P., Taborda, R., Bairros, M., and Dias, J.M.A. (2000). Sediment mixing depth determination for steep and gentle foreshores. *Journal of Coastal Research,* Vol. 16, pp. 830-839.

Folk, R. L. (1954). The distinction between grain size and mineral composition in sedimentary rock nomenclature. *Journal of Geology.* Vol.62, pp.344-359.

Gaughan M.K., (1978). Depth of disturbance of sand in surf zones. *Coastal Engineering*, No.16, pp. 1513-1530. Retrieved on 17th of April, 2013 from: http://journals.tdl.org/icce/index.php/icce/article/viewArticle/3352

Gonzalez, M., Medina R., Bernabeu, A.M., and Novoa, X. (2009). Influence of beach morphodynamics in the deep burial of fuel in beaches. *Journal of Coastal Research.* Vol. 25, pp. 799.

Gonzalez, R., Ciavola, P., Corbau, C., Falati S., and Ferreira Ó. (2004). Mixing depth experiments on an estuarine dissipative beach; St. Georges Beach, Gironde (France). *Journal of Coastal Research.* SI 41, pp. 43-52.

Gordon, Jr., D.C., Keizer, P.D., and Prouse, N.J. (1973). Laboratory studies of the accommodation of some crude and residual fuel oils in sea water. *Journal of the Fisheries Research Board of Canada.* Vol. 30, pp.1611-1618.

Greenwood, B., and Hale, P.B. (1980). Depth of activity, sediment flux and morphological change in a barred beach environment. In: McCann, S.B. (Ed.) *The Coastline of Canada*. Geological Survey Cananda. pp. 89– 109.

Greenwood B., and Mittler, P.R. (1984). Sediment flux and equilibrium slopes in a barred nearshore. *Marine Geology*. Vol.60, pp.79-98.

Greenwood, B., and Sherman, D.J. (1986). Longshore current profiles and lateral mixing across the surf zone of a barred nearshore. *Coastal Engineering.* Vol. 10, pp.149-168.

Hadibarata,T., Tachibana S., and Itoh, K. (2009). Biodegradation of chrysene, an aromatic hydrocarbon by *Polyporus* sp. S133 in liquid medium. *Journal of Hazardous Materials*. Vol. 164, pp. 911-917.

Harayama, S., Kasau, Y., and Hara, A. (2004). Microbial communities in oil-contaminated seawater. *Current Opinion on Biotechnology*. Vol. 15, pp. 205-214.

Haritash, A.K., and Kaushik, C.P. (2009). Biodegradation aspects of Polycyclic Aromatic Hydrocarbons (PAHs): a review. *Journal of Hazardous Materials.* Vol. 169, pp. 1-15.

Head, I.M., and Swannell, R.P.J. (1999). Bioremediation of petroleum hydrocarbon contaminants in marine habitats. *Current Opinion Biotechnology*. Vol.10, pp. 234–239.

Hennig, H.F.K.O. (1979). Quantitative analysis of residual fuel oil in sediment samples by absorption spectrophotometry. *Marine Pollution Bulletin*. Vol. 10, pp. 234-237.

Hyne, N.J. (2001). Nontechnical Guide to Petroleum Geology, *Exploration, Drilling, and Production.* PennWell Corporation.

International Union of Pure and Applied Chemistry (1979). *Nomenclature of Organic Chemistry:* Sections A, B, C, D, E, F, and H. Pergamon Press, Oxford.

Jackson, N.L. and Nordstrom, K.F. (1993). Depth of activation of sediment by plunging breakers on a steep sand beach. *Marine Geology.* Vol. 115 pp.143 151.

Johansson, S.U., Larsson, U., and Boehm, P.D. (1980). The TSESIS oil spill: impact on the pelagic ecosystem. *Marine Pollution Bulletin*. Vol.11, pp. 284–293.

Jonker, M.T.O., Sinke, A.J.C., Brils, J.M., and Koelmans, A.A. (2003). Sorption of polycyclic aromatic hydrocarbons to oil contaminated sediment: unresolved complex? *Environmental Science and Technology*. Vol. 37, pp. 5197-5203.

Keizer. P.D., Ahern, T. P., Dale, J., and Vandermeulen, J.H. (1978). Residues of Bunker C oil in Chedabucto Bay, Nova Scotia 6 years after the ARROW spill. *Journal of the Fisheries Research Board of Canada*. Vol. 35, pp.528-35.

Khelifa, A., Stoffyn-Egli, P., Hill, P.S., and Lee, K. (2002). Characteristics of oil droplets stabilized by mineral particles: effect of oil types and temperature. *Spill Science and Technology Bulletin*.Vol.8, pp. 19-30.

King, C.A.M. (1951). Depth of disturbance of sand on sea beaches by waves. *Journal of Sedimentary Research*. Vol. 21, pp. 131- 140.

Kingston, P.F., Runciman, D., and McDougall, J. (2003). Oil contamination of sedimentary shores of the Gala´pagos islands following the wreck of the Jessica. *Marine Pollution Bulletin.* Vol. 47, pp.303–312.

Kraus, N.C. (1985). Field experiments on vertical mixing of sand in the surf zone. *Journal of Sedimentary Petroleum*. Vol. 55, pp. 3–14.

Hayes, M.O., Michel, J., Montello, T.M., Aurand, D.V., Al-Mansi, A.,Al-Moamen, A.H., Sauer, T.C., and Thayer, G.W. (1993). Distribution and weathering of shoreline oil one year alter Gulf War oil spill. *Marine Pollution Bulletin.* Vol.27, pp.135–142.

Lee, K. (2002). Oil–Particle Interactions in Aquatic Environments: Influence on the Transport, Fate, Effect and Remediation of Oil Spills. *Spill Science and Technology Bulletin.* Vol.8, pp. 3-8.

Lee, K., Prince, R.C., Greer, C.W., Doe, K.G., Wilson, J.E.H., Cobanli, S.E., Wohlgeschaffen, G.D., Alroumi, D., Kinga, T. and Tremblay, G.H. (2003). Composition and toxicity of residual bunker C fuel oil in intertidal sediments after 30 years. *Spill Science & Technology Bulletin*. Vol. 8, pp. 187–199.

Le Floch, S., Guyomarch, J., Merlin, F., Stoffyn-Egli, S., Dixon, J., and Lee, K. (2002). The influence of salinity on oil–mineral aggregate formation. *Spill Science & Technology Bulletin.* Vol. 8, pp. 65-71.

Li, H, Xu, R., and Obbard, J.P. (2006). Biodegradation of pyrene in marine sediments. *Bioremediation Journal.* Vol. 10, pp. 169-177.

Lisi, I., Molfetta, M.G., Bruno, M.F., Di Risio, M., and Damiani, L. (2011). Morphodynamic classification of sandy beaches in enclosed basins: the case study of Alimini (Italy). *Journal of Coastal Research*. Special Issue 64, pp. 180-184.

Luch, A. (2005). *The carcinogenic effects of polycyclic aromatic hydrocarbons.* London: Imperial College Press.

Ma, X., Cogswell, A., Lee, Z., and Lee, K. (2008). Particle size analysis of dispersed oil and oil-mineral aggregates with an automated ultraviolet epi-fluorescence microscopy system. *Environmental Technology*. Vol. 29, pp. 739-748.

Maritime New Zealand (2013). *The Rena Project*. Retrieved on 30th of April, 2013, from http://www.maritimenz.govt.nz/*Rena*/

Mayo, D.W., Page, D.S., Cooley, J., Sorenson, E., Bradley, F., Gilfillan, E.S., and Hanson, S.A. (1978). Weathering characteristics of petroleum hydrocarbons deposited in fine clay marine sediments, Searsport, Maine. *Journal of the Fisheries Research Board of Canada.* Vol. 35, pp.552-67.

MfE.govt.nz (2011). Minister for the Environment; *Rena Long-term Environmental Recovery Plan.* Retrieved on September 12th, 2012 from: http://www.mfe.govt.nz/publications/hazardous/*Rena*-recovery/*Rena*-long-term-environmental-plan.pdf.

MfE.govt.nz (1999). Minister for the Environment; *Guidelines for Assessing and Managing Petroleum Hydrocarbon Contaminated Sites in New Zealand* (Revised 2011) MODULE 2 Hydrocarbon contamination fundamentals. Retrieved on 14th of May 2013, from: http://www.mfe.govt.nz/publications/hazardous/oil-guide-jun99/module-2.pdf

Miller, N.J, and Mudge, S.M. (1997). The effect of biodiesel on the rate of removal and weathering characteristics of crude oil within artificial sand columns. *Spill Science and Technology Bulletin*, Vol.4, pp.17–33.

Minai-Tehrani, D., Minoui, S., and Herfatmanesh, A. (2009). Effect of salinity on biodegradation of polycyclic aromatic hydrocarbons (PAHs) of heavy crude oil in soil. *Bulletin of Environmental Contamination Toxicology*, Vol.82, pp. 179-184.

Moore, J.W., and Ramammoorthy S. (1984). *Organic chemicals in natural waters : applied monitoring and impact assessment*. New York : Springer-Verlag.

Nagpal, N. K. (1993). *Ambient water quality criteria for polycyclic aromatic hydrocarbons (PAHs)*. Water Quality Branch Water Management Division, Ministry of Environment, Lands and Parks Province of British Columbia. Retrieved on: 18th of November, 2013, from: http://www.env.gov.bc.ca/wat/wq/BCguidelines/pahs/index.html#TopOfPage

Nasher, E., Heng, L.Y., Zakaria, Z., and Surif, S. (2013). Concentrations and Sources of Polycyclic Aromatic Hydrocarbons in the Seawater around Langkawi Island, Malaysia. *Journal of Chemistry*. Vol. 2013, pp.10.

Nelson R.K, Kile, B., Plata, D., Sylva, S., Xu, L., Reddy, C., Gaines, R., Frysinger, G., Reichenbach, S. (2006).Tracking the weathering of an oil spill with comprehensive two-dimensional gas chromatography. *Environmental Forensics*. Vol. 7, pp. 33-44.

NOAA Office of Response and Restoration. Emergency Response Division. Retrieved on 30th of April, 2013 from: www.fws.gov/contaminants/Response/NOBargeSpill/No6_fuel_oil.pdf

NRC, National Research Council (2003). *Oil in the sea III: inputs, fates, and effects*. Committee on Oil in the Sea: Inputs Fates and Effects, Ocean Study Board and Marine Board, Divisions of Earth and Life Studies.

New Zealand Geotechnical Society Inc. (2001). *Guideline for Hand Held Shear Vane Test*.

New Zealand Geotechnical Society Inc. (2005). *Field Description of Soil and Rock. Guideline for the field classification and description of soil and rock for engineering purposes*.

Omotoso, O.E., Munoz, V.A., and Mikula, R.J. (2002). Mechanisms of crude oil–mineral interactions. *Spill Science and Technology Bulletin*. Vol.8, pp. 45–54.

Owens, E.H., and Lee, K. (2002). Interaction of oil and mineral fines on shorelines: a review. *Marine Pollution Bulletin*. Vol. 47, pp. 397-405.

Park, S. (2009). *Bay of Plenty Marine Sediment Contaminants Survey 2008*. Environment Bay of Plenty regional Council.

Payne, J.R., Clayton Jr., J.R., McNabb Jr., G.D., Kirstein, C.L., Clary, C.L., Redding, R.T., Evans, J.S., Reimnitz, E., and Kempema, E.W. (1989). Oil–ice–sediment interactions during freezeup and breakup. US Department of Commerce, *National Oceanographic and Atmospheric Administration (NOAA), OCSEAP Final Report*. Vol. 64, pp.382.

Peng, R., Xiong, A. Xue, Y., Fu, X., Gao, F., Zhao, W., Tian, Y., and Yao, Q. (2008). Microbial biodegradation of polyaromatic hydrocarbons. *Federation of European Microbiology (FEMS), Microbiology Reviews*. Vol. 32, pp. 927-955.

Pereira, M.G., and Mudge, S.M. (2004). Cleaning oiled shores: laboratory experiments testing the potential use of vegetable oil diesels. *Chemosphere.* Vol. 54, pp.297–304.

Rashid, M.A. (1974). Degradation of Bunker C Oil under different coastal environments of Chedabucto Bay, Nova Scotia. *Estuarine and Coastal Marine Science*. Vol. 2, pp. 137-144

Rowland, A.P., Lindley, D.K., Hall, G.H., Rossall, M.J., Wilson D.R., Benham, D.G., Harrison, A.F., and Daniels R.E. (2000). Effects of beach sand properties, temperature and rainfall on the degradation rates of oil in buried oil/beach sand mixtures. *Environmental Pollution*. Vol. 109, pp. 109–118.

Sainia, S., Jackson, N.L., and Nordstrom, K.F. (2009). Depth of activation on a mixed sediment beach. *Coastal Engineering*. Vol. 56, pp.788–791.

Santas, R., and Santas P. (2000). Effects of waver action on the bioremediation of crude oil saturated hydrocarbons. *Marine Pollution Bulletin.* Vol. 40, pp. 434-439.

Sherman, D.J., Nordstrom, K.F., Jackson, N.L., and Allen J.R. (1994). Sediment mixing-depths on a low-energy reflective beach. *Journal of Coastal Research.* Vol. 10, pp.297–305.

Short, J.W., and Heintz, R.A. (1997). Identification of Exxon Valdez oil in sediments and tissues from Prince William Sound and the northwestern Gulf of Alaska based on a PAH weathering model. *Environmental Science and Technology.* Vol. 31, pp. 2375-2384.

Speight, J.G. (1999). *The Chemistry and Technology of Petroleum.* Marcel Dekker. pp. 215–216.

Strain, P.M. (1986). The Persistence and Mobility of a Light Crude Oil in a Sandy Beach. *Marine Environmental Research*. Vol. 19, pp. 49-76.

Strand, J.A., Cullinan, V.I., Crecelius, E.A., Fortman, T.J., Citterman, R.J., and Fleischmann, M.I. (1992). Fate of Bunker-C fuel-oil in Washington coastal habitats following the December 1988 Nestucca oil spill. *Northwest Science*. Vol. 66, pp.1-14.

Stoffyn-Egli, P., and Lee, K. (2002). Formation and characterization of oil-mineral aggregates. *Spill Science and Technology*. Vol. 8, pp. 31-44.

Sunamura, T. and Kraus, N.C. (1985). Prediction of average mixing depth of sediment in the surf zone. *Marine Geology*. Vol. 62, pp.1–12.

Swellmap.com, (2013). *Surfing forecast for New Zealand*. Retrieved on: 1st June, 2013, 4th of June, 2013, & 3rd of August, 2013 from: http://www.swellmap.com/surfing/new-zealand

Taborda, R., Cascalho, J., and Sá-Pires, C. (2006). Intra-tidal beach morphological changes and their relationship with sand mixing depth. *Journal of Coastal Research*. Vol. 39, pp. 319-322.

Teal, J.M., Burns, K. and Farrington, J. (1978). Analyses of aromatic hydrocarbons in intertidal sediments resulting from two spills of No. 2 fuel oil in Buzzards Bay, Massachusetts. *Journal of the Fisheries Research Board of Canada*. Vol. 35, pp.510-20.

Teal, J. M., Farrington J.W., Burns, K.A., Stegeman, J.J. Tripp, B.W., Woodin, B., and Phinney, C. (1992). The West Falmouth oil spill after 20 years: Fate of fuel oil compounds and effects on animals. *Marine Pollution Bulletin*, Vol. 24, pp. 607-614.

Ting, W.T.E., Yuan, S.Y., Wu, S.D., and Change, B.V. (2011). Biodegradation of phenanthrene and pyrene by *Ganoderma lucidum. International Biodeterioration and Biodegradation.* Vol. 65, pp. 238-242.

Tronczyński, J., Munschy, C., Héas-Moisan, K., Guiot, N., Truquet, I., Olivier, N., Men, S., and Furaut, A. (2004). Contamination of the Bay of Biscay by polycyclic aromatic hydrocarbons (PAHs) following the T/V "Erika" oil spill. *Aquatic Living Resources*. Vol. 17 pp. 243-259.

Venosa, A.D., and Zhu, X. (2003). Biodegradation of Crude Oil Contaminating Marine Shorelines and Freshwater Wetlands. *Spill Science & Technology Bulletin*. Vol. 8, pp. 163–178.

Viñas, L., Franco M.A, Soriano J A., Gonza´lez J.J., Pon, J., and Albaige´, S.J. (2010). Sources and distribution of polycyclic aromatic hydrocarbons in sediments from the Spanish northern continental shelf. Assessment of spatial and temporal trends. *Environmental Pollution*. Vol. 158, pp. 1551–1560.

Voulgaris, G., and Collins, M.B. (2000). Sediment re-suspension on beaches: response to breaking waves. *Marine Geology*. Vol. 167, pp. 167–187.

Wang, P., and Roberts T.M., (2013). Distribution of surficial and buried oil contaminants across sandy beaches along NW Florida and Alabama coasts following the Deepwater Horizon Oil Spill in 2010. *Just Cerfing.* Vol. 4, pp. 1-6.

Wang, Z., and Stout, S.A. (2007). *Oil spill environmental forensics: fingerprinting and source identification.* Amsterdam; Boston, MA: Elsevier/Academic Press.

Wang, X., Zhang, Y., and Chen, R.F. (2001). Distribution and partitioning of polycylcic aromatic hydrocarbons (PAHs) in different size fractions in sediments from Boston Harbor, United States. *Marine Pollution Bulletin*. Vol. 42, pp.1139-1149.

Wang, Z., Fingus, M., and Page, D.S. (1999). Oil spill identification. *Journal of Chromotography*. Vol. 843, pp. 369-411.

Wang, Z.D.; Fingas, M.; Blenkinsopp, S.; Sergy, G.; Landriault, M.; Sigouin, L.; Foght, J.; Semple, K.; and Westlake, D.W.S. (1998). Comparison of oil composition changes due to biodegradation and physical weathering in different oils. *Journal of Chromatography*. Vol. 809, pp.89-107.

Wang, Z., Fingus, M., and Sergy, G. (1994). Study of 22~ Year-old Arrow oil samples using biomarker compounds by GC/MS. *Environmental Science and Technology*. Vol. 28, pp.1733-1746.

Williams, A.T. (1971). An analysis of some factors involved in the depth of disturbance of beach sand by waves. *Marine Geology*. Vol. 11, pp. 145–158.

Wilkins, A. (2013). GC-MS fingerprint comparison of *Rena* oil and some October-November 2011 and January-February 2012 oiled sand and tarball samples. *Rena Recovery Project Report No 1.*

Wilson, S.C., and Jones, K.C. (1993). Bioremediation of soil contaminated with polynuclear aromatic hydrocarbons (PAHs): a review. *Environmental Pollution.* Vol.81, pp. 229-249.

Wolfe, D.A. (1994). The fate of the oil spilled from the Exxon Valdez. *Environmental Science & Technology*. Vol.28, pp.560A-8A.

Wright, L.D., and Short, A.D. (1984). Morphodynamic variability of surf zones and beaches: a synthesis. *Marine Geology*. Vol. 56, pp. 93– 118.

APPENDICES

9.1 APPENDIX I: SEDIMENT CORE LOGS

Visual core descriptions and photographs of each core.

FACE LOG

Project: *Rena* sediment cores

Borehole:

Co-ordinates: S 37 23.749 E 175 56.297

Site: 19

Core: Waihi mid tide

Depth (m): 61 cm

THE UNIVERSITY OF
WAIKATO
Te Whare Wānanga o Waikato

BOX NUMBER	DEPTH (m)	GRAPHIC LOG	SOIL DESCRIPTION SOIL NAME, colour, structure, weathering, strength; moisture condition; plasticity; grading; bedding; soil fraction; additional observations; geological/pedological name.	
	1		SAND, Hue 5Y 6/3 olive yellow, mSL (still wet) extremely well sorted	
	2 3 4		SAND, Hue 5Y 5/1 gray, mSU (very wet), very well sorted, thin, minor shaded laminations throughout (possibly tatinomagnietite), three whole shells at 30 cm	
	5		SAND, Hue 5Y 7/4 light yellow, crs SL with 5Y 5/1 gray band 8 mm wide at 46 cm and 2 mm, 5Y 8/4 pale yellow band on either side (possibly oxide ferric/ferrous reaction?), well sorted	
	6		SAND, Hue 5Y 7/4 light yellow grading down to a 5Y 6/3 olive yellow, crs SL grading down to crs SL, moderately sorted, shell fragments (3 mm-20 mm) and whole shells (> 30 mm) shell hash band at 53-55 cm	
	7 8		SAND, Hue 5/Y 6/3 olive yellow, mSL, extremely well sorted	
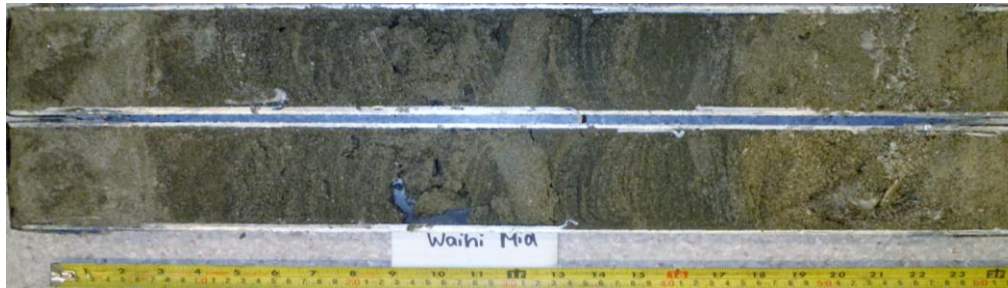
Figure I.1: Site 1, Waihi mid tide core log visual description.

128

FACE LOG

Project:	*Rena* sediment cores
Borehole:	**Co-ordinates:** S 37 23.747 E 175 56.326
Site: 1	**Core: Waihi high tide**
Depth (m): 66 cm	

THE UNIVERSITY OF
WAIKATO
Te Whare Wānanga o Waikato

BOX NUMBER	DEPTH (m)	GRAPHIC LOG	SOIL DESCRIPTION **SOIL NAME, colour, structure, weathering, strength; moisture condition; plasticity; grading; bedding; soil fraction; additional observations; geological/pedological name.**	
	1 2		SAND, Hue 5Y 7/3 light yellow, crs SU, very poorly sorted, whole shells up to 50 mm and 0-6 cm on edge of core barrel a clear gel has formed 0-6 cm	
	3 4		SAND, Hue 5Y 6/2 grayish olive, crs SL, very poorly sorted, whole shells and fragments 20 mm and 50 mm	
	5 6		SAND, Hue 5Y 6/1 gray, mSU, moderately sorted	
	7			

Figure I.2: Site 1, Waihi high tide core log visual description.

129

FACE LOG

Project: *Rena* sediment cores

Borehole:

Co-ordinates: S 37 23.772 E 175 56.336

Site: 2

Core: Waihi- Bowentown mid tide

Depth (m): 102 cm

THE UNIVERSITY OF
WAIKATO
Te Whare Wānanga o Waikato

BOX NUMBER	DEPTH (m)	GRAPHIC LOG	SOIL DESCRIPTION **SOIL NAME, colour, structure, weathering, strength; moisture condition; plasticity; grading; bedding; soil fraction;** **additional observations; geological/pedological name.**	
	1		SAND, Hue 5Y 7/2 light gray, mSL, extremely well sorted Slightly mottled colouring throughout with minor patchy shading	
	2			
	3			
	4			
	5			
	6			
	7		SAND, Hue 5Y 7/2 light gray, mSL, extremely well sorted, titanomagnitite bands 2 mm thick between 58-68 cm	
			SAND, Hue 5Y 8/2 light gray, crs SL, extremely well sorted fining to below	
	8		SAND, Hue 5Y, 8/2 light gray, mSU, extremely well sorted	
			SAND Hue 5Y 7/3 light yellow, crs SL, a coarse 1 cm thick band slighter darker, very well sorted	
	9		SAND, Hue 5Y 8/2 light gray, mSU, extremely well sorted	
	10			
	11			

Figure I.3: Site 2, Bowentown mid tide core log visual description.

130

FACE LOG

Project: *Rena* sediment cores

Borehole:

Co-ordinates: S 37 23.783 E 175 56.323

Site: 2

Core: Waihi -Bowentown high tide

Depth (m): 114 cm

THE UNIVERSITY OF
WAIKATO
Te Whare Wānanga o Waikato

BOX NUMBER	DEPTH (m)	GRAPHIC LOG	SOIL DESCRIPTION **SOIL NAME, colour, structure, weathering, strength; moisture condition; plasticity; grading; bedding; soil fraction;** additional observations; geological/pedological name.	
			SAND, Hue 5Y 7/1 light gray, mSU, well sorted	
	1		SAND, Hue 5Y 4/1 gray, mSU, very well sorted, titanomagnetite band 10 mm thick	
	2		SAND, Hue 5Y 7/2 light gray, mSU, extremely well sorted, grading to 5/1 with increasing titanomagnetite (~40%) at 28 cm	
	3		SAND Hue 5Y 4/1 gray - 2/1black, mSU, extremely well sorted, 80% titanomagnitite with minor lighter patches	
	4			
	5		SAND, Hue 5Y 7/2 light gray, crs SL at 53 cm fining to mSU at 84 cm. minor (5%) thin titanomagnetite bands	
	6			
	7			
	8			
	9		SAND Hue 5Y 4/1 gray- 2/1 black, mSU, extremely well sorted, defined 2 mm wide striations of titanomagnetite	
	10		SAND Hue 5Y 7/2 light gray, mSU, extremely well sorted, minor (~5%) thin titanomagnetite in all directions	
	11			
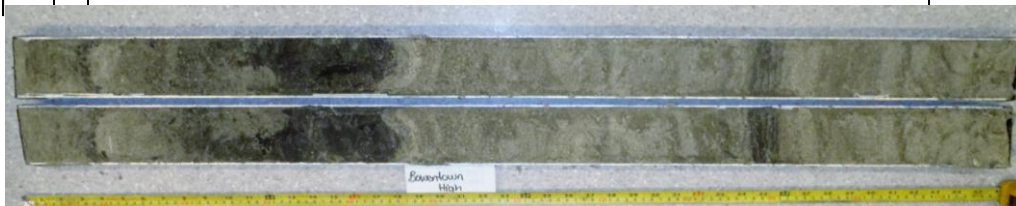
Figure I.4: Site 2, Bowentown high tide core log visual description.

131

FACE LOG

Project: *Rena* sediment cores

Borehole:

Co-ordinates: S 37 35.546 E 176 06.591

Site: 2

Core: Matakana Island-Tank Road mid tide

Depth (m): 90 cm

THE UNIVERSITY OF
WAIKATO
Te Whare Wānanga o Waikato

BOX NUMBER	DEPTH (m)	GRAPHIC LOG	SOIL DESCRIPTION **SOIL NAME, colour, structure, weathering, strength; moisture condition; plasticity; grading; bedding; soil fraction; additional observations; geological/pedological name.**
	1		SAND, Hue 5Y 8/2 light gray, mSU, extremely well sorted, begins coarsening gradually at 30 cm with large shell fragments (2%) to crs SL at 68 cm, shells are >2cm in size
	2		
	3		
	4		
	5		
	6		
	7		
	8		SAND, Hue 5Y 8/2 light gray, crs SL, well sorted, titanomagnetite 2/1 black, in bands at 68 and 70 cm ~2 mm thick, accumulation of medium shell fragments 1-2 mm in size at 78-83 cm (5%)
	9		

Figure I.5: Site 3, Matakana Island, Tank Road mid tide core visual description.

132

FACE LOG

Project:	*Rena* sediment cores
Borehole:	**Co-ordinates:** S 37 35.554 E 176 06 583
Site: 3	**Core: Matakana Island-Tank Road high tide**
Depth (m):	69 cm

THE UNIVERSITY OF
WAIKATO
Te Whare Wānanga o Waikato

BOX NUMBER	DEPTH (m)	GRAPHIC LOG	SOIL DESCRIPTION **SOIL NAME, colour, structure, weathering, strength; moisture condition; plasticity; grading; bedding; soil fraction; additional observations; geological/pedological name.**	
	1 2 3		SAND, Hue 5Y 8/1 light gray, mSU, extremely well sorted, mottled with 2/1 black, titanomagnetite, 1 large shell at 5-7 cm, 30 mm in size	
	4		SAND, Hue 5Y 7/1 light gray, mSU, slightly darker mottling of 2/1 black titanomagnetite, extremely well sorted	
	5 6 7		SAND, Hue 5Y 8/1 light gray, mSU, extremely well sorted, with patches of 7/1 light gray	

Figure I.6: Site 3, Matakana Island, Tank Road high tide core visual description.

FACE LOG

Project: *Rena* sediment cores

Borehole:

Co-ordinates: S 37 38.154 E 176 09.675

Site: 4

Core: Matakana Island- Panepane Point mid tide

Depth (m): 100 cm

THE UNIVERSITY OF
WAIKATO
Te Whare Wānanga o Waikato

BOX NUMBER	DEPTH (m)	GRAPHIC LOG	SOIL DESCRIPTION SOIL NAME, colour, structure, weathering, strength; moisture condition; plasticity; grading; bedding; soil fraction; additional observations; geological/pedological name.	
			SAND, Hue 5Y 8/2 light gray, crs SL, extremely well sorted. Slight mottling in colour with titanomagnitite Hue 5Y 2/1 black	
	1		SAND, Hue 5Y 8/2 light gray, crs SU, extremely well sorted, mottled with titanomagnetite, Hue 2/1 black, patches at 50 cm, 64 cm and 73 cm that are 3-4 cm wide that are slightly darker (7/2), possibly due to being wetter than the rest of the core	
	2			
	3			
	4			
	5			
	6			
	7			
	8			
	9		SAND, Hue 5Y 7/2 light gray, crs SU, very well sorted, more mottled and slightly coarser	
			SAND, Hue 5Y 8/2 light gray, crs SL, extremely well sorted, mottled with 5Y 2/1 black	
	10			

Figure I.7: Site 4, Matakana Island, Panepane Point mid tide core visual description.

FACE LOG

Project:	***Rena* sediment cores**	
Borehole:	**Co-ordinates:** S 37 38.165E 176 09.662	
Site: 4	**Core: Matakana Island Panepane Point high tide**	
Depth (m):	84 cm	

THE UNIVERSITY OF
WAIKATO
Te Whare Wānanga o Waikato

BOX NUMBER	DEPTH (m)	GRAPHIC LOG	**SOIL DESCRIPTION** **SOIL NAME, colour, structure, weathering, strength; moisture condition; plasticity; grading;** **bedding; soil fraction;** **additional observations; geological/pedological name.**	
	1		SAND, Hue 5Y 8/2 light gray, mSU, extremely well sorted. Slight mottled black 8/2 (15%)	
			SAND, Hue 5Y 7/2 crs SL, slightly darker than above, extremely well sorted	
			SAND Hue 5Y 8/3, mSU, with a few brown streaks at 11 cm (Hue 5Y 5/4 yelllowish brown) extremely well sorted	
	2		SAND Hue 5 Y 8/2 light gray, mSU, extremely well sorted.~15% Mottled black 8/2	
	3			
	4		SAND, Hue 5Y 8/2 light gray mSU, very well sorted, titanomagnetite bands 8/3 olive black 2 thick, mostly 2 mm wide with one 2 cm think band at 37.5 cm-39.5 cm	
	5			
	6		SAND, Hue 5Y 7/1 light gray, mSU, very well sorted, mottled black with minor 2 % shell fragments < 2 mm	
	7			
	8		SAND, Hue 5Y 5/1 gray, mSU, very well sorted, band of titanomagnitite but not as dark as on an angle 74 mm to 80 mm on the other side of the core	
			SAND, Hue 5Y 8/2 light gray, mSU, very well sorted, 5% lg shell fragments ~5 mm in size	
	9			

Figure I.8: Matakana Island, Panepane Point high tide core visual description.

FACE LOG

Project: *Rena* sediment cores

Borehole:

    Co-ordinates: S 37 38.583 E176 10.425

Site: 5

    Core: Centre Bank

Depth (m): 71 cm

THE UNIVERSITY OF
WAIKATO
Te Whare Wānanga o Waikato

BOX NUMBER	DEPTH (m)	GRAPHIC LOG	SOIL DESCRIPTION **SOIL NAME, colour, structure, weathering, strength; moisture condition; plasticity; grading; bedding; soil fraction;** **additional observations; geological/pedological name.**	
	1 2 3		SAND, Hue 5Y 7/3, crs SU, very poorly sorted, whole shells < 5 cm and fragments ~5 mm-10 mm, on edge of core at 0-6 cm a gel has formed (silca) binding grains	
	4 5		SAND, Hue 5Y 6/2 grayish olive, crs SL, very poorly sorted, darker than above, whole shells and fragments between 5 mm and 20 mm	
	6		SAND, Hue 5Y 6/1 gray, mSU, moderately sorted, band of whole and large shell fragments at 48-51 ranging between 10-20 mm, also a few silty patches, Hue 5Y 6/1 gray, fSL	
	7 8		SAND, Hue 5Y 6/2 grayish olive, crs SL, poorly sorted, with large shell fragments (10mm), at 64 cm a band of reddish brown sediment, and a few silty patches Hue 5Y 6/1 gray	

Figure I.9: Site 5, Centre Bank core visual description.

FACE LOG

Project: *Rena* sediment cores

Borehole: **Co-ordinates:** S 37 37.840 E 176 10.689

Site: 6 **Core: Mount Maunganui low tide**

Depth (m): 72 cm

THE UNIVERSITY OF
WAIKATO
Te Whare Wānanga o Waikato

BOX NUMBER	DEPTH (m)	GRAPHIC LOG	SOIL DESCRIPTION **SOIL NAME, colour, structure, weathering, strength; moisture condition; plasticity; grading; bedding; soil fraction;** **additional observations; geological/pedological name.**	
	1		SAND,Hue 5Y 6/2 grayish olive, mSU, very well sorted, with minimal black 2/1	
	2		SAND, Hue 5Y 7/2 light gray, crs SU, moderately sorted, contains shell fragments of colour and <15 mm in size	
	3 4 5		SAND, Hue 5Y 6/2 grayish olive, crs SU, very well sorted,with ~2 % shell fragments 5-15 mm, slight colour banding with dark and light stripes ~2 mm thick	
	6 7 8		SAND, Hue 5Y 6/2 grayish olive, crs SL, very well sorted with > <u>crs</u> SU shell fragments in solid bands at 55 cm, 58 cm, and 62 cm 10-20 mm thick. 5 % shell fragments	

Figure I.10: Site 6, Mount Maunganui low tide core visual description.

137

FACE LOG

Project: *Rena* sediment cores

Borehole:

Co-ordinates: S 37 37.844 E 176 10.686

Site: 6

Core: Mount Maunganui mid tide

Depth (m): 76.5 cm

THE UNIVERSITY OF
WAIKATO
Te Whare Wānanga o Waikato

BOX NUMBER	DEPTH (m)	GRAPHIC LOG	SOIL DESCRIPTION **SOIL NAME, colour, structure, weathering, strength; moisture condition; plasticity; grading; bedding; soil fraction;** **additional observations; geological/pedological name.**	
	1		SAND, Hue 5Y 7/1 light gray, mSU, well sorted, shell fragments slightly larger (15%) obvious larger quartz grains	
			SAND, Hue 5Y 7/3 light yellow, crs SU, poorly sorted, shell fragments and whole shells 30-40 mm in size with bands of shell hash throughout, with obvious quartz grains (crs SU)	
	2			
	3			
	4			
	5			
	6		SAND (possibly gravel), Hue 5Y 7/1 light gray, crs SU, very poorly sorted, shell hash, large shell of varying colour, obvious quartz grains (crs SL)	
	7		SAND, Hue 5Y 7/1 light yellow, crs SU, poorly sorted, 30 % Shell fragments < 20 mm in size, obvious quartz grains (crs SL)	
	8			
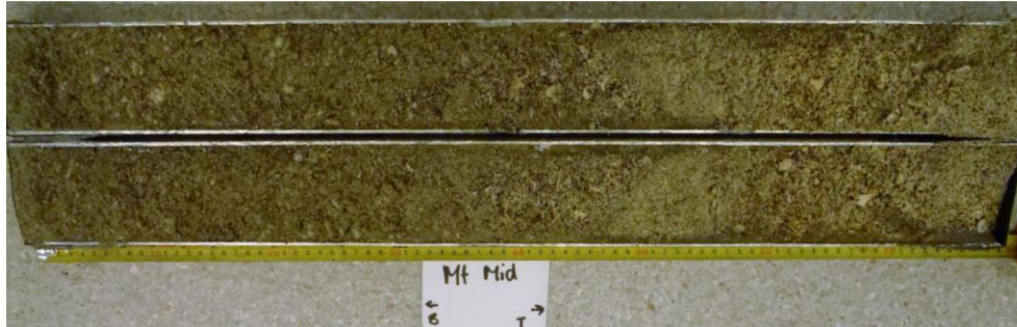
Figure I.11: Site 6, Mount Maunganui mid tide core visual description.

138

FACE LOG

Project: *Rena* sediment cores

Borehole:

Co-ordinates: S 37 37.510 E 176 10.406

Site: 6

Core: Mount Maunganui high tide

Depth (m): 82 cm

THE UNIVERSITY OF
WAIKATO
Te Whare Wānanga o Waikato

BOX NUMBER	DEPTH (m)	GRAPHIC LOG	SOIL DESCRIPTION SOIL NAME, colour, structure, weathering, strength; moisture condition; plasticity; grading; bedding; soil fraction; additional observations; geological/pedological name.	
1	1 2 3		SAND, Hue 5Y 8/2 light gray, crs SL, well sorted, mottled with 2/1 black and small shell	
			SAND, Hue 5Y 8/2 light gray, crs SL, very poorly sorted, shell fragments > 40 mm, 5mm size fragments 20 %, large shell fragments 50 %, sand 30 %	
	4 5 6		SAND, Hue 5Y 8/2 light gray, crs SL, moderately sorted with small shell fragments (~5 mm) amongst crs SL grains, 5% large shells (>1cm)	
			SAND, Hue 5Y 8/2 light gray, crs SL, poorly sorted, small shell fragments (2-5mm) make up shell hash	
7	7		SAND, Hue 5Y 8/2 light gray, crs SL, well sorted, titanomagnetite banding, 5mm wide, 5Y 5/1 gray, every 20 mm	
			SAND, Hue 5Y 8/2 light gray, crs SU, poorly sorted, shell hash band ~5 mm size shells	
8	8		SAND, Hue 5Y 8/2 light gray, crs SL, well sorted, mottled with 2/1 black 10% shell fragments 10 mm in size	
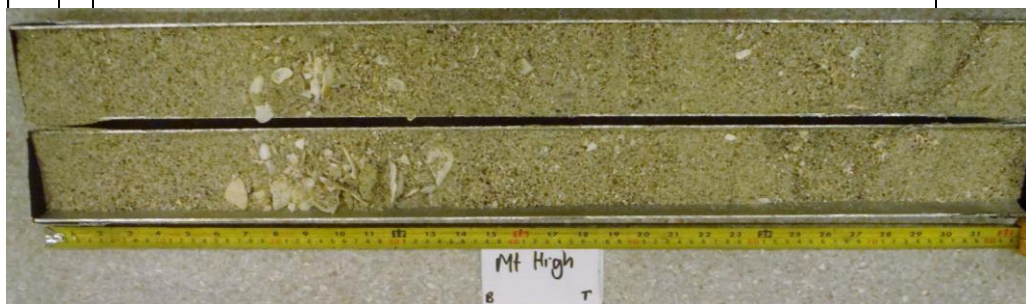
Figure I.12: Site 6, Mount Maunganui high tide core visual description.

139

FACE LOG

Project:	*Rena* **sediment cores**
Borehole:	**Co-ordinates:** S 37 39.508 E 176 12.953
Site: 7	**Core: Omanu mid tide**
Depth (m):	87 cm

THE UNIVERSITY OF
WAIKATO
Te Whare Wānanga o Waikato

BOX NUMBER	DEPTH (m)	GRAPHIC LOG	SOIL DESCRIPTION **SOIL NAME, colour, structure, weathering, strength; moisture condition; plasticity; grading; bedding; soil fraction;** **additional observations; geological/pedological name.**	
	1		SAND, Hue 5Y 7/2 light gray, mSU, extremely well sorted, mottled with 2/1 black titanomagnetite grains	
	2 3 4		SAND, Hue 5Y 6/2, grayish olive, crs SL, very well sorted, grading to coarser and darker grains, mottled 2/1 black, shell fragments crs SL	
	5 6		SAND, Hue 5Y 7/2 light gray, mSU, extremely well sorted, mottled with 2/1 black	
	7 8 9		SAND, Hue 5Y 6/2 grayish olive, mSU, extremely well sorted, mottled with 2/1 black titanomagnetite	

Figure I.13: Site 7, Omanu Beach mid tide core visual description.

FACE LOG

Project: *Rena* sediment cores

Borehole:

Co-ordinates: S 37 39.514 E 176 12.944

Site: 7

Core: Omanu high tide

Depth (m): 121 cm

BOX NUMBER	DEPTH (m)	GRAPHIC LOG	SOIL DESCRIPTION SOIL NAME, colour, structure, weathering, strength; moisture condition; plasticity; grading; bedding; soil fraction; additional observations; geological/pedological name.	
	1		SAND, Hue 5Y 8/1 light gray, mSL, extremely well sorted. Mottled colouring with 2/1 black titanomagnetite grains	
	2			
	3			
	4		SAND, Hue 5Y 7/1 light gray , mSL, extremely well sorted	
	5		SAND, Hue 5Y 8/1 light gray, mSL, extremely well sorted	
	6			
	7		SAND, Hue 5Y 7/1 light gray, mSL, extremely well sorted, banding of lighter 8/1 light gray and darker 7/1 light gray grains in varying widths and angles	
	8			
	9		SAND, Hue 5Y 8/1 light gray, mSL, very well sorted, mottled 2/1 black	
	10			
	11			
	12			

Figure I.14: Site 7, Omanu Beach high tide core visual description.

141

FACE LOG

Project: *Rena* sediment cores

Borehole:

Co-ordinates: S 37 41.412   E 176 16.436

Site: 8

Core: Harrison's low tide

Depth (m):   142 cm

THE UNIVERSITY OF
WAIKATO
Te Whare Wānanga o Waikato

BOX NUMBER	DEPTH (m)	GRAPHIC LOG	SOIL DESCRIPTION
			SOIL NAME, colour, structure, weathering, strength; moisture condition; plasticity; grading; bedding; soil fraction; additional observations; geological/pedological name.

SAND, Hue 5Y 7/2 light gray, crs SL, very well sorted

SAND, Hue 5Y 7/2 light gray, crs SU, very well sorted. Minor shell fragments (2-5%) ranging in size from 2mm-4mm, grading in colour to 8/2 pale yellow with mottling of 2/1 black

SAND, Hue 5Y 7/2 light gray, crs SL, minor titanomagnetite banding (6/1), extremely well sorted a defined titanomagnetite band (2/1) at 114 cm, 5mm wide

SAND, Hue 5Y 7/2 light gray, crs SU, moderately sorted, shell fragments & whole shells >5mm

SAND, Hue 5Y 6/1 gray, crs SU, extremely well sorted

SAND, Hue 5Y 7/2 light gray, crs SU, shell fragments and whole shells (2%) >5mm

Figure I.15: Site 8, Harrison's Cut low tide core visual description.

FACE LOG

Project: *Rena* sediment cores

Co-ordinates: S 37 41.416 E 176 16.430

site: 8

Core: Harrison's mid tide

Depth (m): 120 cm

THE UNIVERSITY OF
WAIKATO
Te Whare Wānanga o Waikato

BOX NUMBER	DEPTH (m)	GRAPHIC LOG	SOIL DESCRIPTION **SOIL NAME, colour, structure, weathering, strength; moisture condition; plasticity; grading; bedding; soil fraction;** **additional observations; geological/pedological name.**
	1 2		SAND, Hue 5Y 7/3 light yellow, with 2/1 black mottling, mSU, very well sorted with sparse (1%) shell fragments <12mm in size.
	3 4		SAND, Hue 5Y 8/4 pale yellow, and 2/1 mSU, very well sorted, small, slightly yellower patch on one side of the core at 31-34cm 34cm 31cm
	5 6		SAND, Hue 5Y 7/3 light yellow, mSU, very well sorted, sparse shell fragments (5%) and whole shells <12mm
	7 8		SAND, Hue 5Y 6/1 gray, crs SU with 2/1 black particles, darker than above, moderately sorted. Shell fragments and whole shells <6mm in moderate amounts (20%)
	9		SAND, Hue 5Y 7/3 light yellow with 2/1 black grains (10%), poorly sorted. shell fragments and whole shells <20mm in size (20%)
	10 11		SAND, Hue 5Y 6/1 gray, darker than above, poorly sorted. Shell fragments and whole shells at <20mm in size
	12		SAND, Hue 5Y 6/2 grayish olive with 2/1 black, well sorted

Figure I.16: Site 8, Harrison's Cut mid tide core visual description.

143

FACE LOG

Project: **Rena beach sediments: Harrison's High**

Borehole: **Co-ordinates:**   S 37 41.442 E 176 16.425

Site: 8   **Grid:**

Depth (m):   114 cm

THE UNIVERSITY OF
WAIKATO
Te Whare Wānanga o Waikato

BOX NUMBER	DEPTH (m)	GRAPHIC LOG	SOIL DESCRIPTION — SOIL NAME, colour, structure, weathering, strength; moisture condition; plasticity; grading; bedding; soil fraction; additional observations; geological/pedological name.	
	1		SAND, Hue 5Y 7/2 light gray, crs SL, extremely well sorted, light and black (2/1) mottling, dry	
	2–4		SAND, Hue 5Y 7/2 light gray, crs SL, extremely well sorted, mottling. Slightly darker than above maybe due to being wet.	
	5		SAND, Hue 5Y 6/1 gray, crs SL, moderately sorted, contains 5% large shell fragments <10mm	
	6		SAND, Hue 5Y 6/1 gray, crs SL, moderately sorted, no shell fragments	
	7		SAND, Hue 5Y 6/1 gray, crs SU, moderately sorted, 10% shell fragments and whole shells	
	8		SAND, Hue 5Y 6/1 gray, crs SL, well sorted, no obvious shell fragments	
	9		SAND, Hue 5Y 6/1 gray, moderately sorted with crs SL and crs SU grains	
	10–11		SAND, Hue 5Y 6/1 gray, crs SU, well sorted. Slighty finer grains then above and better sorted	
	12			

Figure I.17: Site 8, Harrison's Cut high tide core visual description.

FACE LOG

Project: *Rena* sediment cores

Borehole:

Co-ordinates: S 37 42.371 E 176 19.391

Site: 9

Core: Taylor's low tide

Depth (m): 84 cm core

THE UNIVERSITY OF
WAIKATO
Te Whare Wānanga o Waikato

BOX NUMBER	DEPTH (m)	GRAPHIC LOG	SOIL DESCRIPTION SOIL NAME, colour, structure, weathering, strength; moisture condition; plasticity; grading; bedding; soil fraction; additional observations; geological/pedological name.	
	1		SAND , Hue 5Y 6/2 gray, mSU, extremely well sorted, mottled with 2/1 black but, only slightly	
	2		SAND, Hue 5Y 6/2 gray, crs SU, moderately sorted with shell fragments <10mm in size at 2% shell colours: 5Y 8/3, 3/1, 7/4 and 2.5Y 8/6 yellow and 5YR 6/6 orange	
	3			
	4			
	5			
	6		CLAY, Hue 5Y 7/4 light yellow, fSL, extremely well sorted, 2mm (clay or silt).	
			SAND, Hue 5Y 6/2 grayish olive, crs SU, moderately sorted with 10% shell fragments <10mm	
	7		CLAY, Hue 5Y 7/4 light yellow, fSL, extremely well sorted, 2mm (clay or silt).	
			SAND, Hue 5Y 6/2 grayish olive, crs SU, moderately sorted with 10% shell fragments <10mm	
	8		SAND, Hue 5Y 6/2 grayish olive, crs SU, moderately sorted, 5% shell fragments at <10mm	
	9			
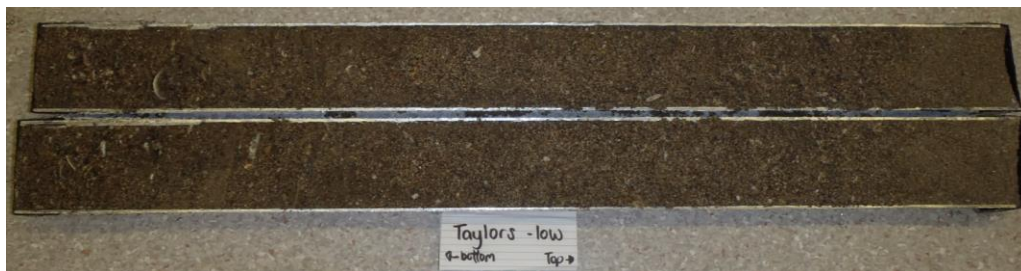
Figure I.18: Site 9, Taylor's Reserve low tide core visual description.

145

FACE LOG

Project:	***Rena* sediment cores**
Borehole:	**Co-ordinates:** S 37 42.603 E 176 19.636
Site: 9	**Core: Taylor's mid tide**
Depth (m):	64 cm

THE UNIVERSITY OF
WAIKATO
Te Whare Wānanga o Waikato

BOX NUMBER	DEPTH (m)	GRAPHIC LOG	SOIL DESCRIPTION **SOIL NAME, colour, structure, weathering, strength; moisture condition; plasticity; grading; bedding; soil fraction;** **additional observations; geological/pedological name.**	
	1		SAND, Hue 5Y 6/1 gray, crs SL, very well sorted, very minor colour changes of 10mm banding between 38-52cm	
	2			
	3			
	4			
	5			
	6		SAND , Hue 5Y 6/2 grayish olive, crs SU, very well sorted, larger grains than above	
	7			
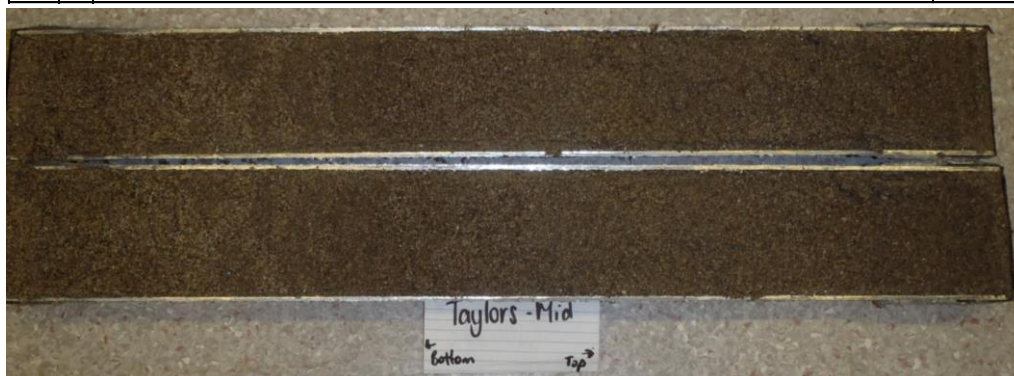
Figure I.19: Site 9, Taylor's Reserve mid tide core visual description.

146

FACE LOG

Project: *Rena* sediment cores

Co-ordinates: S 37 42.620 E 176 19.653

THE UNIVERSITY OF
WAIKATO
Te Whare Wānanga o Waikato

site: 9

Core: Taylor's high tide

Depth (m): 86cm

BOX NUMBER	DEPTH (m)	GRAPHIC LOG	SOIL DESCRIPTION **SOIL NAME, colour, structure, weathering, strength; moisture condition; plasticity; grading; bedding; soil fraction;** **additional observations; geological/pedological name.**	
	1		SAND, 5Y 7/3 light yellow, mSU, very well sorted with 2% larger grains and shell fragments 2-3mm in size	
			SAND, Hue 5Y 7/2 light gray, mSL, slightly lighter than above, extremely well sorted	
	2		SAND, 5Y 7/3 light yellow, mSU, extremely well sorted, slightly darker striations ~2-4mm wide	
	3			
	4			
	5			
	6			
	7		SAND, 5Y 7/2 light gray, mSU, extremely well sorted, lighter than above	
	8		SAND, 5y 7/3 light yellow, mSU, extremely well sorted	
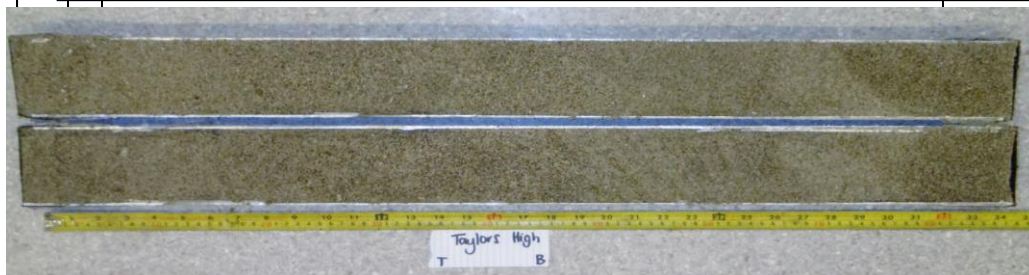
Figure I.20: Site 9, Taylor's Reserve high tide core visual description.

FACE LOG

Project: *Rena* sediment cores

Borehole:

    Co-ordinates: S 37 44.860 E 176 24.975

Site: 10

    Core: Maketu-Ford Road mid tide

Depth (m): 82 cm

THE UNIVERSITY OF
WAIKATO
Te Whare Wānanga o Waikato

BOX NUMBER	DEPTH (m)	GRAPHIC LOG	SOIL DESCRIPTION SOIL NAME, colour, structure, weathering, strength; moisture condition; plasticity; grading; bedding; soil fraction; additional observations; geological/pedological name.	
	1		SAND, 5Y 5/2 grayish olive, crs SU, very well sorted, < 1 % shell fragments up to 15 mm ~1-3 mm wide	
	2			
	3			
	4			
	5			
	6			
	7		SAND, Hue 5Y 5/2 grayish olive, crs SL, very sell sorted with 2/1 black titanomagnetite banding	
	8		SAND, Hue 5Y 5/2 grayish olive, crs SU, extremely well sorted	
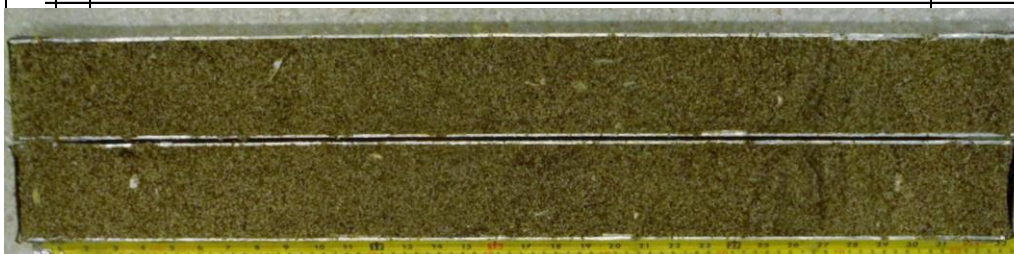
Figure I.21: Site 10, Maketu Ford Road (Kaituna Cut) mid tide core visual description.

FACE LOG

Project: *Rena* sediment cores

Borehole: **Co-ordinates:** S 37 44.866 E 176 24.975

Site: 10   **Core: Maketu- Ford Road high tide**

Depth (m): 69 cm

THE UNIVERSITY OF
WAIKATO
Te Whare Wānanga o Waikato

BOX NUMBER	DEPTH (m)	GRAPHIC LOG	SOIL DESCRIPTION **SOIL NAME, colour, structure, weathering, strength; moisture condition; plasticity; grading; bedding; soil fraction;** additional observations; geological/pedological name.

SAND, Hue 5Y 6/3 olive yellow, crs SL, very well sorted with 2/1 black mottling, sparse (2 %) < 2 cm shell fragments and small shells

SAND, Hue 5Y 6/3 olive yellow, crs SL, very well sorted with 10 % wood pieces > 40 mm

SAND, Hue 5Y 6/3 olive yellow, crs SL, very well sorted, with 2/1 black thick bands throughout 42-45 cm a 2/1 black band wider on one side then the other 40-47cm

banding 2/1 black again at 50-56 cm
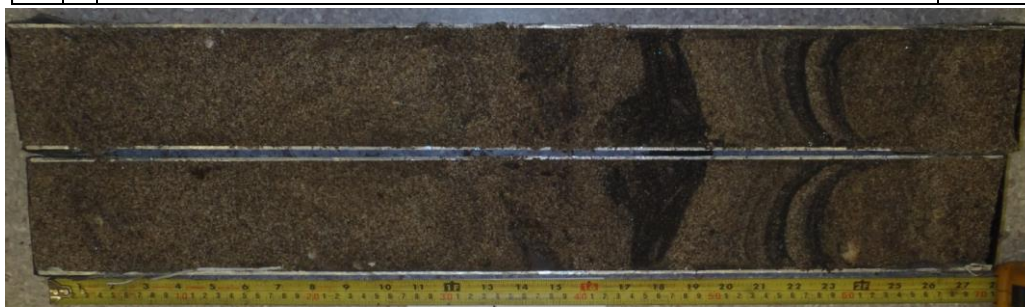
Figure I.22: Site 10, Maketu Ford Road (Kaituna Cut) high tide core visual description.

149

FACE LOG

Project: *Rena* sediment cores

Borehole:

Co-ordinates: S 37 45.263 E 176 26.985

Site: 11

Core: Maketu Spit mid tide

Depth (m): 95 cm

THE UNIVERSITY OF
WAIKATO
Te Whare Wānanga o Waikato

BOX NUMBER	DEPTH (m)	GRAPHIC LOG	SOIL DESCRIPTION **SOIL NAME, colour, structure, weathering, strength; moisture condition; plasticity; grading; bedding; soil fraction;** additional observations; geological/pedological name.	
	1		SAND, Hue 5Y 6/2 grayish olive with 2/1 black patch on one side of core, mSL, extremely well sorted, titanomagnetite	
	2		SAND, Hue 5Y 6/2 grayish olive, mSL, extremely well sorted, with patches of darker and lighter shades (wet)	
	3		SAND, Hue 5Y 6/2 grayish olive, mSU, very well sorted with patches of 7/4 light yellow, crs SL	
	4		SAND, Hue 5Y 6/2 grayish olive, mSU, very well sorted with a 2 mm thick 2/1 band 36 - 44 cm (on angle)	
	5		SAND, Hue 5Y 6/2 grayish olive, mSU, very well sorted, with straiations of 7/4 light yellow, crs	
	6		SAND, Hue 5Y 8/1 light gray, crs SL,well sorted, with 2/1 black obvious laminations ~2-3mm wide with 5-10 mm spacings, with obvious quartz grains	
	7		SAND, Hue 5Y 8/1 light gray, crs SU, well sorted, coarsening and yellowing to 5Y 8/2 light gray and crs SL, few ~ 5 % shell fragments ~5 mm with same size dark rocks and quartz	
	8			
	9		SAND, Hue 5Y 7/1 light gray, crs SL, well sorted, minor shell fragments 5 %, 2 mm in size	
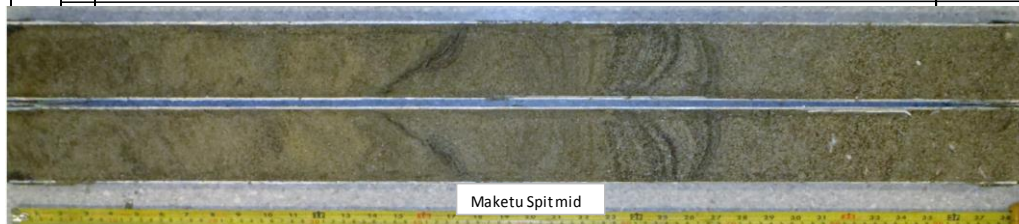
Maketu Spit mid

Figure I.23: Site 11, Maketu Spit mid tide core visual description.

150

FACE LOG

Project: *Rena* **sediment cores**

Borehole: **Co-ordinates:** S 37 45.271 E 176 26.985

Site: 11   **Grid: Maketu Spit high tide**

Depth (m):   91 cm

BOX NUMBER	DEPTH (m)	GRAPHIC LOG	SOIL DESCRIPTION **SOIL NAME, colour, structure, weathering, strength; moisture condition; plasticity; grading; bedding; soil fraction;** **additional observations; geological/pedological name.**	
	1		SAND, Hue 5Y 5/1 gray, mSU, extremely well sorted, mottled with titanomagnetite	
			SAND, Hue 5Y 7/1 light gray, mSU, extremely well sorted	
	2		SAND, Hue 5Y 4/2 grayish olive, mSU, extremely well sorted, patches of 2/1 black and 4/1 lighter patches, solid band of 2/1 black 30 mm thick at 27-30 cm	
	3			
	4		SAND, Hue 5Y 7/2 light gray, crs SL, very well sorted with ~5% shell fragments crs SU in size	
	5		SAND, Hue 5Y 2/1 black titanomagnetite banding, with 7/2 light gray inbetween, crs SL, very well sorted	
	6		SAND, Hue 5Y 4/2 grayish olive, crs SL, well sorted with ~ 10 % shell fragments crs SU in size mottled and patchy 5Y 4/2- 70% and 7/2 light gray 30%	
	7			
	8		SAND, Hue 5Y 8/2 light gray, crs SL, very well sorted, grading to mSU and darkening to 5Y 6/1 gray, at the base as it fines	
	9			

Figure I.24: Site 11, Maketu spit high tide core visual description.

151

FACE LOG

Project:	***Rena* sediment cores**
Borehole:	**Co-ordinates:** S 37 45.428 E 176 27.088
Site: 12	**Core: Maketu Estuary 1**
Depth (m):	65 cm

THE UNIVERSITY OF
WAIKATO
Te Whare Wānanga o Waikato

BOX NUMBER	DEPTH (m)	GRAPHIC LOG	SOIL DESCRIPTION **SOIL NAME, colour, structure, weathering, strength; moisture condition; plasticity; grading; bedding; soil fraction; additional observations; geological/pedological name.**	
1	1		SAND, Hue 5Y 6/3 olive yellow, crs SL, well sorted, slight colour variation in first 10 cm with and light patches, crs SL shell fragments ~5 %	
	2		SAND, Hue 5Y 5/2 grayish olive, mSU, well sorted, shell fragments ~10 %, crs SL in size	
	3		SAND, Hue 5Y 8/3 pale yellow, crs SU, moderately sorted, shell fragments, crs SU & crs SL patch, yellow band 2 cm wide	
			SAND, 5Y 8/3 olive yellow, crs SL, moderately sorted with 5mm shell fragments ~5 %	
	4		ORGANIC, wood or seaweed, Hue 5Y 3/2 2/1 dark brown to black, white stones scattered possibly seeds or pumice ~crs SU 10 %	
			SAND, Hue 5Y 6/1 gray, crs SL, well sorted, high quartz content	
	5		SAND, Hue 5Y 6/1, mSL, extremely well sorted, 1mm wide brown bands (iron rich) at 51 and not extending across entire width of core. Slight striations	
	6			
	7		SAND, Hue 5Y 6/1 gray, crs SU, well sorted, quartz and shell fragments ~5 % at < 5 mm	
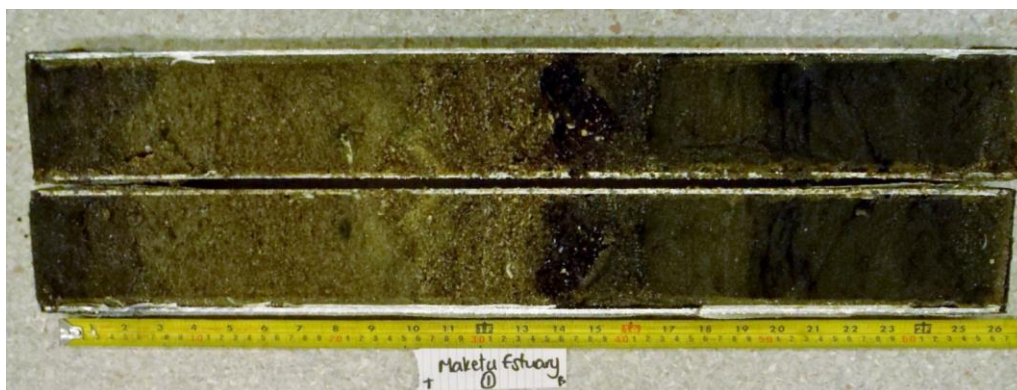
Figure I.25: Maketu Estuary #1 core visual description.

FACE LOG

Project: *Rena* sediment cores

Borehole:

    Co-ordinates: S 37 45.412 E 176 27.053

Site: 12

    Core: **Maketu Estuary 2**

Depth (m):   72 cm

THE UNIVERSITY OF
WAIKATO
Te Whare Wānanga o Waikato

BOX NUMBER	DEPTH (m)	GRAPHIC LOG	SOIL DESCRIPTION **SOIL NAME, colour, structure, weathering, strength; moisture condition; plasticity; grading; bedding; soil fraction;** **additional observations; geological/pedological name.**	
	1		SAND, Hue 5Y 2/1 black 70%, 6/2 grayish olive 30%, mSL, very well sorted	
			SAND, Hue 5Y 6/3 olive yellow, crs SU, moderately sorted, mottled slightly with 2/1 black and quartz, 15 % shell fragments and whole shells 20 mm in size	
	2			
	3		SAND, Hue 5Y 6/1 gray, crs SL, well sorted, almost looks banded with minor 1-2 mm bands of lighter and darker shades	
	4		SAND, Hue 5Y 7/1 light gray, crs SU, and crs SL, moderately sorted, strongly mottled with 2/1 black and quartz, < 40 mm shell fragments 20 %	
	5			
	6			
	7			

Figure I.26: Maketu Estuary #2 core visual description.

9.2 APPENDIX II: GRAIN SIZE ANALYSIS

Summary statistics as graphs, from laser sizing of sediment cores.
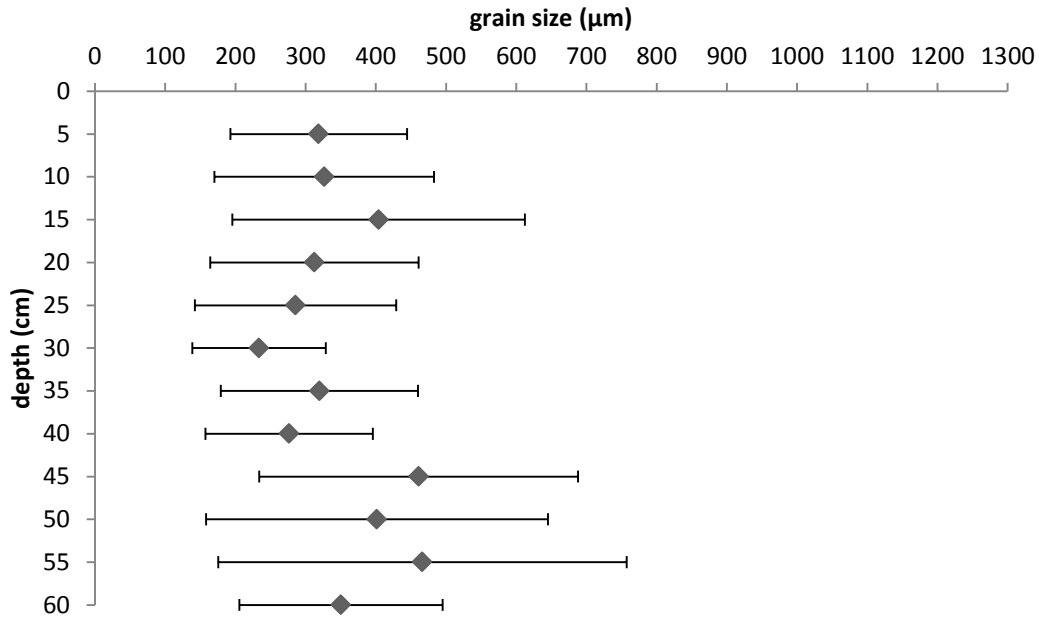
Figure II.27:Grain size results for site 1, the mid tide core at Waihi Beach, Waihi with the error bars showing standard deviation.
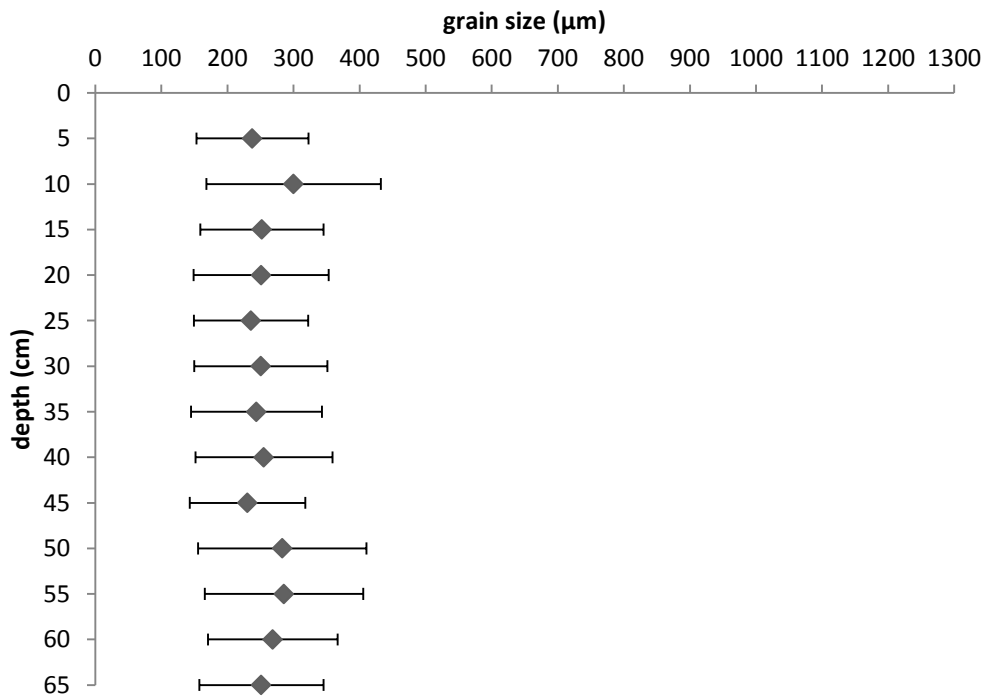
Figure II.28: Grain size results for site 1, the high tide core at Waihi Beach, Waihi with the error bars showing standard deviation.

154
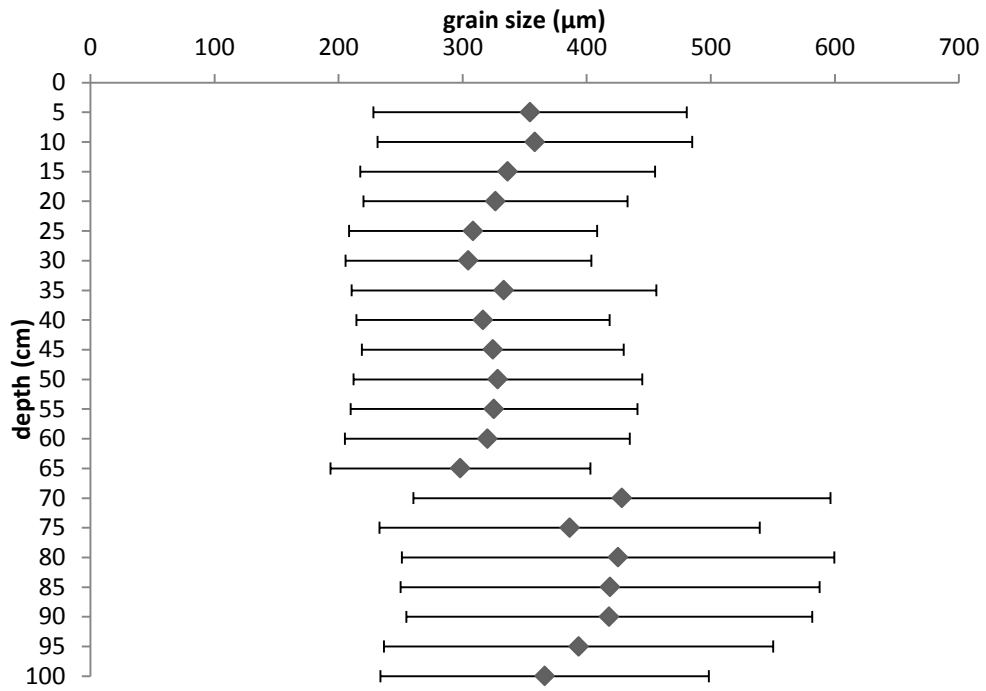
Figure II.29:Grain size results for site 2, the mid tide core at Bowentown Beach, Waihi with the error bars showing standard deviation.
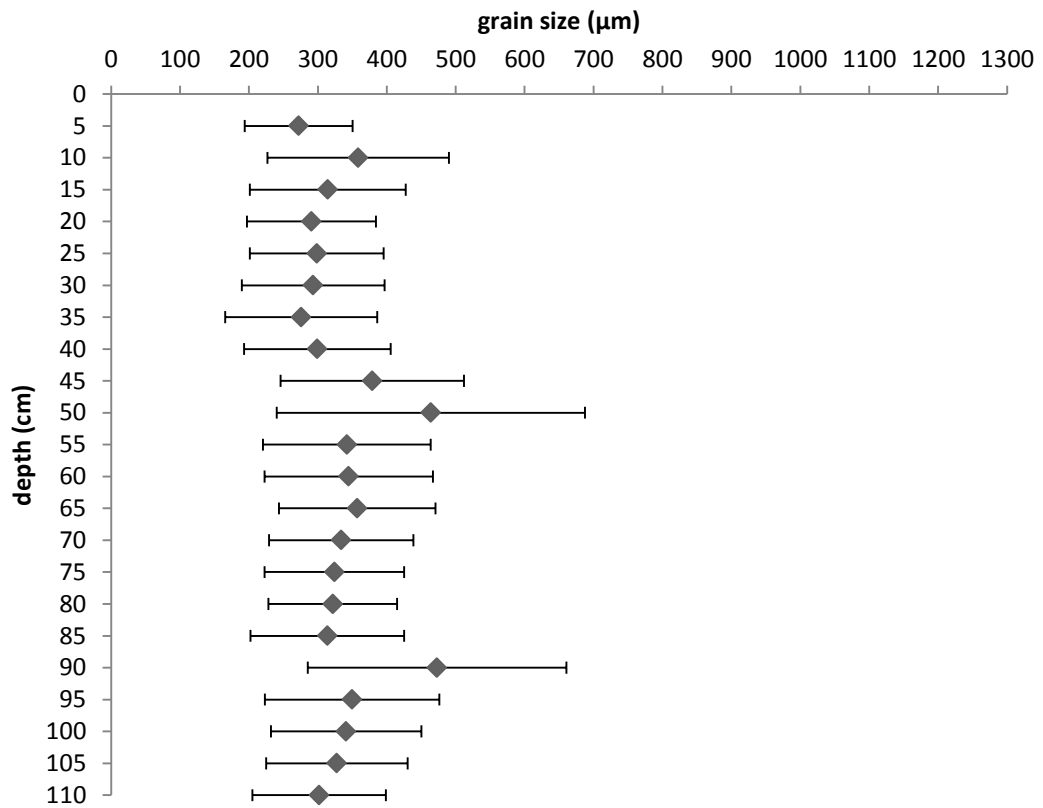
Figure.II.30: Grain size results for site 2, the high tide core at Bowentown Beach, Waihi with the error bars showing standard deviation.
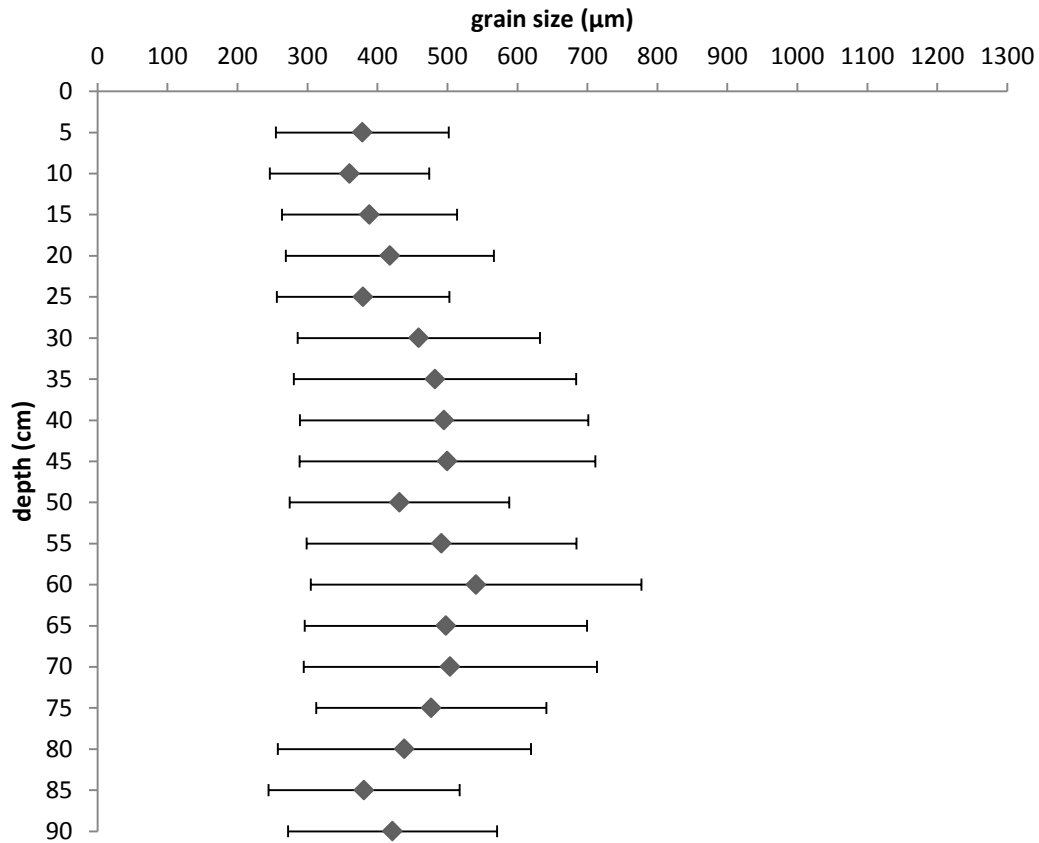
Figure II.31: Grain size results for site 3, the mid tide core at Tank Road, Makatana Island with the error bars showing standard deviation.
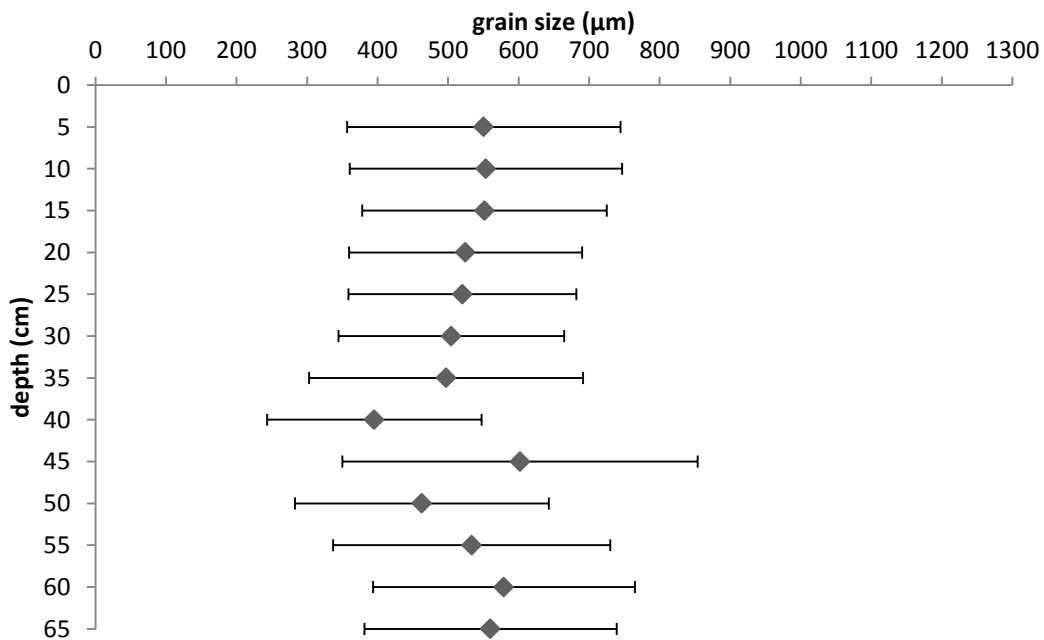
Figure II.32: Grain size results for site 3, the high tide core at Tank Road, Makatana Island with the error bars showing standard deviation.

156
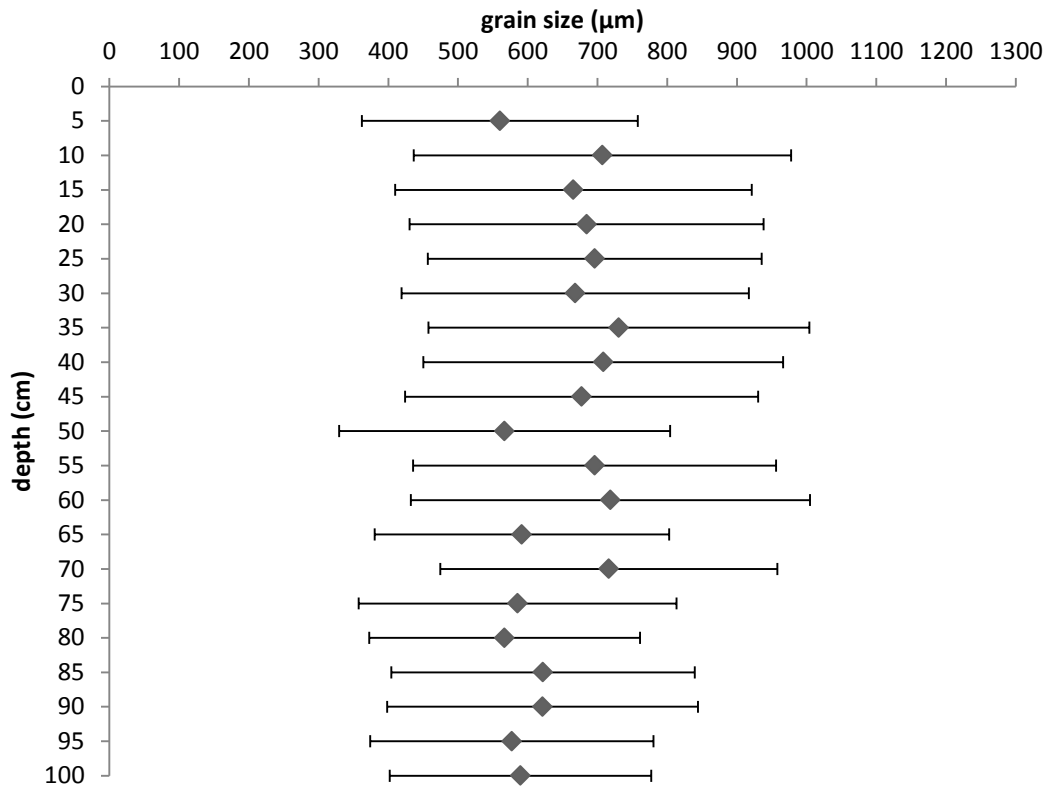
Figure II.33: Grain size results for site 4, the mid tide core at Panepane Point, Makatana Island with the error bars showing standard deviation.
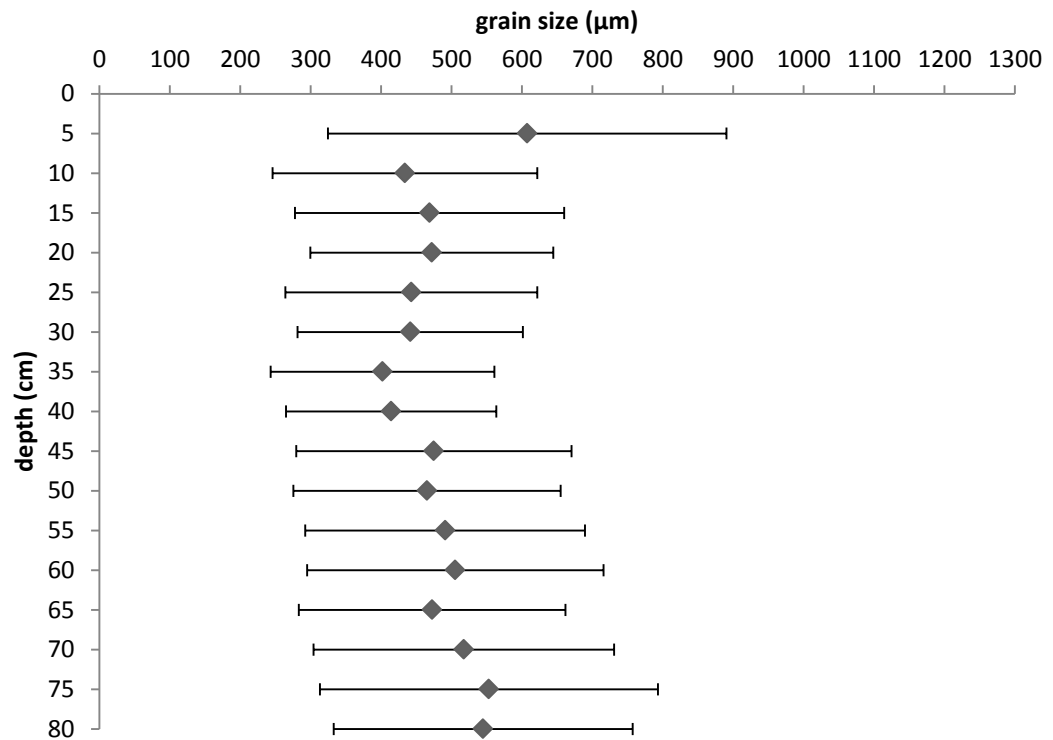
Figure II. 34: Grain size results for site 4, the high tide core at Panepane Point, Makatana Island with the error bars showing standard deviation.
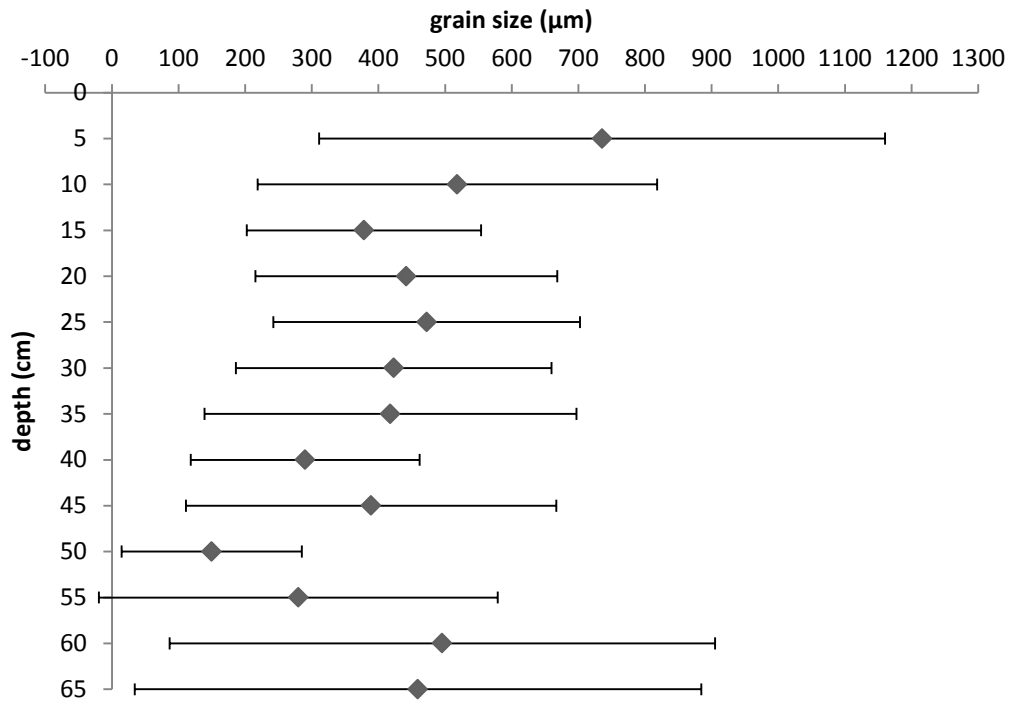
Figure II.35: Grain size results for site 5, the core at Centre Bank , Tauranga Harbour with the error bars showing standard deviation.
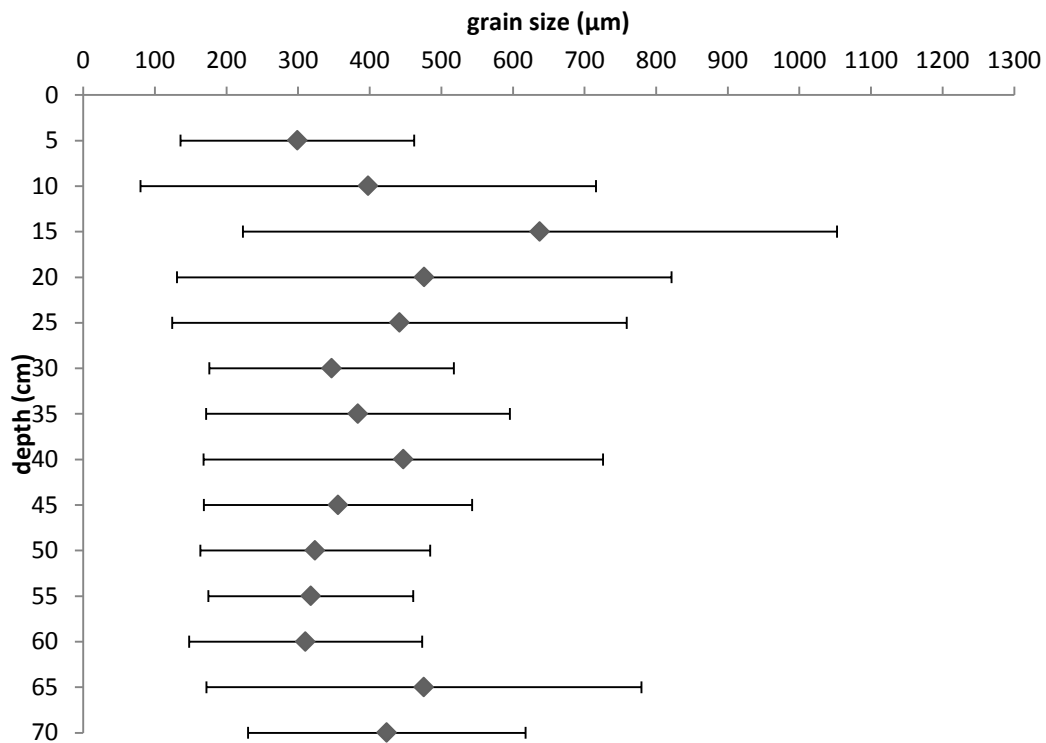
Figure II.10: Grain size resluts for site 6, the low tide core at Mt Maunganui beach , Tauranga with the error bars showing standard deviation.
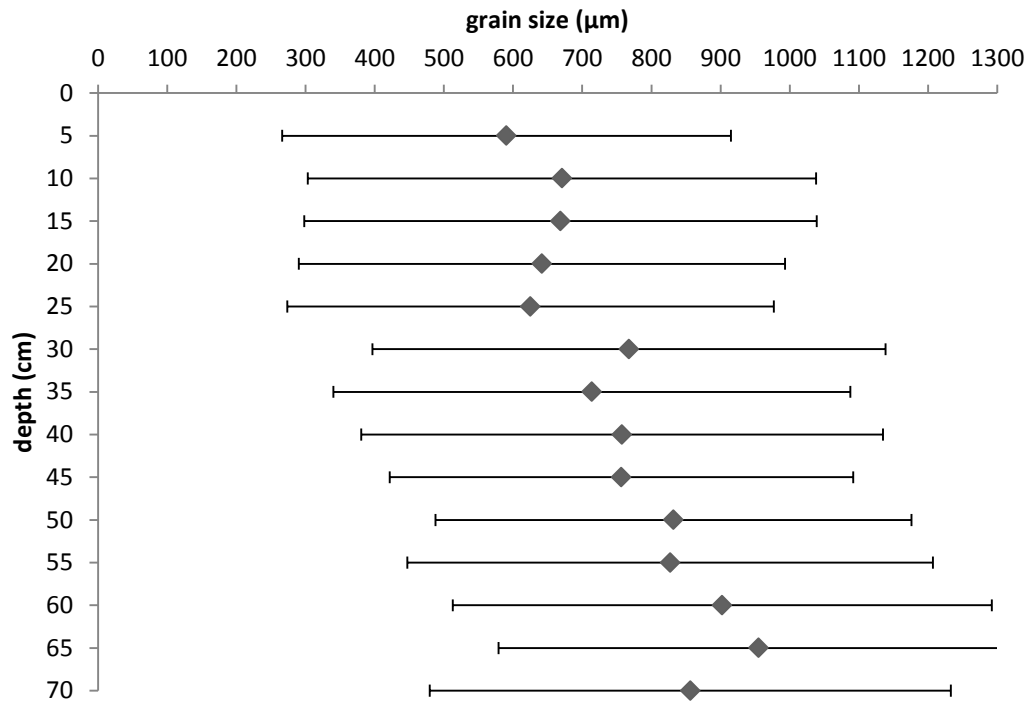
Figure II.11: Grain size results for site 6, the mid tide core at Mt Maunganui beach , Tauranga with the error bars showing standard deviation.
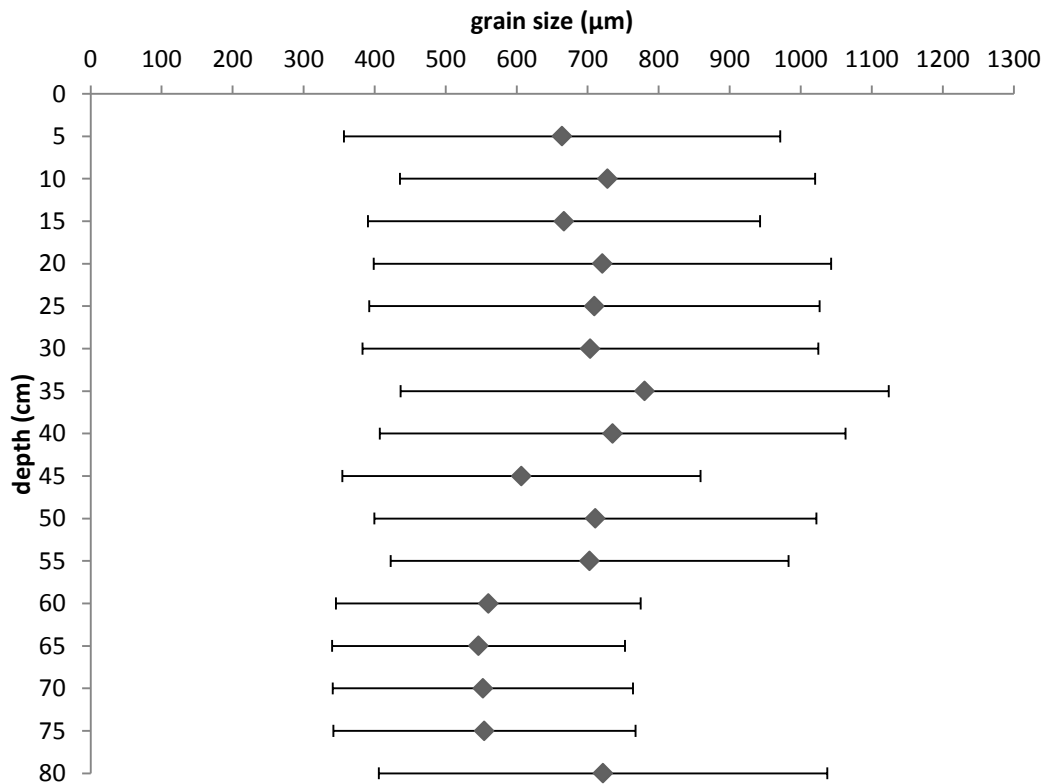
Figure II.12: Grain size results for site 6, the high tide core at Mt Maunganui beach , Tauranga with the error bars showing standard deviation.

159
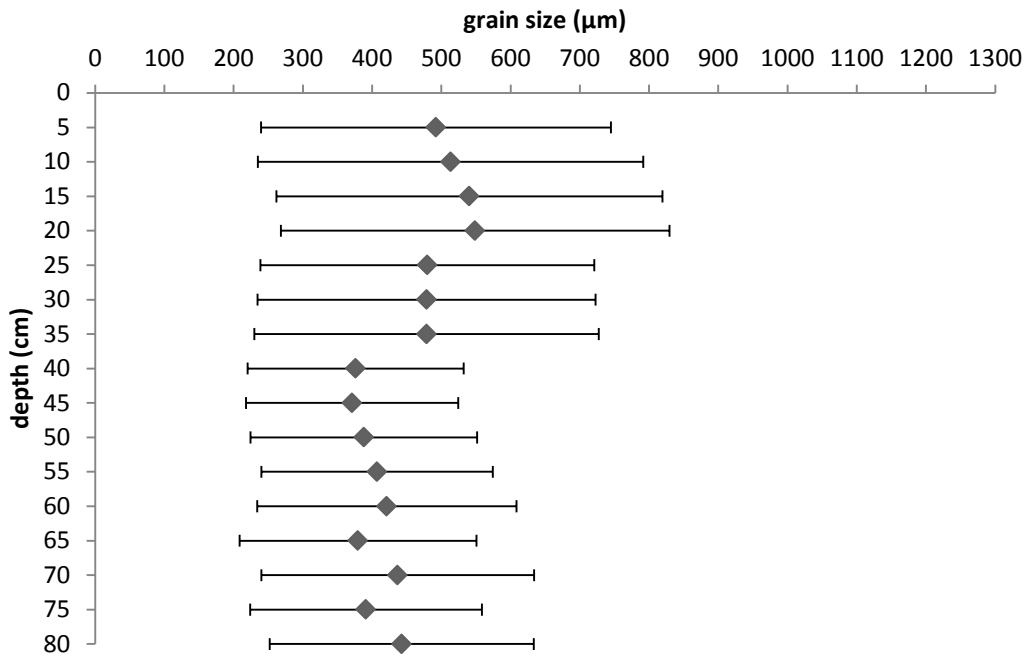
Figure II.13: Grain size results for site 7, the mid tide core at Omanu Surf Club, Papamoa, Tauranga with the error bars showing standard deviation.
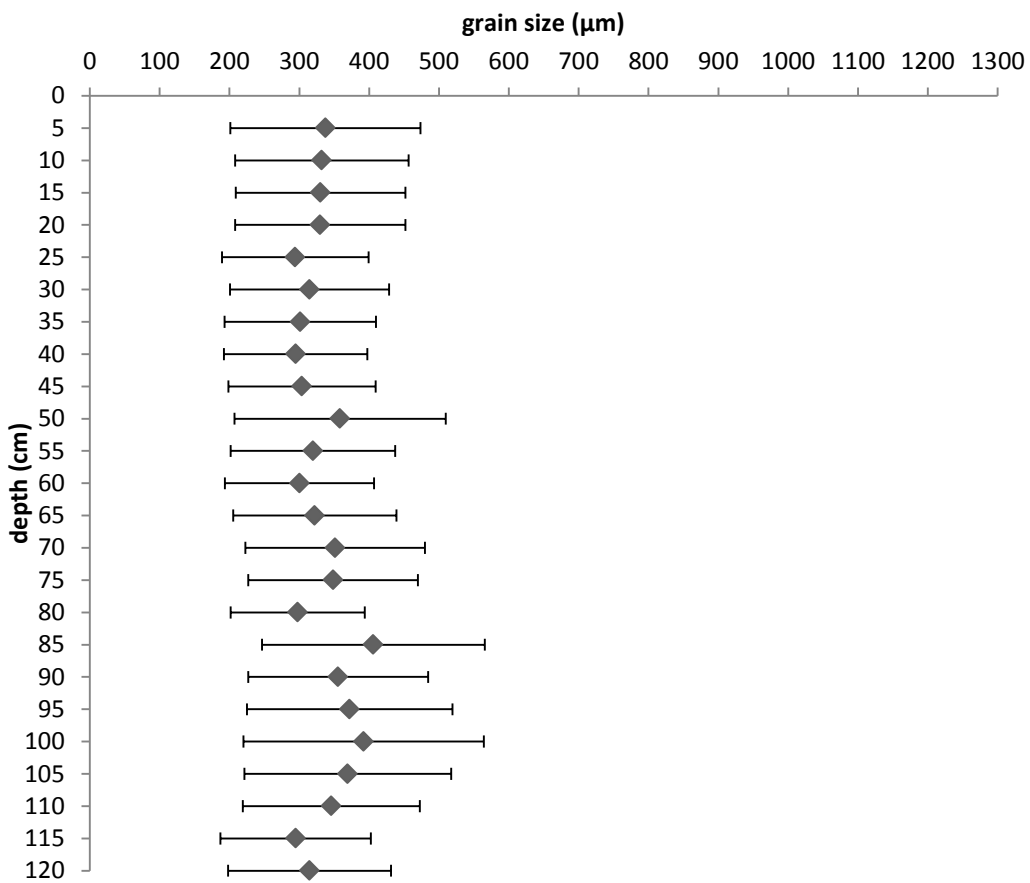
Figure II.14: Grain size results for site 7, the high tide core at Omanu Surf Club, Papamoa, Tauranga with the error bars showing standard deviation.
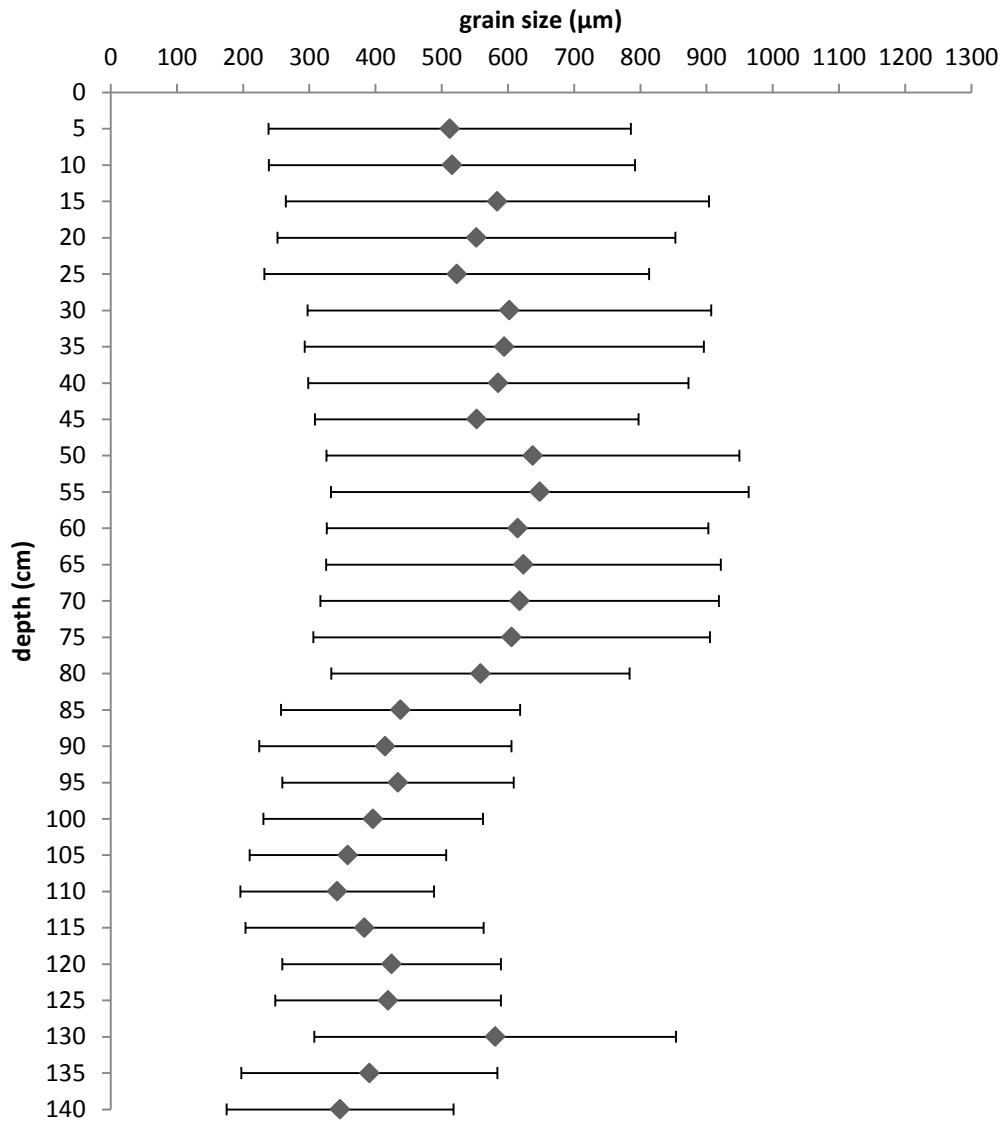
Figure II.15: The grain size for site 8, the low tide core at Harrision's Cut, Papamoa, Tauranga with the error bars showing standard deviation
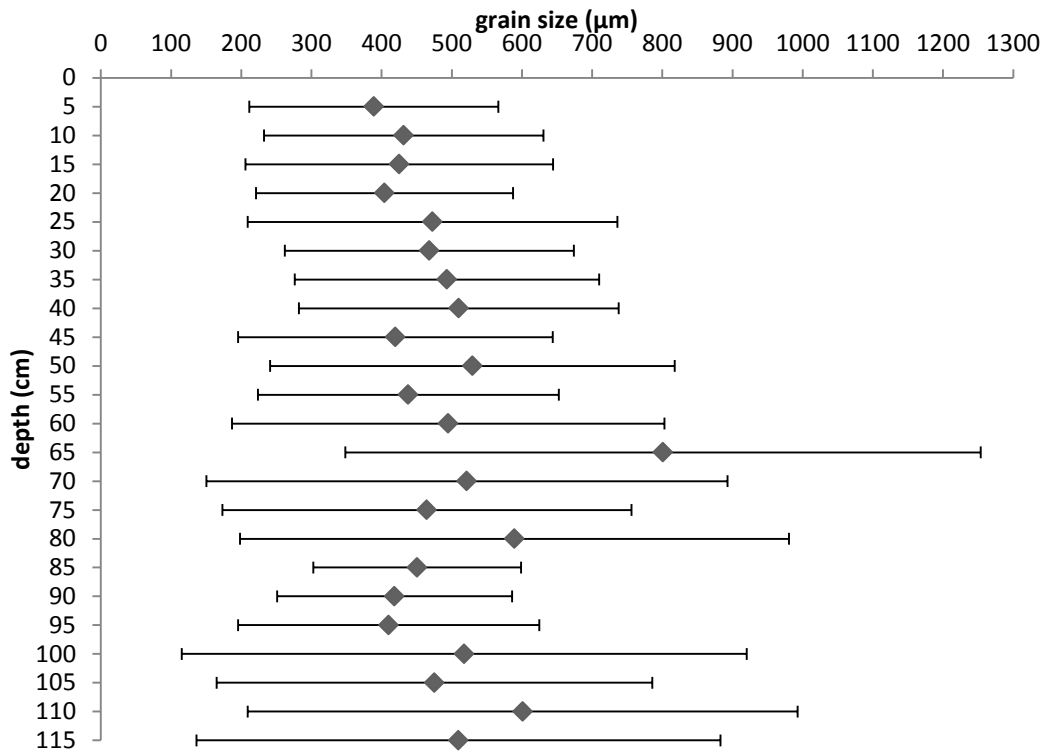
Figure II.16: The grain size for site 8, the mid tide core at Harrision's Beach, Papamoa, Tauranga with the error bars showing standard deviation.
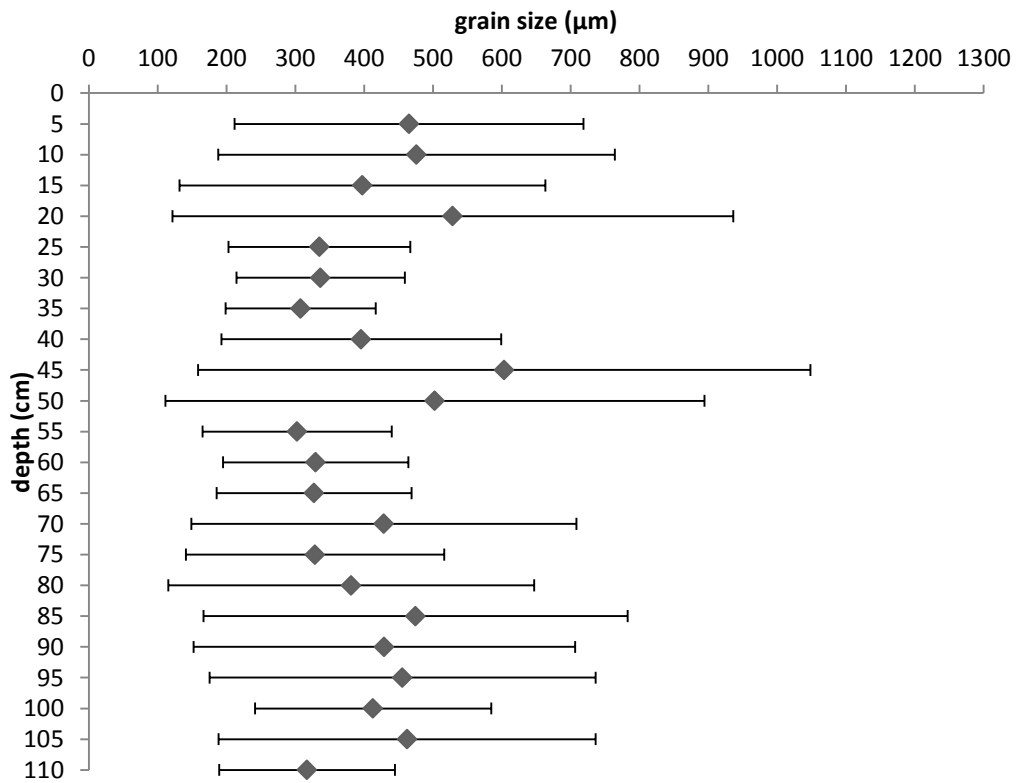
Figure II.17: The mean grain size for site 8, the high tide core at Harrision's Beach, Papamoa, Tauranga with the error bars showing standard deviation.

162
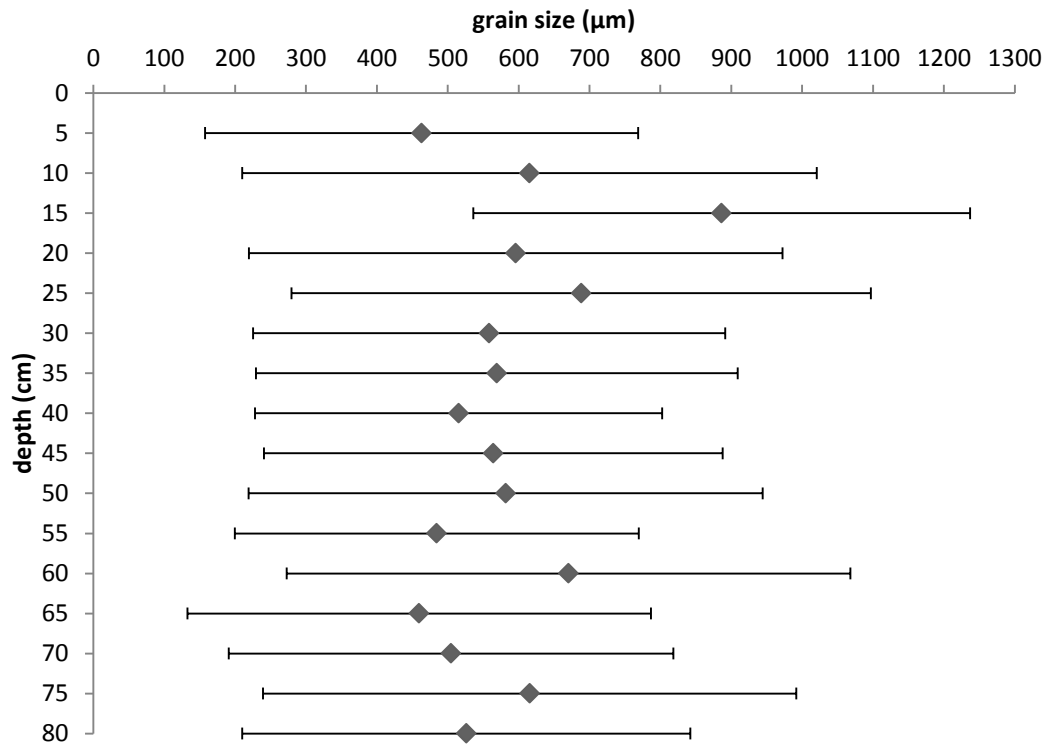
Figure II.18: The grain size for site 9, the low tide core at Taylor's Beach, Papamoa, Tauranga with the error bars showing standard deviation.
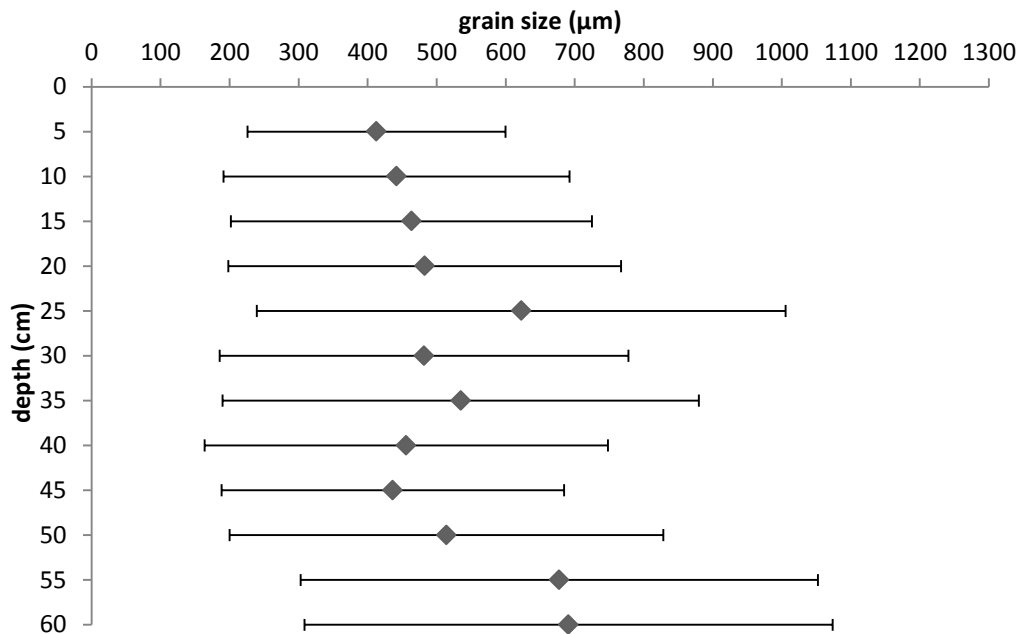
Figure II.19: The grain size for site 9, the mid tide core at Taylor's Beach, Papamoa, Tauranga with the error bars showing standard deviation.
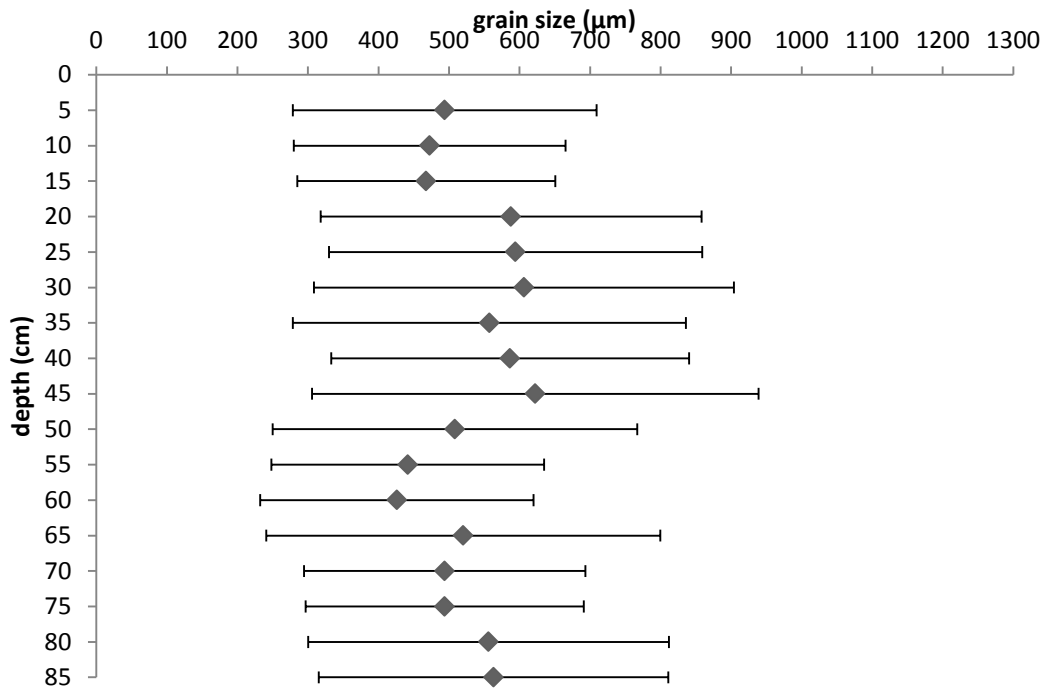
Figure II.20: The grain size for site 9, the high tide core at Taylor's Beach, Papamoa, Tauranga with the error bars showing standard deviation.
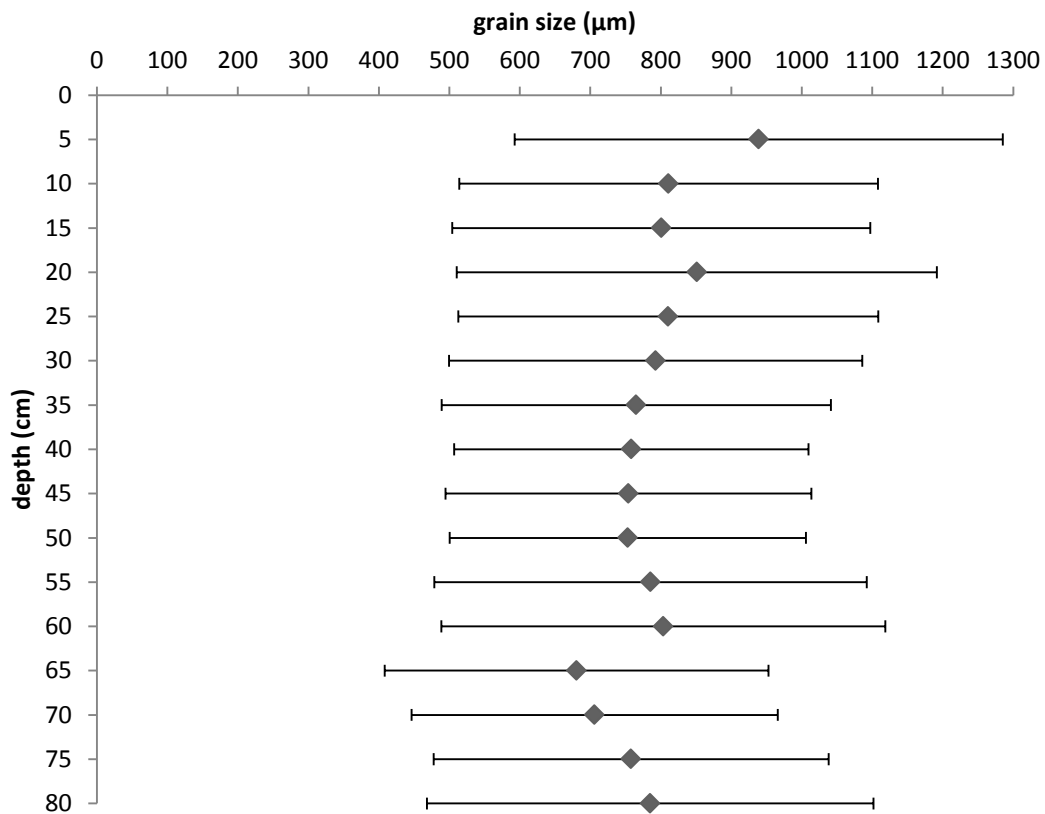
Figure II.21: Grain size results for site 1II, the mid tide core at Ford Road, Maketu with the error bars showing standard deviation.
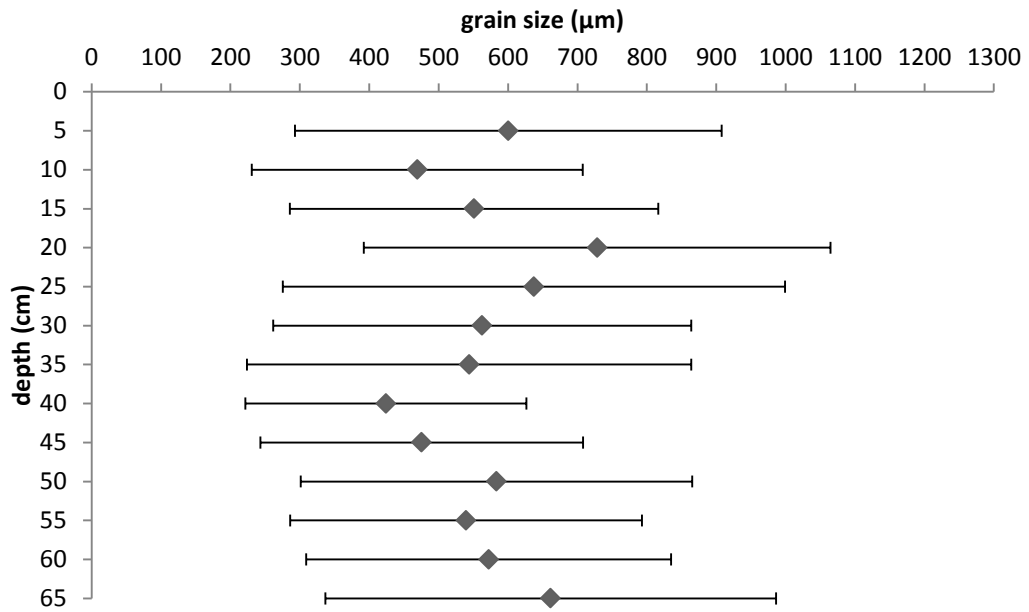
Figure II.22: Grain size results for site 1II, the high tide core at Ford Road, Maketu with the error bars showing standard deviation.
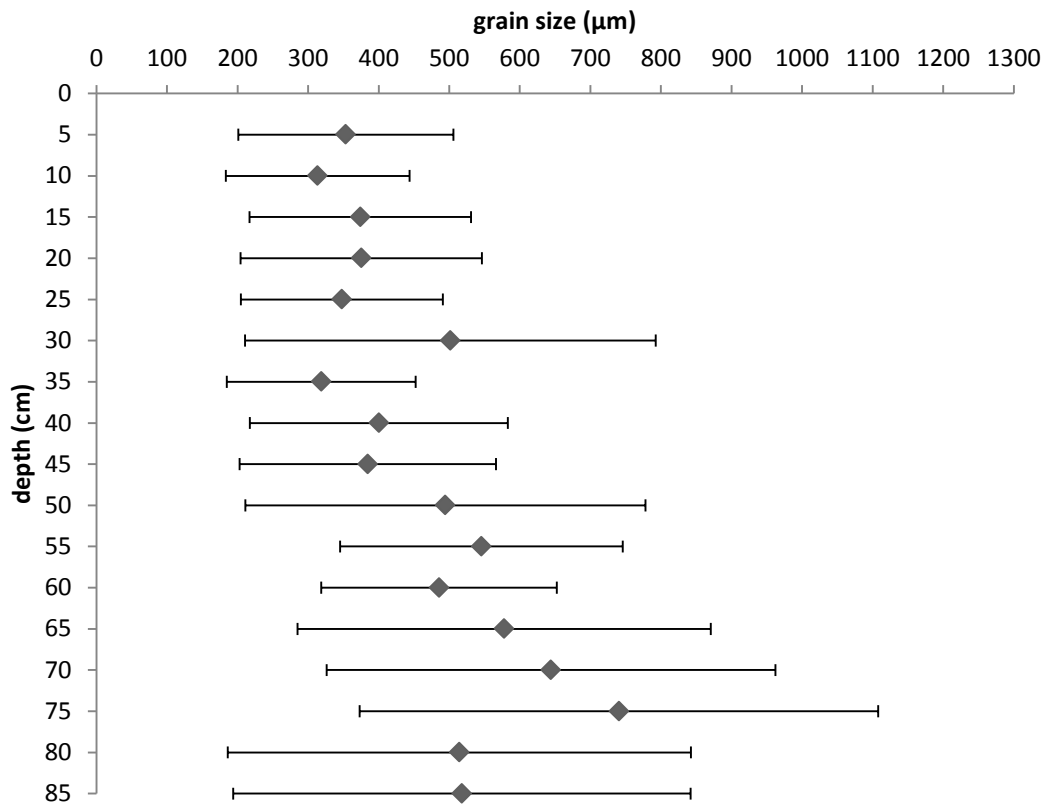
Figure II.23: Grain size results for site 11, the mid tide core at Maketu Spit, Maketu with the error bars showing standard deviation.
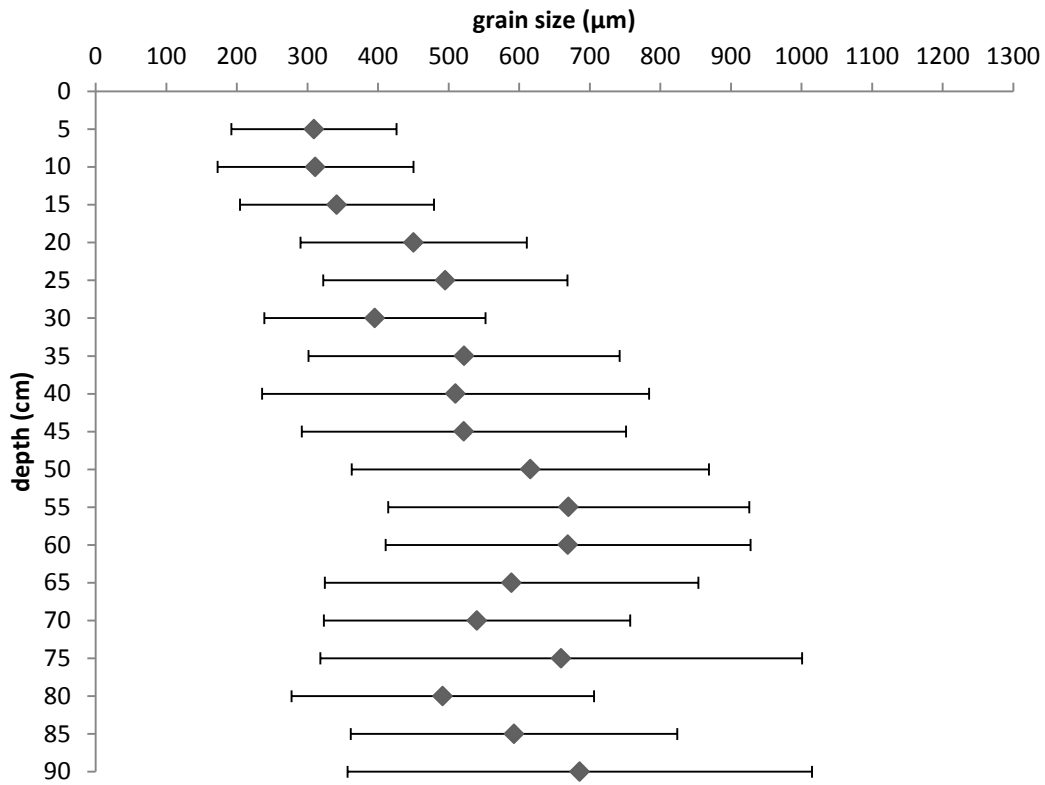
Figure II.24: Grain size results for site 11, the high tide core at Maketu Spit, Maketu with the error bars showing standard deviation.
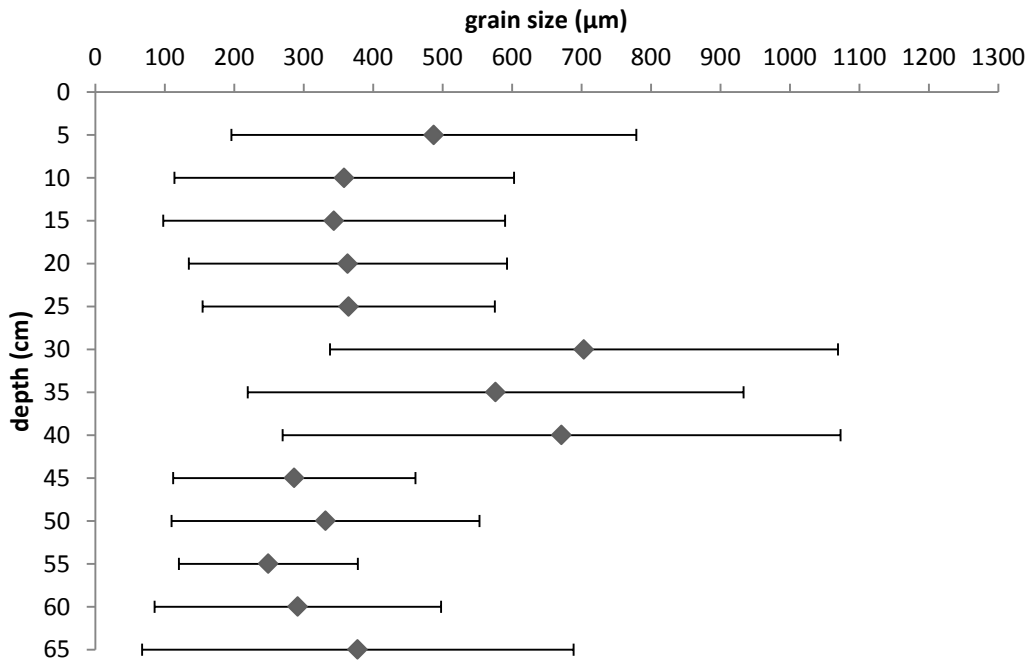
Figure II.25: Grain size results for site 12, core # 1 at Maketu Estuary, Maketu with the error bars showing standard deviation.
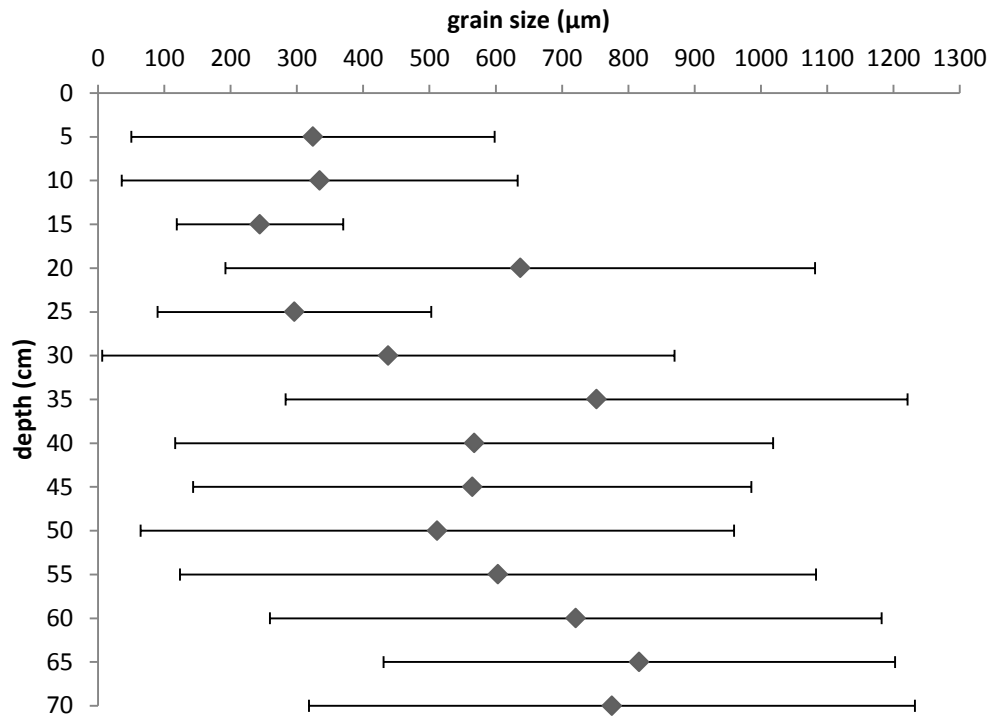
Figure II.26: Grain size results for site 12, core # 2 at Maketu Estuary, Maketu with the error bars showing standard deviation.

9.3 APPENDIX III: QUALITATIVE CHEMISTRY RESULTS

This appendix contains the main qualitative GC/MS chemistry chromatograms analysed by the University's Chemistry Department that are discussed in this thesis.
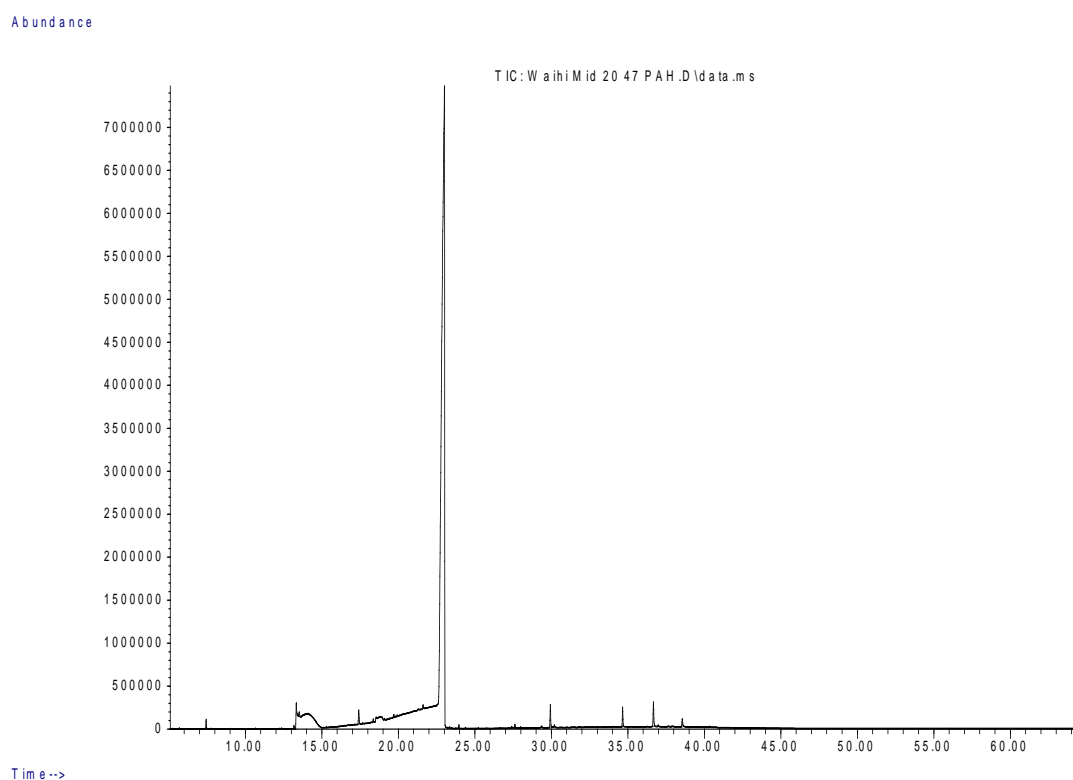
Figure II.36: Site 1, Waihi surf club mid tide core for sediment, 0-20 cm deep. GC/MS total ion chromatograph results from *Rena* PAH fingerprint analysis.
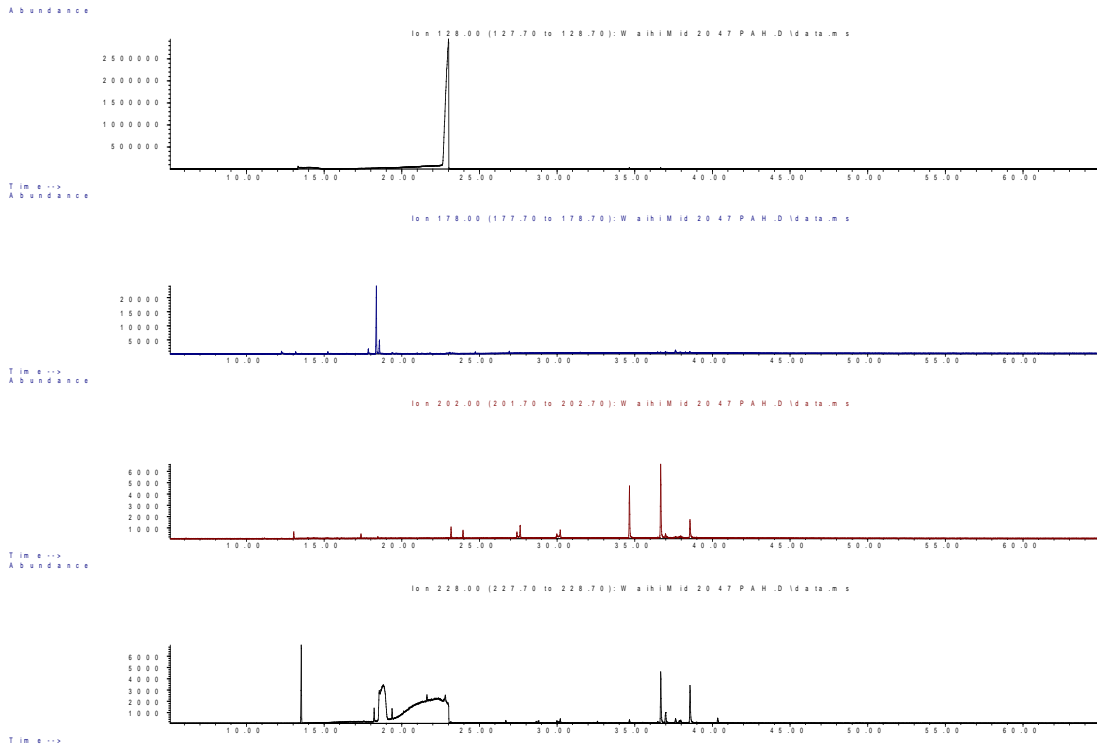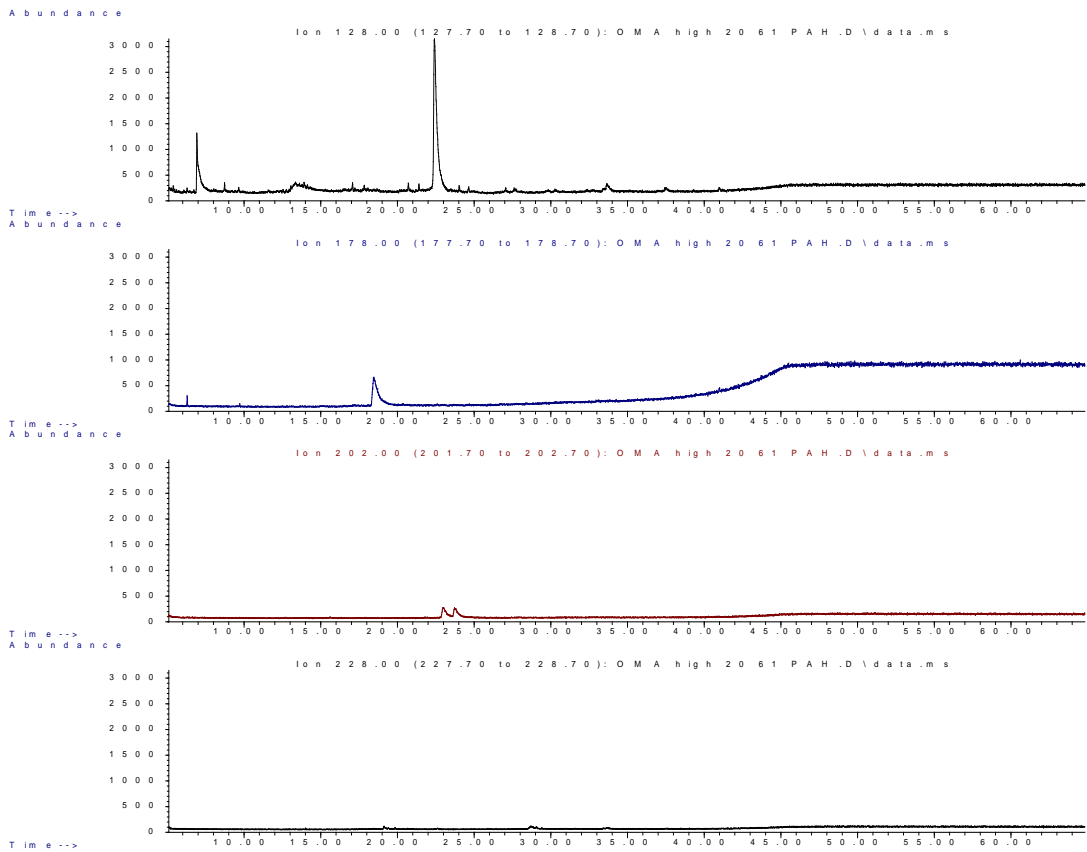
Figure II.37: Site 1, Waihi surf club mid tide core for sediment 0-20 cm deep. GC/MS chromatograph results from *Rena* PAH fingerprint analysis for naphthalene 128 (top), phenanthrene 178 (second), pyrene 202 (third) and benzo(a)anthracene and chrysene 228 at the bottom.
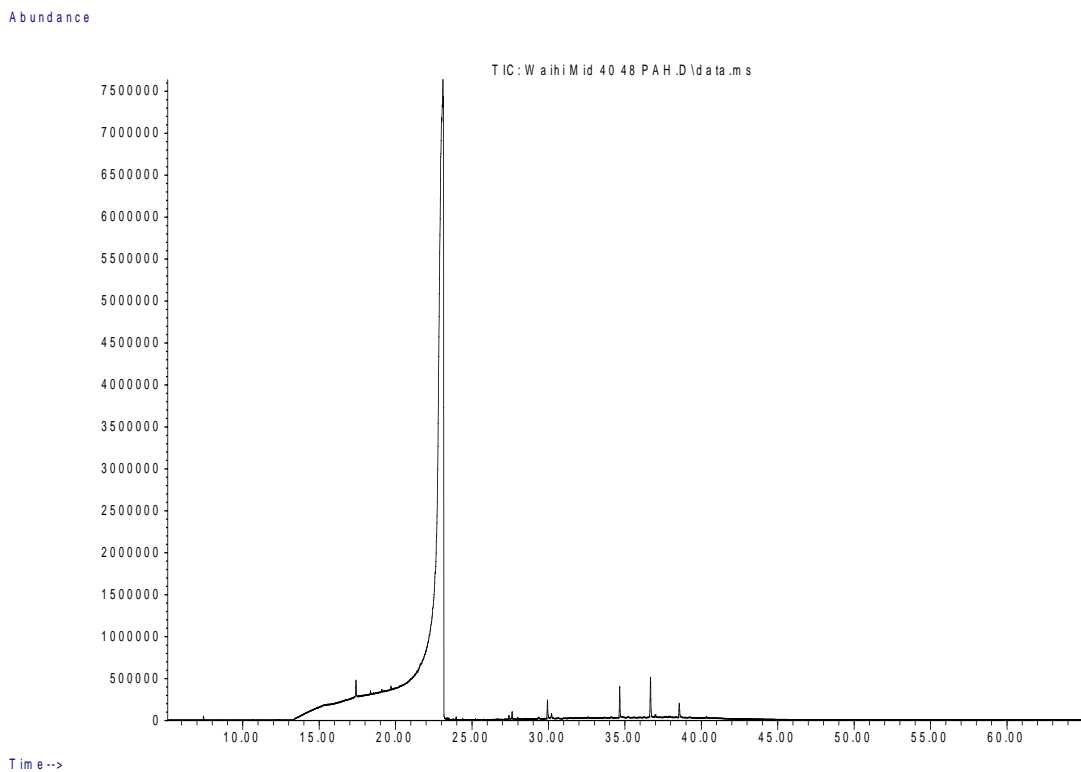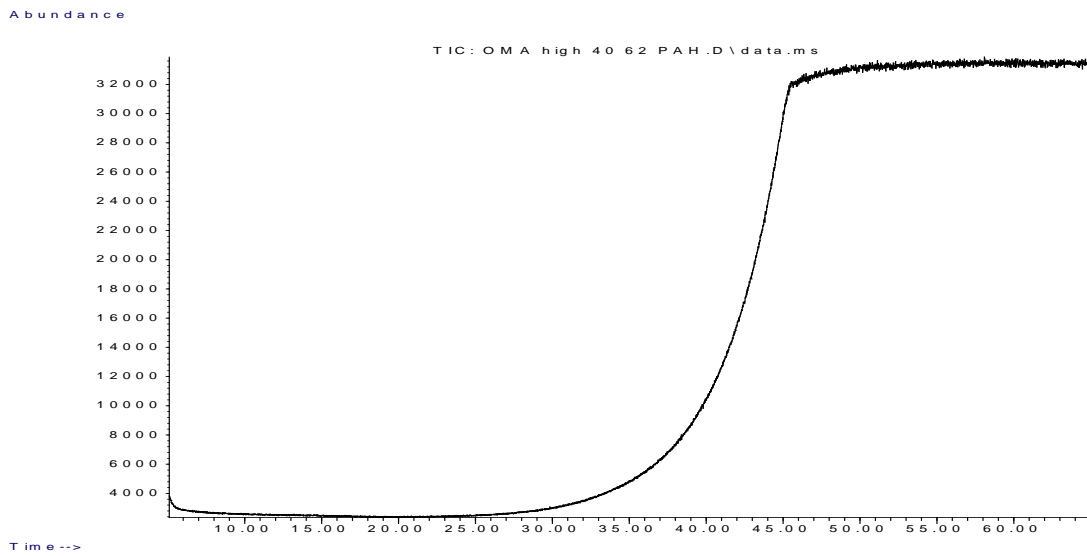

Figure II.38: Site 1, Waihi surf club mid tide core for sediment, 20-40 cm deep. GC/MS total ion chromatograph results from *Rena* PAH fingerprint analysis.
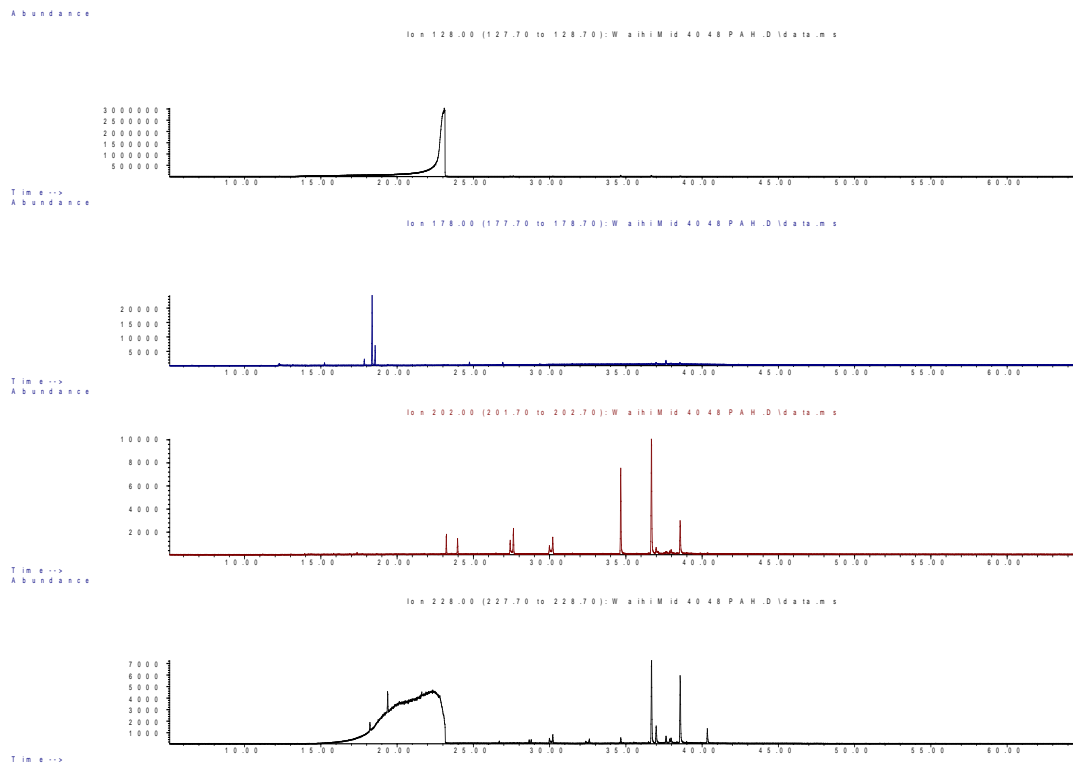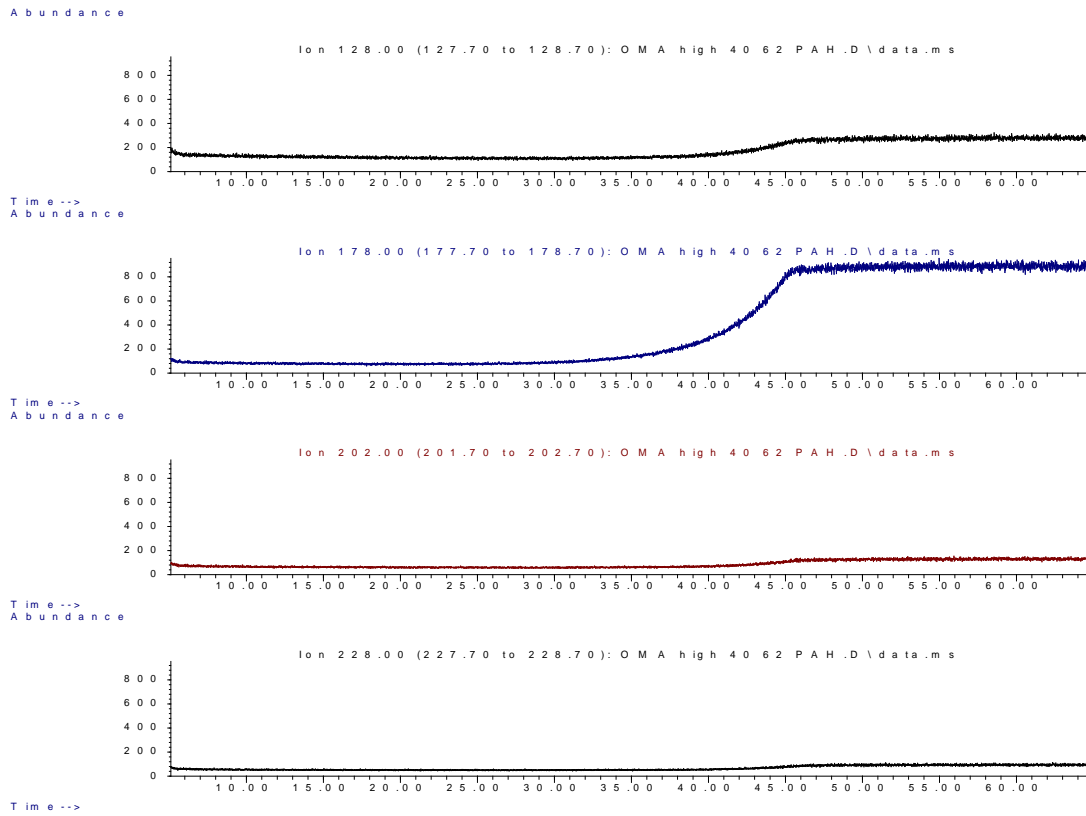
Figure II.39: Site 1,Waihi surf club mid tide core for sediment 20-40 cm deep. GC/MS chromatograph results from *Rena* PAH fingerprint analysis for naphthalene 128 (top), phenanthrene 178 (second), pyrene 202 (third) and benzo(a)anthracene and chrysene 228 at the bottom.
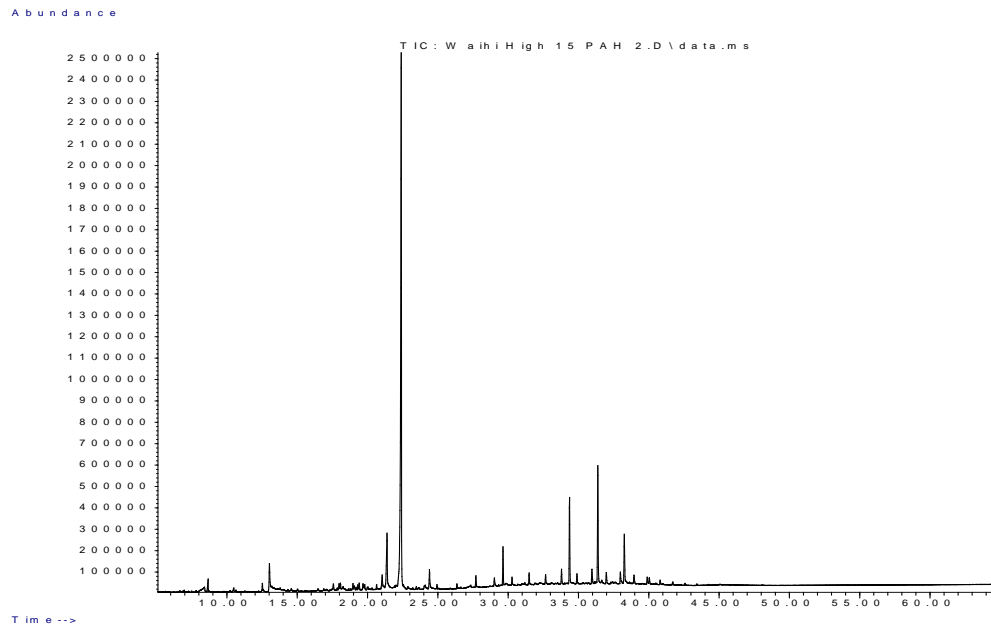
Figure III. 40: Site 1, Waihi surf club high tide core for sediment, 0-20 cm deep. GC/MS total ion chromatograph results from *Rena* PAH fingerprint analysis.

170
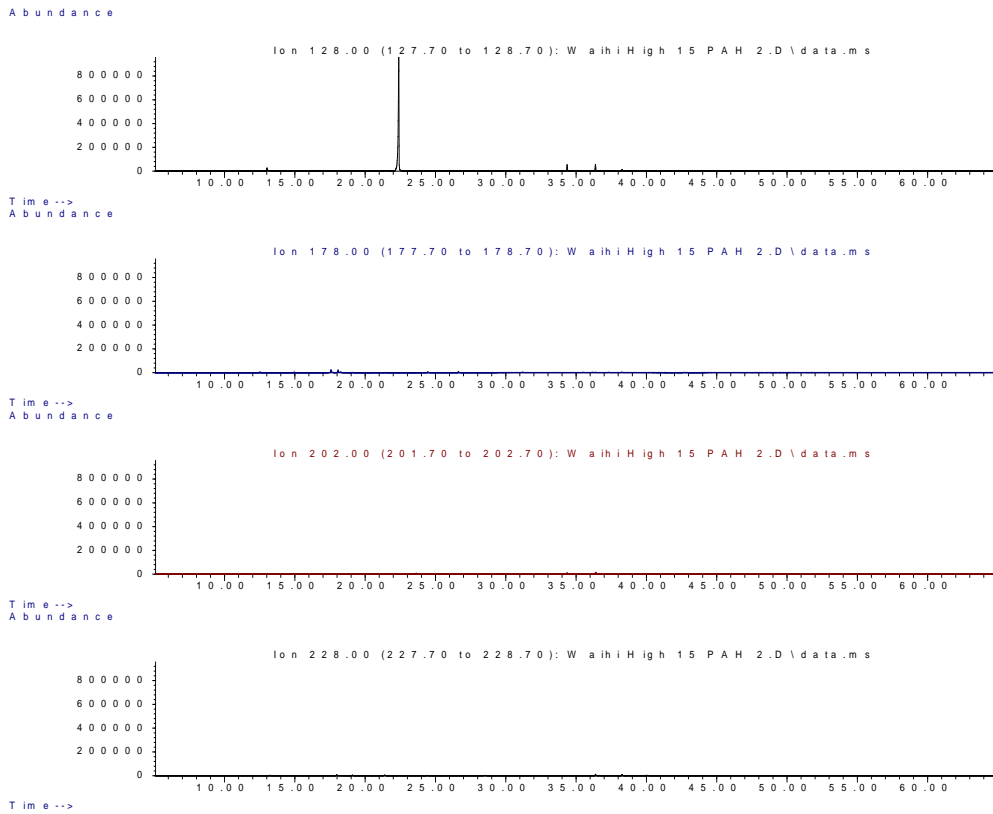
Figure III.41: Site 1,Waihi surf club high tide core for sediment 0-20 cm deep. GC/MS chromatograph results from *Rena* PAH fingerprint analysis for naphthalene 128 (top), phenanthrene 178 (second), pyrene 202 (third) and benzo(a)anthracene and chrysene 228 at the bottom.
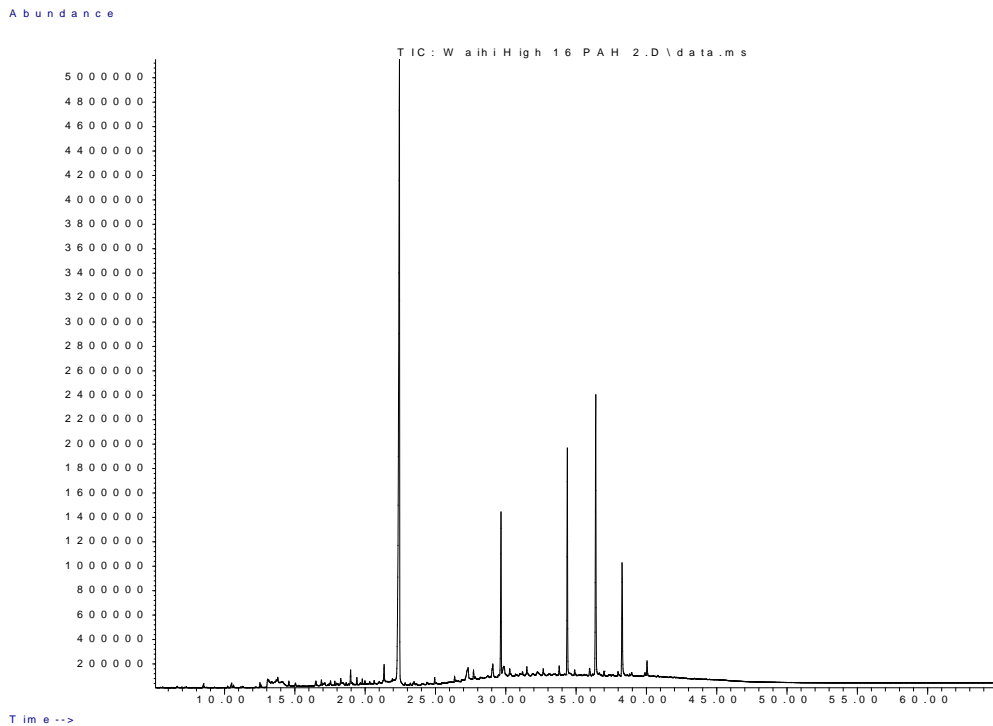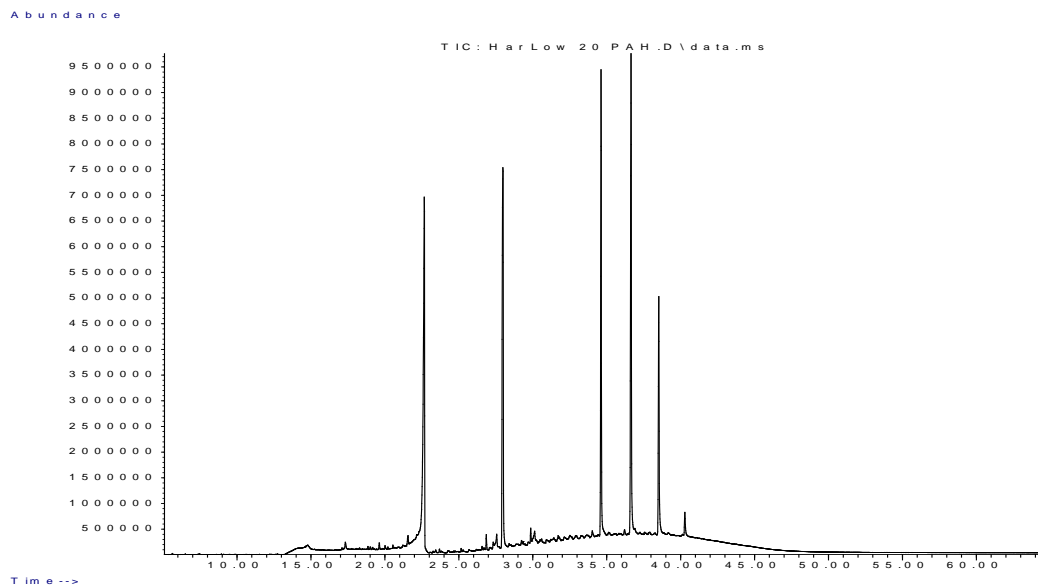

Figure III.42: Site 1,Waihi surf club high tide core for sediment, 20-40 cm deep. GC/MS total ion chromatograph results from *Rena* PAH fingerprint analysis.
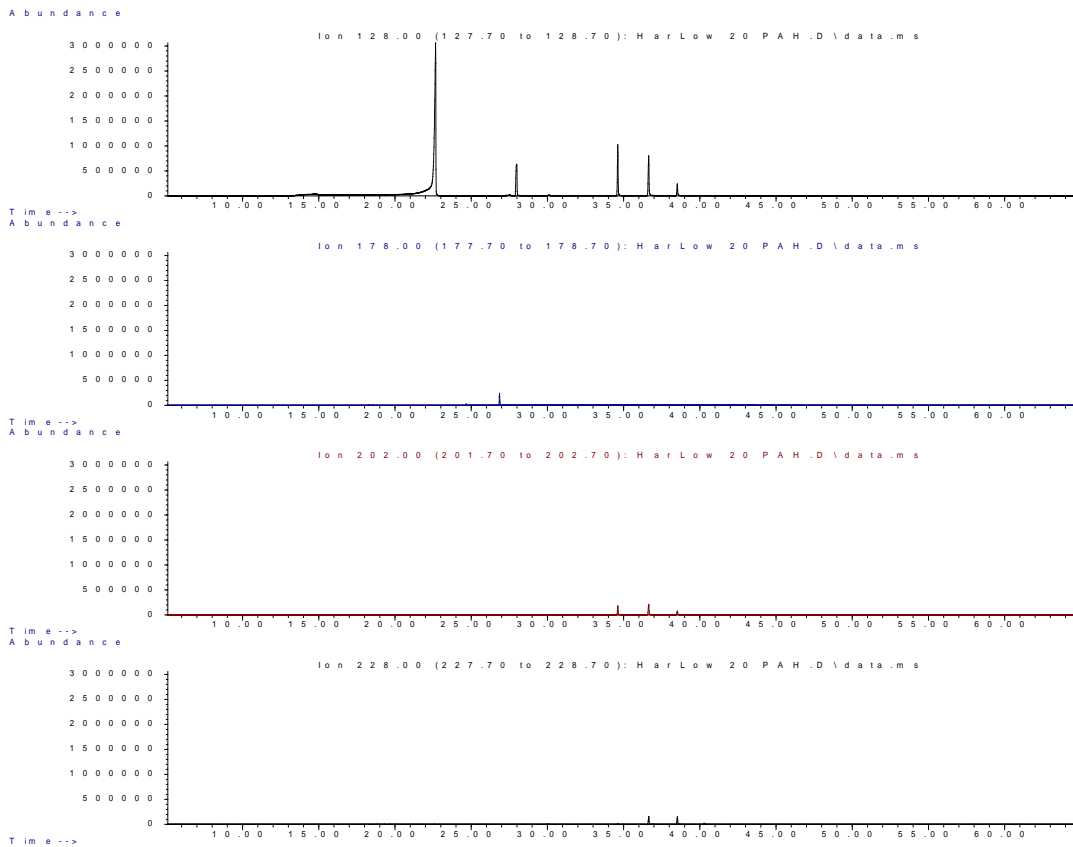
171
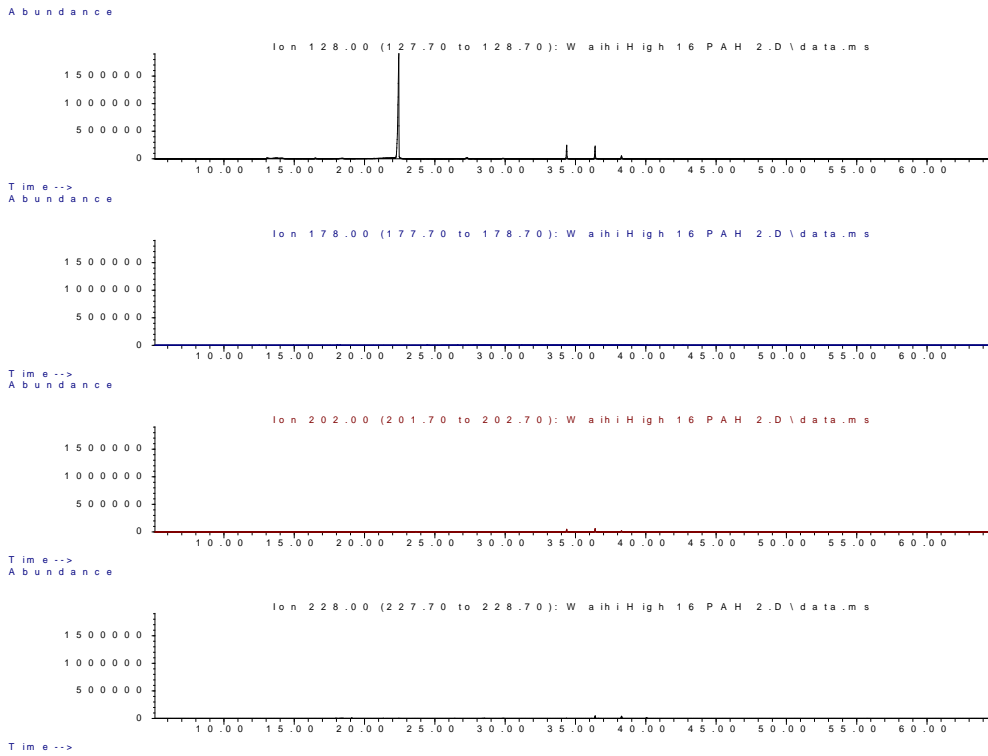
Figure III.43: Site 1, Waihi surf club high tide core for sediment 20-40 cm deep. GC/MS chromatograph results from *Rena* PAH fingerprint analysis for naphthalene 128 (top), phenanthrene 178 (second), pyrene 202 (third) and benzo(a)anthracene and chrysene 228 at the bottom.
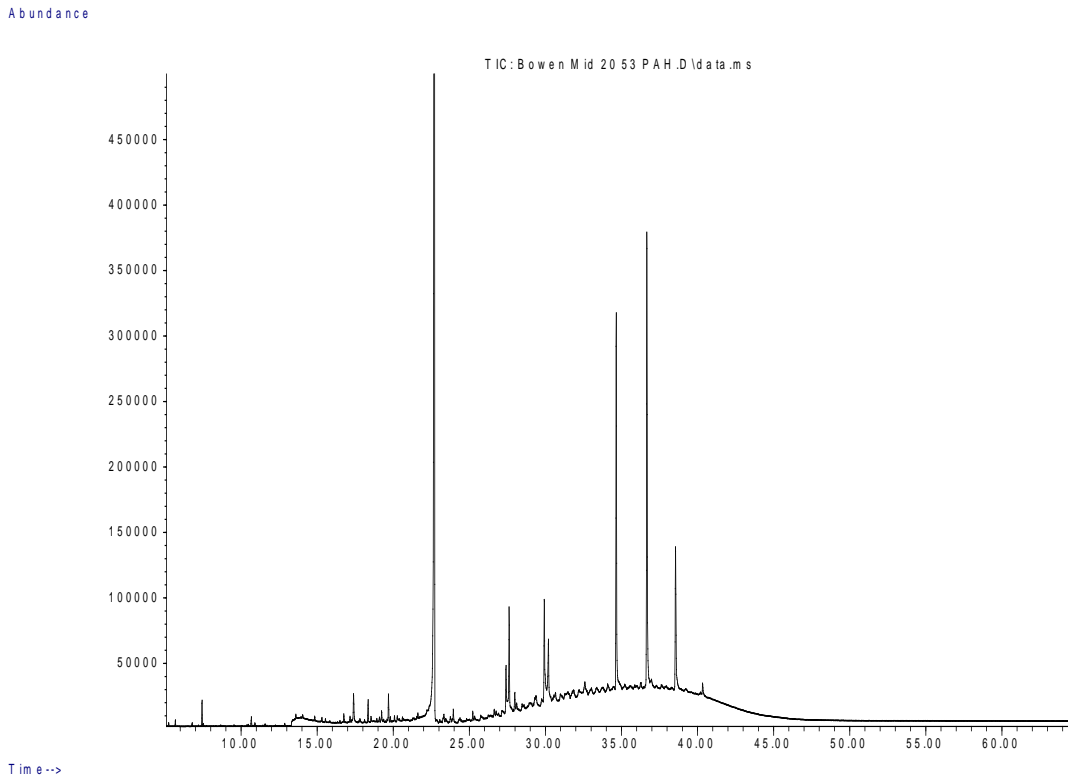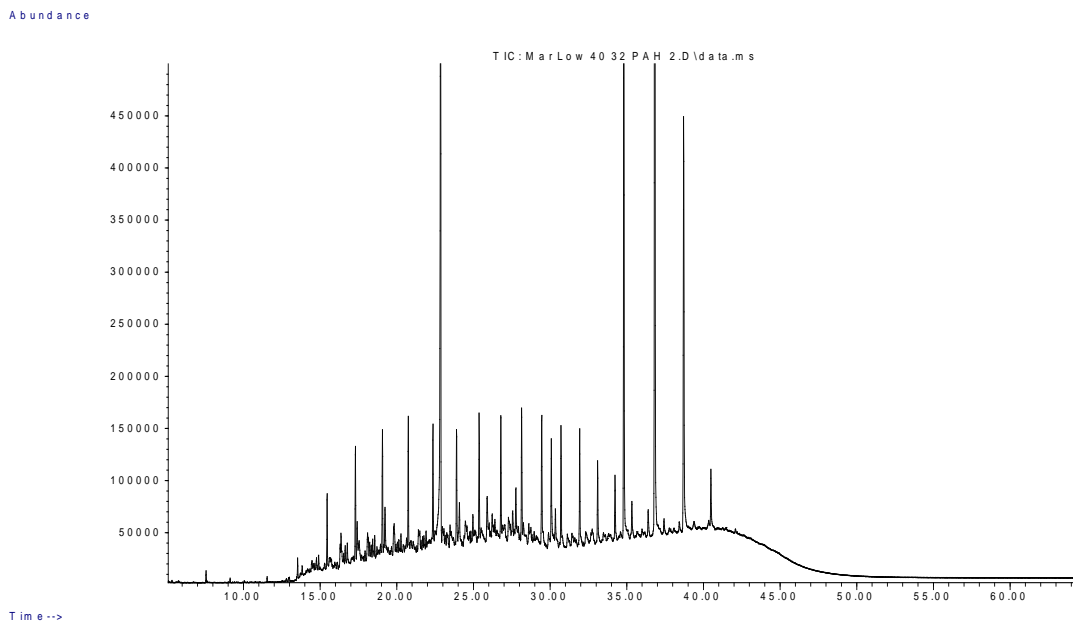

Figure III.44: Site 2, Bowentown mid tide core for sediment, 0-20 cm deep. GC/MS total ion chromatograph results from *Rena* PAH fingerprint analysis.
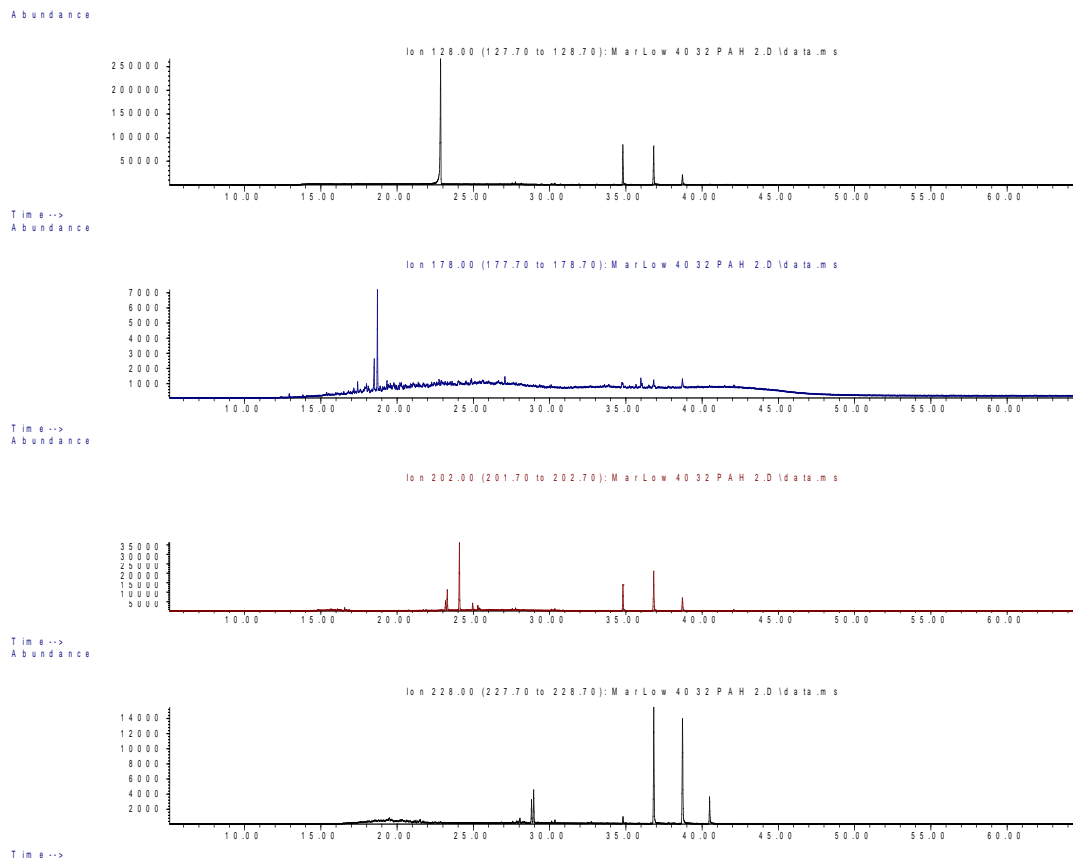
172
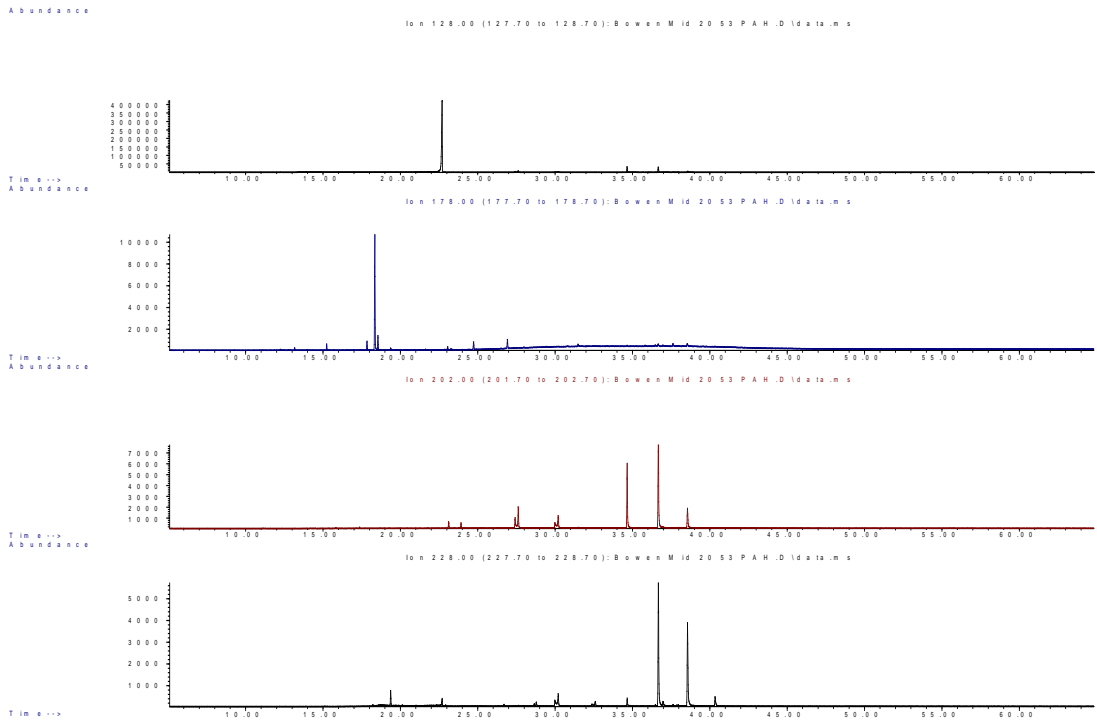
Figure 9III.45: Site 2, Bowentown mid tide core for sediment 0-20 cm deep. GC/MS chromatograph results from *Rena* PAH fingerprint analysis for naphthalene 128 (top), phenanthrene 178 (second), pyrene 202 (third) and benzo(a)anthracene and chrysene 228 at the bottom.
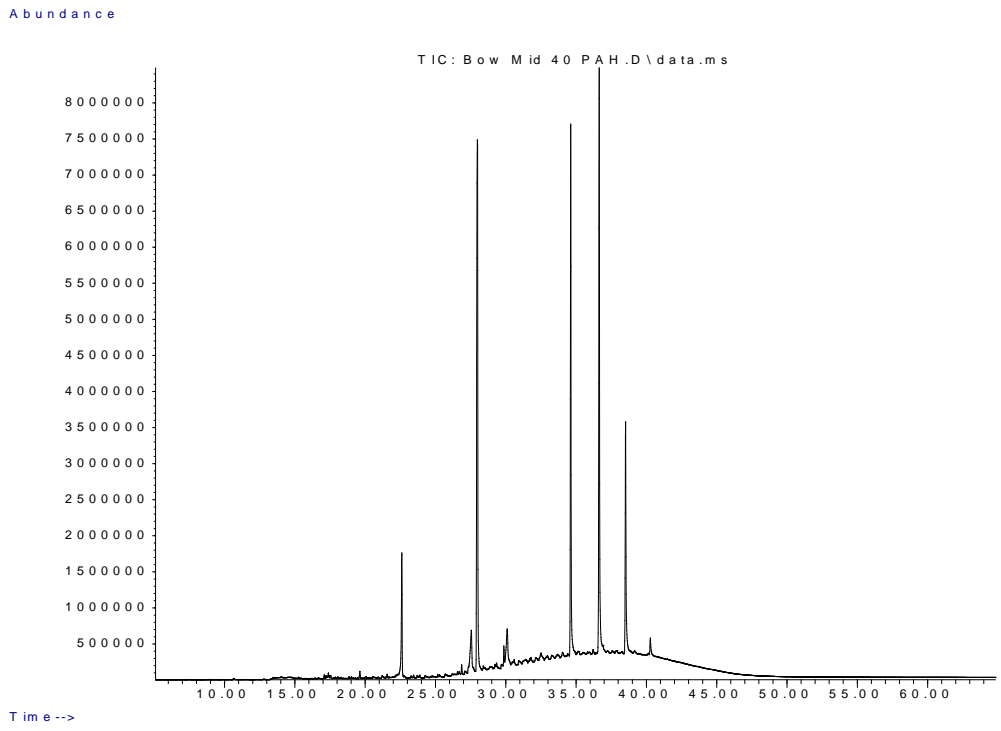
Figure III.46: Site 2, Bowentown mid tide core for sediment, 20-40 cm deep. GC/MS total ion chromatograph results from Rena PAH fingerprint analysis.

173
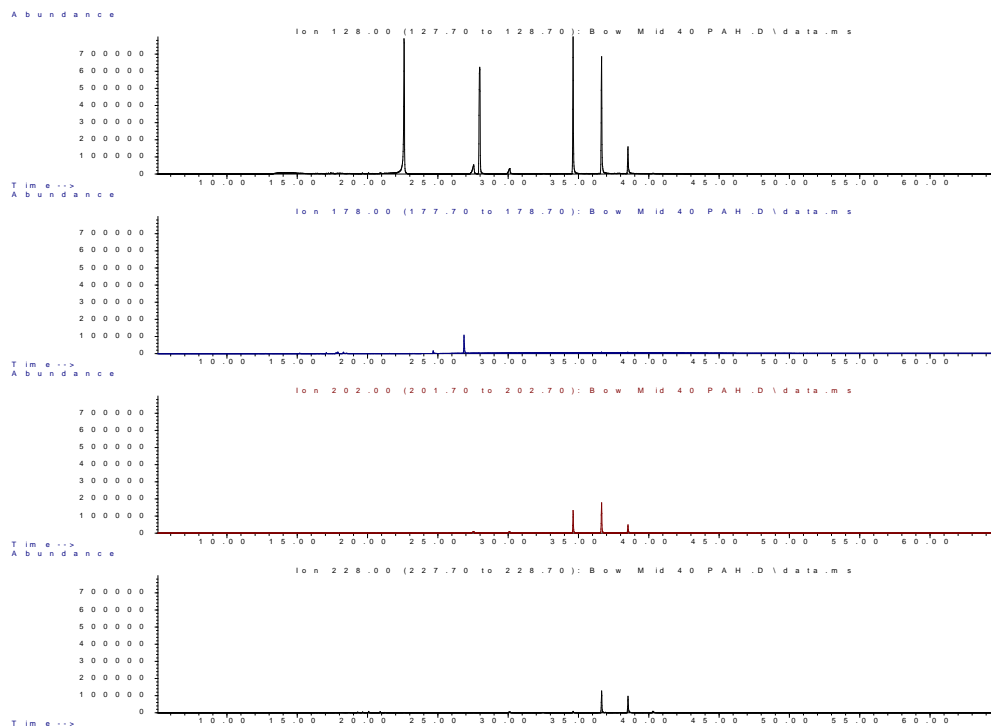
Figure 9III.47: Site 2, Bowentown mid tide core for sediment 20-40 cm deep. GC/MS chromatograph results from Rena PAH fingerprint analysis for naphthalene 128 (top), phenanthrene 178 (second), pyrene 202 (third) and benzo(a)anthracene and chrysene 228 at the bottom.
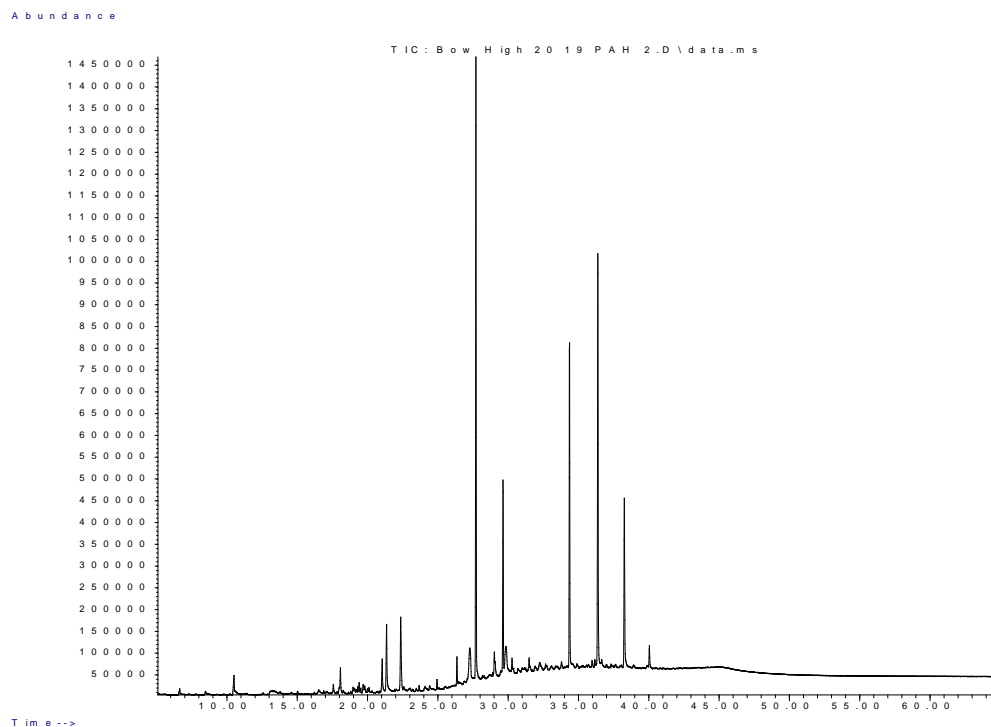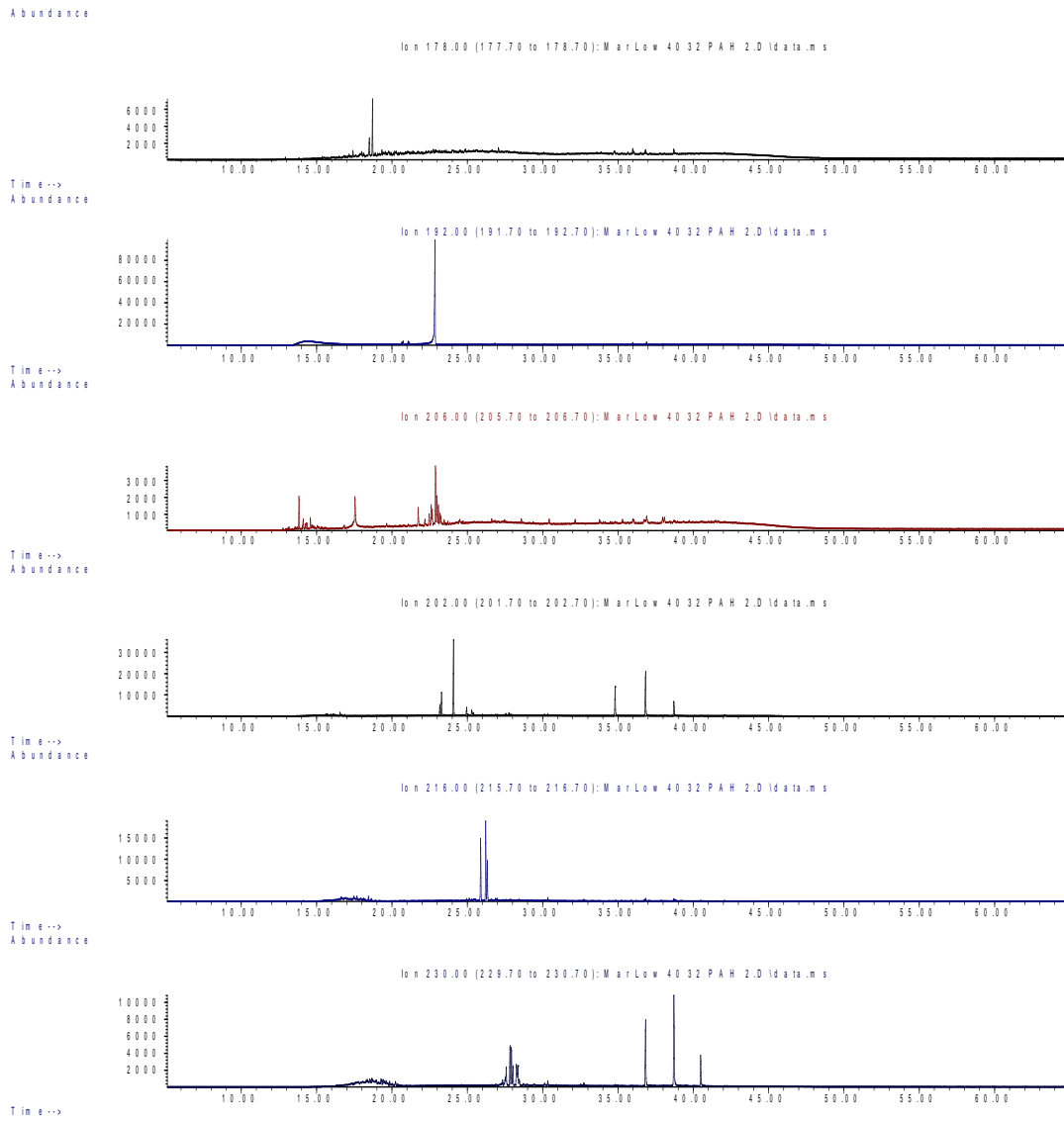

Figure III.48: Site 2, Bowentown high tide core for sediment, 0-20 cm deep. GC/MS total ion chromatograph results from *Rena* PAH fingerprint analysis.
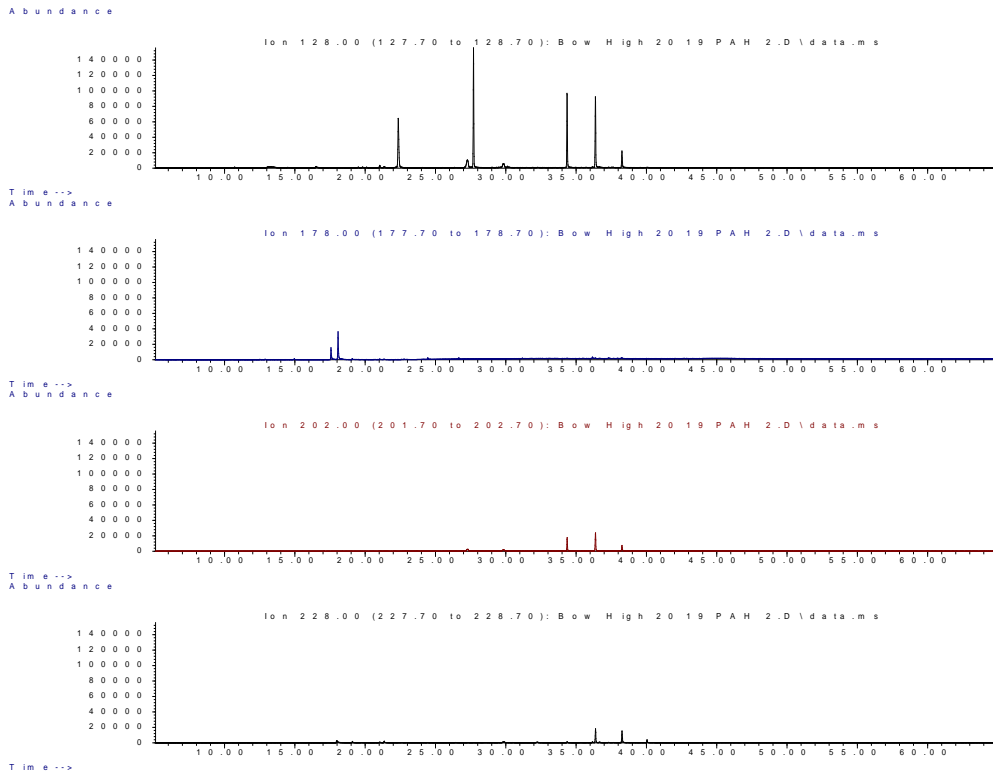
Figure III.49: Site 2, Bowentown high tide core for sediment 0-20cm deep. GC/MS chromatograph results from *Rena* PAH fingerprint analysis for naphthalene 128 (top), phenanthrene 178 (second), pyrene 202 (third) and benzo(a)anthracene and chrysene 228 at the bottom.
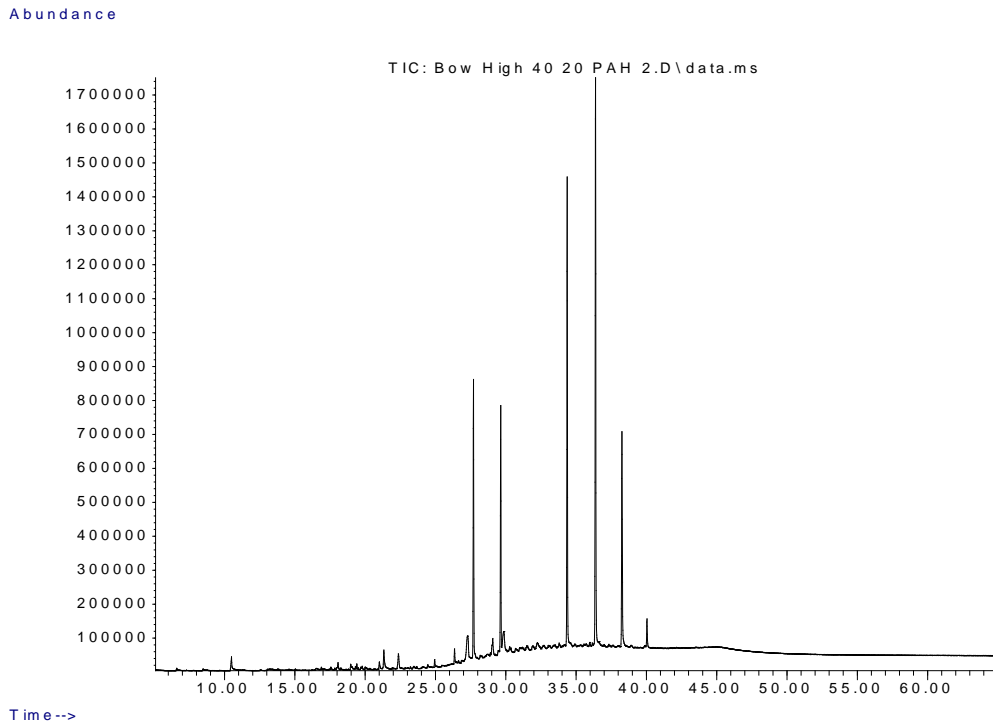
Figure III.50: Site 2, Bowentown high tide core for sediment, 20-40 cm deep. GC/MS total ion chromatograph results from *Rena* PAH fingerprint analysis.
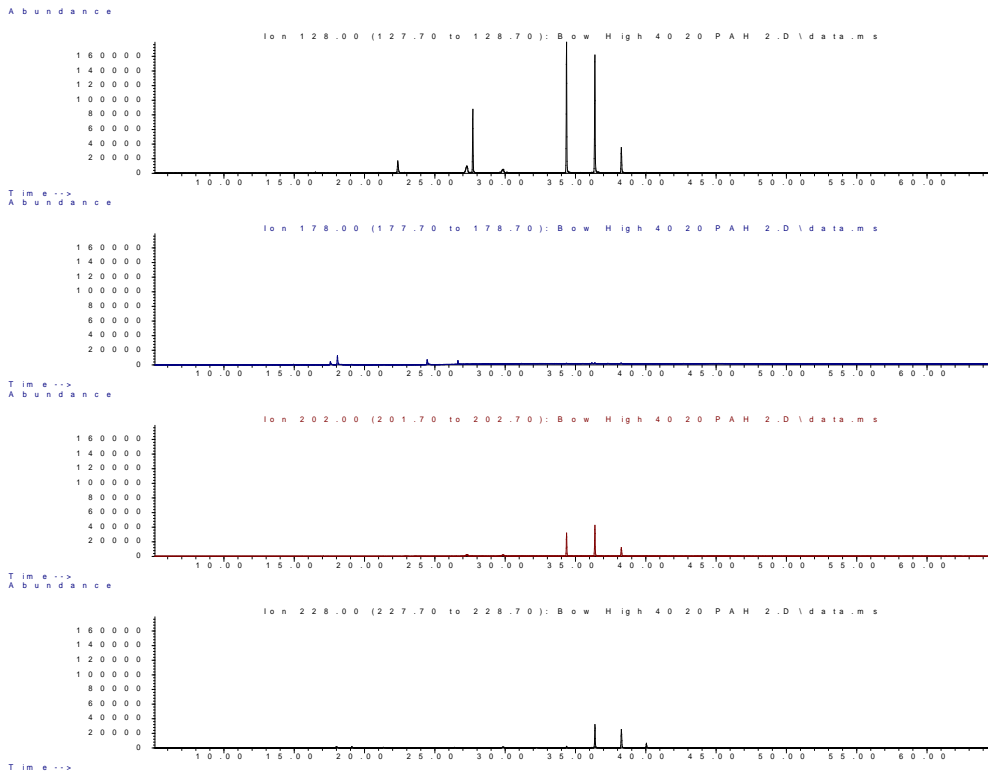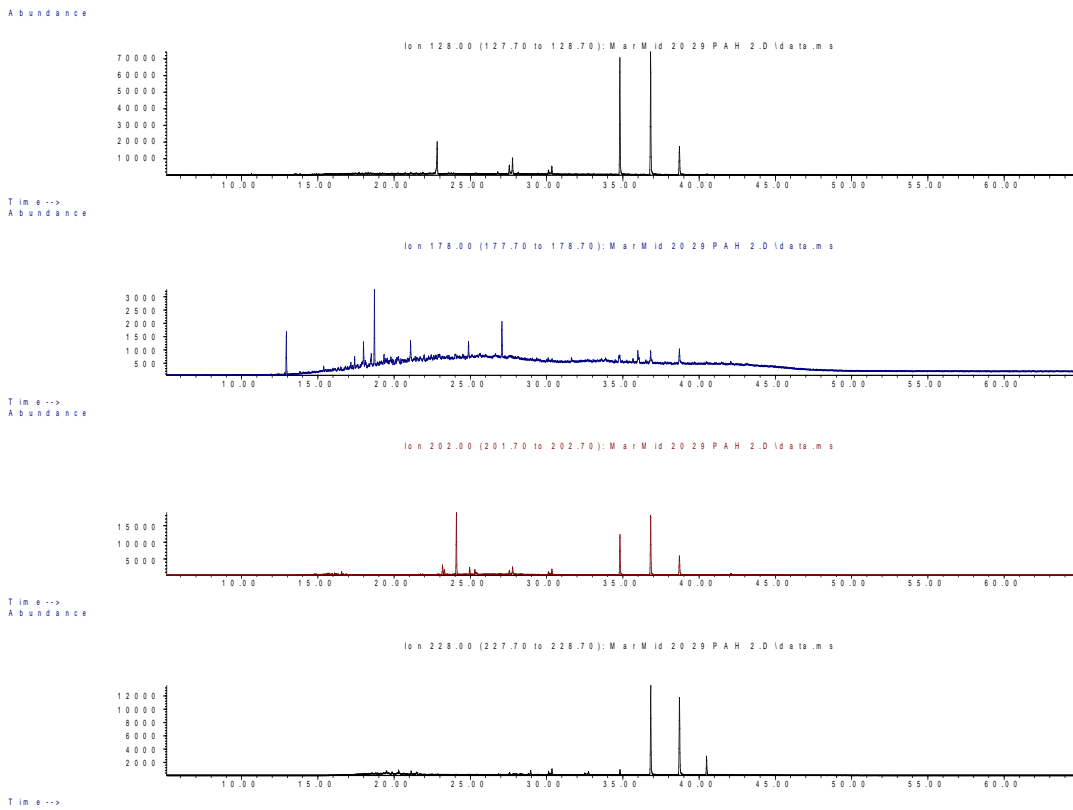
Figure III.51: Site 2, Bowentown high tide core for sediment 20-40 cm deep. GC/MS chromatograph results from *Rena* PAH fingerprint analysis for naphthalene 128 (top), phenanthrene 178 (second), pyrene 202 (third) and benzo(a)anthracene and chrysene 228 at the bottom.
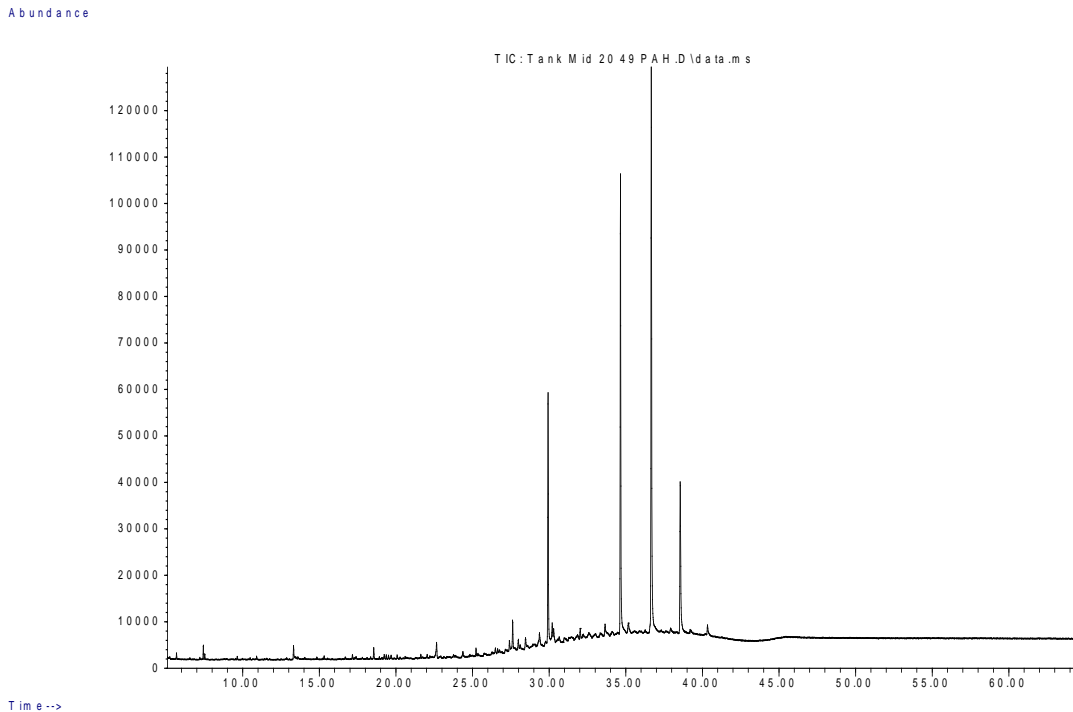
Figure III.52: Site 3, Tank Road mid tide core for sediment, 0-20 cm deep. GC/MS total ion chromatograph results from *Rena* PAH fingerprint analysis.

176
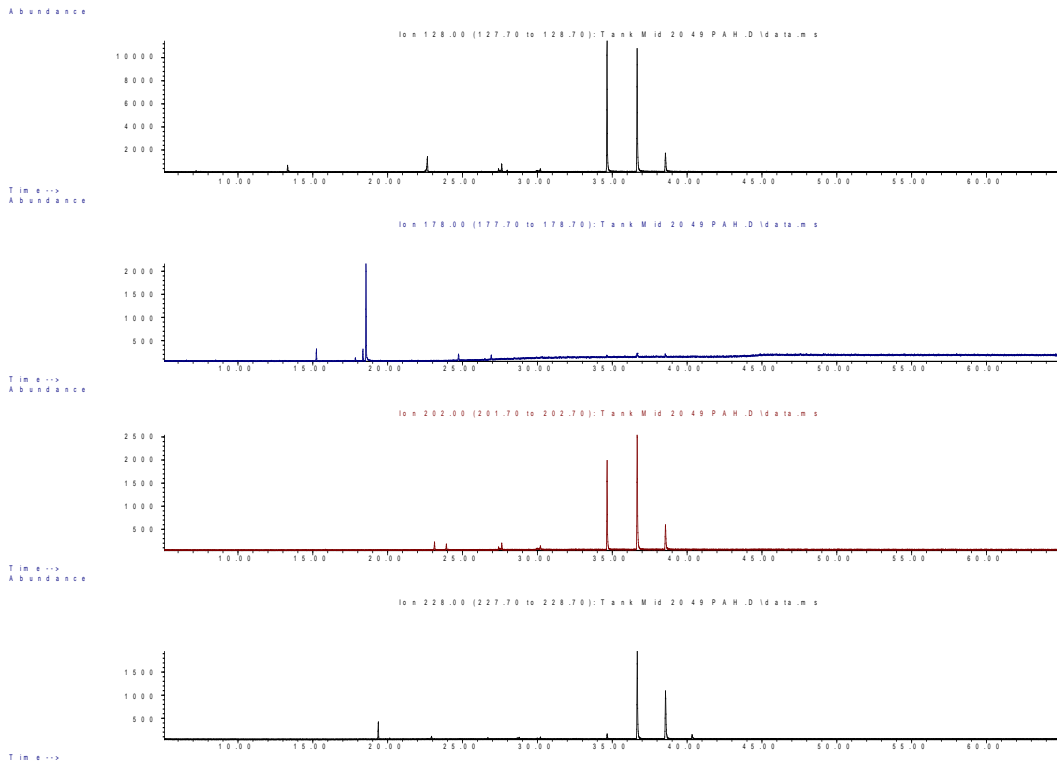
Figure III.53: Site 3, Tank Road mid tide core for sediment 0-20 cm deep. GC/MS chromatograph results from *Rena* PAH fingerprint analysis for naphthalene 128 (top), phenanthrene 178 (second), pyrene 202 (third) and benzo(a)anthracene and chrysene 228 at the bottom.
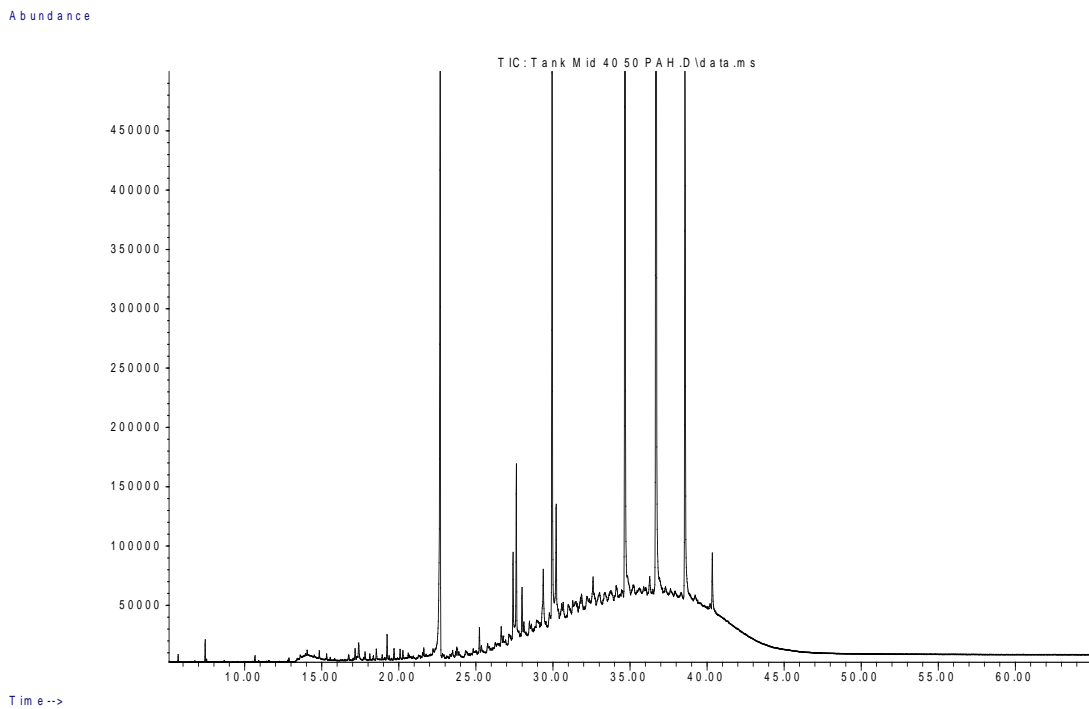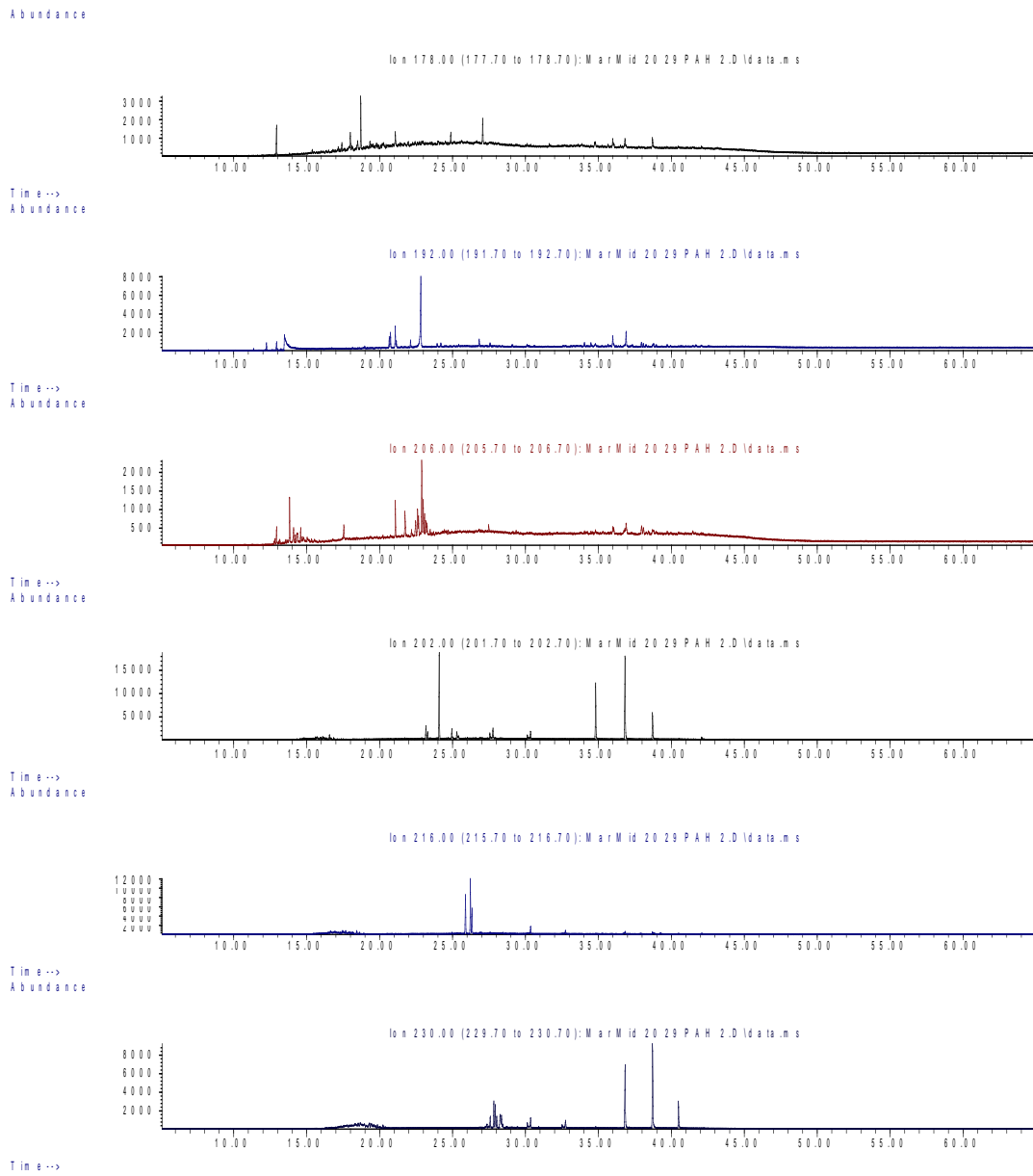

Figure III.54: Site 3, Tank Road mid tide core for sediment, 20-40 cm deep. GC/MS total ion chromatograph results from *Rena* PAH fingerprint analysis.

177
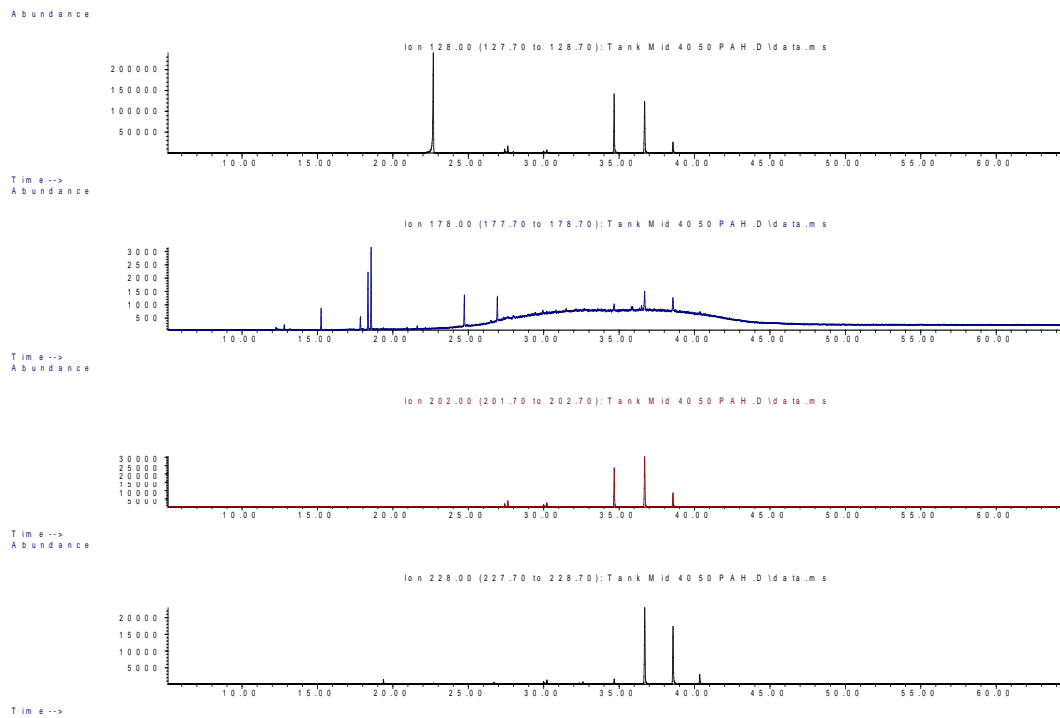
Figure III.55: Site 3, Tank Road mid tide core for sediment 20-40 cm deep. GC/MS chromatograph results from *Rena* PAH fingerprint analysis for naphthalene 128 (top), phenanthrene 178 (second), pyrene 202 (third) and benzo(a)anthracene and chrysene 228 at the bottom.
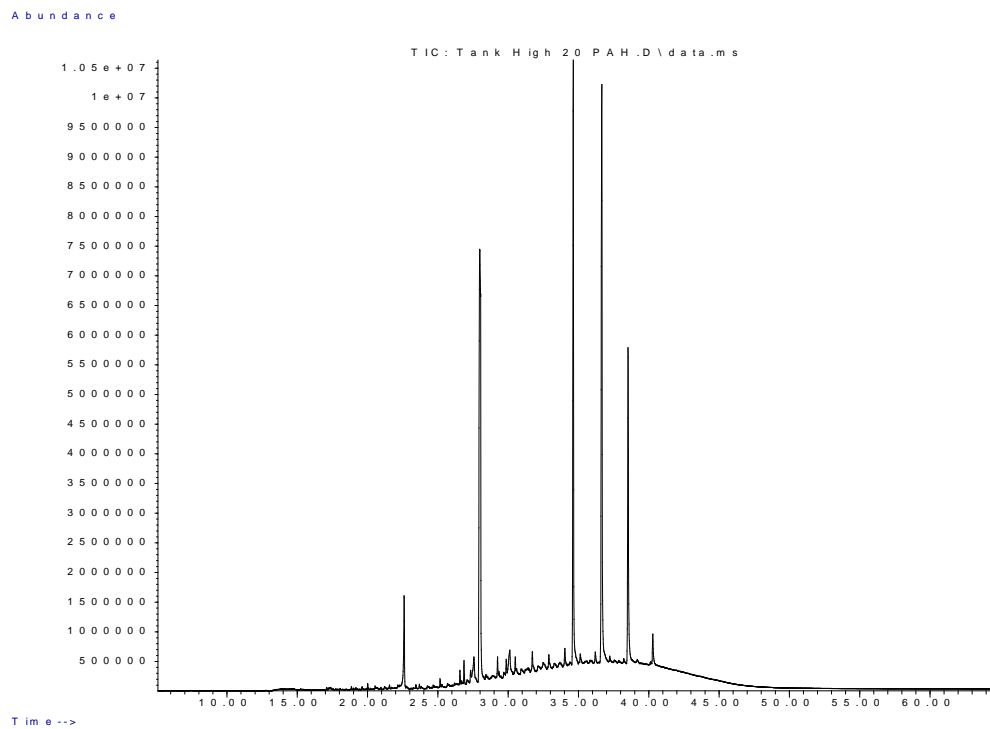
Figure III.56: Site 3, Tank Road high tide core for sediment, 0-20 cm deep. GC/MS total ion chromatograph results from *Rena* PAH fingerprint analysis.
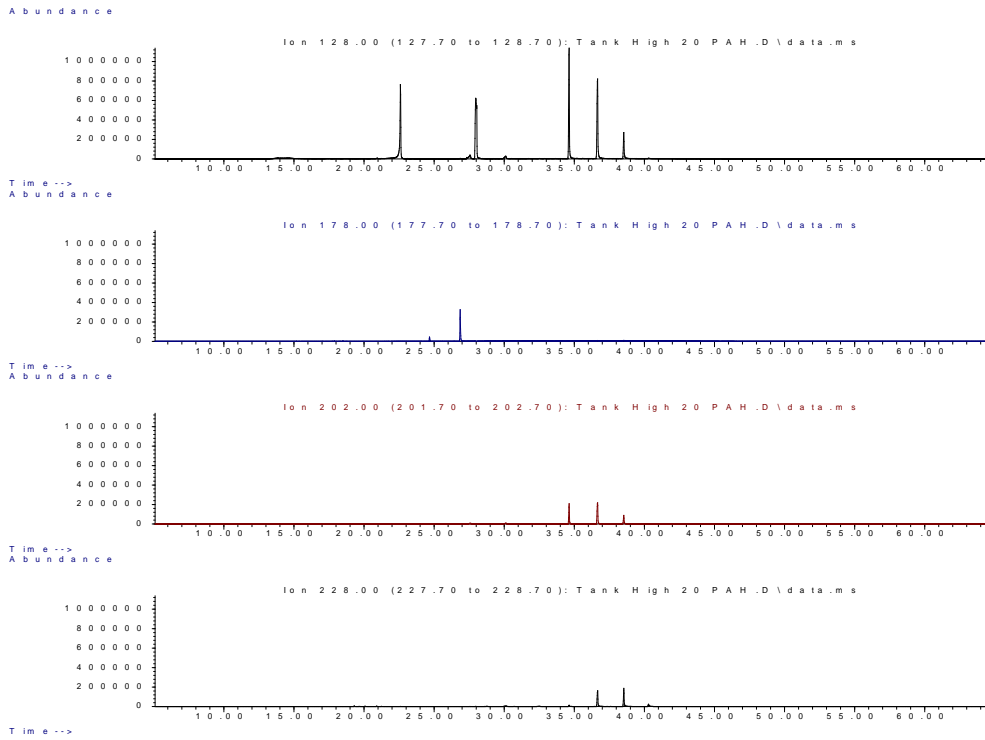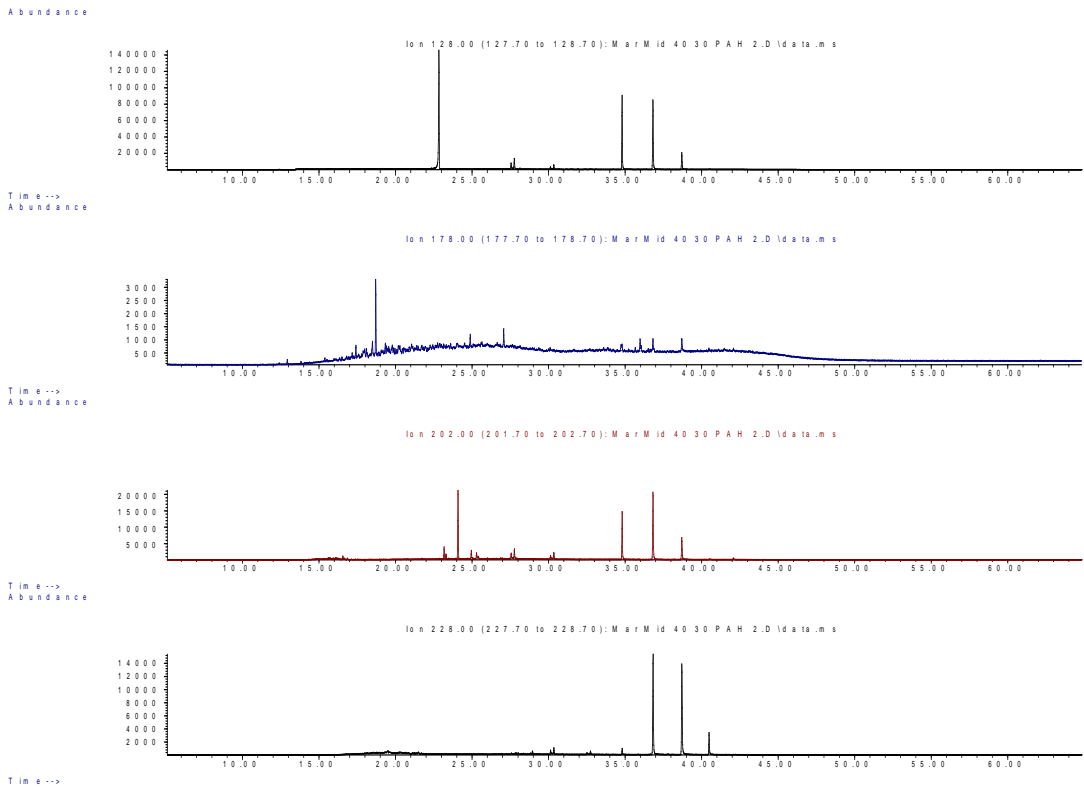
Figure III.57: Site 3, Tank Road mid tide core for sediment 0-20 cm deep. GC/MS chromatograph results from *Rena* PAH fingerprint analysis for naphthalene 128 (top), phenanthrene 178 (second), pyrene 202 (third) and benzo(a)anthracene and chrysene 228 at the bottom.
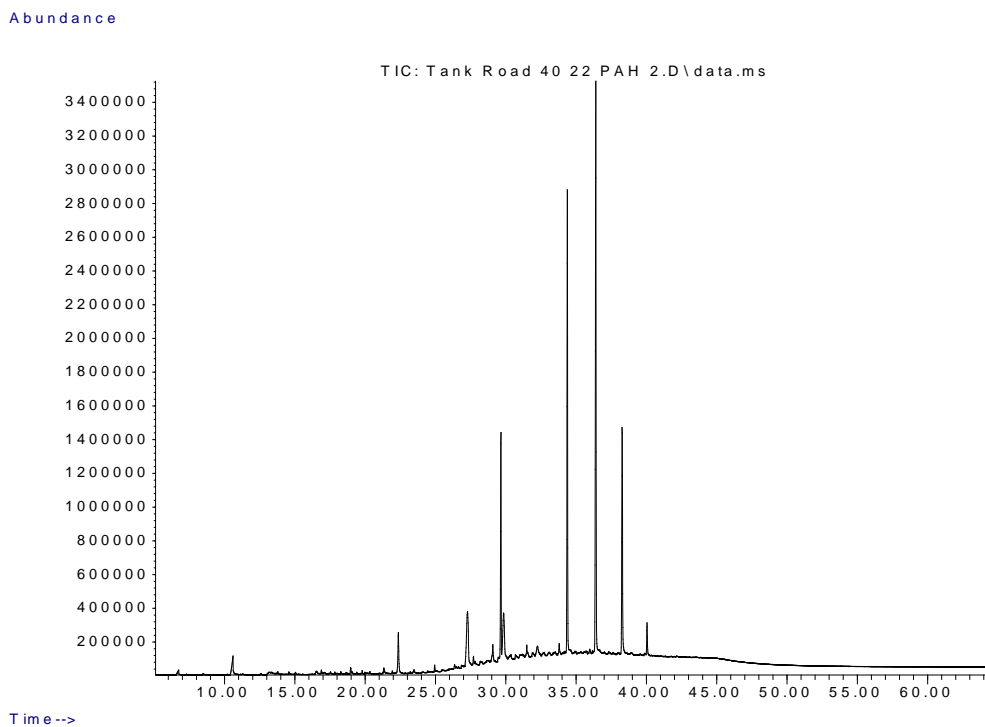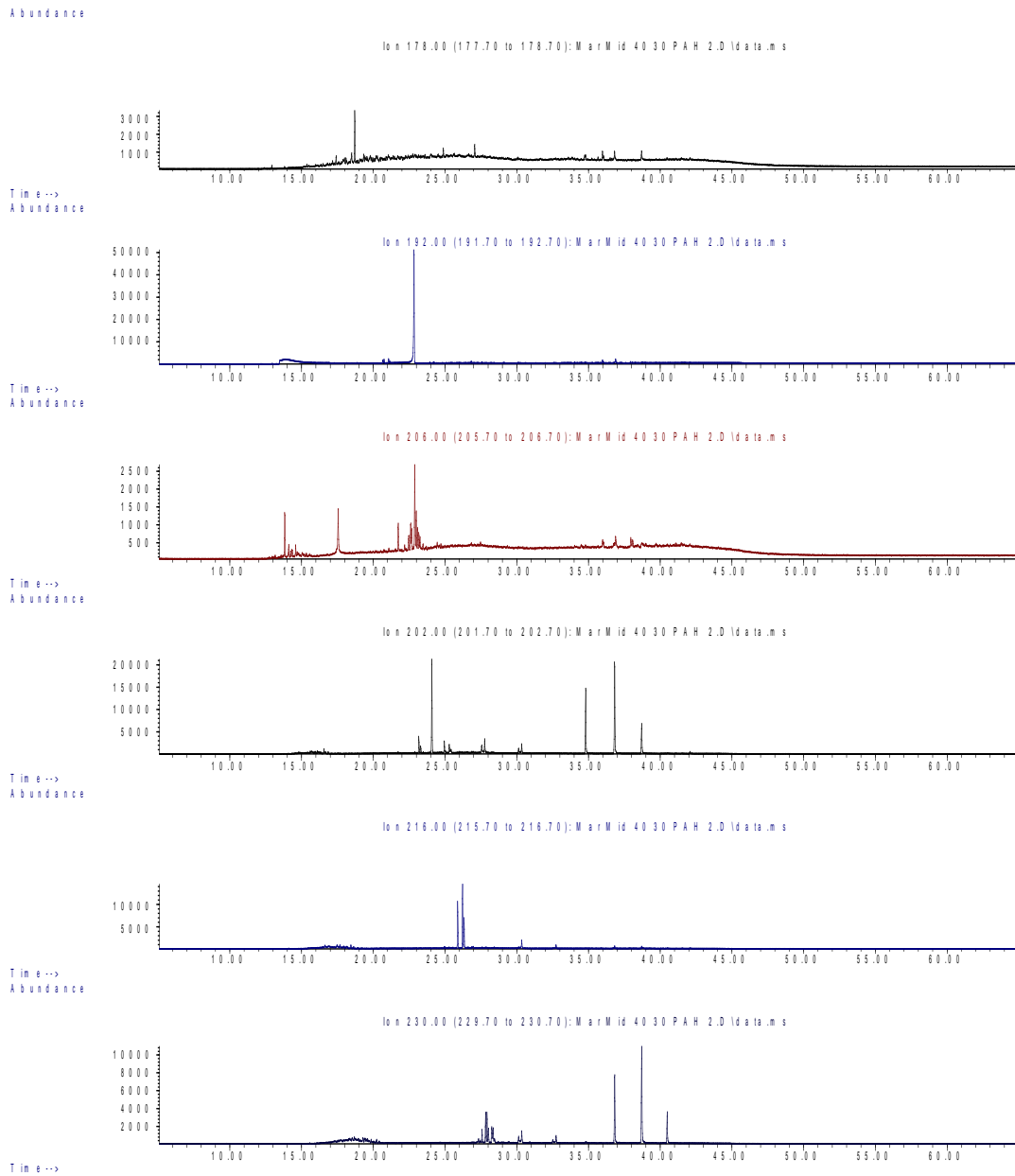

Figure III.58: Site 3, Tank Road high tide core for sediment, 20-40 cm deep. GC/MS total ion chromatograph results from *Rena* PAH fingerprint analysis.
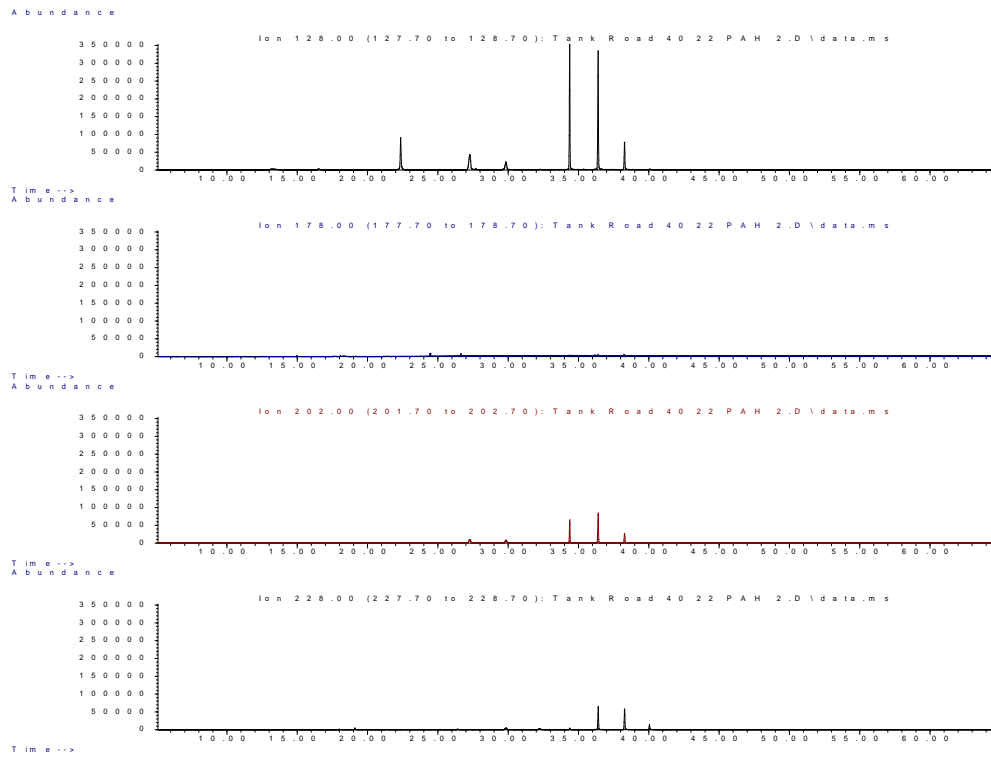
Figure III.59: Site 3, Tank Road mid tide core for sediment 20-40 cm deep. GC/MS chromatograph results from *Rena* PAH fingerprint analysis for naphthalene 128 (top), phenanthrene 178 (second), pyrene 202 (third) and benzo(a)anthracene and chrysene 228 at the bottom.
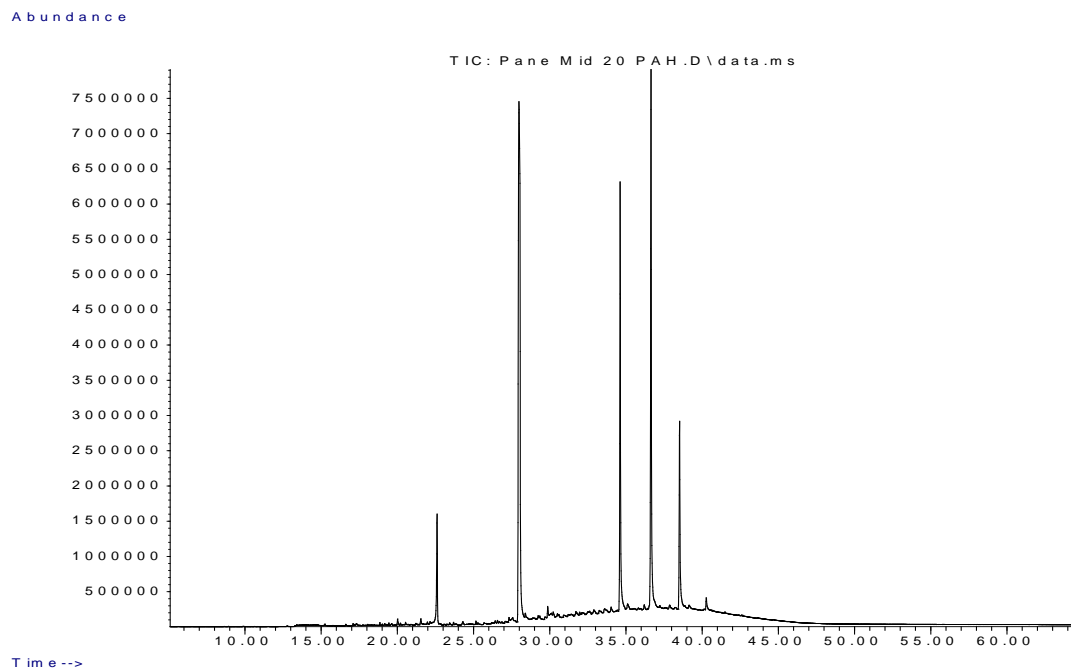
Figure III.60: Site 4, Panepane Point mid tide core for sediment, 0-20 cm deep. GC/MS total ion chromatograph results from *Rena* PAH fingerprint analysis.
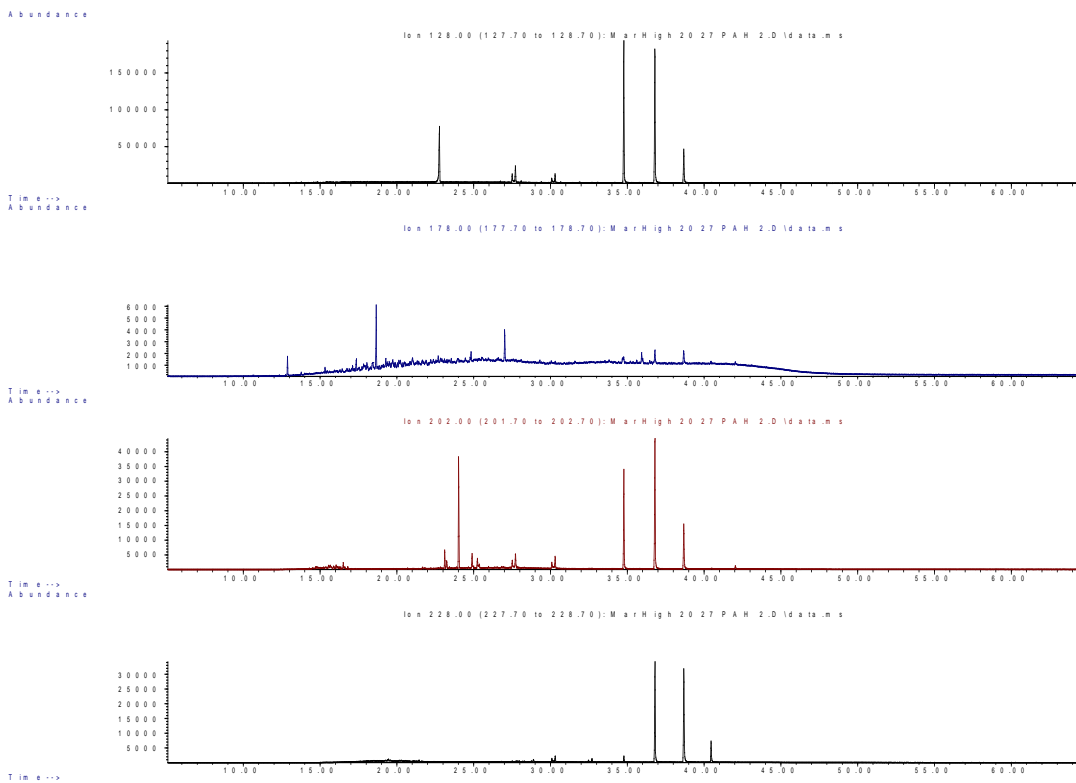
180
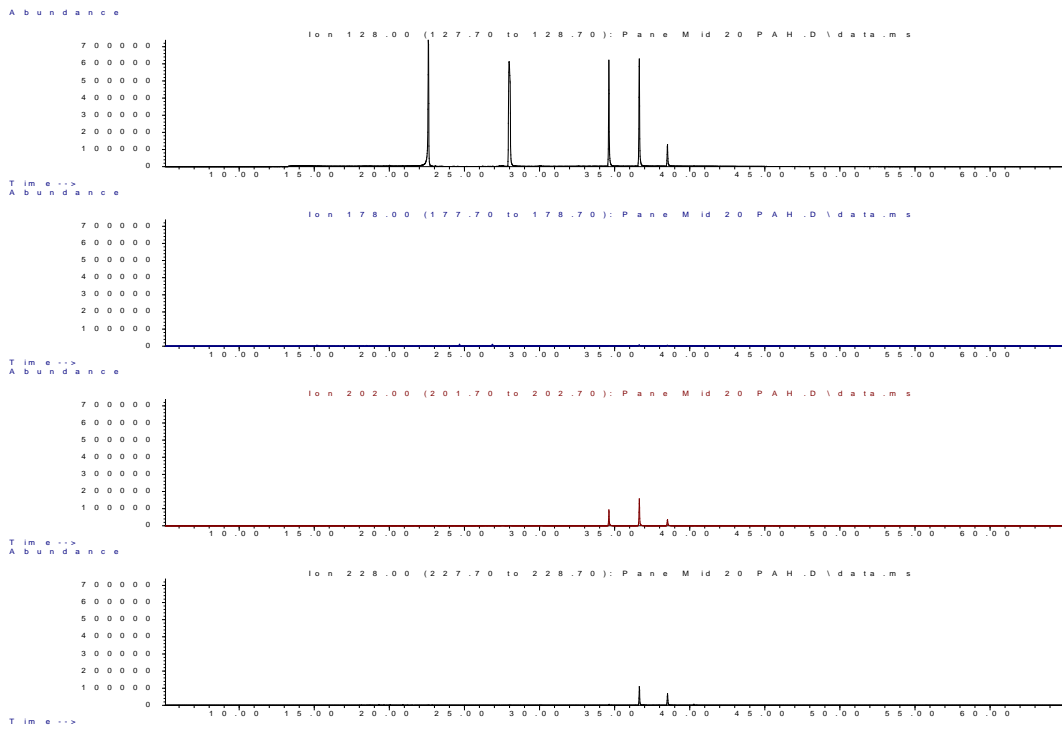
Figure III.61: Site 4, Panepane Point mid tide core for sediment 0-20 cm deep. GC/MS chromatograph results from Rena PAH fingerprint analysis for naphthalene 128 (top), phenanthrene 178 (second), pyrene 202 (third) and benzo(a)anthracene and chrysene 228 at the bottom.
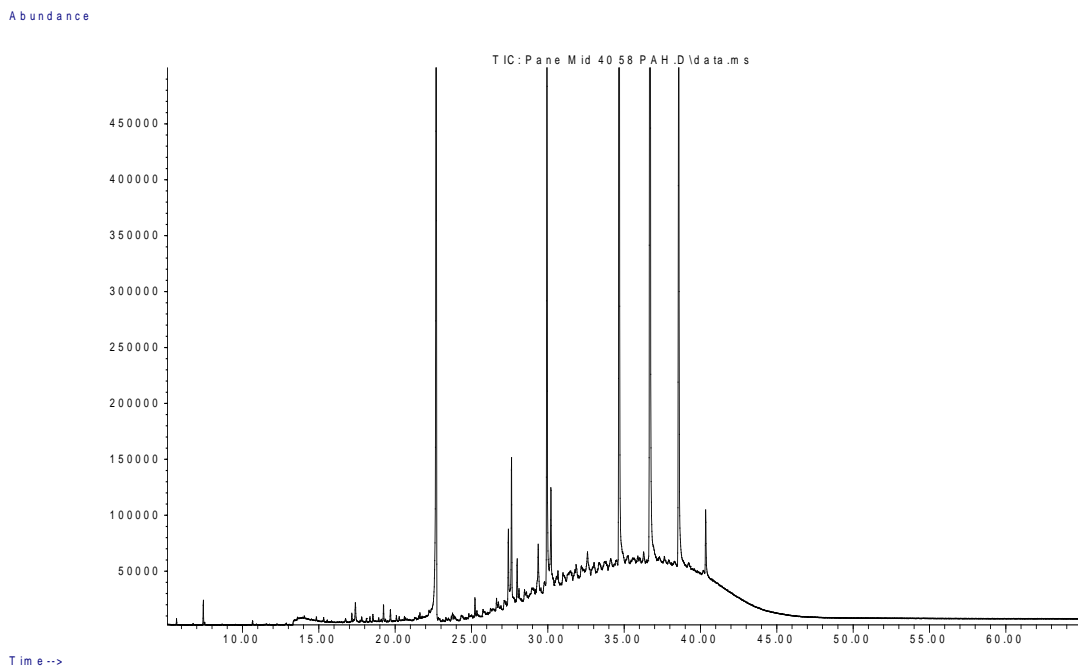
Figure III.62: Site 4, Panepane Point mid tide core for sediment, 20-40 cm deep. GC/MS total ion chromatograph results from *Rena* PAH fingerprint analysis.
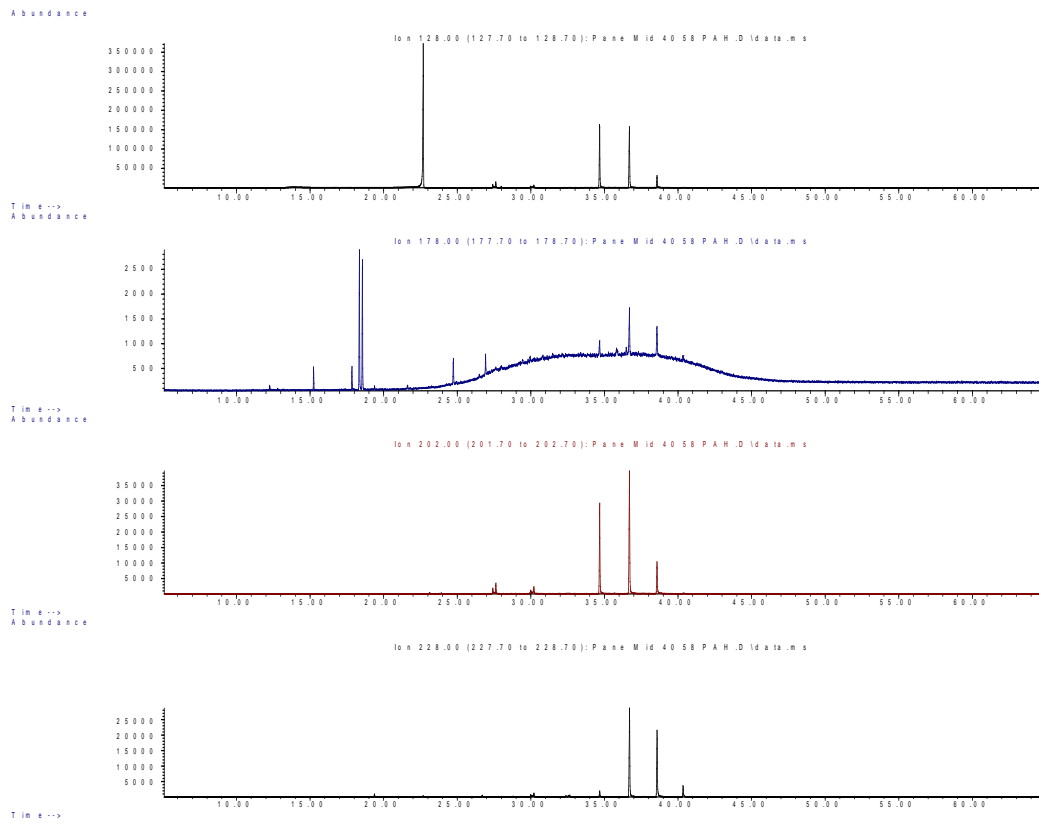
Figure III.63: Site 4, Panepane Point mid tide core for sediment 20-40 cm deep. GC/MS chromatograph results from *Rena* PAH fingerprint analysis for naphthalene 128 (top), phenanthrene 178 (second), pyrene 202 (third) and benzo(a)anthracene and chrysene 228 at the bottom.
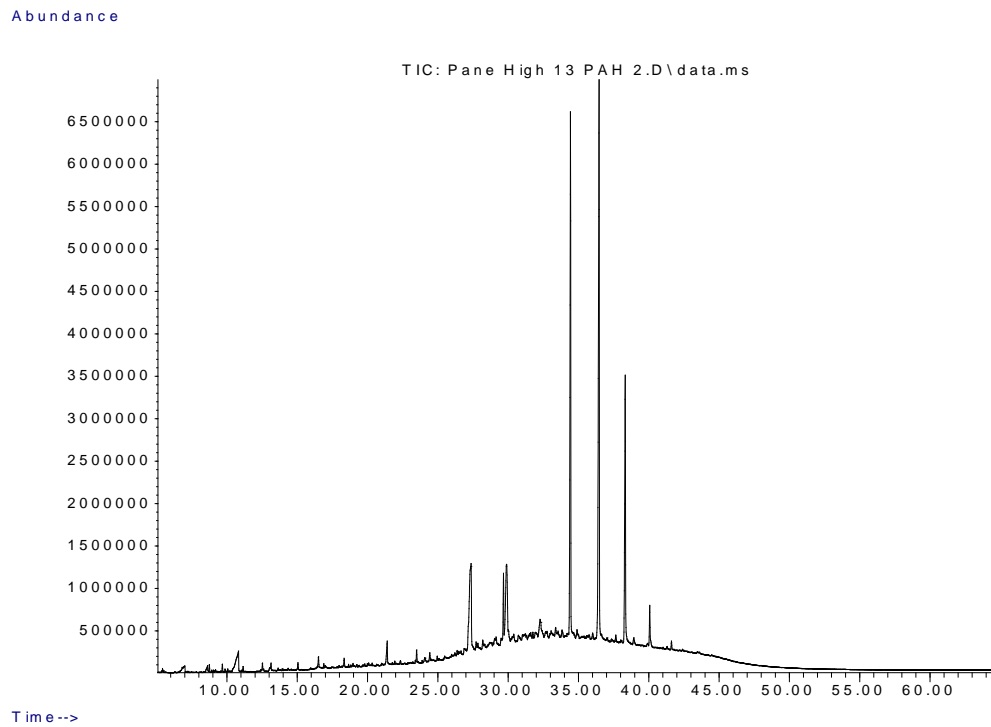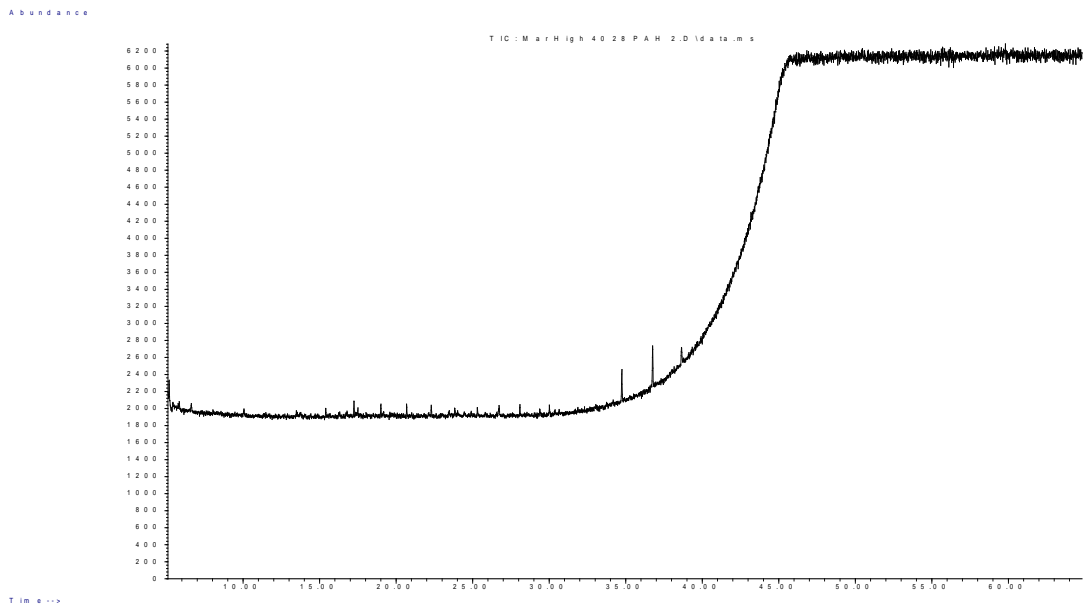

Figure III.64: Site 4, Panepane Point high tide core for sediment, 0-20 cm deep. GC/MS total ion chromatograph results from *Rena* PAH fingerprint analysis.

182
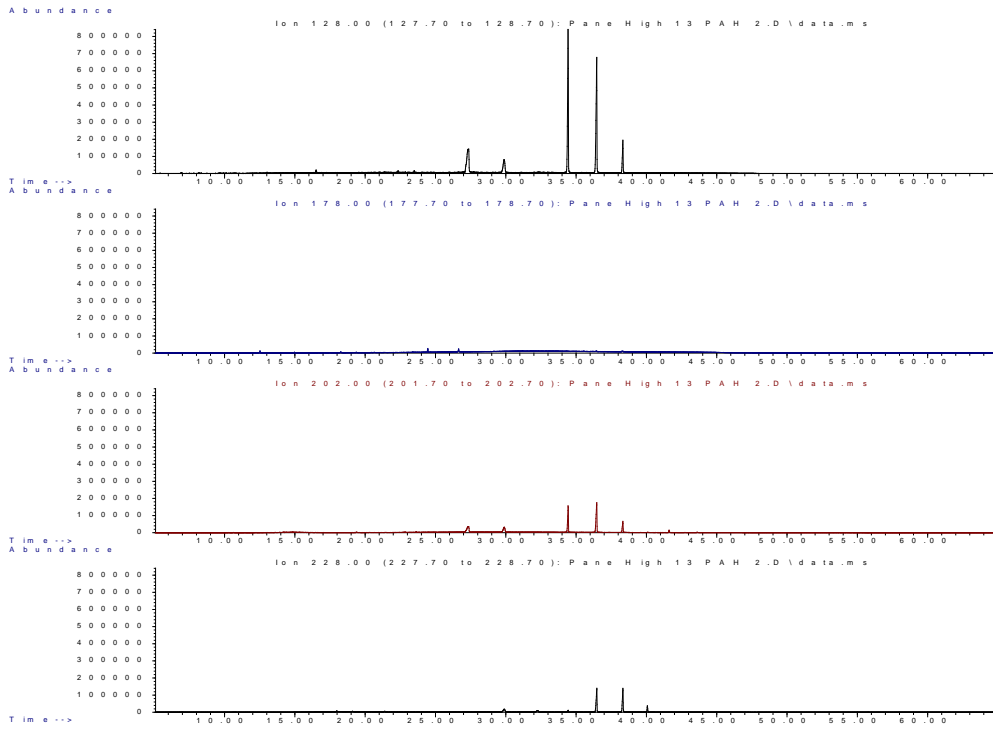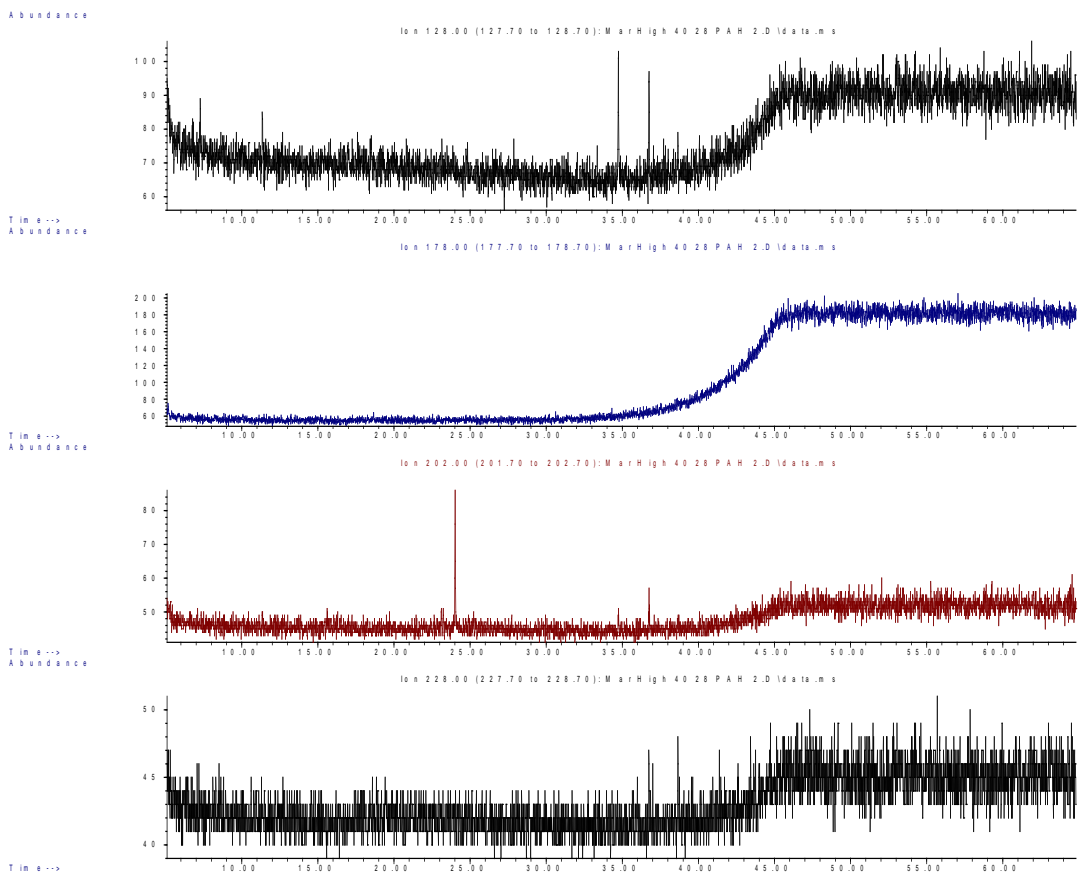
Figure III.65: Site 4, Panepane Point high tide core for sediment 0-20 cm deep. GC/MS chromatograph results from *Rena* PAH fingerprint analysis for naphthalene 128 (top), phenanthrene 178 (second), pyrene 202 (third) and benzo(a)anthracene and chrysene 228 at the bottom.
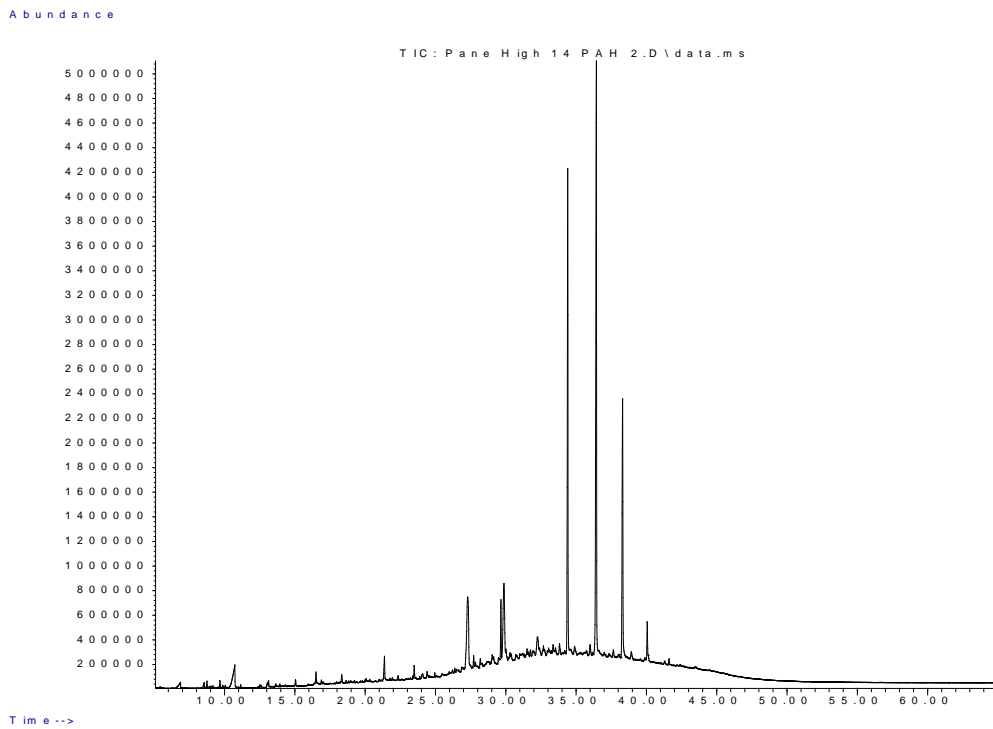
Figure III.66: Site 4, Panepane Point high tide core for sediment, 20-40 cm deep. GC/MS total ion chromatograph results from *Rena* PAH fingerprint analysis.
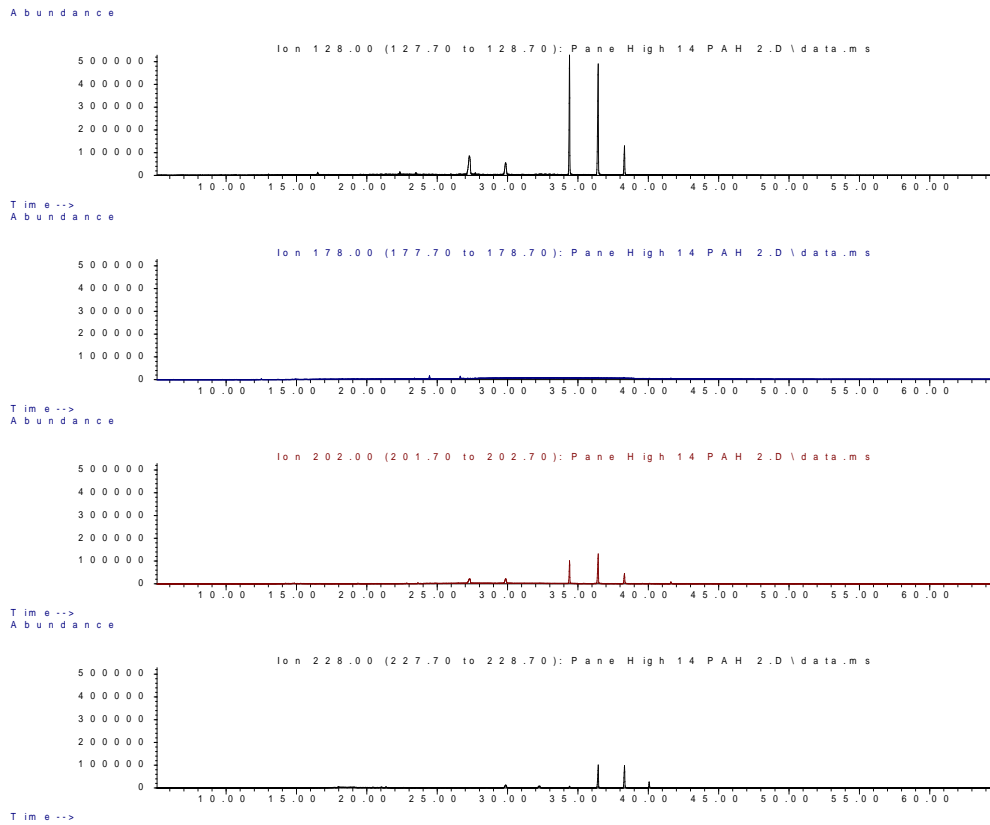
Figure III.67: Site 4, Panepane Point high tide core for sediment 20-40 cm deep. GC/MS chromatograph results from *Rena* PAH fingerprint analysis for naphthalene 128 (top), phenanthrene 178 (second), pyrene 202 (third) and benzo(a)anthracene and chrysene 228 at the bottom.
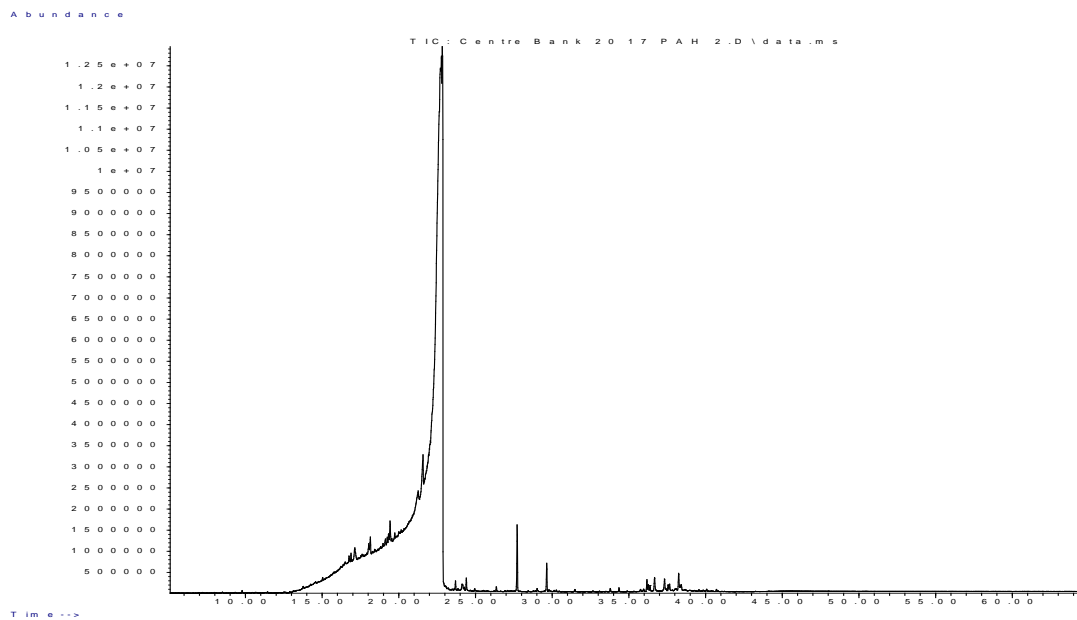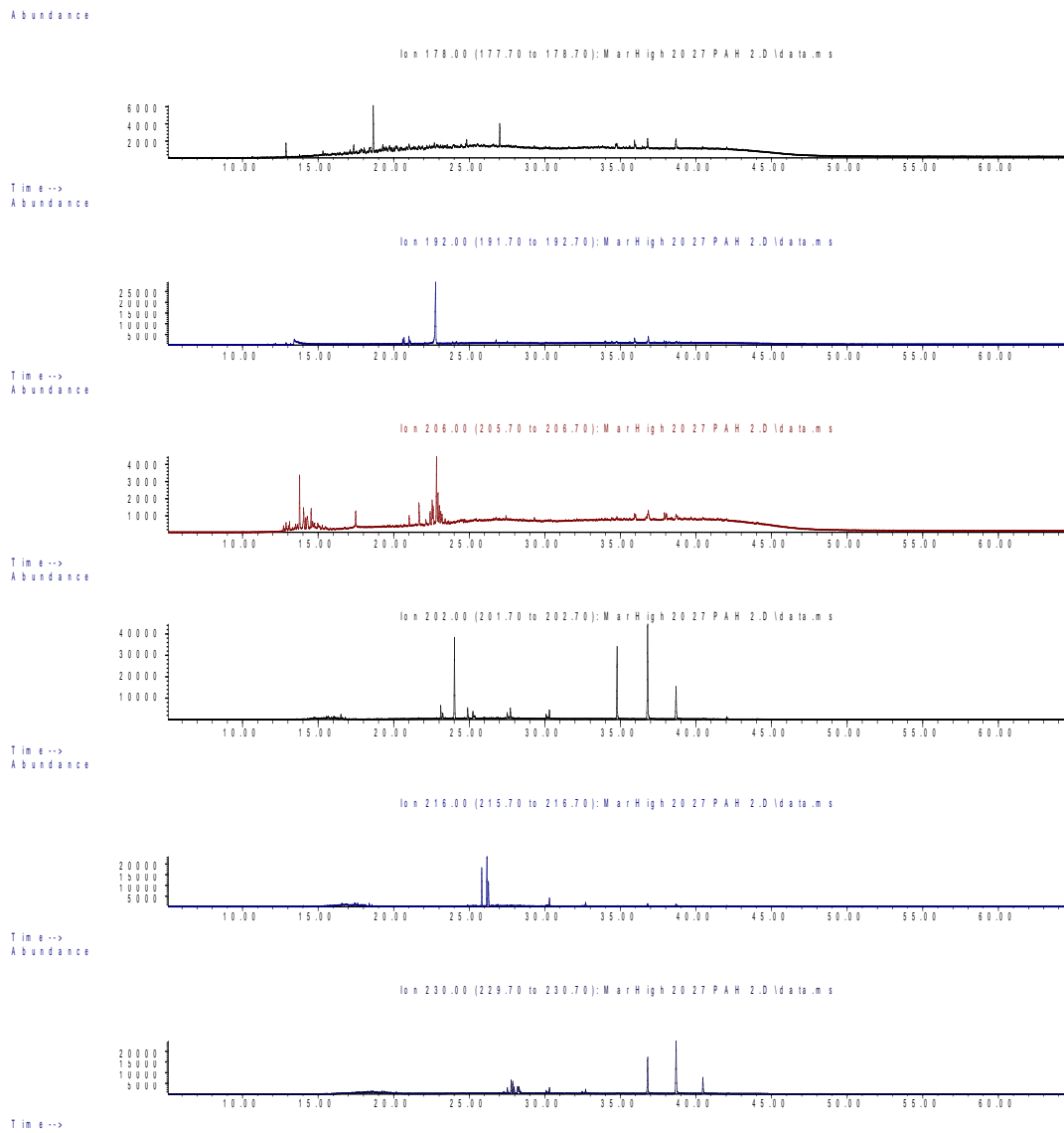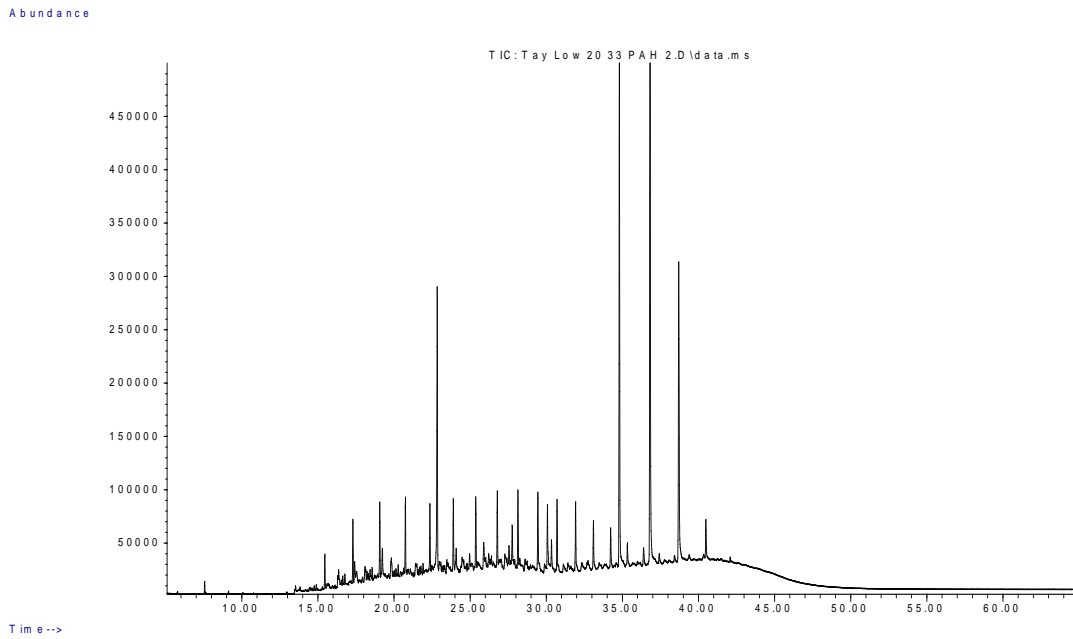

Figure III.68: Site 5, Centre Bank core for sediment 0-20 cm deep. GC/MS total ion chromatograph results from *Rena* PAH fingerprint analysis.
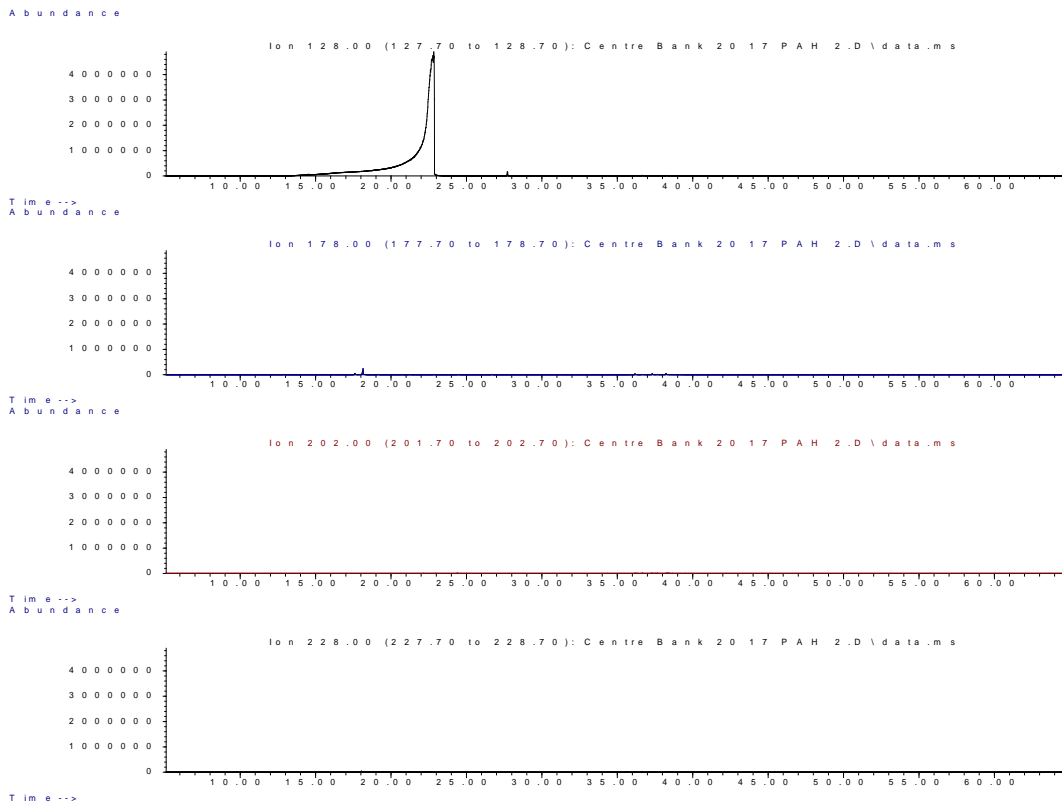
Figure III.69: Site 5, Centre Bank core for sediment 0-20 cm deep. GC/MS chromatograph results from *Rena* PAH fingerprint analysis for naphthalene 128 (top), phenanthrene 178 (second), pyrene 202 (third) and benzo(a)anthracene and chrysene 228 at the bottom.
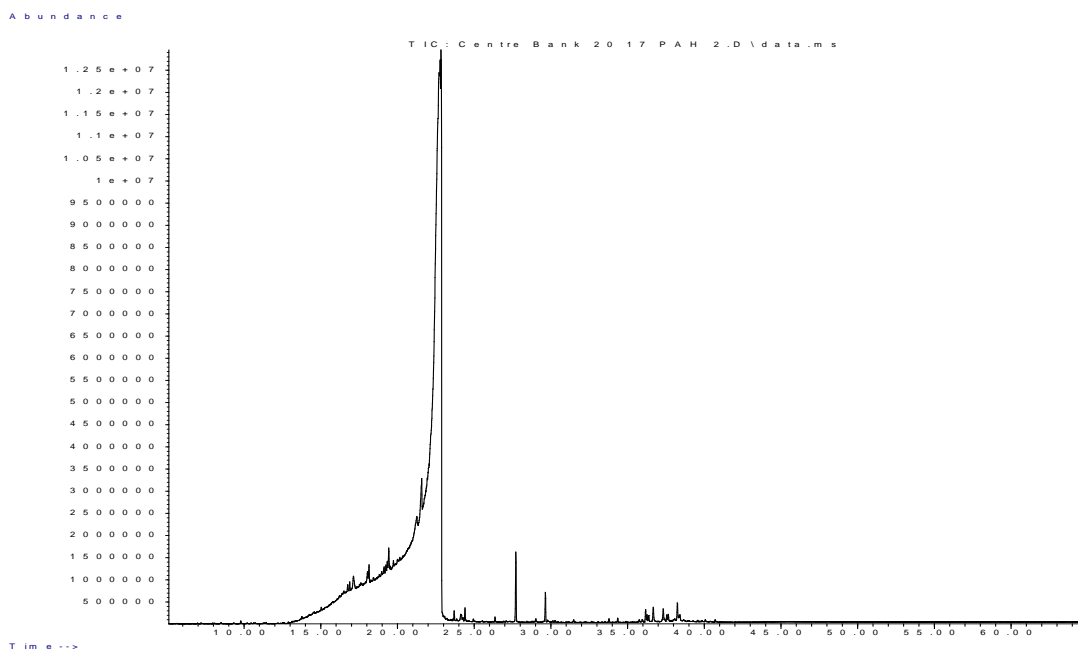
Figure III.70: Site 5, Centre Bank core for sediment 20-40 cm deep. GC/MS total ion chromatograph results from *Rena* PAH fingerprint analysis.
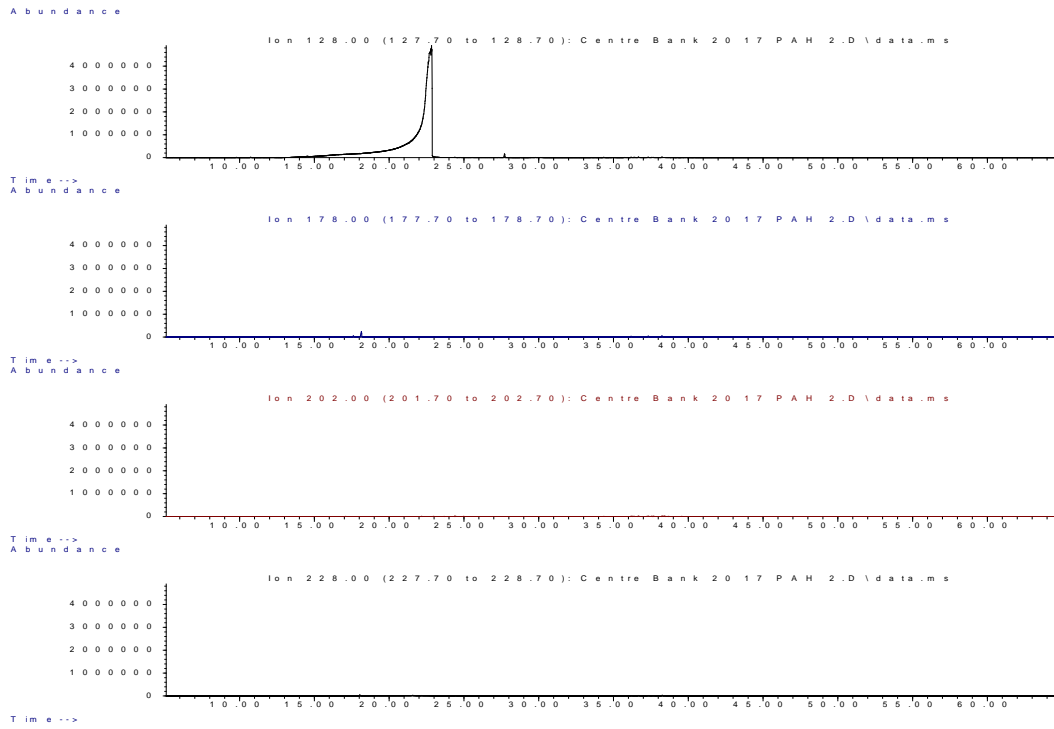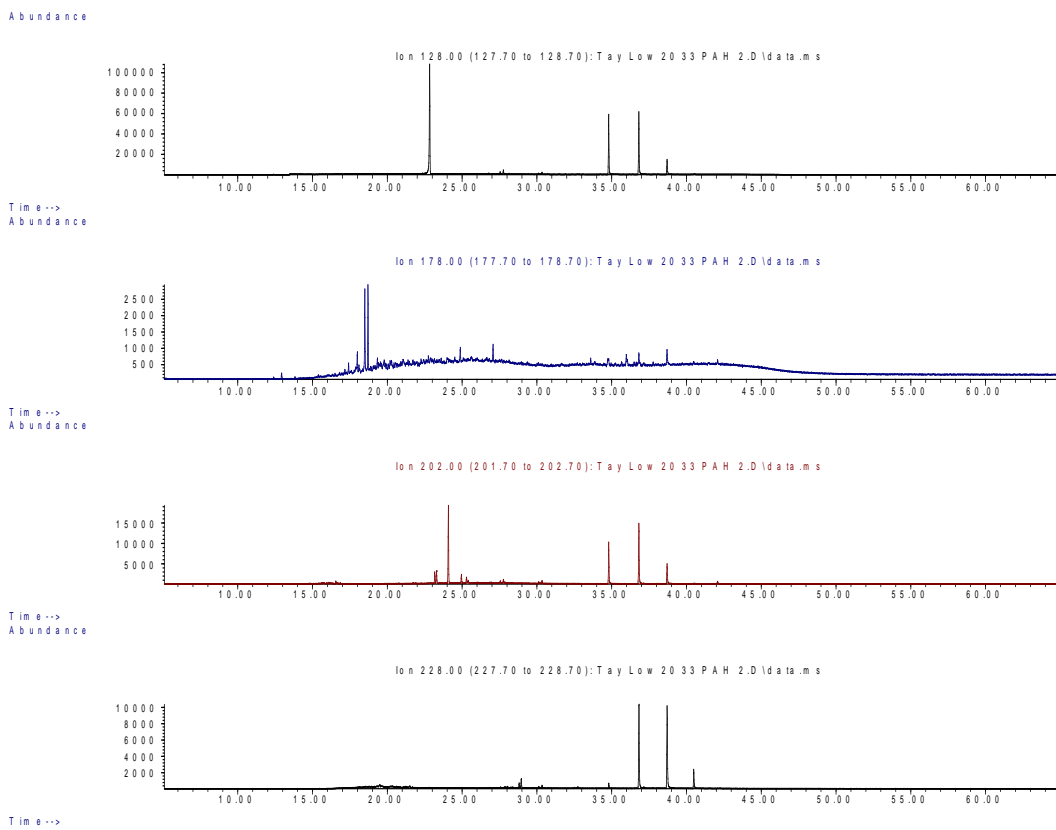
Figure III.71: Site 5, Centre Bank core for sediment 20-40 cm deep. GC/MS chromatograph results from *Rena* PAH fingerprint analysis for naphthalene 128 (top), phenanthrene 178 (second), pyrene 202 (third) and benzo(a)anthracene and chrysene 228 at the bottom.
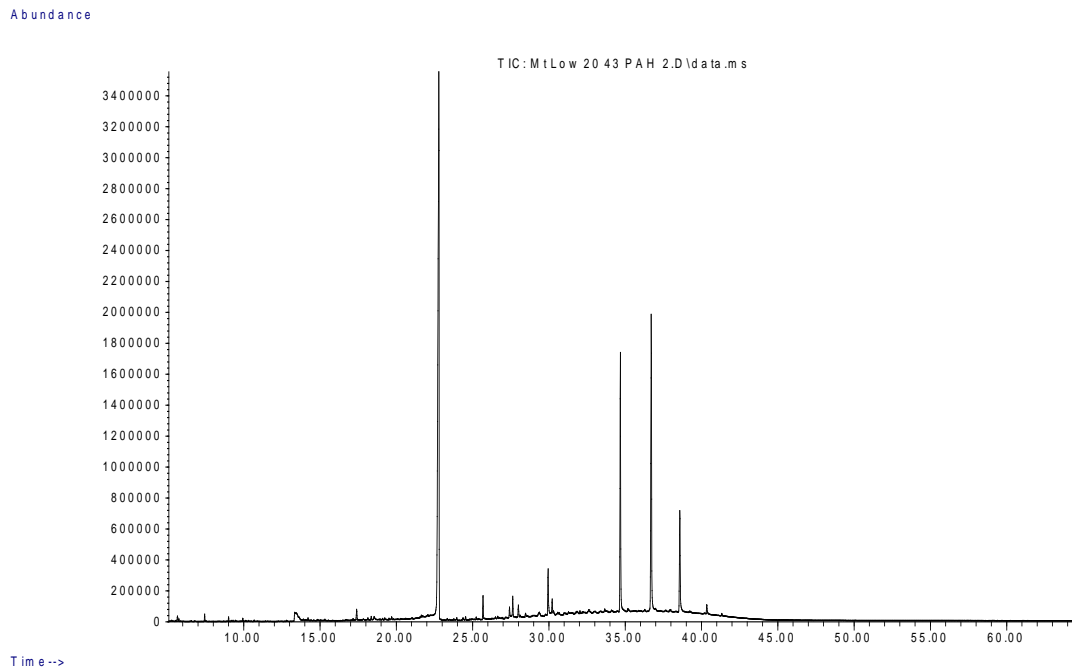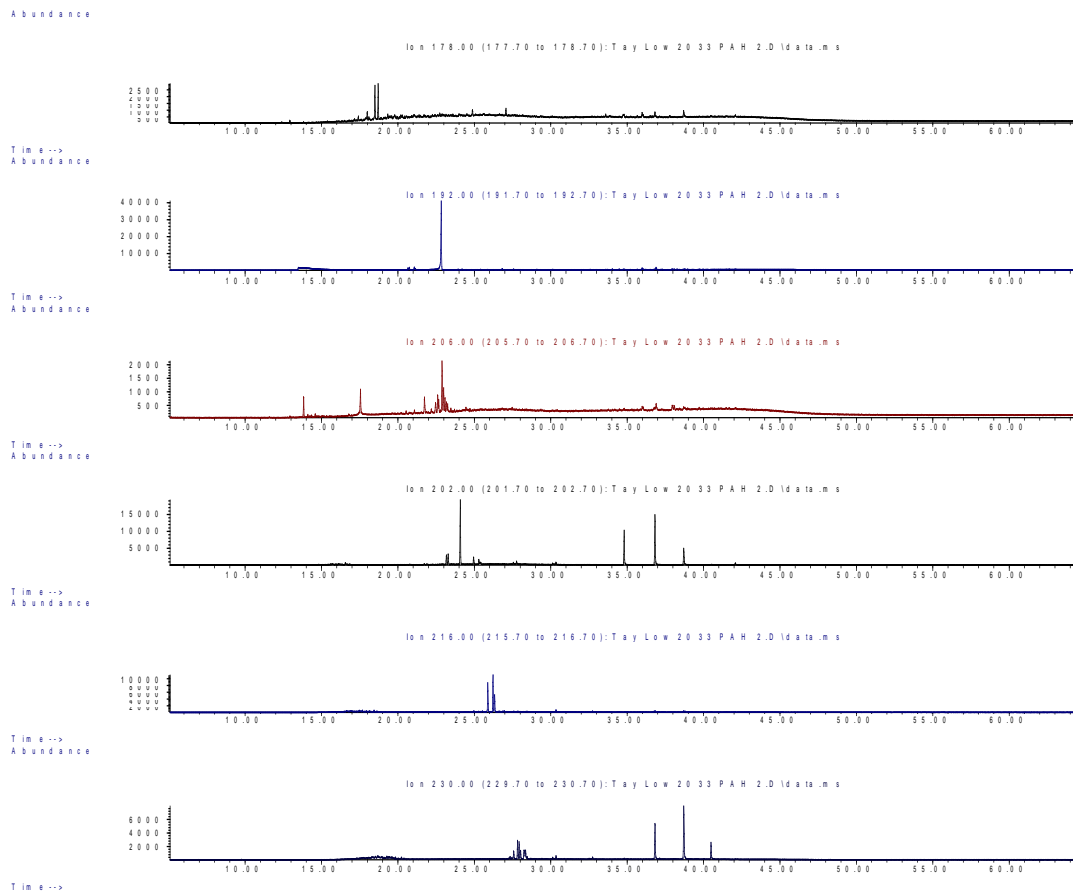

Figure III.72: Site 6, Mount Maunganui low tide core for sediment 0-20 cm deep. GC/MS total ion chromatograph results from *Rena* PAH fingerprint analysis.
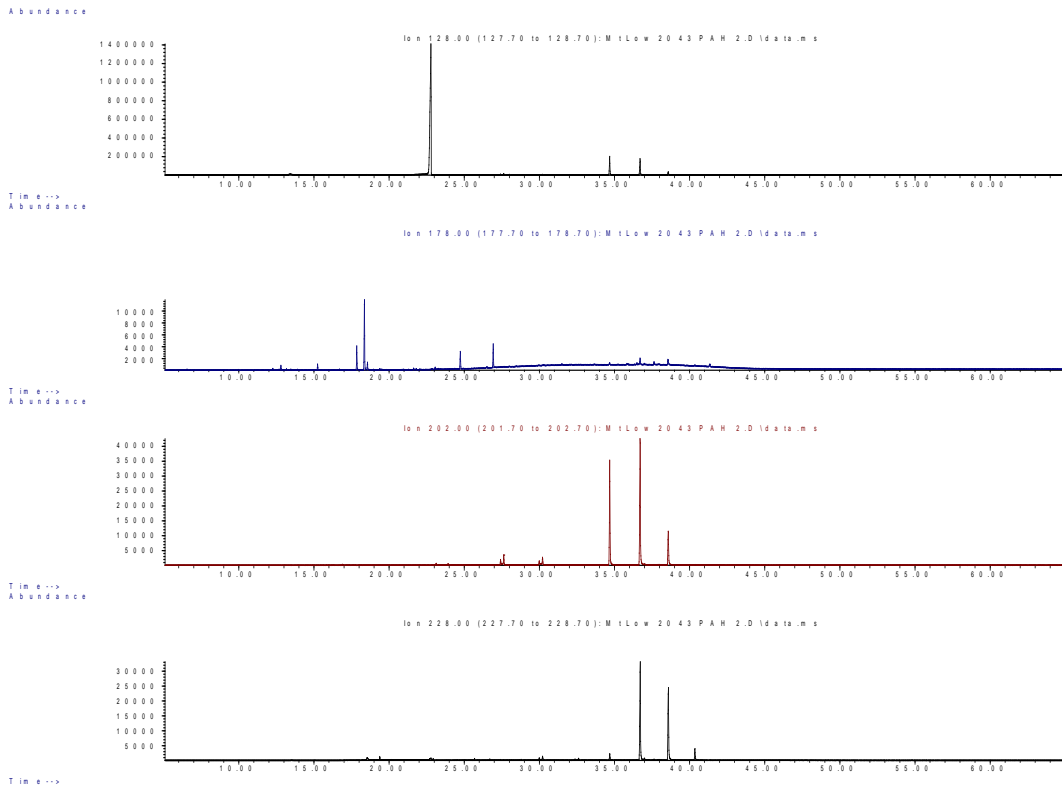
Figure 9II.73: Site 6, Mount Maunganui low tide core for sediment, 0-20 cm deep. GC/MS chromatograph results from *Rena* PAH fingerprint analysis for naphthalene 128 (black), phenanthrene 178 (blue), pyrene 202 (red) and benzo(a)anthracene and chrysene 228 (black) at the bottom.
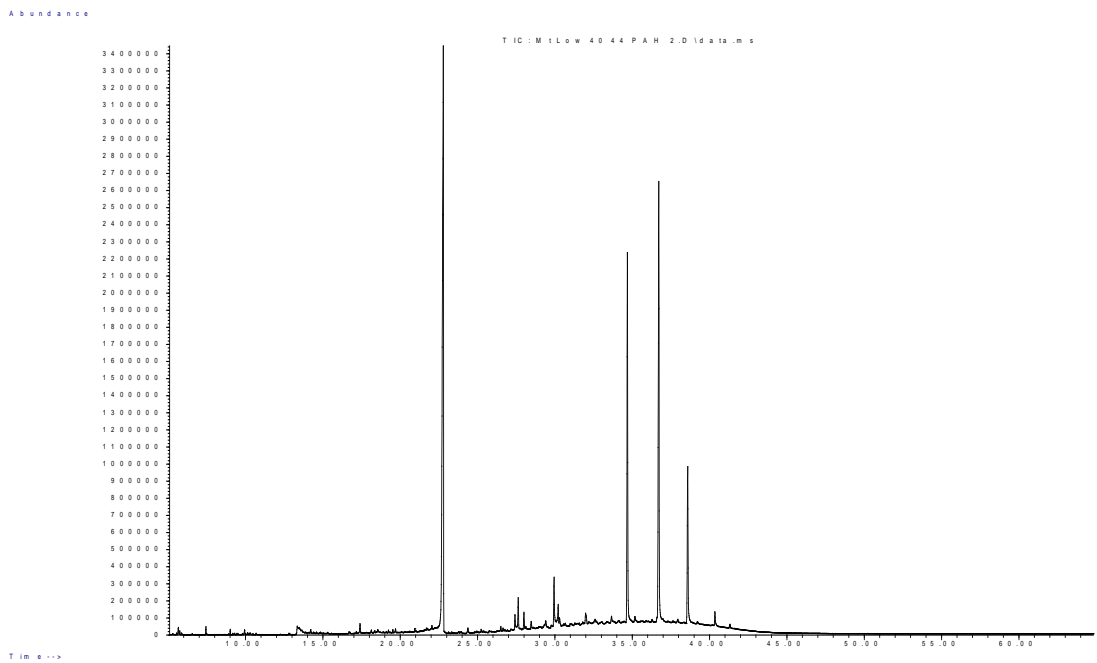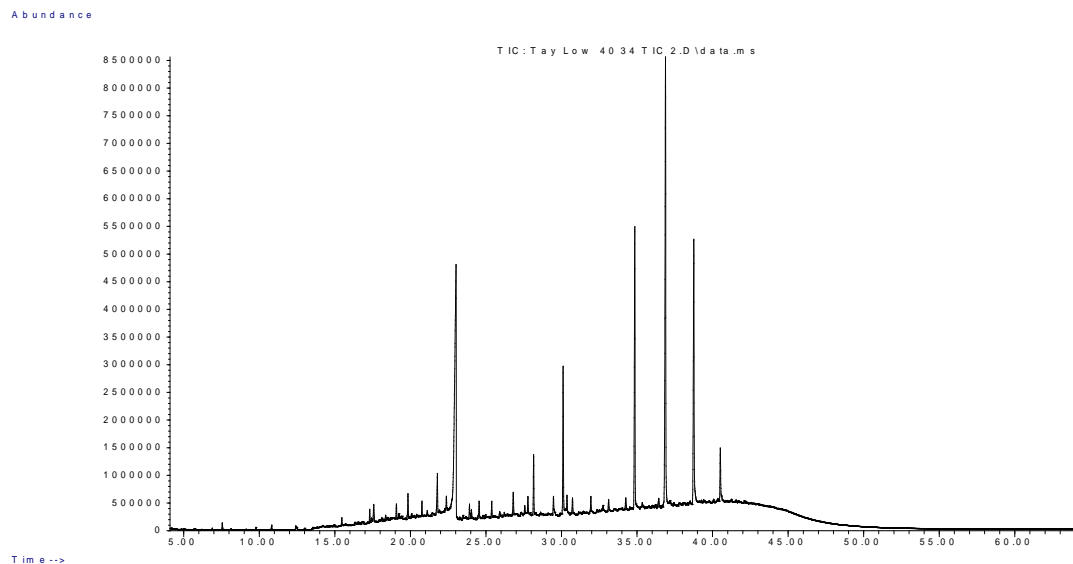

Figure III.74: Site 6, Mount Maunganui low tide core for sediment 20-40 cm deep. GC/MS total ion chromatograph results from *Rena* PAH fingerprint analysis.
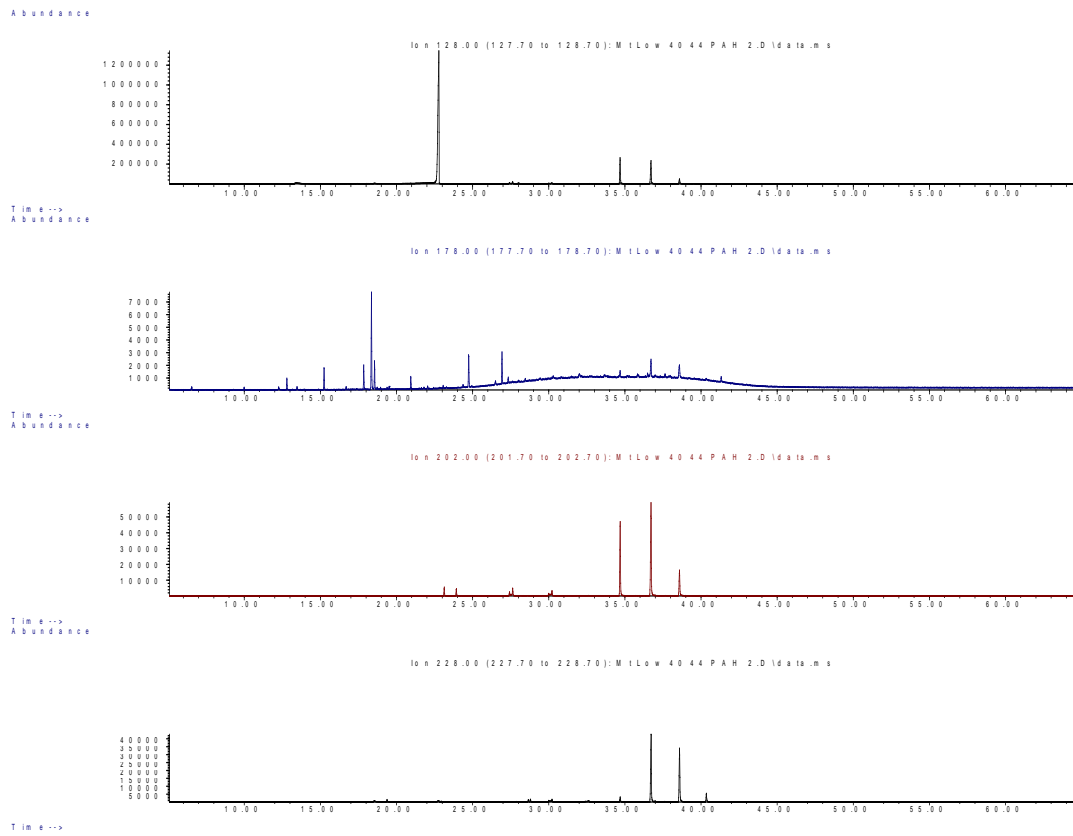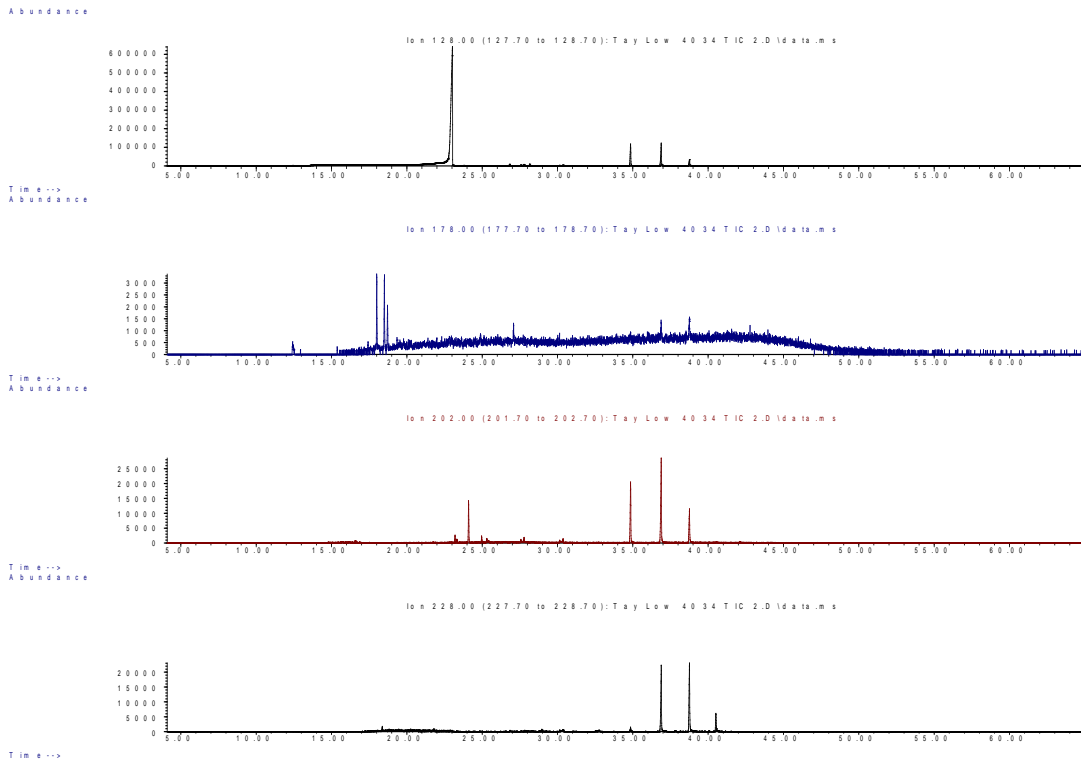
Figure III.75: Site 6, Mount Maunganui low tide core for sediment, 20-40 cm deep. GC/MS chromatograph results from *Rena* PAH fingerprint analysis for Naphthalene 128 (black), phenanthrene 178 (blue), pyrene 202 (red) and benzo(a)anthracene and chrysene 228 (black) at the bottom.
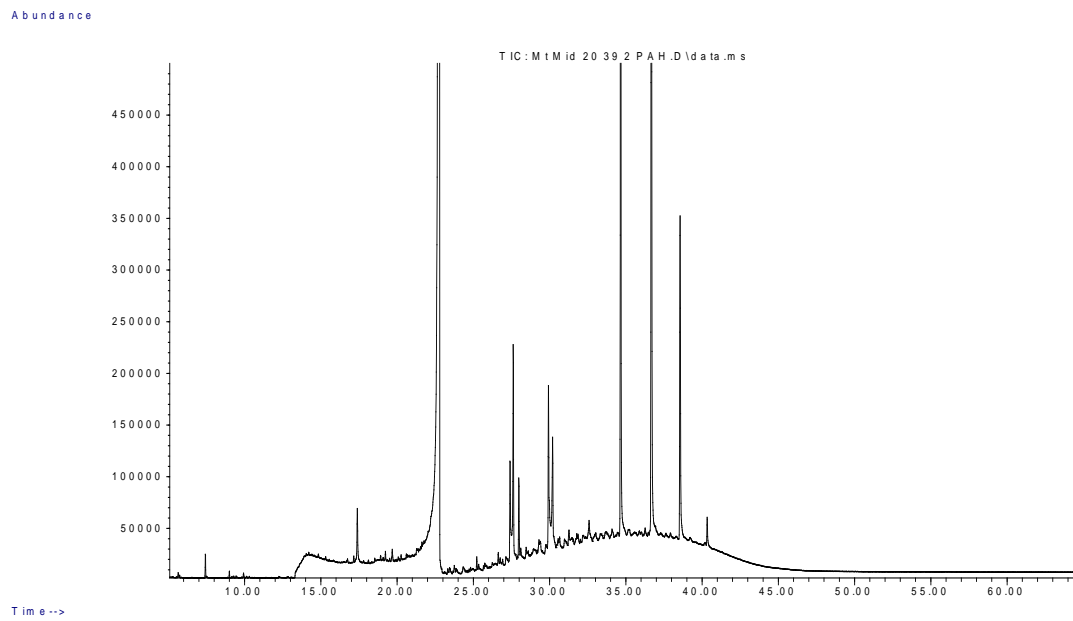
Figure III.76: Site 6, Mount Maunganui mid tide core for sediment 0-20 cm deep. GC/MS total ion chromatograph results from *Rena* PAH fingerprint analysis.
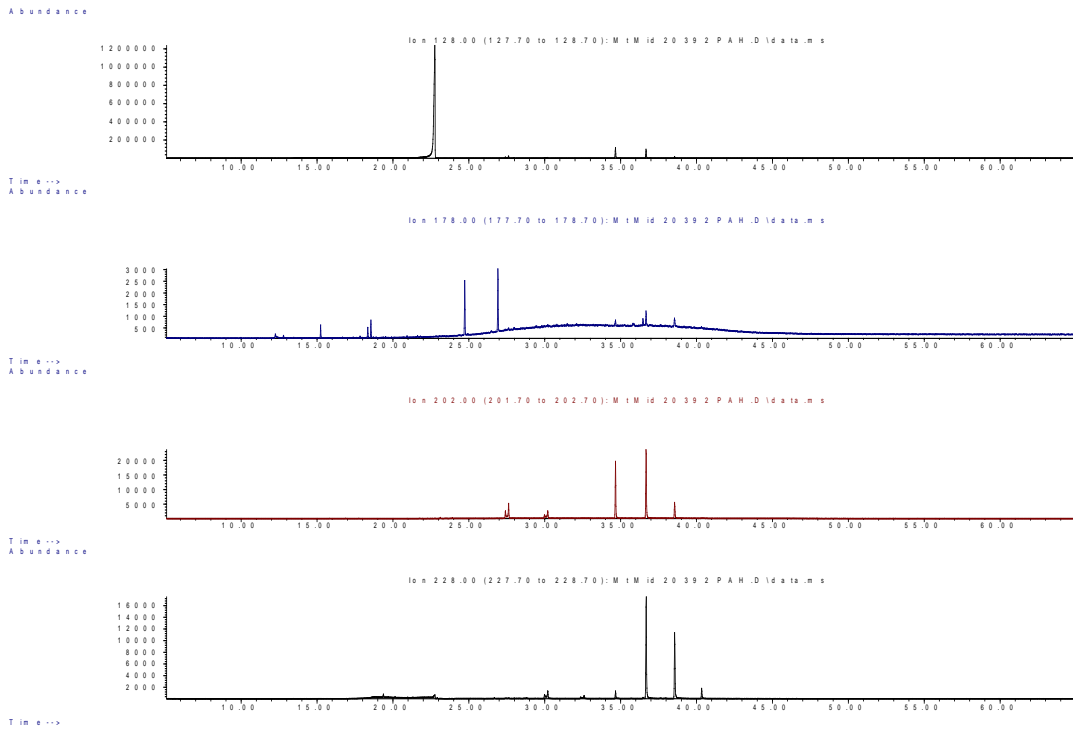
Figure III.77 Site 6, Mount Maunganui mid tide core for sediment, 0-20 cm deep. GC/MS chromatograph results from *Rena* PAH fingerprint analysis for Naphthalene 128 (black), phenanthrene 178 (blue), pyrene 202 (red) and benzo(a)anthracene and chrysene 228 (black) at the bottom.
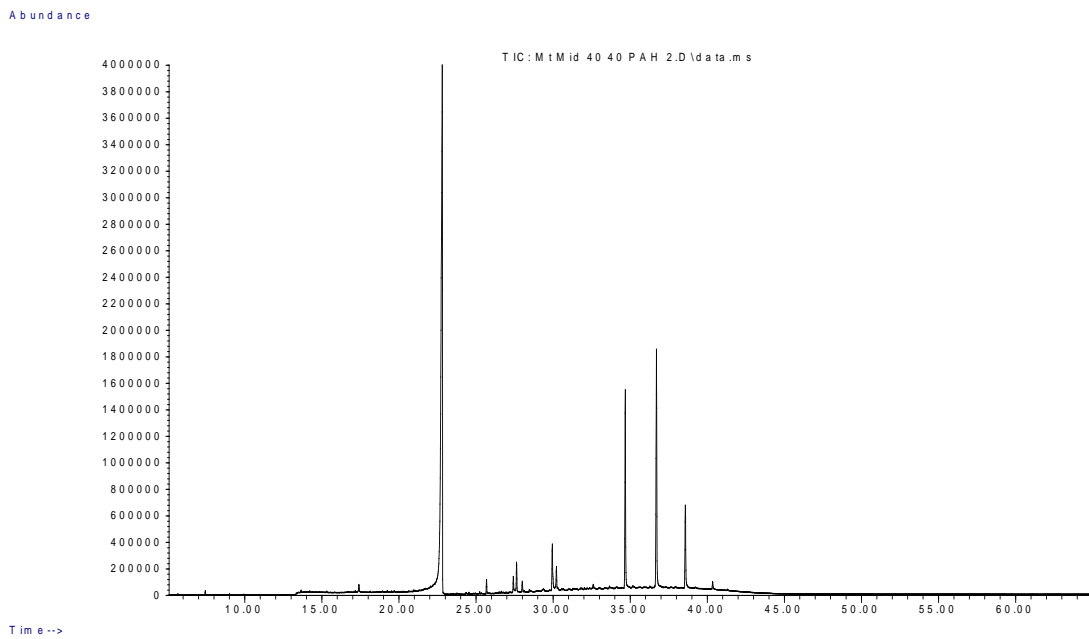
Figure III.78: Site 6, Mount Maunganui mid tide core for sediment, 20-40 cm deep. GC/MS total ion chromatograph results from *Rena* PAH fingerprint analysis.

189
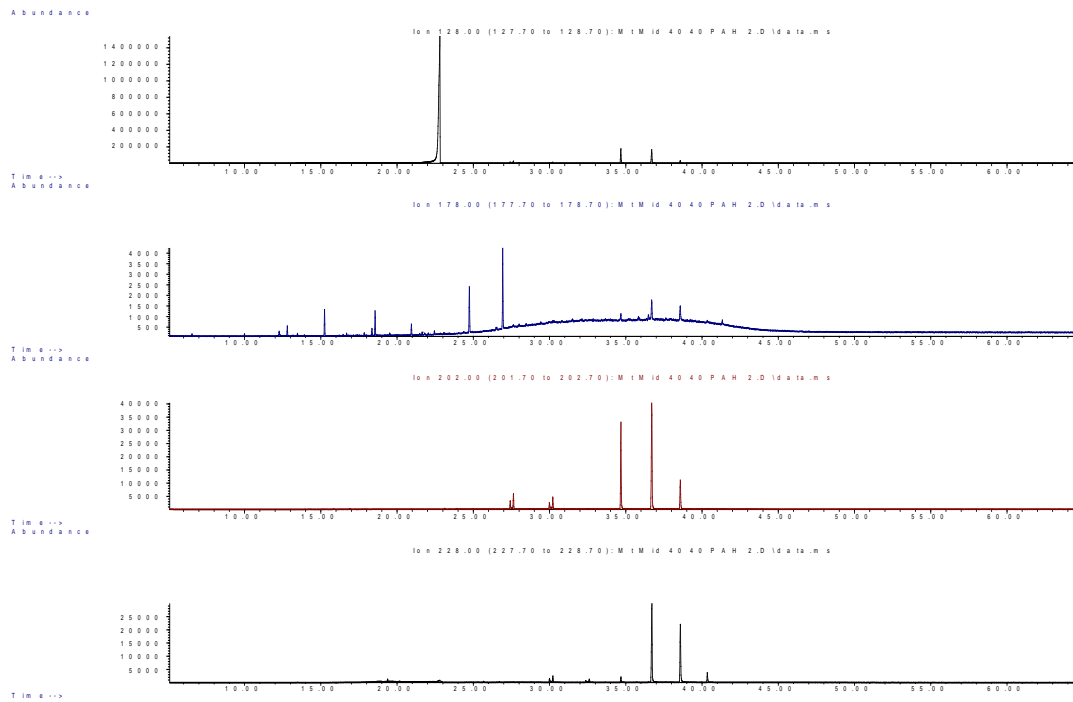
Figure III.79: Site 6, Mount Maunganui mid tide core for sediment 20-40 cm deep. GC/MS chromatograph results from *Rena* PAH fingerprint analysis for naphthalene 128 (top), phenanthrene 178 (second), pyrene 202 (third) and benzo(a)anthracene and chrysene 228 at the bottom.
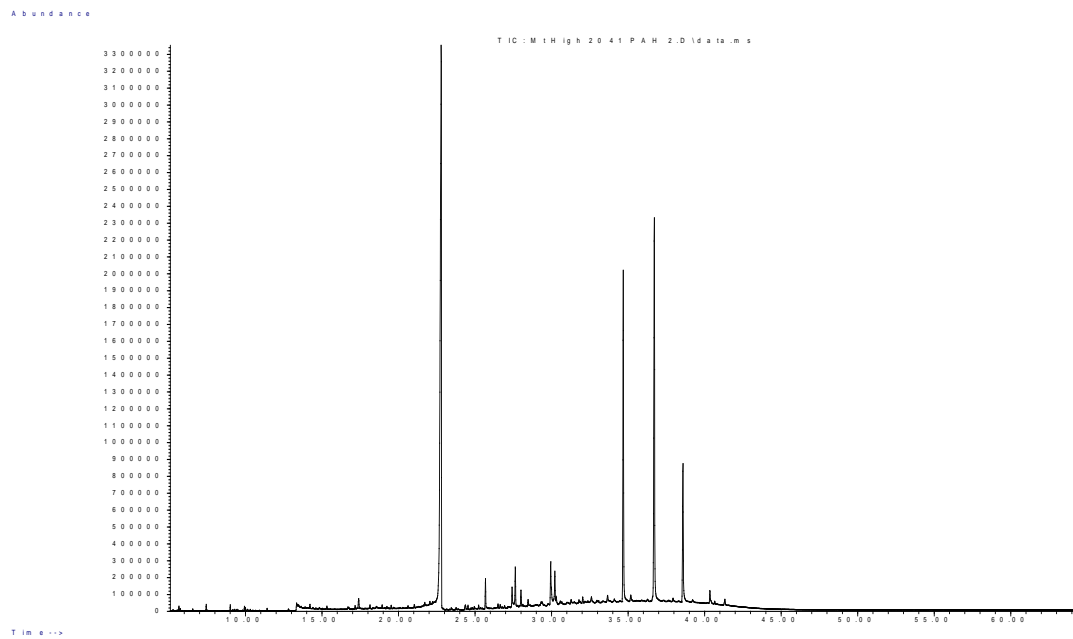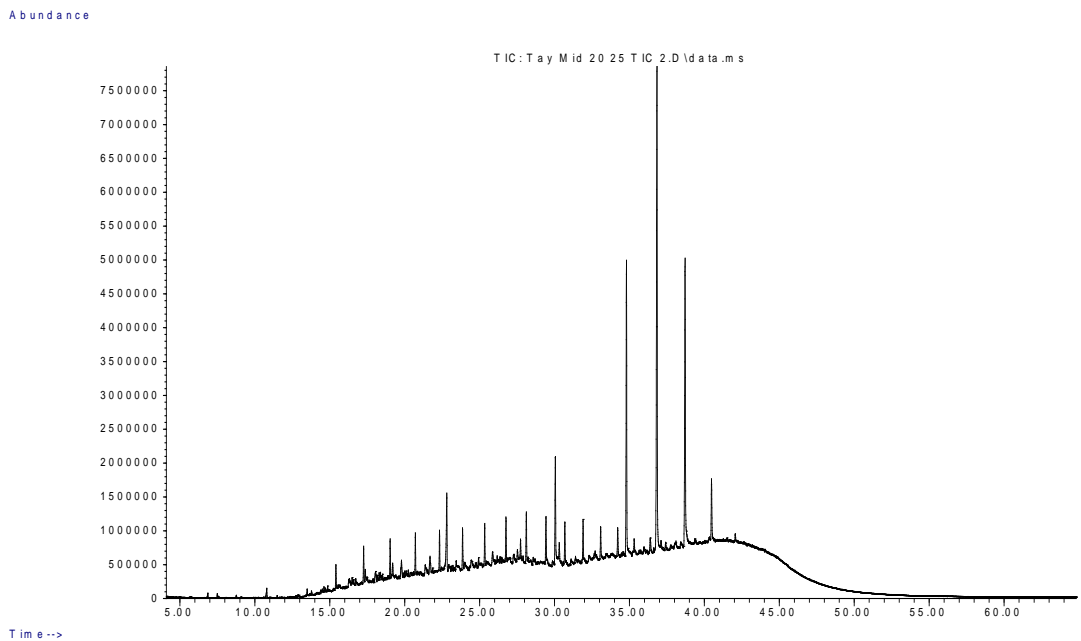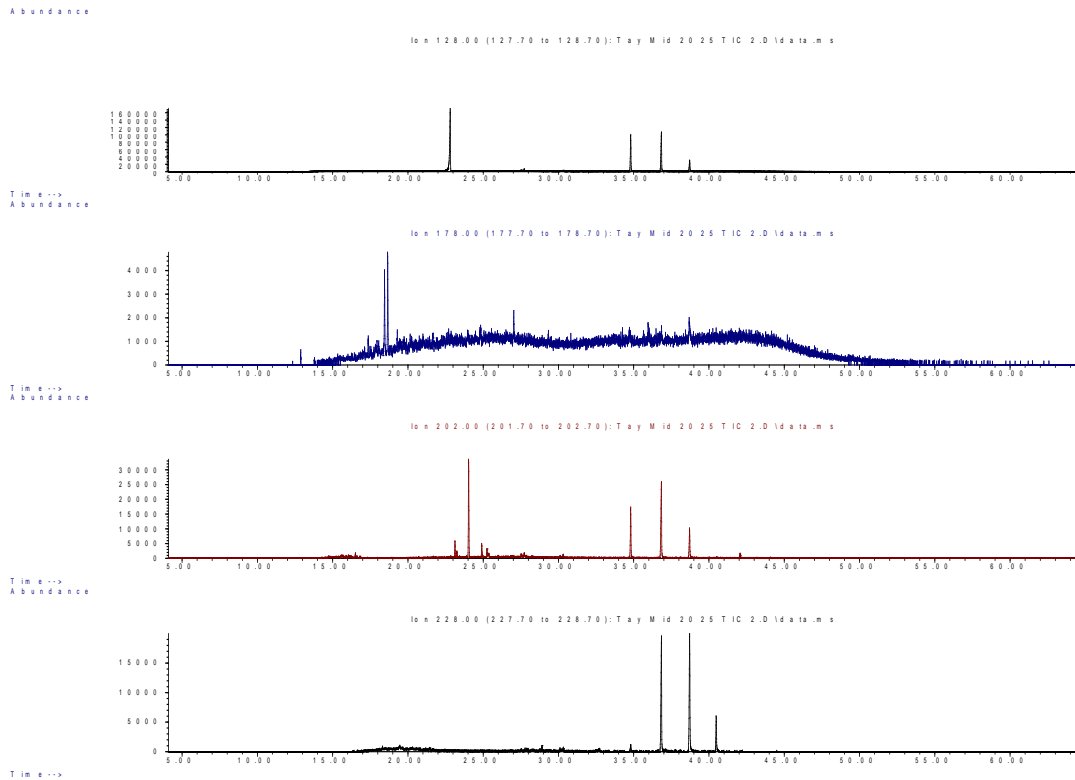

Figure III.80: Site 6, Mount Maunganui high tide core for sediment, 0-20 cm deep. GC/MS total ion chromatograph results from *Rena* PAH fingerprint analysis.

190
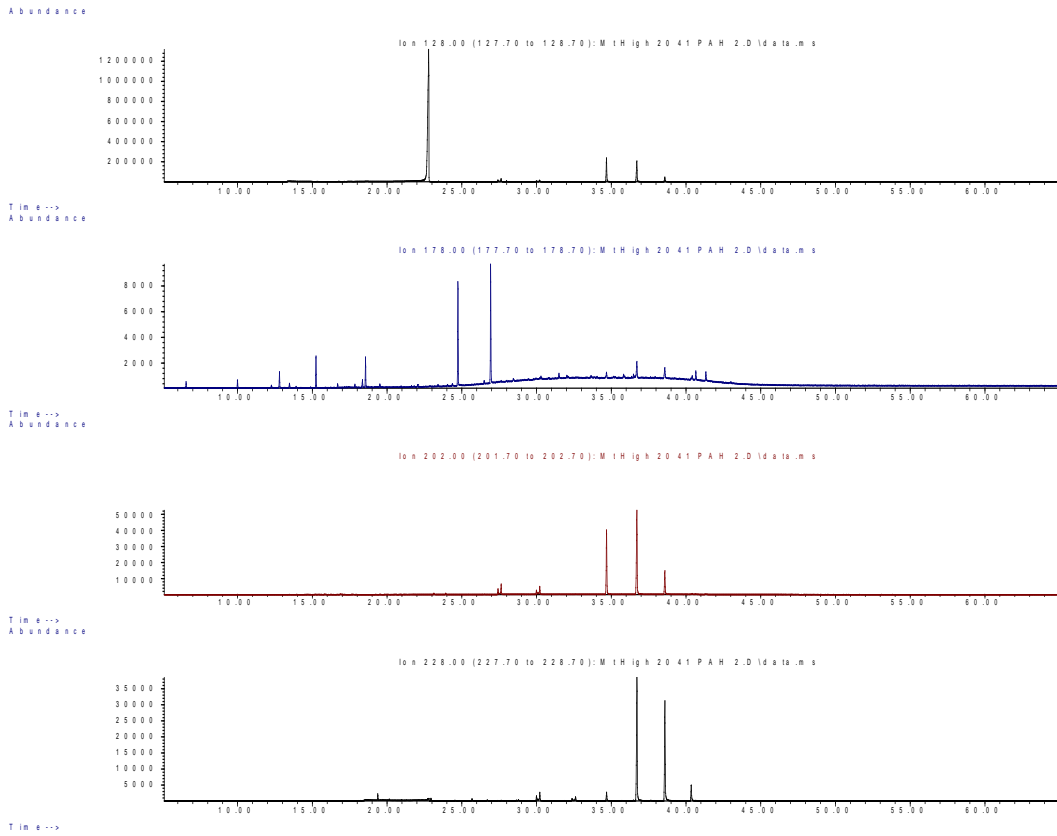
Figure III.81: Site 6, Mount Maunganui high tide core for sediment 0-20 cm deep. GC/MS chromatograph results from *Rena* PAH fingerprint analysis for naphthalene 128 (black),phenanthrene 178 (blue), pyrene 202 (red) and benzo(a)anthracene and chrysene 228 (black) at the bottom.
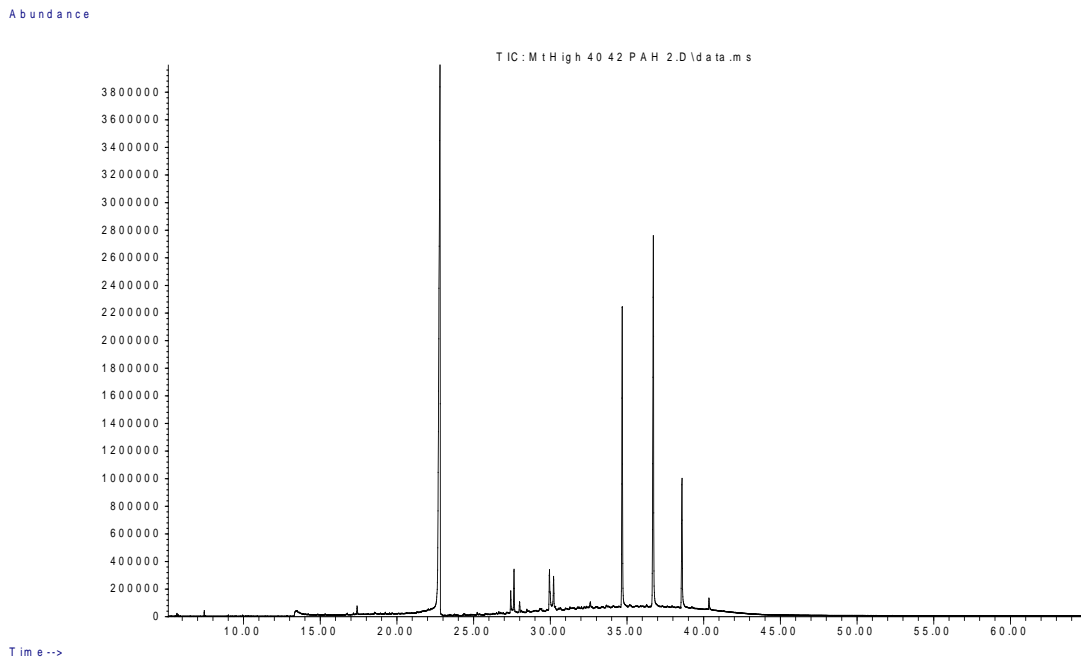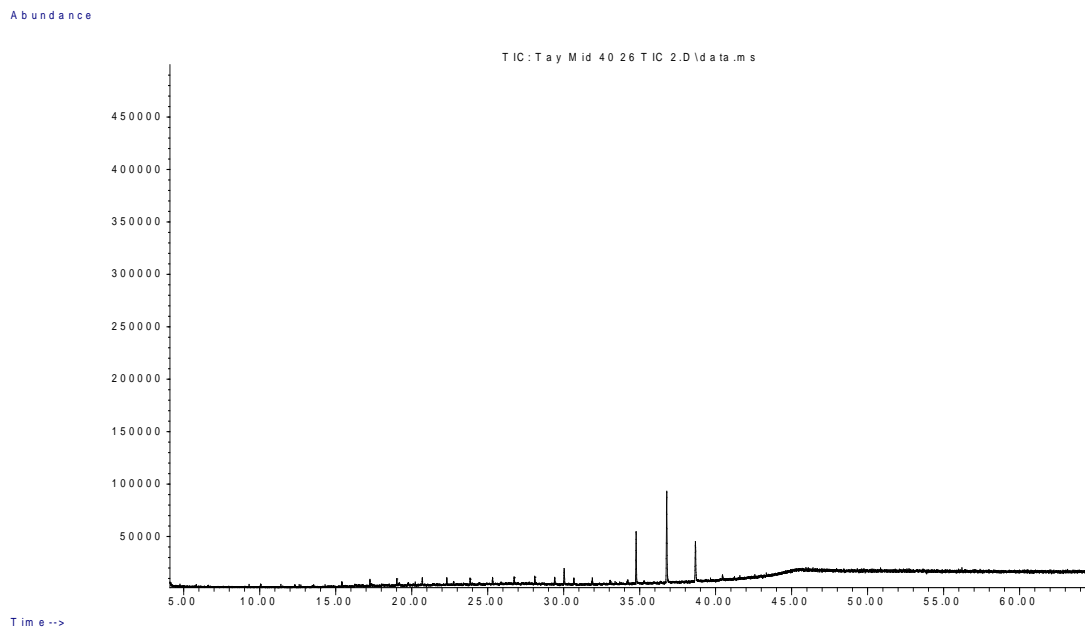

Figure III.82:Site 6, Mount Maunganui high tide core for sediment, 20-40 cm deep. GC/MS total ion chromatograph results from *Rena* PAH fingerprint analysis.
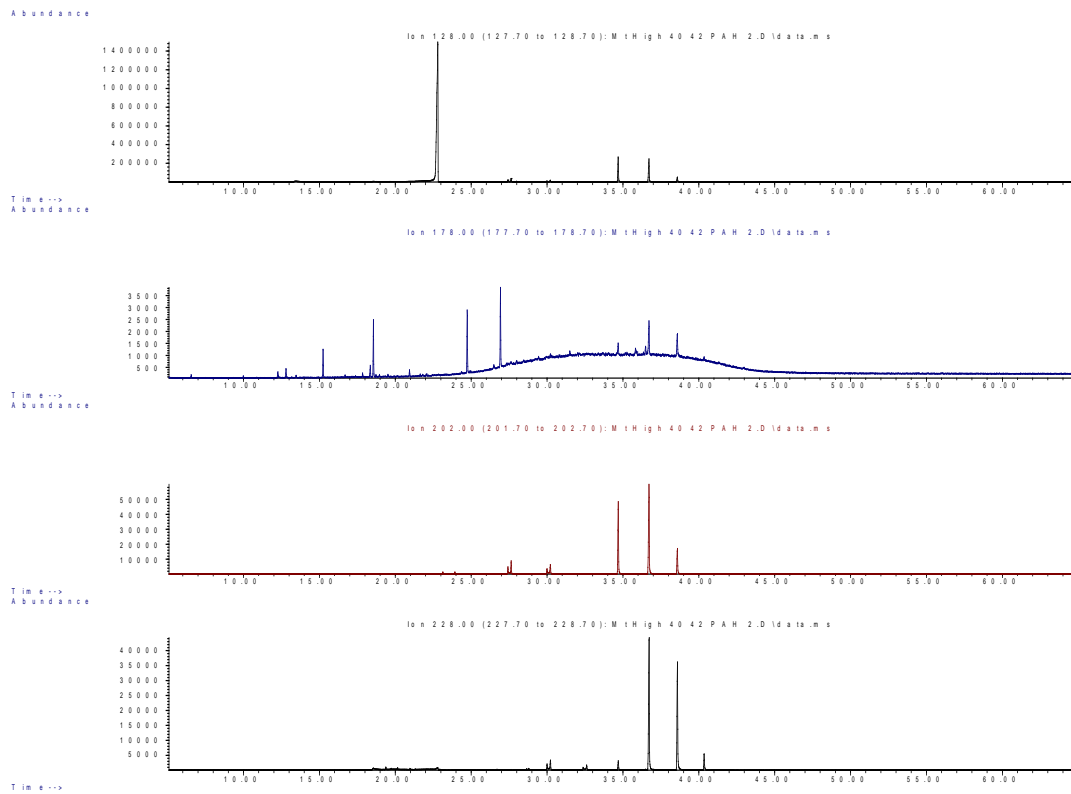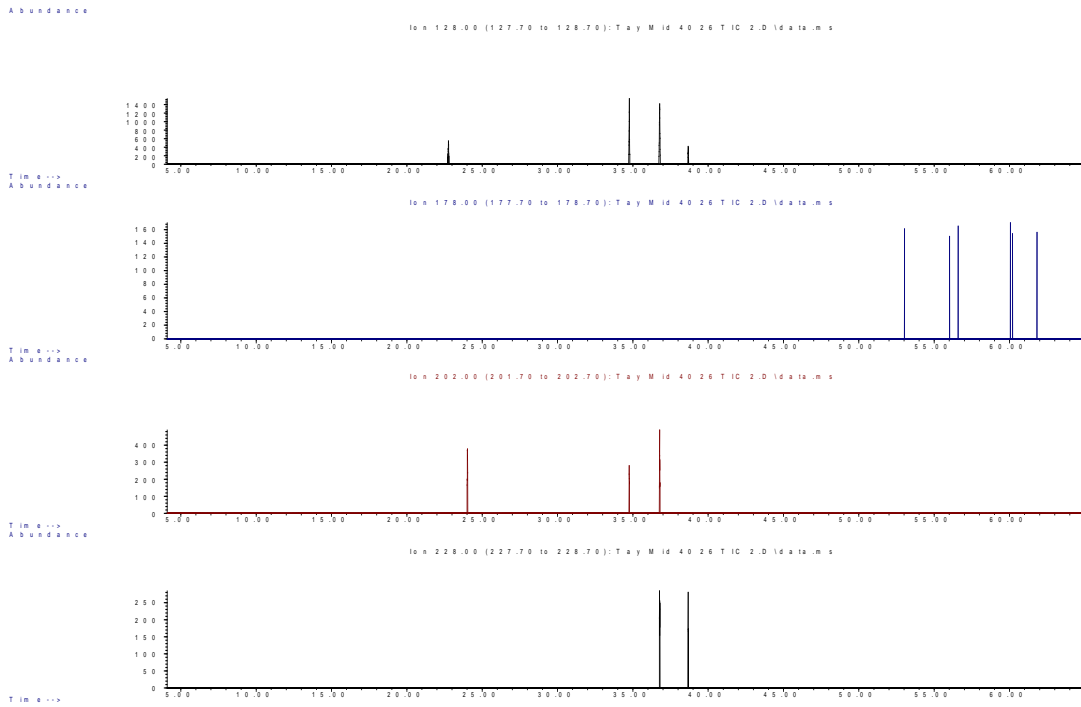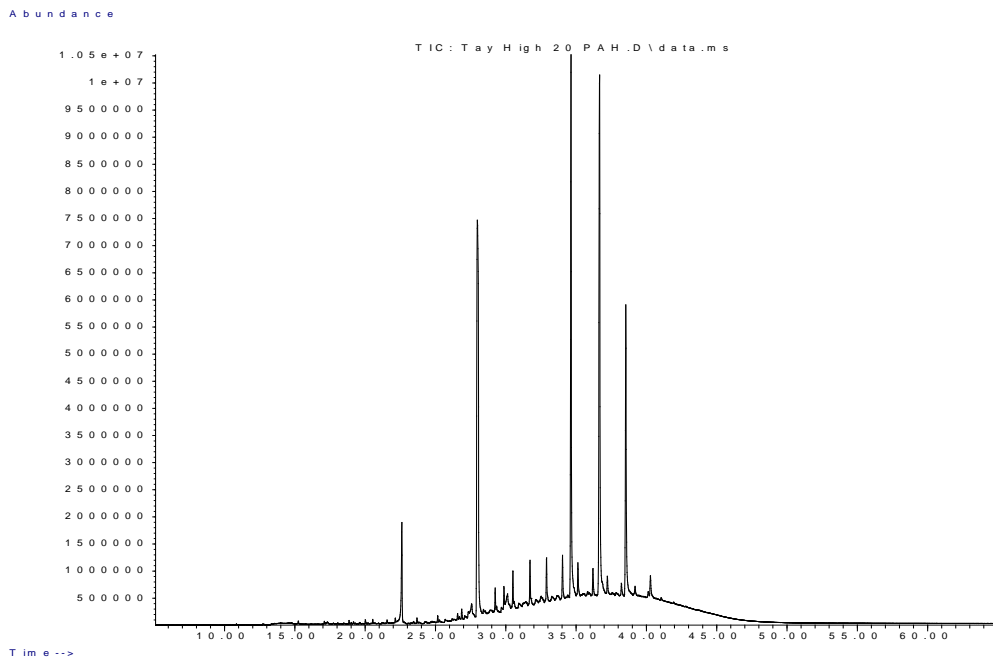
Figure III.83: Site 6, Mount Maunganui high tide core for sediment 20-40 cm deep. GC/MS chromatograph results from *Rena* PAH fingerprint analysis for naphthalene 128 (top), phenanthrene 178 (second), pyrene 202 (third) and benzo(a)anthracene and chrysene 228 at the bottom.
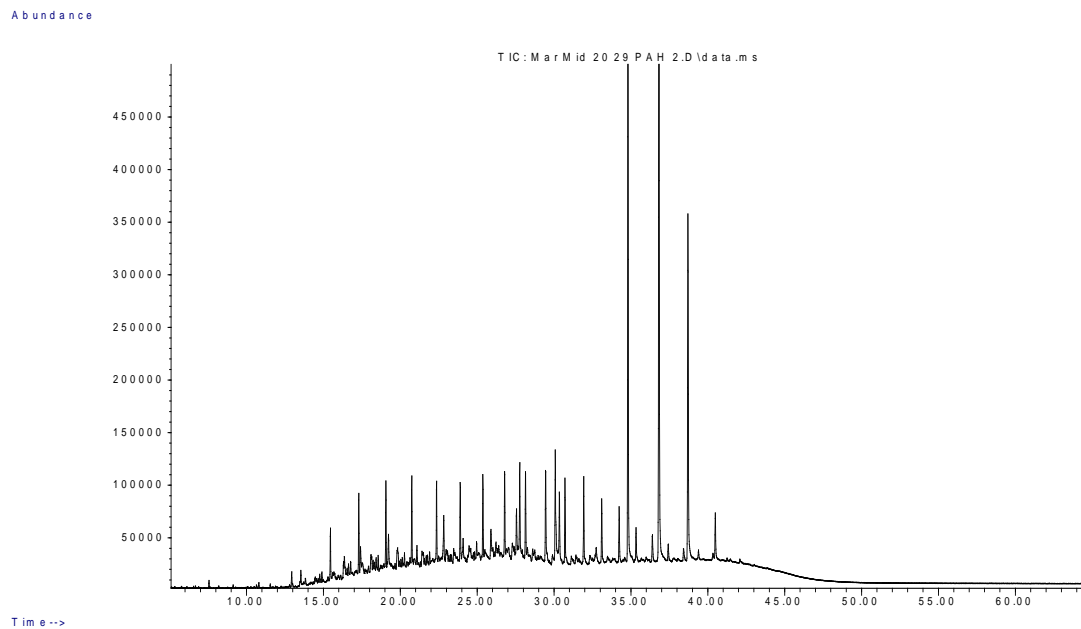
Figure III.84: Site 7, Omanu mid tide core for sediment, 0-20 cm deep. GC/MS total ion chromatograph results from *Rena* PAH fingerprint analysis.
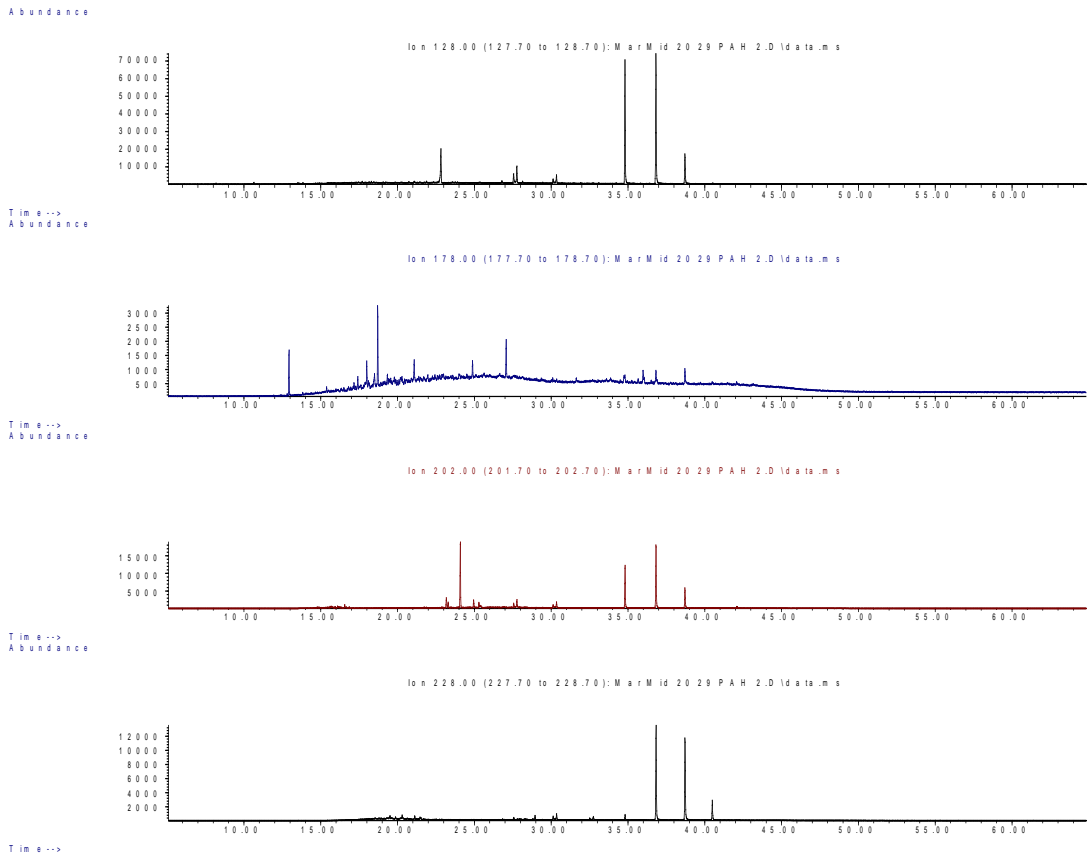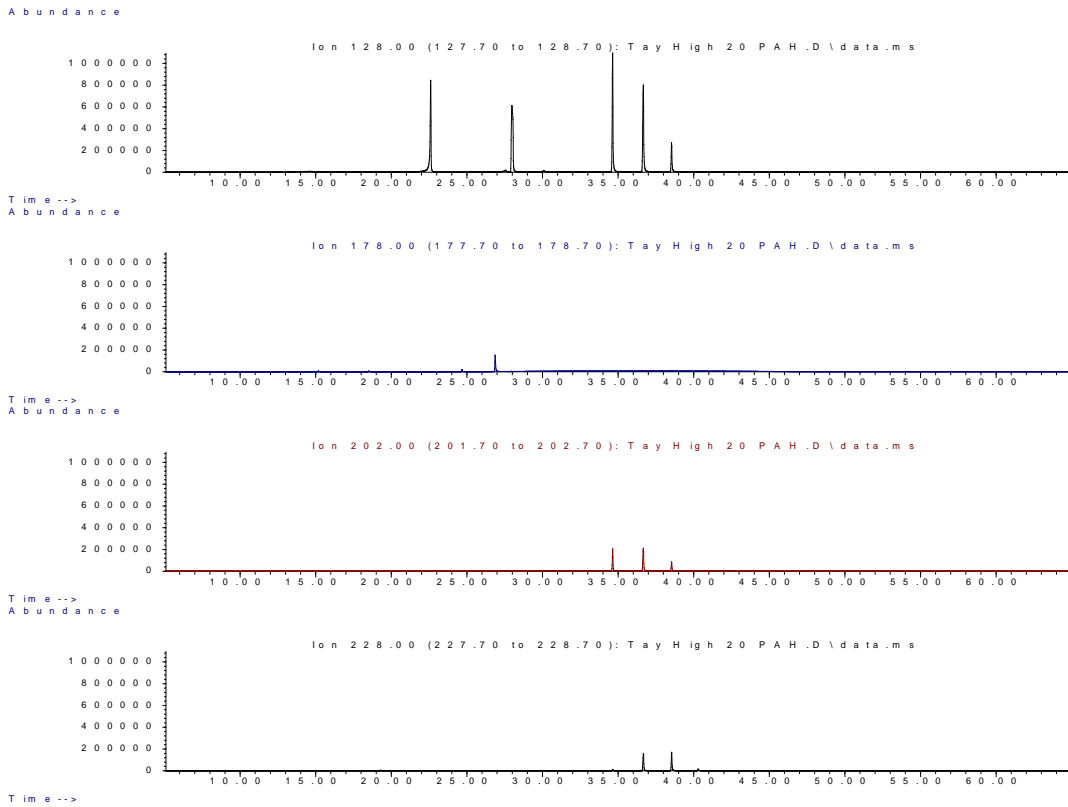
Figure III.85: Site 7, Omanu mid tide core for sediment 0-20 cm deep. GC/MS chromatograph results from *Rena* PAH fingerprint analysis for naphthalene 128 (top), phenanthrene 178 (second), pyrene 202 (third) and benzo(a)anthracene and chrysene 228 at the bottom.
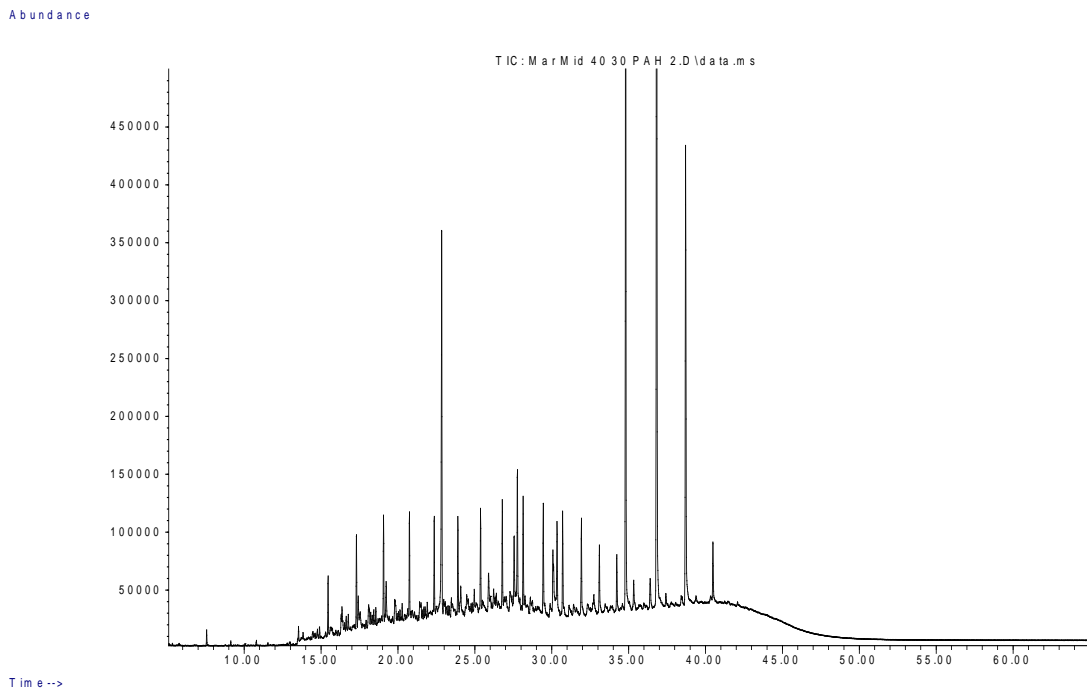
Figure III.86: Site 7, Omanu mid tide core for sediment, 20-40 cm deep. GC/MS total ion chromatograph results from *Rena* PAH fingerprint analysis.

193
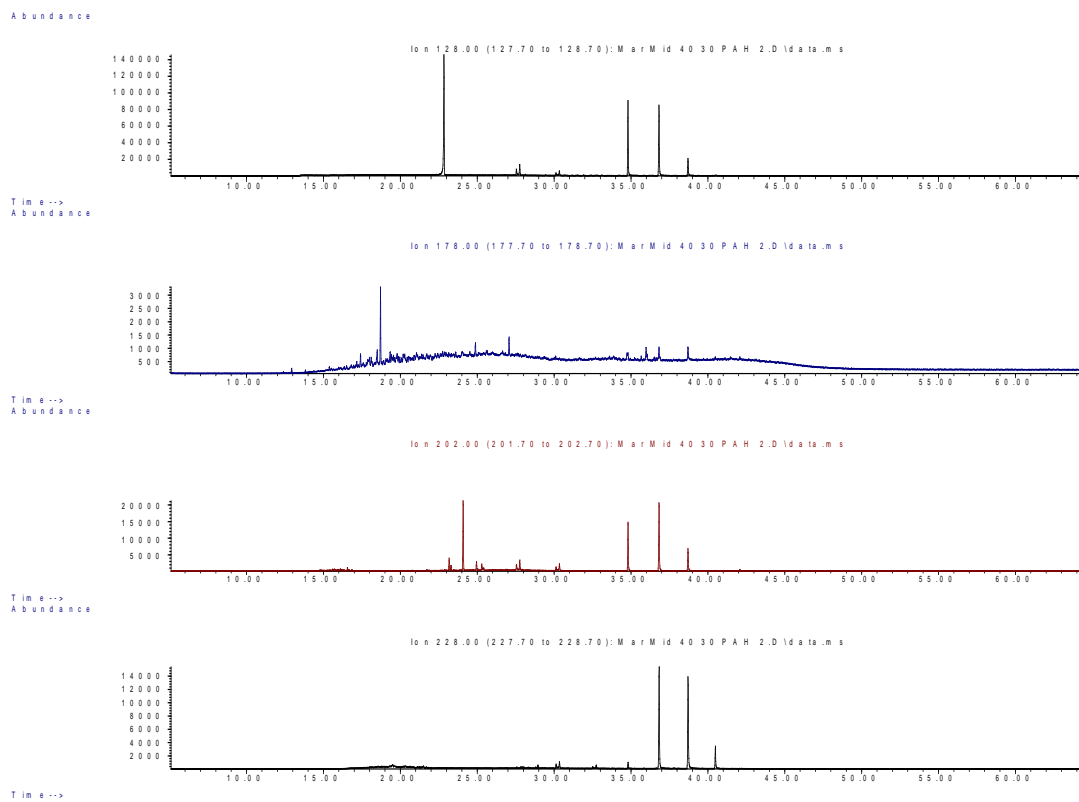
Figure III.87: Site 7, Omanu mid tide core for sediment 20-40 cm deep. GC/MS chromatograph results from *Rena* PAH fingerprint analysis for naphthalene 128 (top), phenanthrene 178 (second), pyrene 202 (third) and benzo(a)anthracene and chrysene 228 at the bottom.
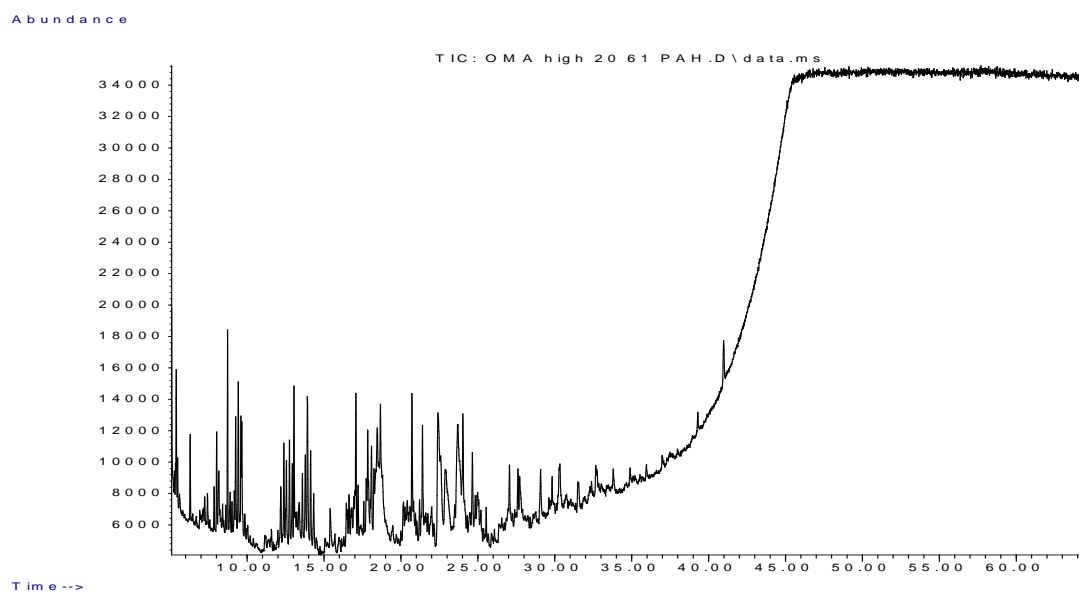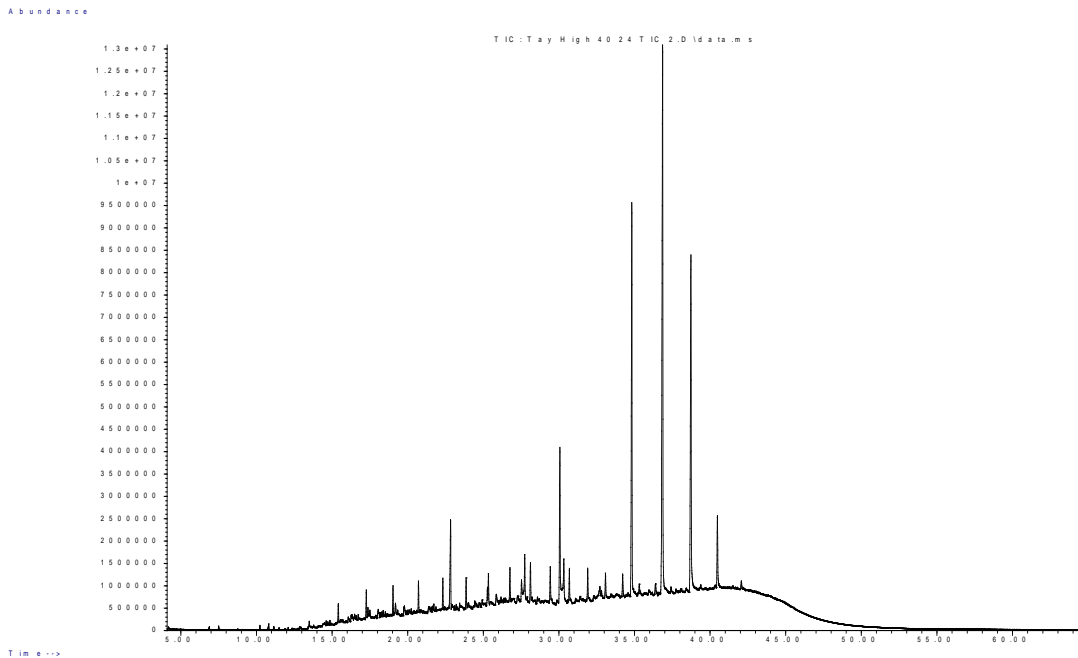

Figure III.88: Site 7, Omanu high tide core for sediment, 0-20 cm deep. GC/MS total ion chromatograph results from *Rena* PAH fingerprint analysis.
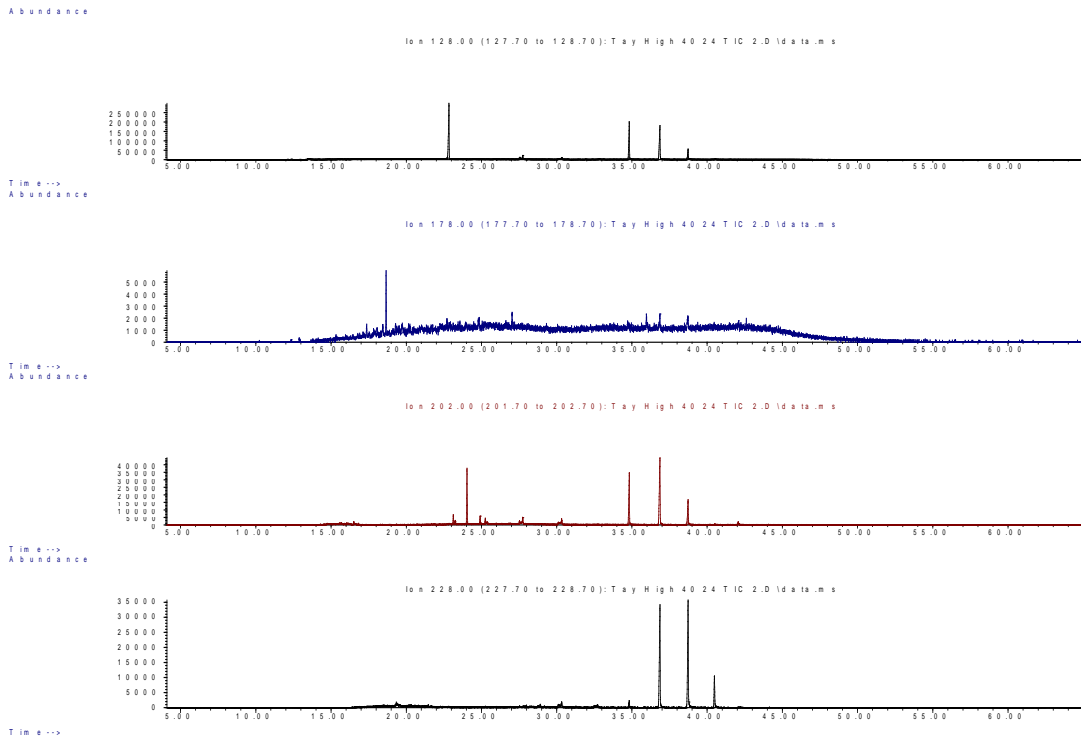
Figure III.89: Site 7, Omanu high tide core for sediment 0-20 cm deep. GC/MS chromatograph results from *Rena* PAH fingerprint analysis for naphthalene 128 (top), phenanthrene 178 (second), pyrene 202 (third) and benzo(a)anthracene and chrysene 228 at the bottom.
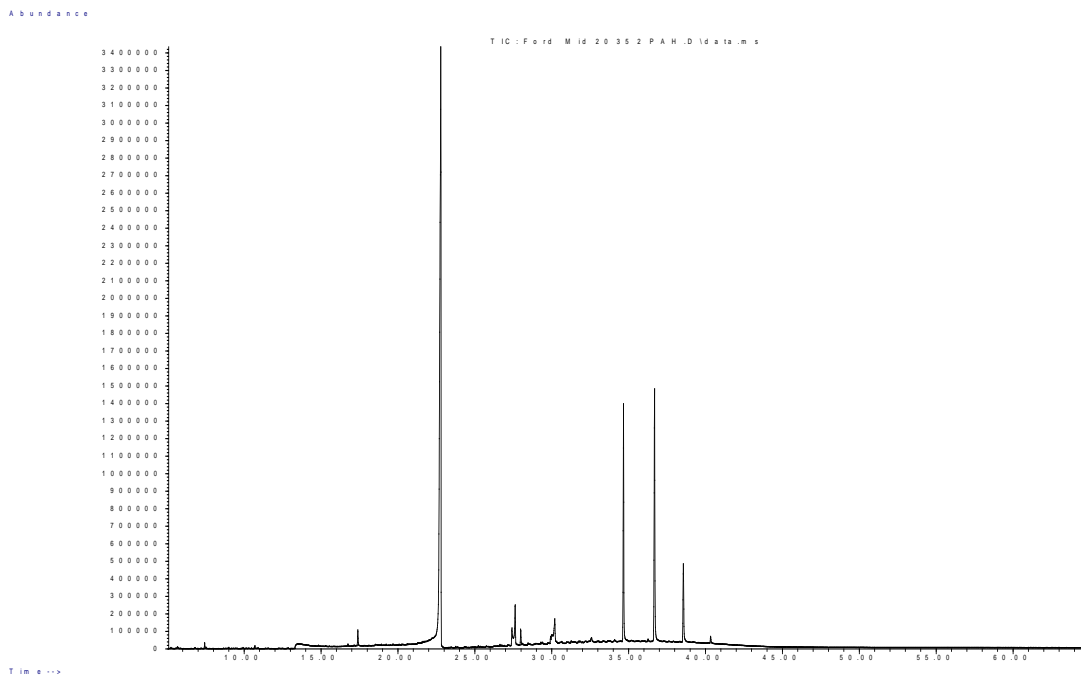

Figure III.90: Site 7, Omanu high tide core for sediment, 20-40 cm deep. GC/MS total ion chromatograph results from *Rena* PAH fingerprint analysis.
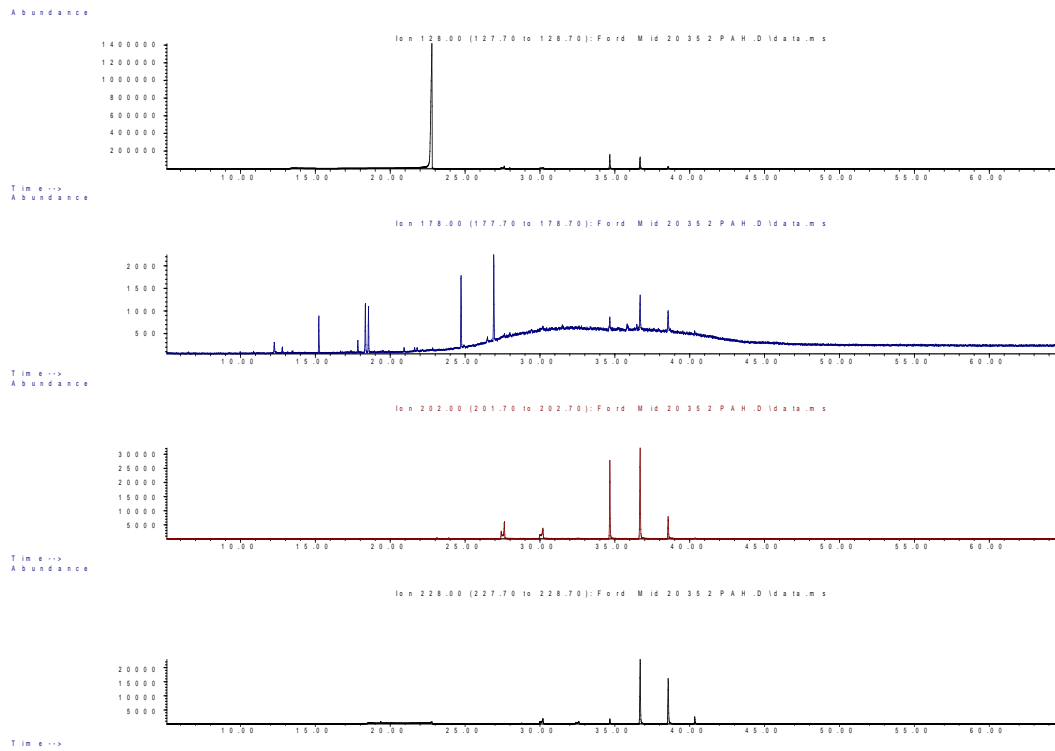
Figure III.91: Site 7, Omanu high tide core for sediment 20-40 cm deep. GC/MS chromatograph results from *Rena* PAH fingerprint analysis for naphthalene 128 (top), phenanthrene 178 (second), pyrene 202 (third) and benzo(a)anthracene and chrysene 228 at the bottom.

Figure III.92: Site 8, Harrison's Cut low tide core, 0-20 cm deep. GC/MS total ion chromatograph results from Rena PAH fingerprint analysis.

Figure III.93: Site 8, Harrison's Cut low tide core for sediment 0-20 cm deep. GC/MS chromatograph results from *Rena* PAH fingerprint analysis for naphthalene 128 (top), phenanthrene 178 (second), pyrene 202 (third) and benzo(a)anthracene and chrysene 228 at the bottom.
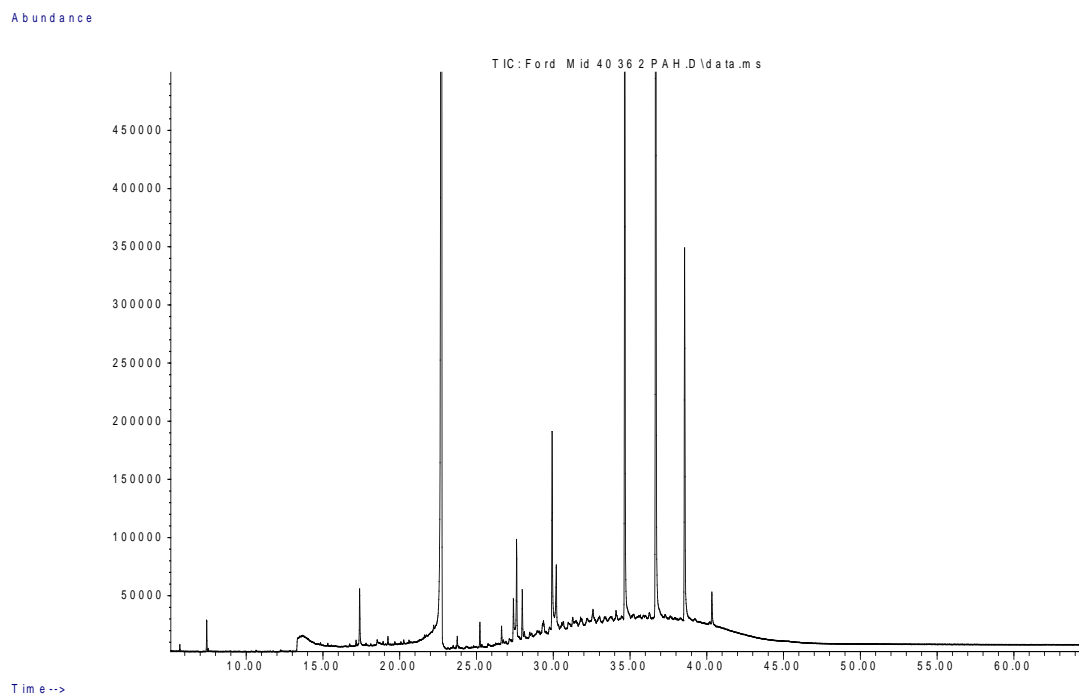

Figure III.94: Site 8, Harrison's Cut low tide core, 20-40 cm deep. GC/MS total ion chromatograph results from *Rena* PAH fingerprint analysis.

Figure III.95: Site 8, Harrison's Cut low tide core for sediment 20-40 cm deep. GC/MS chromatograph results from *Rena* PAH fingerprint analysis for naphthalene 128 (top), phenanthrene 178 (second), pyrene 202 (third) and benzo(a)anthracene and chrysene 228 at the bottom.
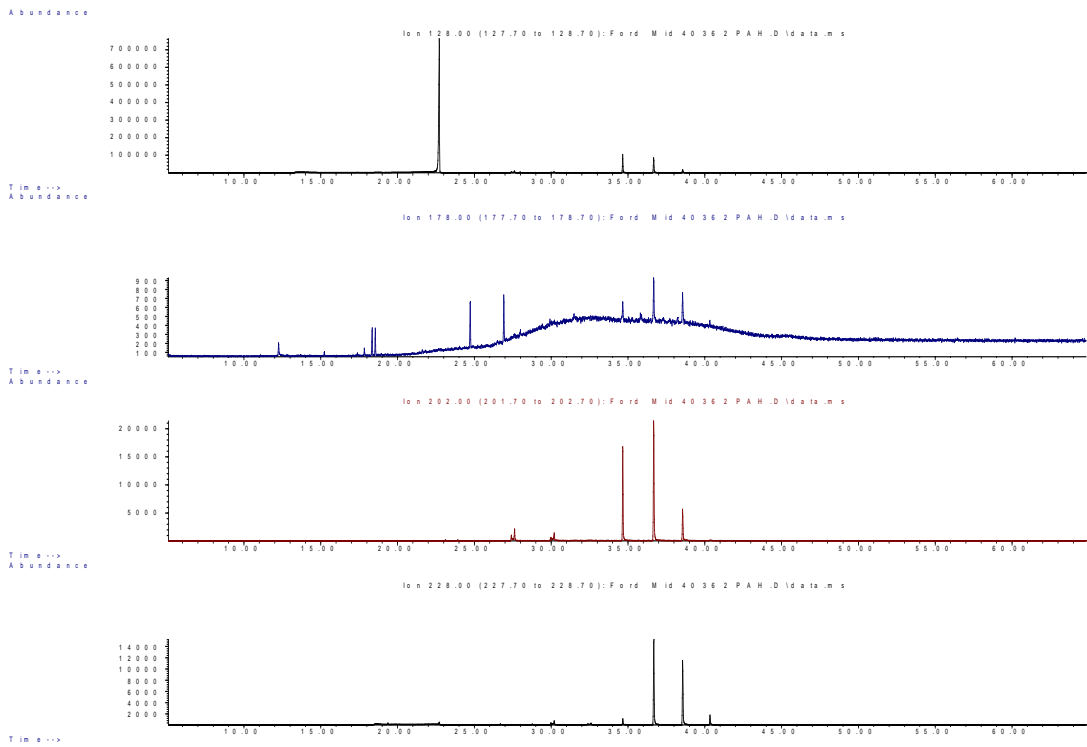
Figure III.96:Site 8, Harrison's Cut low tide core for sediment 20-40 cm deep. GC/MS chromatograph results from *Rena* PAH fingerprint analysis for mono-alkylated phenanthenes at the top, di alkylated phenanthrenes (second), tri-alkylated phenanthrenes (third), pyrene (fourth) mono-alkylated pyrenes (fifth) and di- alkylated phenanthrenes on the bottom.
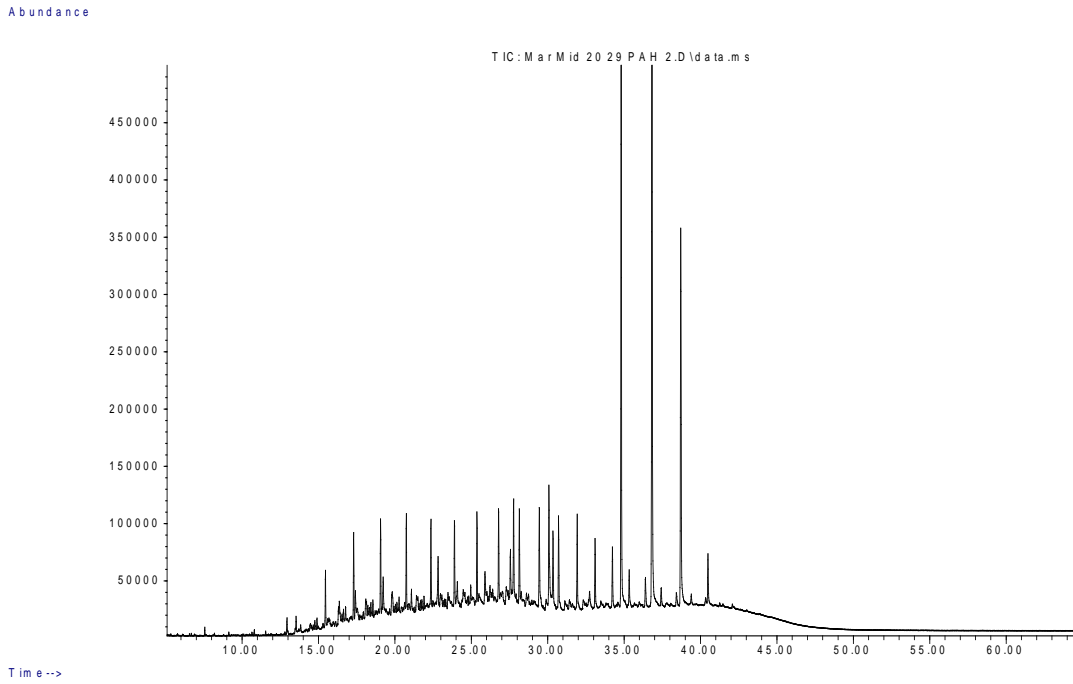
Figure III.97:Site 8, Harrison's Cut, mid tide core, 0-20 cm deep. GC/MS total ion chromatograph results from *Rena* PAH fingerprint analysis.

Figure III.98: Site 8, Harrison's Cut mid tide core for sediment 0-20cm deep. GC/MS chromatograph results from *Rena* PAH fingerprint analysis for naphthalene 128 (top), phenanthrene 178 (second), pyrene 202 (third) and benzo(a)anthracene and chrysene 228 at the bottom.
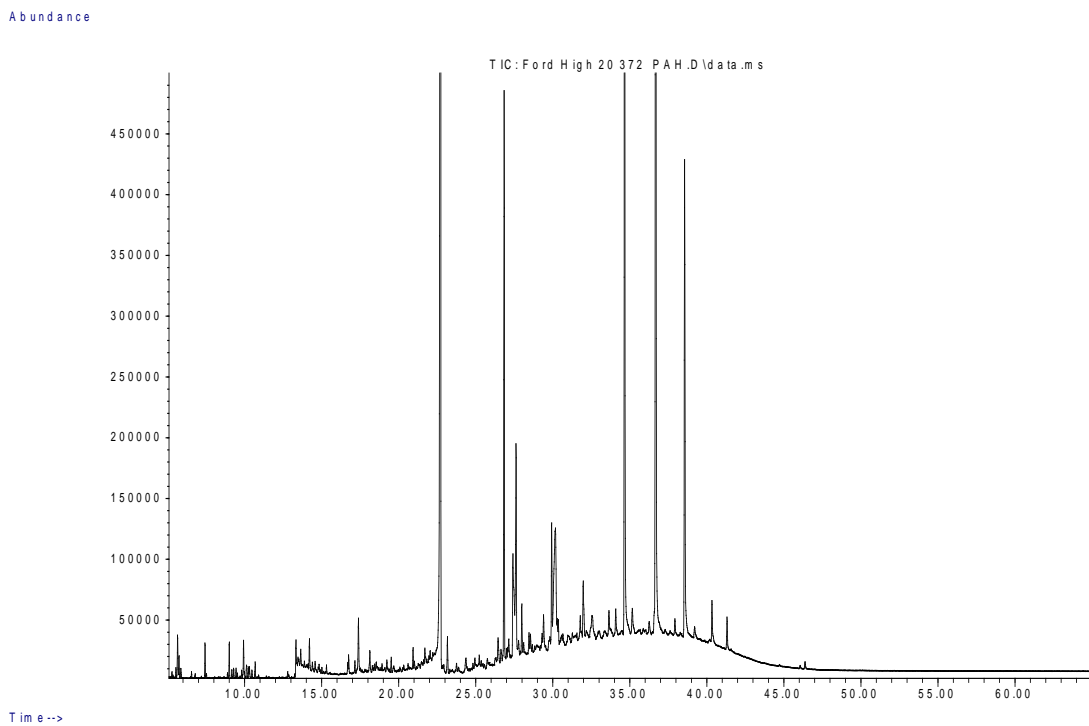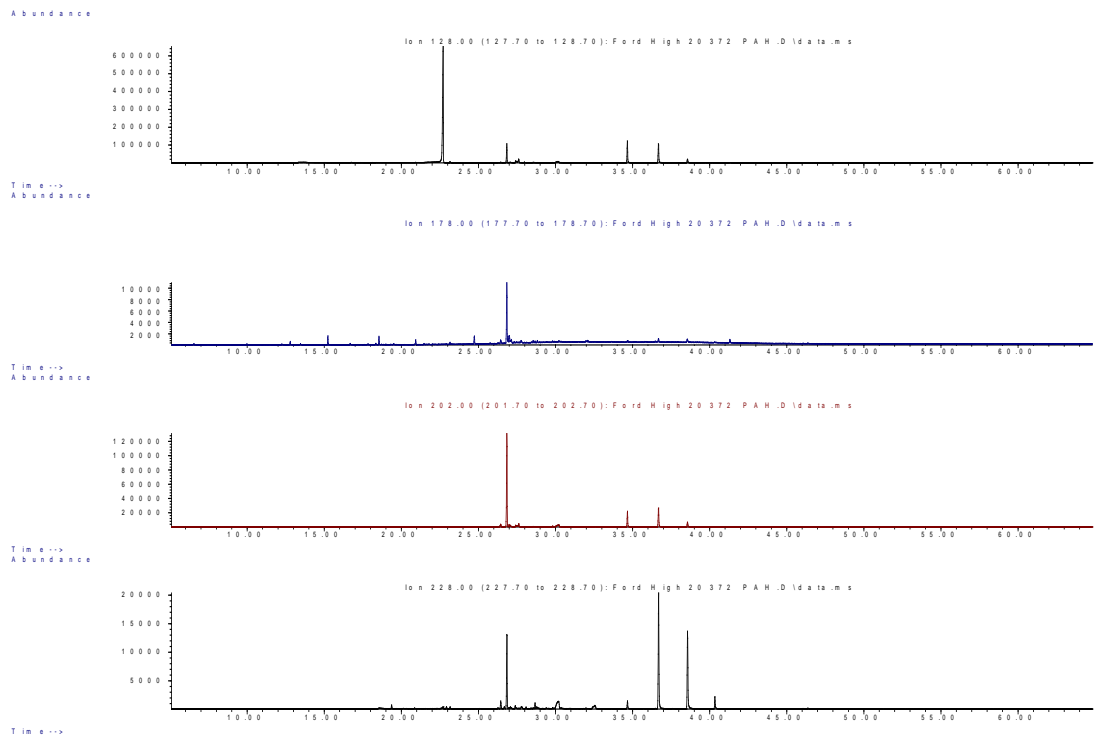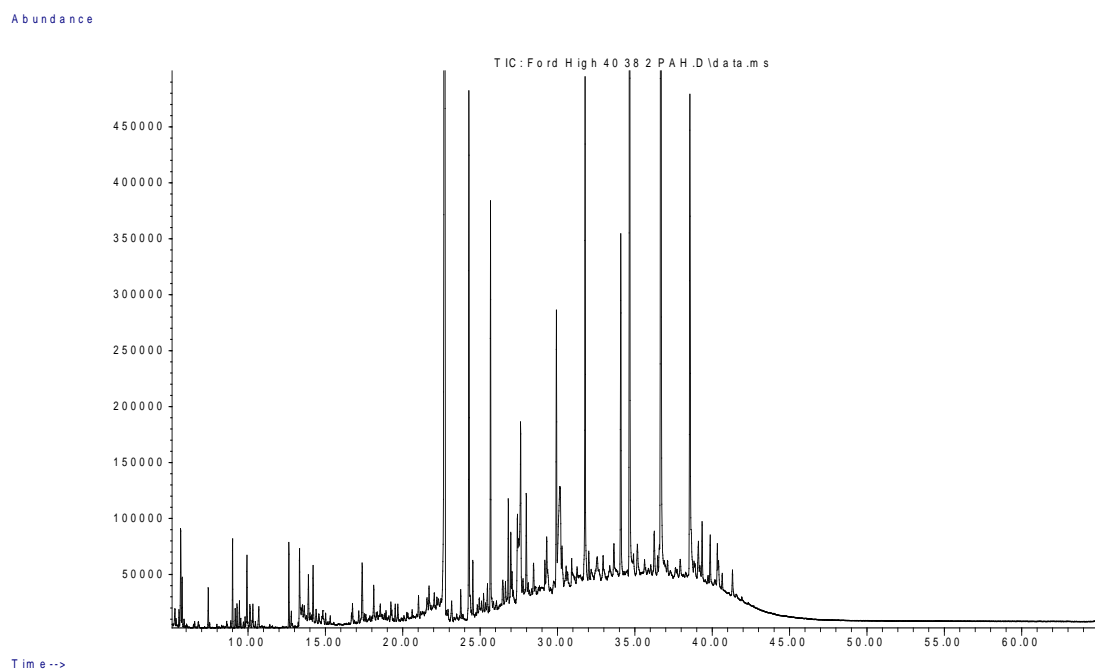
Figure III.99: Site 8, Harrison's Cut mid tide core for sediment 0-20 cm deep. GC/MS chromatograph results from *Rena* PAH fingerprint analysis for mono-alkylated phenanthenes at the top, di alkylated phenanthrenes (second), tri-alkylated phenanthrenes (third), pyrene (fourth) mono-alkylated pyrene s (fifth) and di- alkylated phenanthrenes on the bottom.
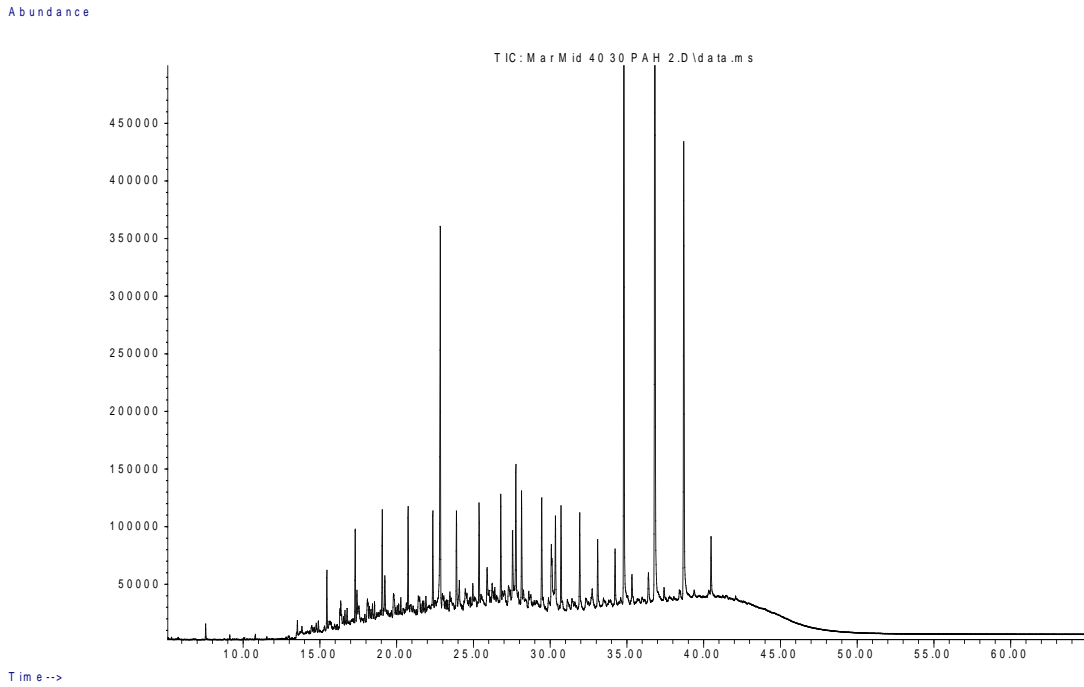
Figure III.100: Harrison's Cut site 8, mid tide core, 20-40 cm deep. GC/MS total ion chromatograph results from *Rena* PAH fingerprint analysis.
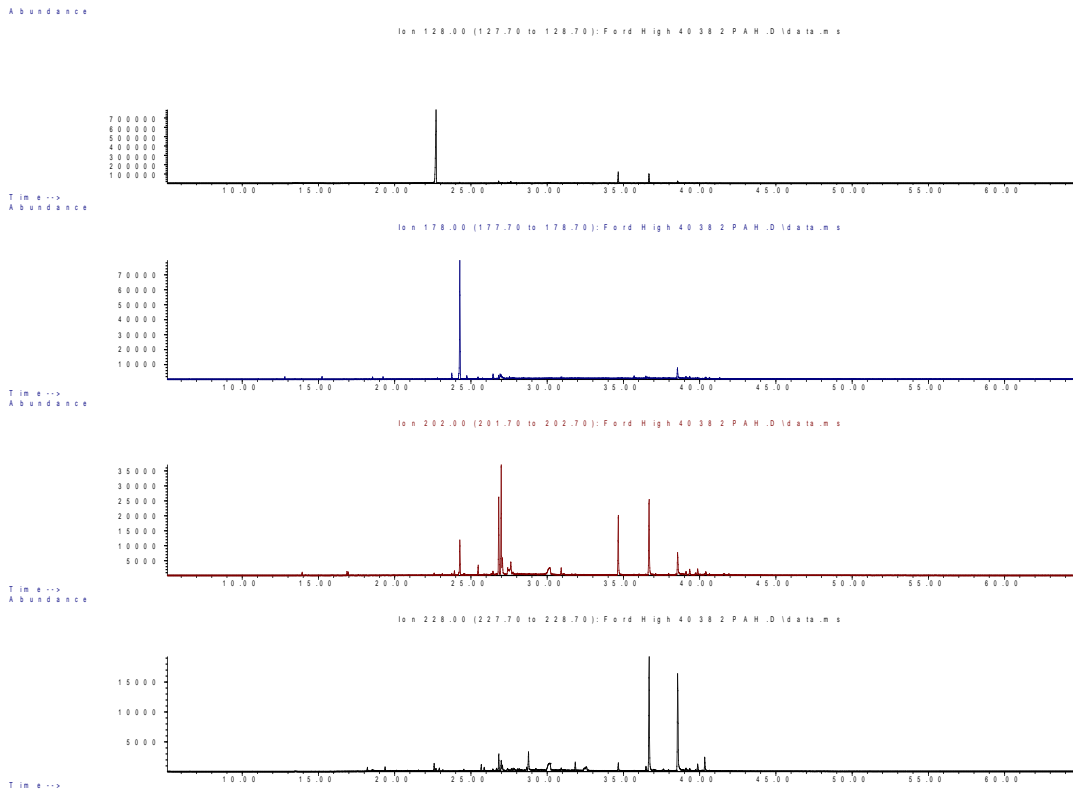

Figure III.101:Site 8,Harrison's Cut mid tide core for sediment 20-40 cm deep. GC/MS chromatograph results from *Rena* PAH fingerprint analysis for naphthalene 128 (top), phenanthrene 178 (second), pyrene 202 (third) and benzo(a)anthracene and chrysene 228 at the bottom.
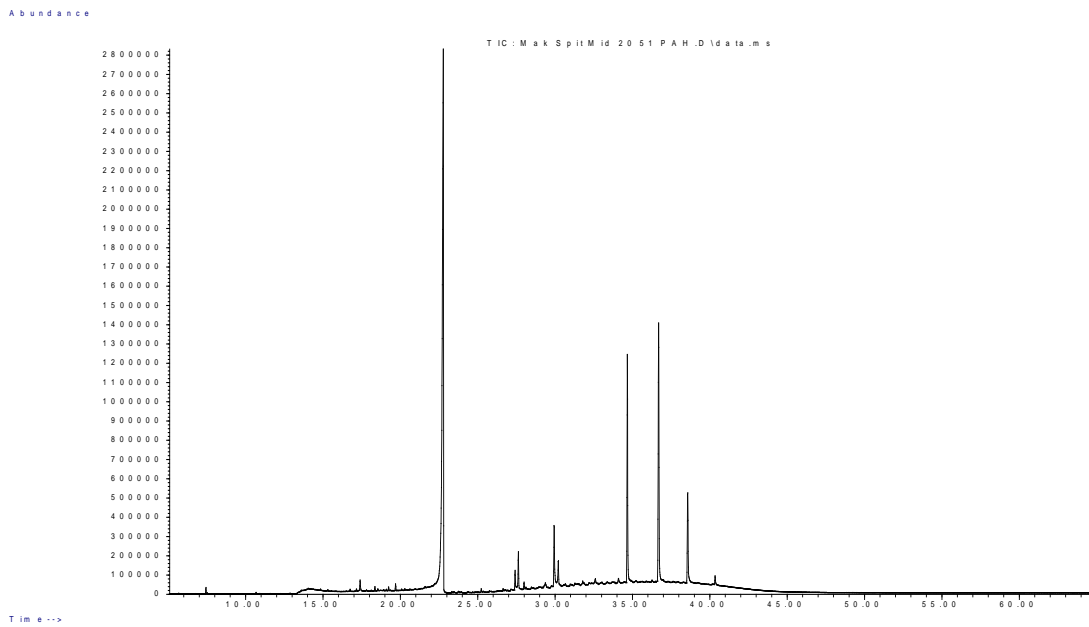
Figure III.102 Site 8, Harrison's Cut mid tide core for sediment 20-40 cm deep. GC/MS chromatograph results from *Rena* PAH fingerprint analysis for mono-alkylated phenanthenes at the top, di alkylated phenanthrenes (second), tri-alkylated phenanthrenes (third), pyrene (fourth) mono-alkylated pyrenes (fifth) and di- alkylated phenanthrenes on the bottom.
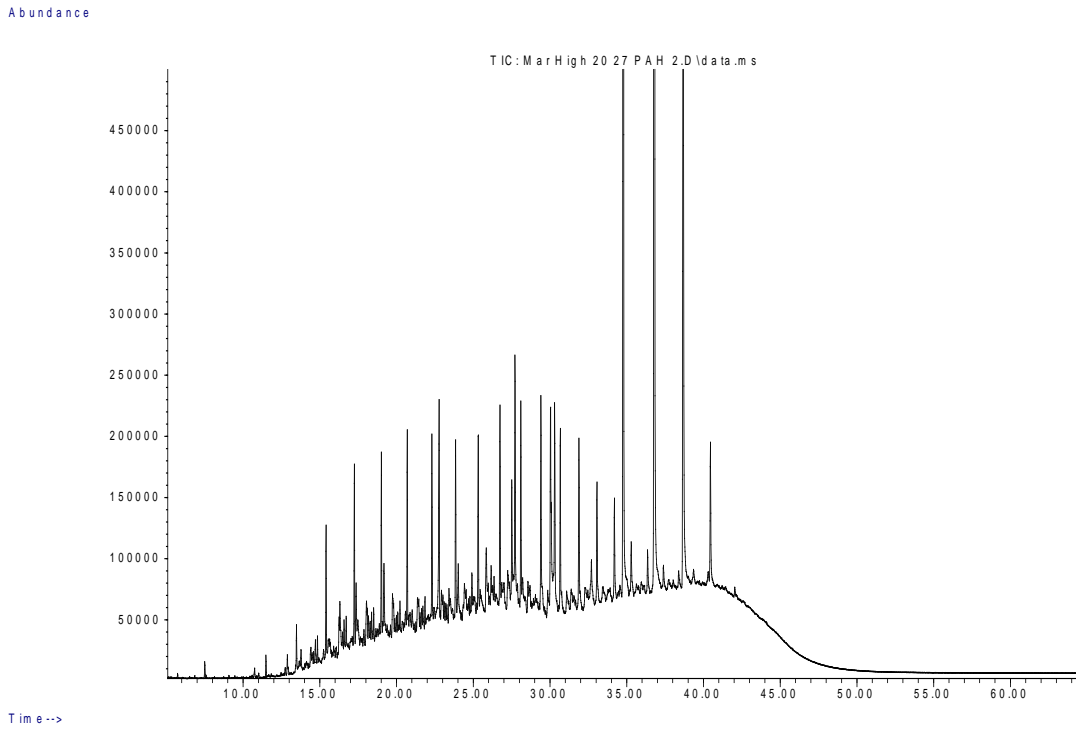
Figure III.103 Site 8, Harrison's Cut site 3 high tide core 0-20 cm. GC/MS total ion chromatograph results from *Rena* PAH fingerprint analysis.
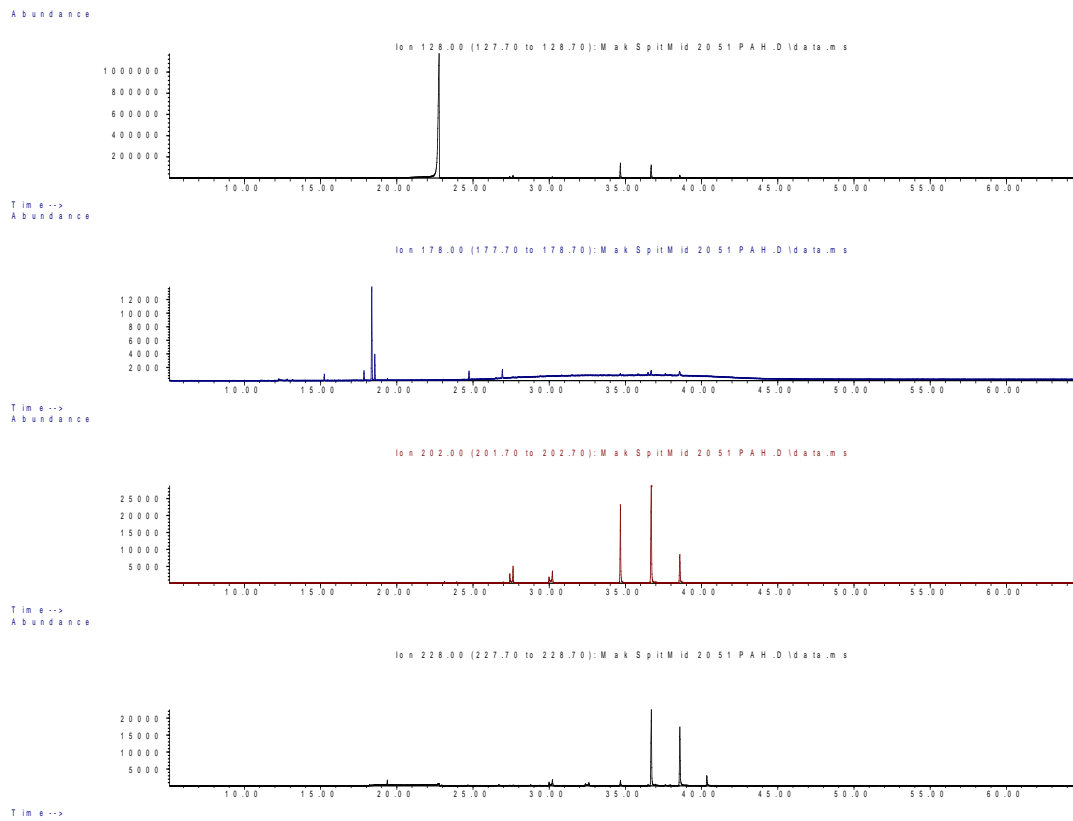

Figure III.104:Site 8, Harrison's Cut high tide core for sediment 0-20 cm deep. GC/MS chromatograph results from *Rena* PAH fingerprint analysis for naphthalene 128 (top), phenanthrene 178 (second), pyrene 202 (third) and benzo(a)anthracene and chrysene 228 at the bottom.
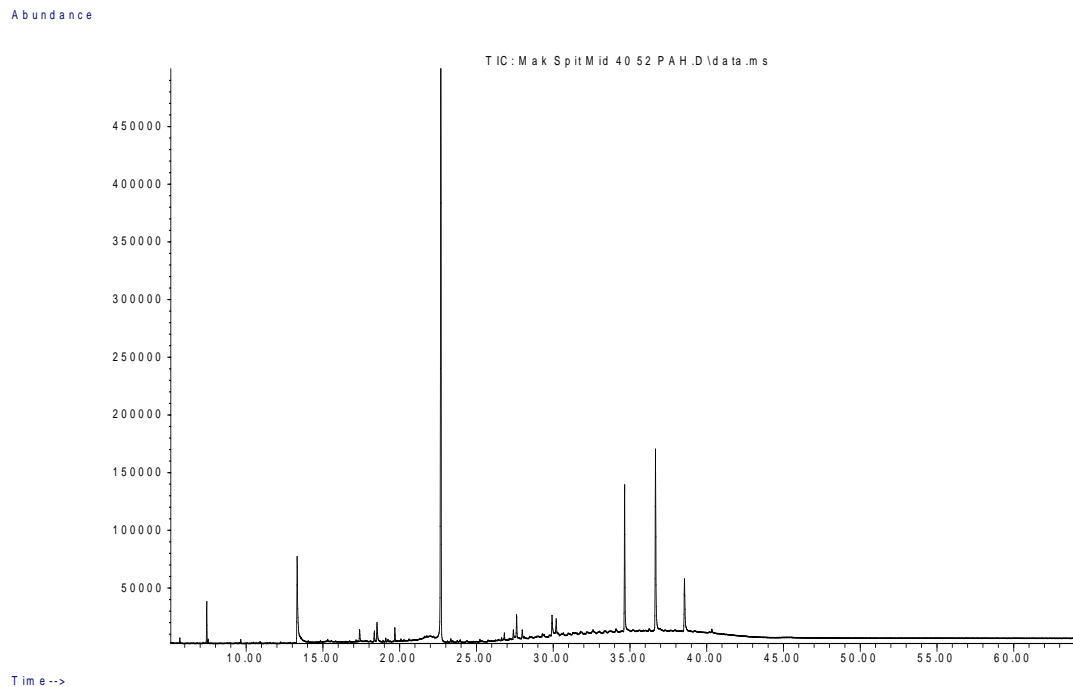
Figure III.105 Harrison's Cut site 8, high tide core for sediment 20-40 cm deep. GC/MS total ion chromatograph results from *Rena* PAH fingerprint analysis.

Figure III.106,Site 8, Harrison's Cut high tide core for sediment 20-40 cm deep. GC/MS chromatograph results from *Rena* PAH fingerprint analysis for naphthalene 128 (top), phenanthrene 178 (second), pyrene 202 (third) and benzo(a)anthracene and chrysene 228 at the bottom.
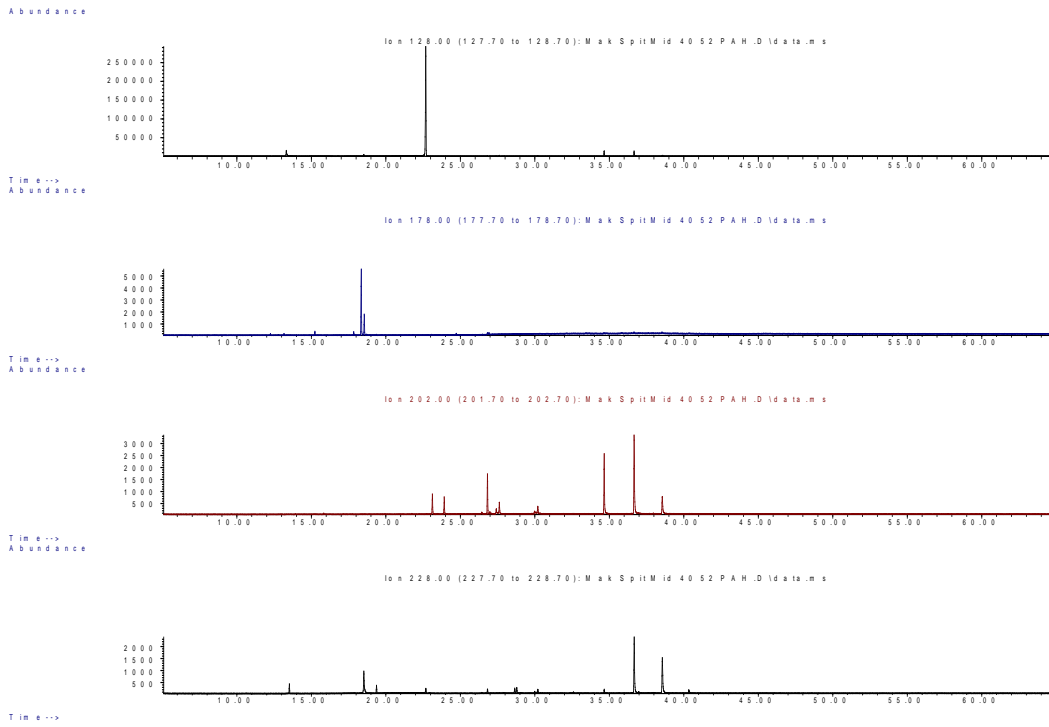
Figure III.107 Site 8, Harrison's Cut high tide core for sediment 0-20 cm deep. GC/MS chromatograph results from *Rena* PAH fingerprint analysis for mono-alkylated phenanthenes at the top, di alkylated phenanthrenes (second), tri-alkylated phenanthrenes (third), pyrene (fourth) mono-alkylated pyrenes (fifth) and di- alkylated phenanthrenes on the bottom.

Figure III.108: Site 9, Taylor's Reserve low tide core for sediment 0-20 cm deep. GC/MS total ion chromatograph results from *Rena* PAH fingerprint analysis.

Figure III.109: Site 9, Taylor's Reserve low tide core for sediment 0-20 cm deep. GC/MS chromatograph results from *Rena* PAH fingerprint analysis for naphthalene 128 (top), phenanthrene 178 (second), pyrene 202 (third) and benzo(a)anthracene and chrysene 228 at the bottom.
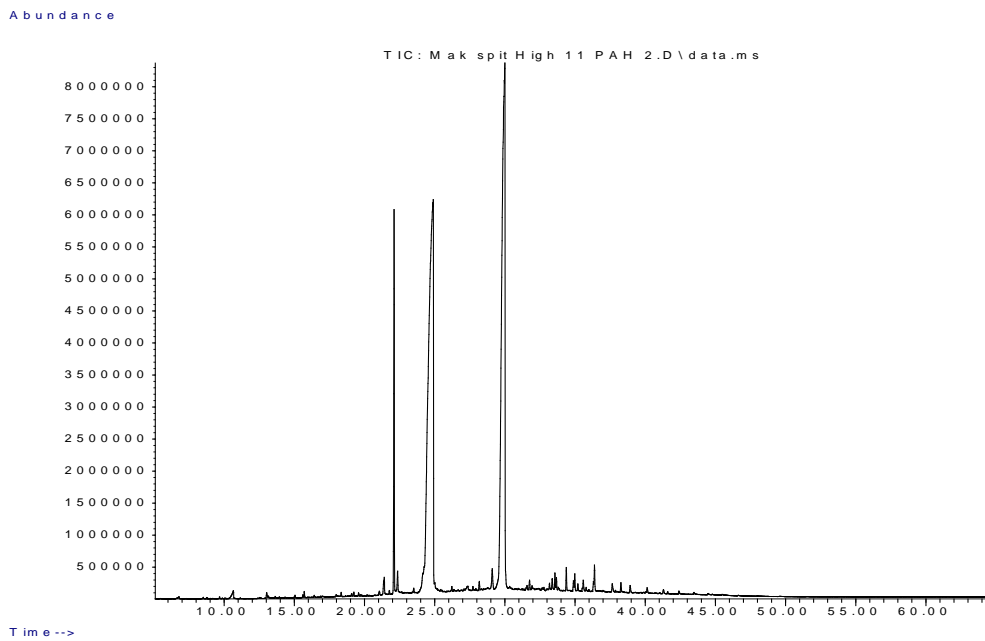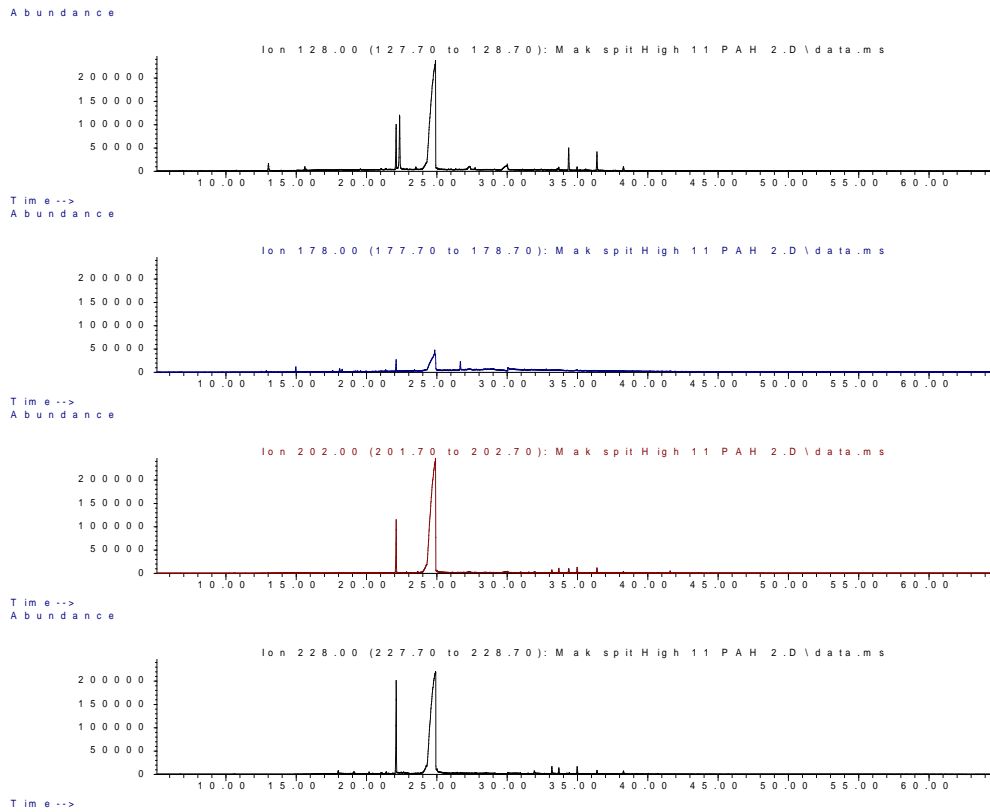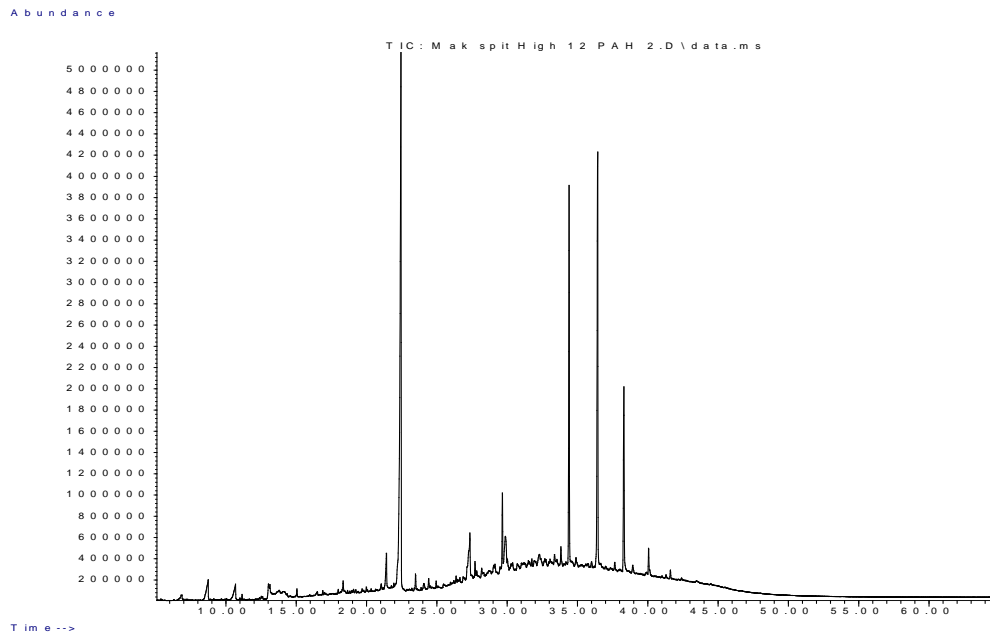
Figure III.110 Site 9,Taylor's low tide core for sediment 0-20 cm deep. GC/MS chromatograph results from *Rena* PAH fingerprint analysis for mono-alkylated phenanthenes at the top, di alkylated phenanthrenes (second), tri-alkylated phenanthrenes (third), pyrene (fourth) mono-alkylated pyrene s (fifth) and di- alkylated phenanthrenes on the bottom.

Figure III.111: Site 9, Taylor's Reserve low tide core for sediment 20-40 cm deep. GC/MS total ion chromatograph results from *Rena* PAH fingerprint analysis.
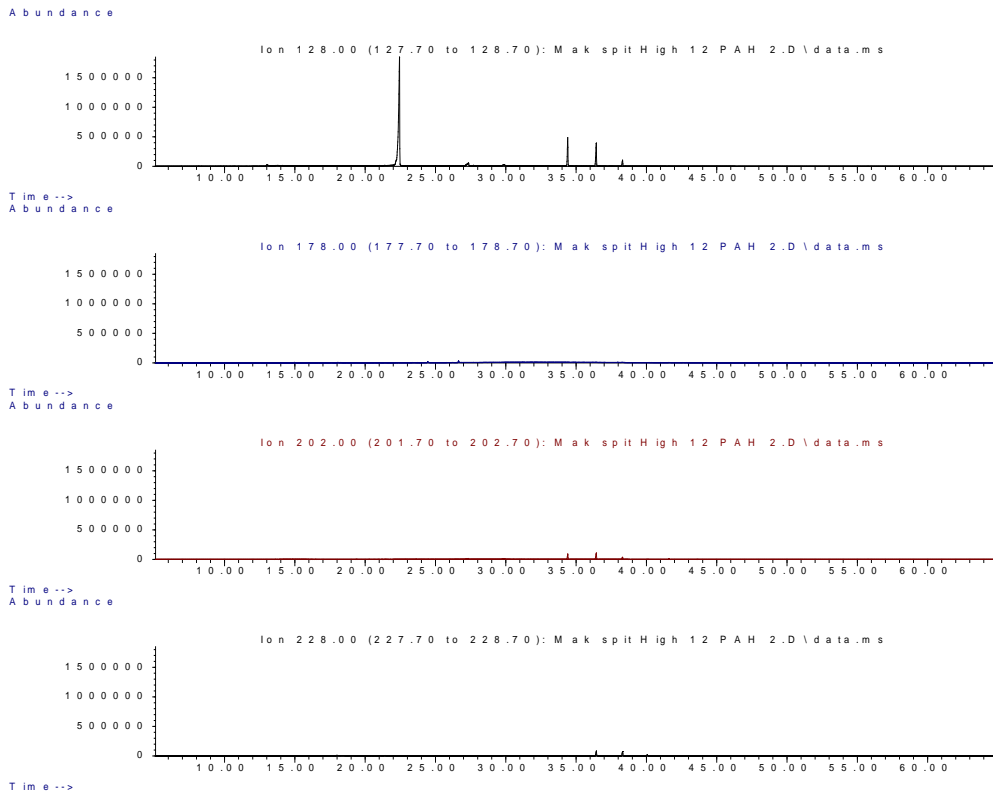
208

Figure III.112: Site 9, Taylor's Reserve low tide core for sediment 20-40 cm deep. GC/MS chromatograph results from *Rena* PAH fingerprint analysis for naphthalene 128 (top), phenanthrene 178 (second), pyrene 202 (third) and benzo(a)anthracene and chrysene 228 at the bottom.
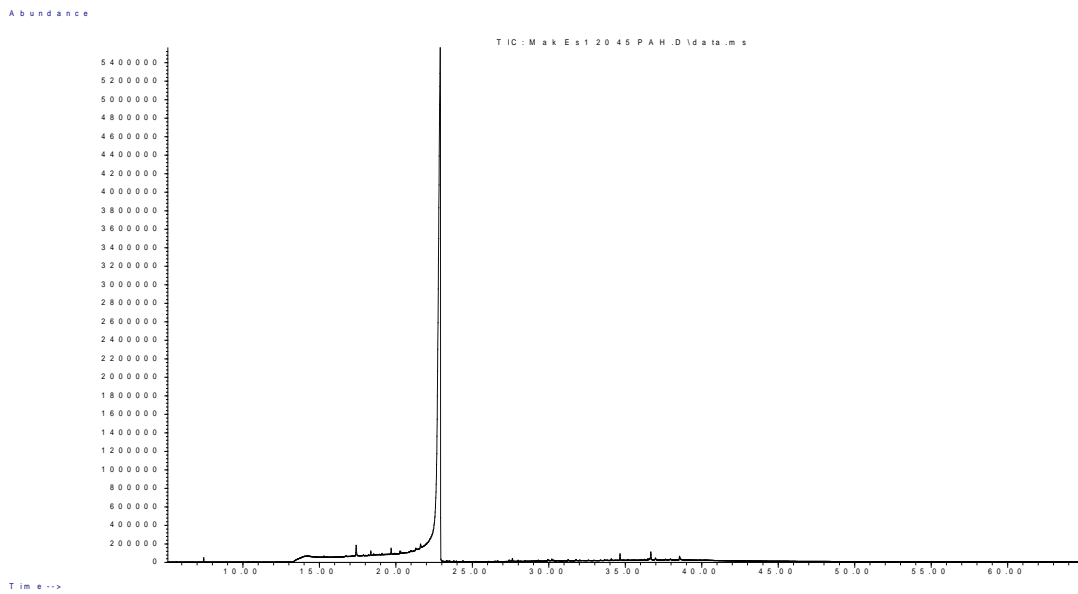

Figure III.113: Site 9, Taylor's Reserve mid tide core for sediment 0-20 cm deep. GC/MS total ion chromatograph results from *Rena* PAH fingerprint analysis.

Figure III.114: Site 9, Taylor's Reserve mid tide core for sediment 0-20 cm deep. GC/MS chromatograph results from *Rena* PAH fingerprint analysis for naphthalene 128 (black), phenanthrene 178 (blue), pyrene 202 (red) and benzo(a)anthracene and chrysene 228 (black) at the bottom.

Figure III.115 Site 9, Taylor's Reserve mid tide core for sediment 20-40 cm deep. GC/MS total ion chromatograph results from *Rena* PAH fingerprint analysis.

Figure III.116: Site 9,Taylor's Reserve mid tide core for sediment 20-40 cm deep. GC/MS chromatograph results from *Rena* PAH fingerprint analysis for naphthalene 128 (black), phenanthrene 178 (blue), pyrene 202 (red) and benzo(a)anthracene and chrysene 228 (black) at the bottom.
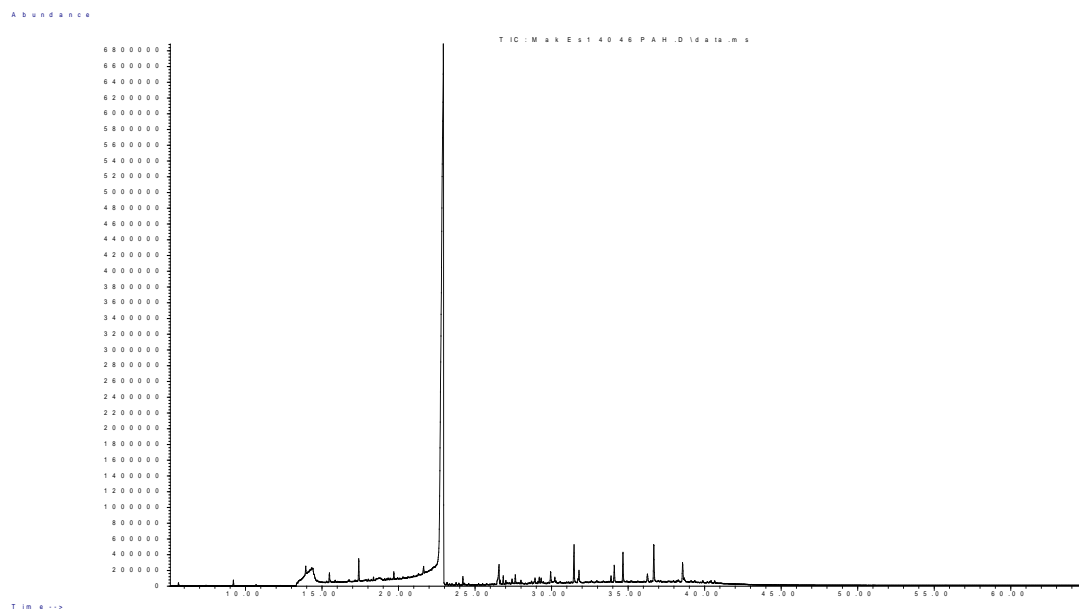

Figure III.117: Site 9, Taylor's Reserve high tide core for sediment 0-20 cm deep. GC/MS total ion chromatograph results from *Rena* PAH fingerprint analysis.

Figure III.118: Site 9, Taylor's Reserve high tide core for sediment 0-20 cm deep. GC/MS chromatograph results from *Rena* PAH fingerprint analysis for naphthalene 128 (black), phenanthrene 178 (blue), pyrene 202 (red) and benzo(a)anthracene and chrysene 228 (black) at the bottom.

Figure III.119: Site 9, Taylor's Reserve high tide core for sediment 20-40 cm deep. GC/MS total ion chromatograph results from *Rena* PAH fingerprint analysis.

Figure III.120: Site 9, Taylor's Reserve high tide core for sediment 20-40 cm deep. GC/MS chromatograph results from *Rena* PAH fingerprint analysis for naphthalene 128 (black), phenanthrene 178 (blue), pyrene 202 (red) and benzo(a)anthracene and chrysene 228 (black) at the bottom.
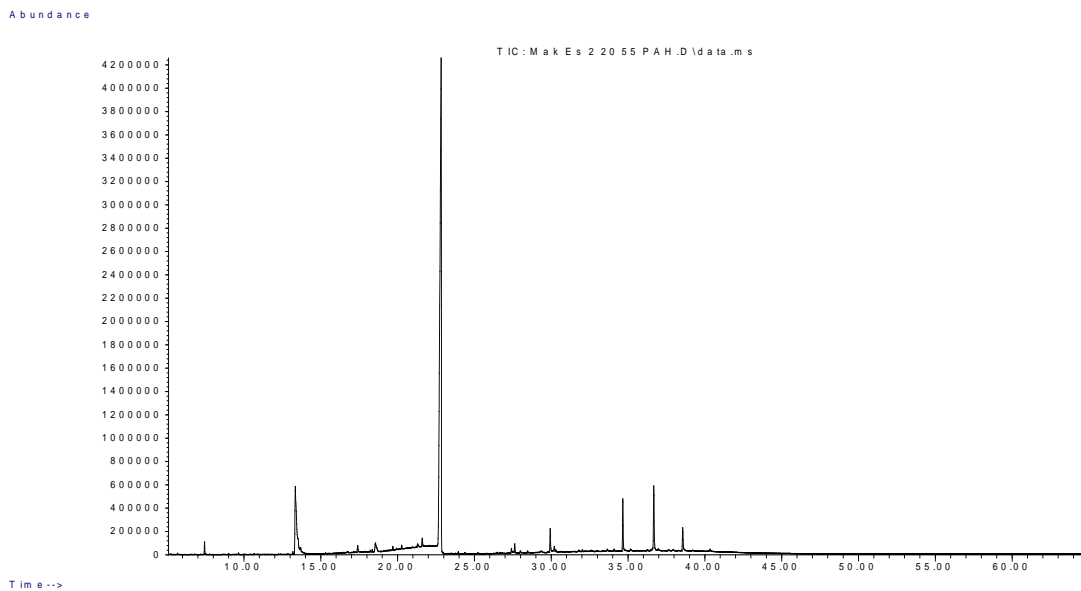

Figure III.121: Site 10, Ford Road mid tide core for sediment, 0-20 cm deep. GC/MS total ion chromatograph results from *Rena* PAH fingerprint analysis.
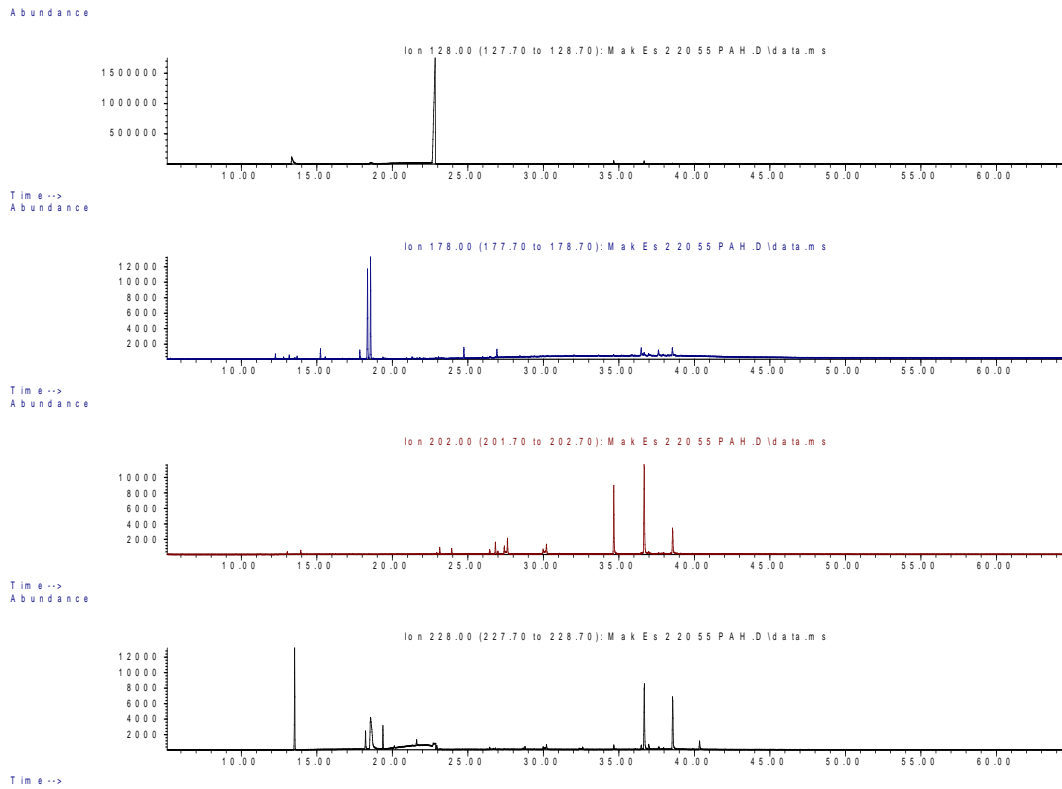
Figure III.122: Site 10, Ford Road mid tide core for sediment 0-20 cm deep. GC/MS chromatograph results from *Rena* PAH fingerprint analysis for naphthalene 128 (top), phenanthrene 178 (second), pyrene 202 (third) and benzo(a)anthracene and chrysene 228 at the bottom.
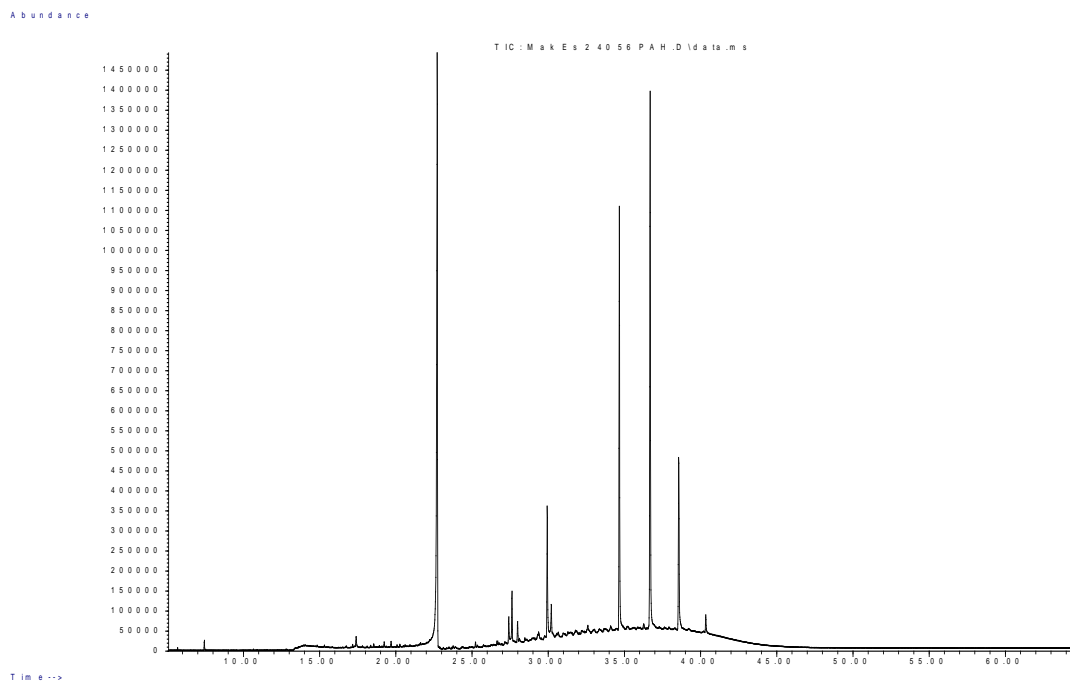

Figure III.123: Site 10, Ford Road mid tide core for sediment, 20-40 cm deep. GC/MS total ion chromatograph results from *Rena* PAH fingerprint analysis.
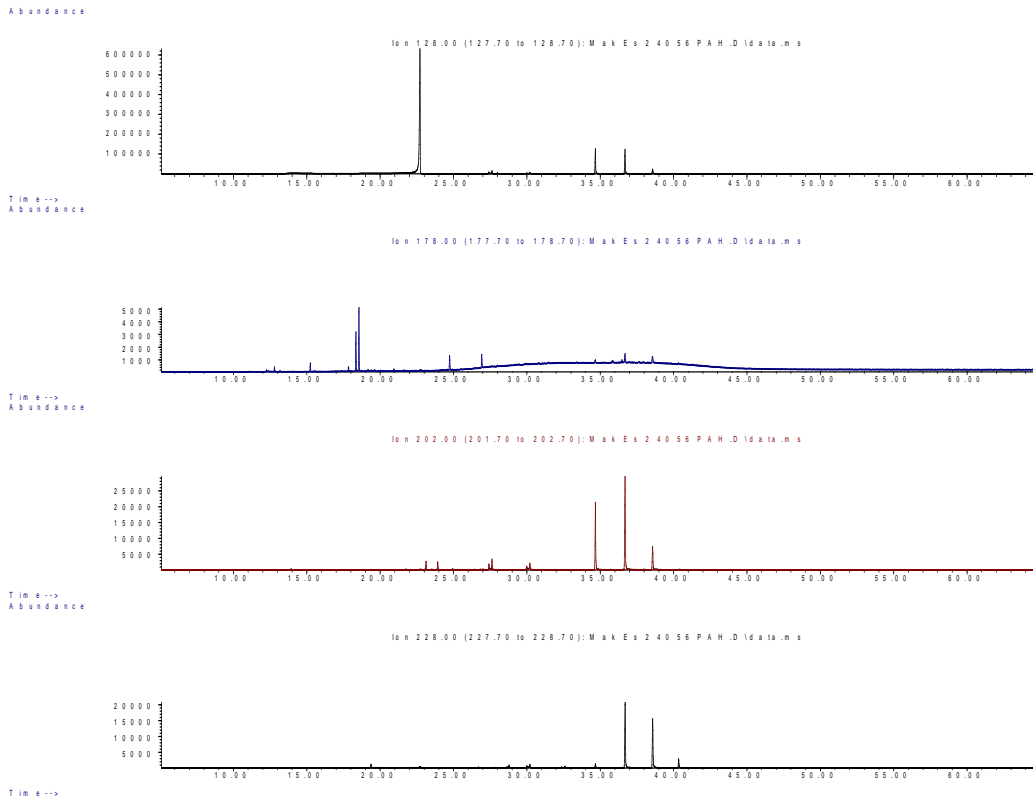
Figure III.124: Site 10, Ford Road mid tide core for sediment 20-40 cm deep. GC/MS chromatograph results from *Rena* PAH fingerprint analysis for naphthalene 128 (top), phenanthrene 178 (second), pyrene 202 (third) and benzo(a)anthracene and chrysene 228 at the bottom.

Figure III.125: Site 10, Ford Road high tide core for sediment, 0-20 cm deep. GC/MS total ion chromatograph results from *Rena* PAH fingerprint analysis.

215

Figure III.126: Site 10, Ford Road high tide core for sediment 0-20 cm deep. GC/MS chromatograph results from *Rena* PAH fingerprint analysis for naphthalene 128 (top), phenanthrene 178 (second), pyrene 202 (third) and benzo(a)anthracene and chrysene 228 at the bottom.

Figure III.127: Site 10, Ford Road high tide core for sediment, 20-40 cm deep. GC/MS total ion chromatograph results from *Rena* PAH fingerprint analysis.

Figure III.128: Site 10, Ford Road high tide core for sediment 20-40 cm deep. GC/MS chromatograph results from *Rena* PAH fingerprint analysis for naphthalene 128 (top), phenanthrene 178 (second), pyrene 202 (third) and benzo(a)anthracene and chrysene 228 at the bottom.

Figure III.129: Site 11, Maketu Spit mid tide core for sediment, 0-20cm deep. GC/MS total ion chromatograph results from *Rena* PAH fingerprint analysis.

Figure III.130: Site 11, Maketu Spit mid tide core for sediment 0-20 cm deep. GC/MS chromatograph results from *Rena* PAH fingerprint analysis for naphthalene 128 (top), phenanthrene 178 (second), pyrene 202 (third) and benzo(a)anthracene and chrysene 228 at the bottom.

Figure III.131: Site 11, Maketu Spit mid tide core for sediment, 20-40 cm deep. GC/MS total ion chromatograph results from *Rena* PAH fingerprint analysis.

Figure III.132: Site 11, Maketu Spit mid tide core for sediment 20-40 cm deep. GC/MS chromatograph results from *Rena* PAH fingerprint analysis for Naphthalene 128 (top), phenanthrene 178 (second), pyrene 202 (third) and benzo(a)anthracene and chrysene 228 at the bottom.

Figure III. 133:Site 11, Maketu Spit high tide core for sediment, 0-20 cm deep. GC/MS total ion chromatograph results from *Rena* PAH fingerprint analysis.

Figure III.134: Site 11, Maketu Spit high tide core for sediment 0-20 cm deep. GC/MS chromatograph results from *Rena* PAH fingerprint analysis for Naphthalene 128 (top), phenanthrene 178 (second), pyrene 202 (third) and benzo(a)anthracene and chrysene 228 at the bottom.

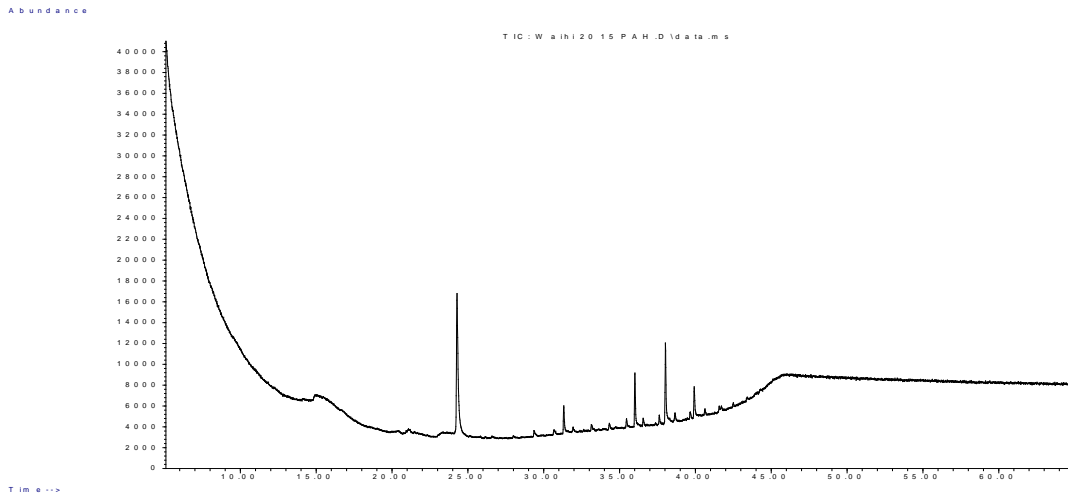Figure III. 135: Site 11, Maketu Spit high tide core for sediment, 20-40 cm deep. GC/MS total ion chromatograph results from *Rena* PAH fingerprint analysis.

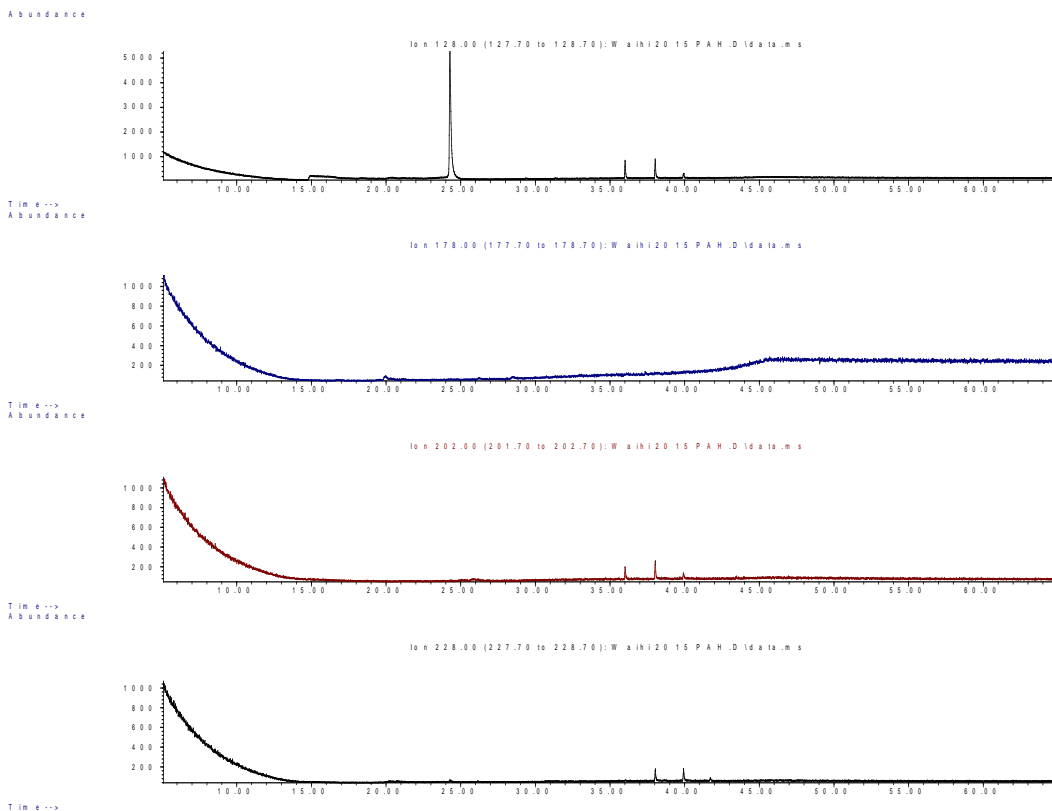Figure III.136: Site 11, Maketu Spit high tide core for sediment 20-40 cm deep. GC/MS chromatograph results from *Rena* PAH fingerprint analysis for naphthalene 128 (top), phenanthrene 178 (second), pyrene 202 (third) and benzo(a)anthracene and chrysene 228 at the bottom.

Figure III.137: Site 12, Maketu Estuary 1 core for sediment, 0-20cm deep. GC/MS total ion chromatograph results from *Rena* PAH fingerprint analysis.
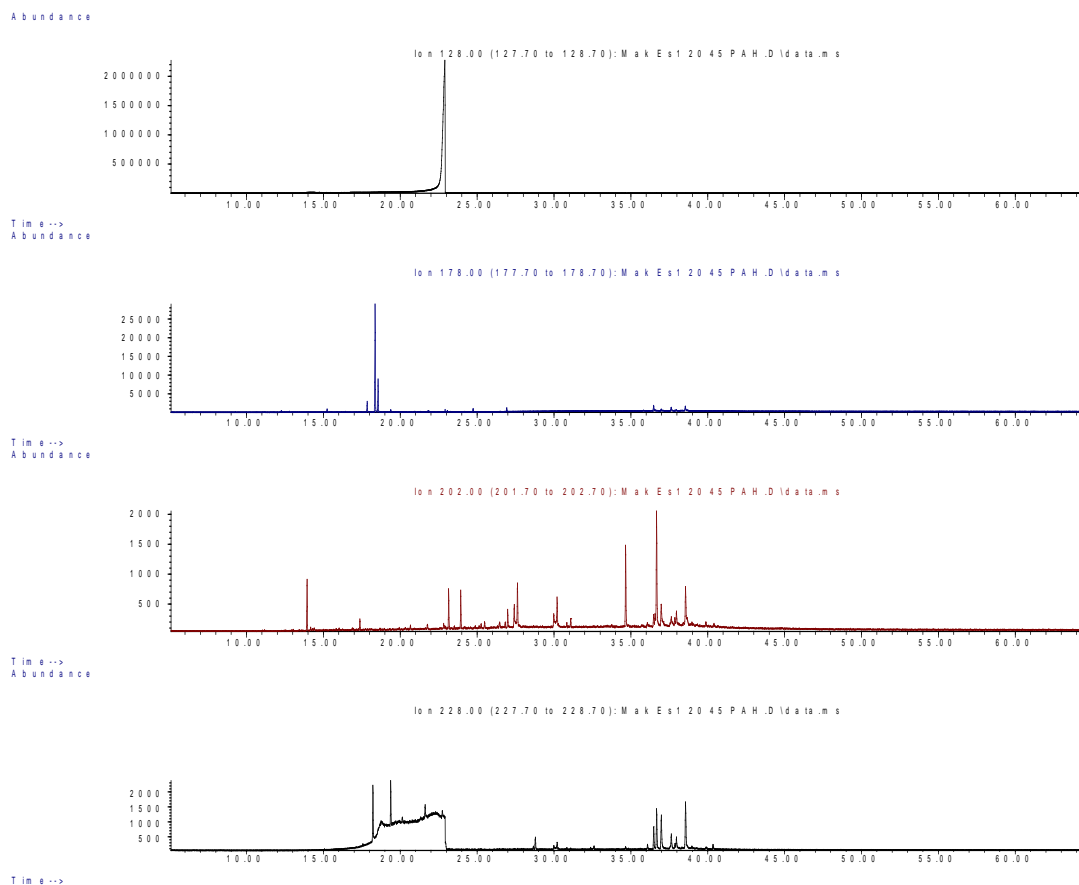
Figure III.138: Site 12, Maketu Estuary 1 core for sediment 0-20 cm deep. GC/MS chromatograph results from *Rena* PAH fingerprint analysis for naphthalene 128 (black), phenanthrene 178 (blue), Pyrene 202 (red) and Benzo(a)anthracene and Chrysene 228 (black) at the bottom

Figure III.139: Site 12, Maketu Estuary 1 core for sediment, 20-40 cm deep. GC/MS total ion chromatograph results from *Rena* PAH fingerprint analysis.

222
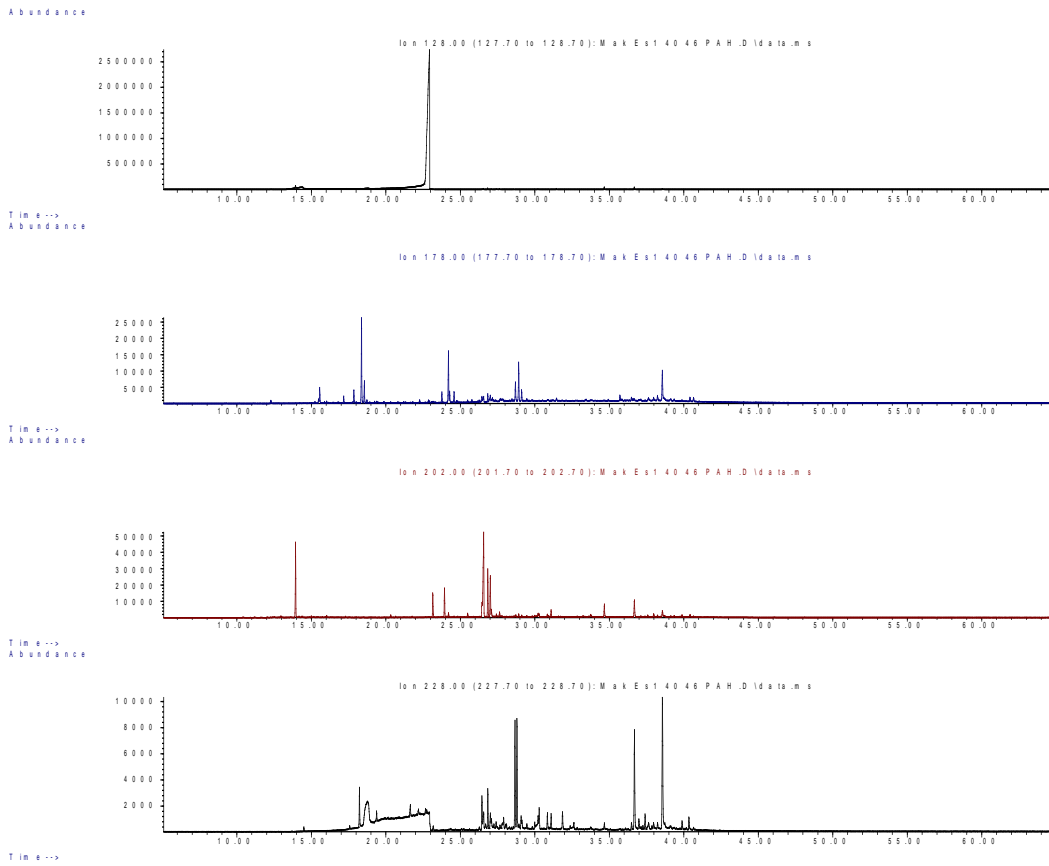
Figure III.140: Site 12, Maketu Estuary 1 core for sediment 20-40 cm deep. GC/MS chromatograph results from *Rena* PAH fingerprint analysis for Naphthalene 128 (top), phenanthrene 178 (second), pyrene 202 (third) and benzo(a)anthracene and chrysene 228 at the bottom.
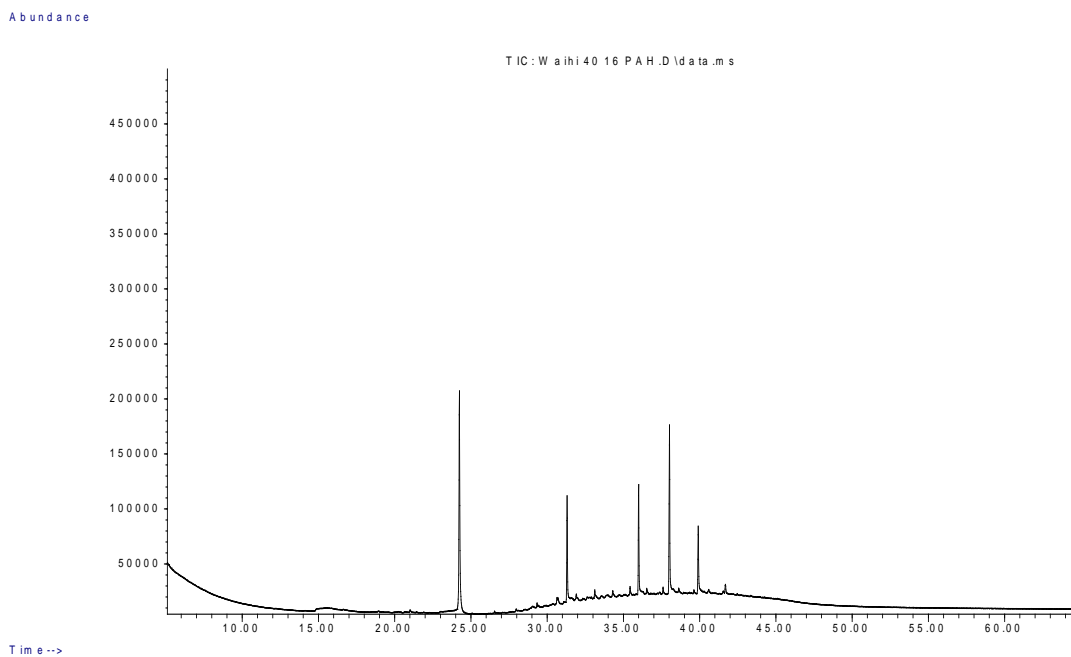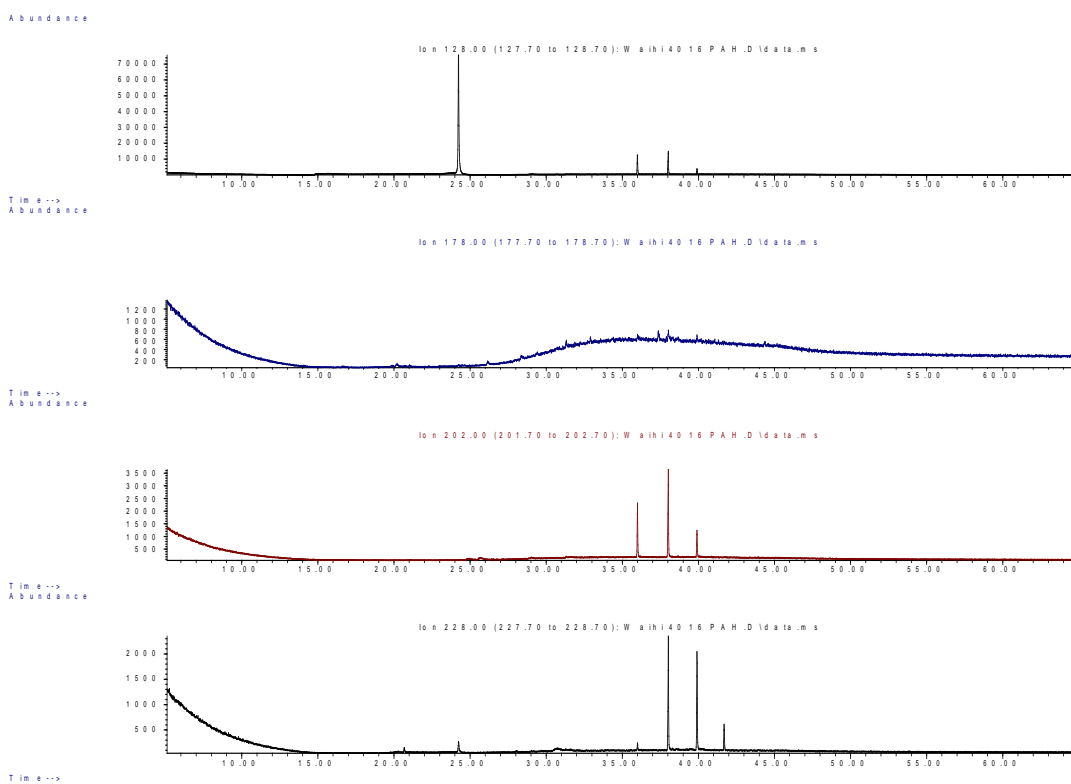

Figure III.141: Site 12, Maketu Estuary 2 core for sediment, 0-20 cm deep. GC/MS total ion chromatograph results from *Rena* PAH fingerprint analysis.

Figure III.142: Site 12, Maketu Estuary 2 core for sediment 0-20 cm deep. GC/MS chromatograph results from *Rena* PAH fingerprint analysis for Naphthalene 128 (top), phenanthrene 178 (second), pyrene 202 (third) and benzo(a)anthracene and chrysene 228 at the bottom.
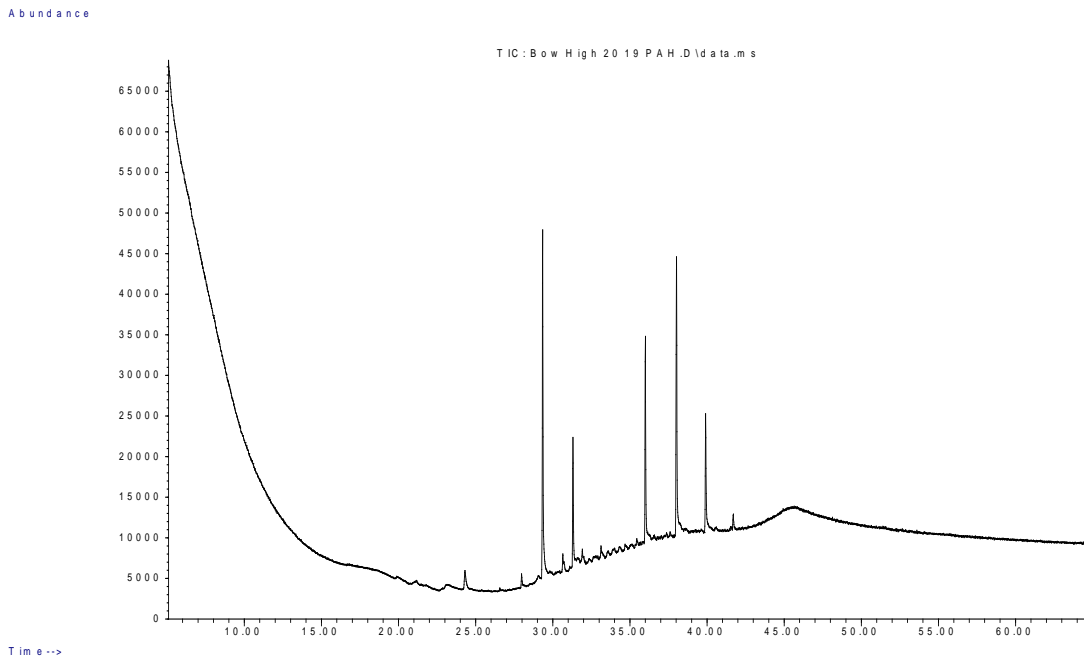

Figure III.143: Site 12, Maketu Estuary 2 core for sediment, 20-40 cm deep. GC/MS total ion chromatograph results from *Rena* PAH fingerprint analysis.
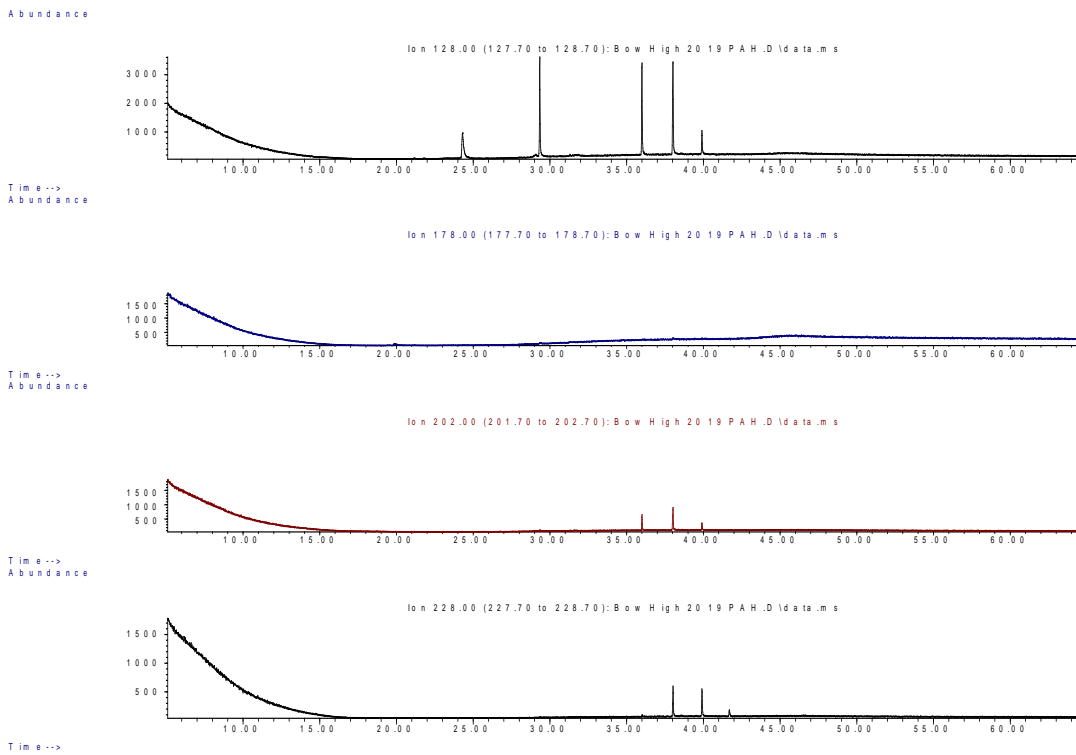
Figure III.144: Site 12, Maketu Estuary 2 core for sediment 20-40 cm deep. GC/MS chromatograph results from *Rena* PAH fingerprint analysis for naphthalene 128 (top), phenanthrene 178 (second), pyrene 202 (third) and benzo(a)anthracene and chrysene 228 at the bottom.

9.4 APPENDIX IV: HILL'S LABORATORIES GC/MS RESULTS

This appendix consists of the qualitative GC/MS analysis results carried out by Hill's Laboratories.

Table IV.1: Hill's Laboratory results from GC/MS analysis of 16 priority PAHs.

Sample	Site	Location/ depth	Sample date	Analysis date	Naphthalene mg/kg dry wt	pyrene 202 mg/kg dry wt	phenanthrene 178 mg/kg dry wt	benz(a)anthracene/ chrysene 228 mg/kg dry wt
8	4	Taylor's Reserve low 20-40 cm	4/12/2012	26/08/2013	< 0.010	< 0.002	< 0.002	< 0.002
14	7	Mt Maunganui low 20-40 cm	6/12/2012	26/08/2013	< 0.010	< 0.002	< 0.002	< 0.002
20	10	Maketu Spit mid 20-40 cm	6/12/2012	26/08/2013	< 0.010	< 0.002	< 0.002	< 0.002
21	11	Maketu Spit high 0-20 cm	6/12/2012	26/08/2013	< 0.010	< 0.002	< 0.002	< 0.002
22	11	Maketu Spit high 20-40 cm	6/12/2012	26/08/2013	< 0.010	< 0.002	< 0.002	< 0.002
25	13	Omanu high 0-20 cm	7/12/2012	26/08/2013	< 0.010	0.002	0.008	< 0.002
26	13	Omanu high 20-40 cm	7/12/2012	26/08/2013	< 0.010	< 0.002	< 0.002	< 0.002
33	14	Centre Bank 0-20 cm	12/12/2012	26/08/2013	< 0.010	< 0.002	< 0.002	< 0.002
34	14	Centre Bank 20-40 cm	12/12/2012	26/08/2013	< 0.010	< 0.002	< 0.002	< 0.002
35	15	Maketu Estuary 1 0-20 cm	8/01/2013	26/08/2013	< 0.010	< 0.002	< 0.002	< 0.002
36	15	Maketu Estuary 1 20-40 cm	8/01/2013	26/08/2013	< 0.010	< 0.002	< 0.002	< 0.002
45	20	Waihi- Surf club high	10/01/2013	26/08/2013	< 0.010	< 0.002	< 0.002	< 0.002

46	20	0-20 cm Waihi-Surf club high	10/01/2013	26/08/2013	< 0.010	< 0.002	< 0.002	< 0.002
49	22	20-40 cm Waihi-Bowentown high	10/01/2013	26/08/2013	< 0.010	< 0.002	< 0.002	< 0.002
50	22	0-20 cm Waihi-Bowentown high	10/01/2013	26/08/2013	< 0.010	< 0.002	< 0.002	< 0.002
53	24	20-40 cm Matakana Panepane high	26/01/2013	26/08/2013	< 0.010	< 0.002	< 0.002	< 0.002
54	24	0-20 cm Matakana Panepane high	26/01/2013	26/08/2013	< 0.010	< 0.002	< 0.002	< 0.002
58	26	20-40 cm Matakana Tank Rd high	26/01/2013	26/08/2013	< 0.010	< 0.002	< 0.002	< 0.002
		20-40 cm						

9.5 APPENDIX V: CHEMISTRY RESULTS

The qualitative chemistry results in this appendix were considered unreliable due to a column blockage that may have occurred in the GC/MS during analysis.
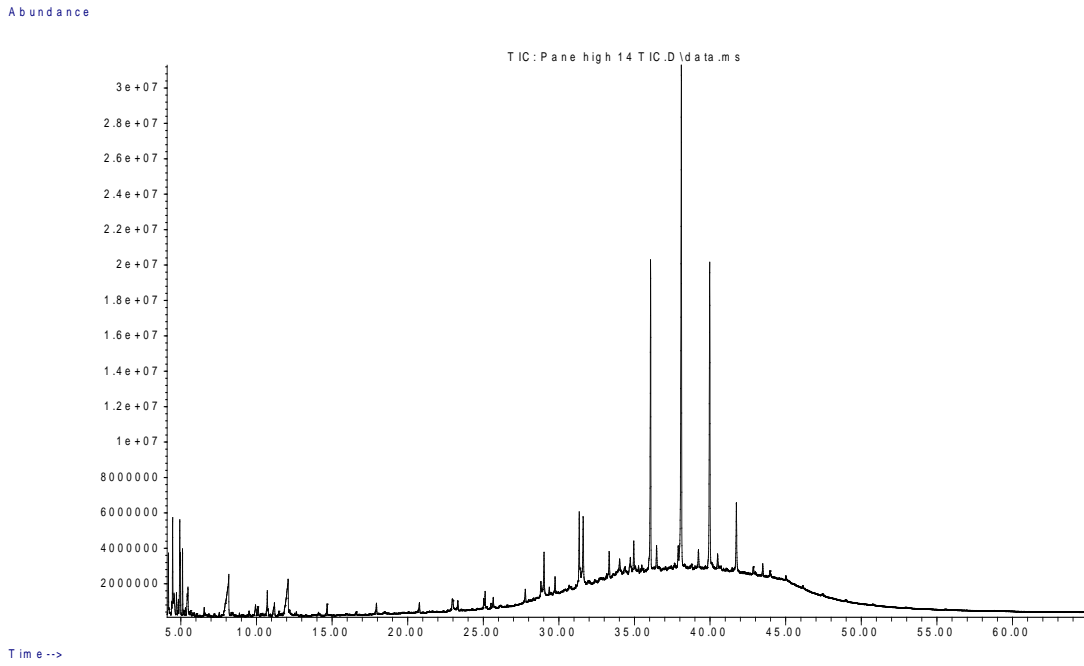

Figure V.145: Waihi surf club high tide core for sediment, 0-20 cm deep. GC/MS total ion chromatograph results from *Rena* PAH fingerprint analysis.
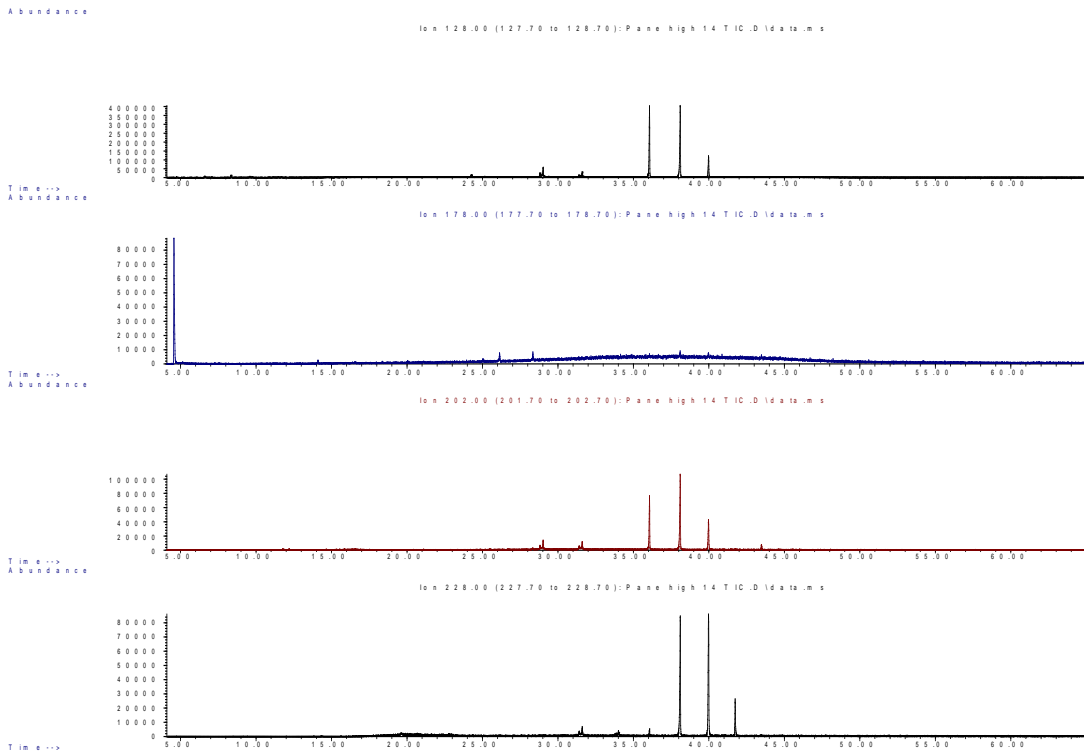

Figure V.146: Waihi surf club high tide core for sediment 0-20 cm deep. GC/MS chromatograph results from *Rena* PAH fingerprint analysis for naphthalene 128 (top), phenanthrene 178 (second), pyrene 202 (third) and benzo(a)anthracene and chrysene 228 at the bottom.
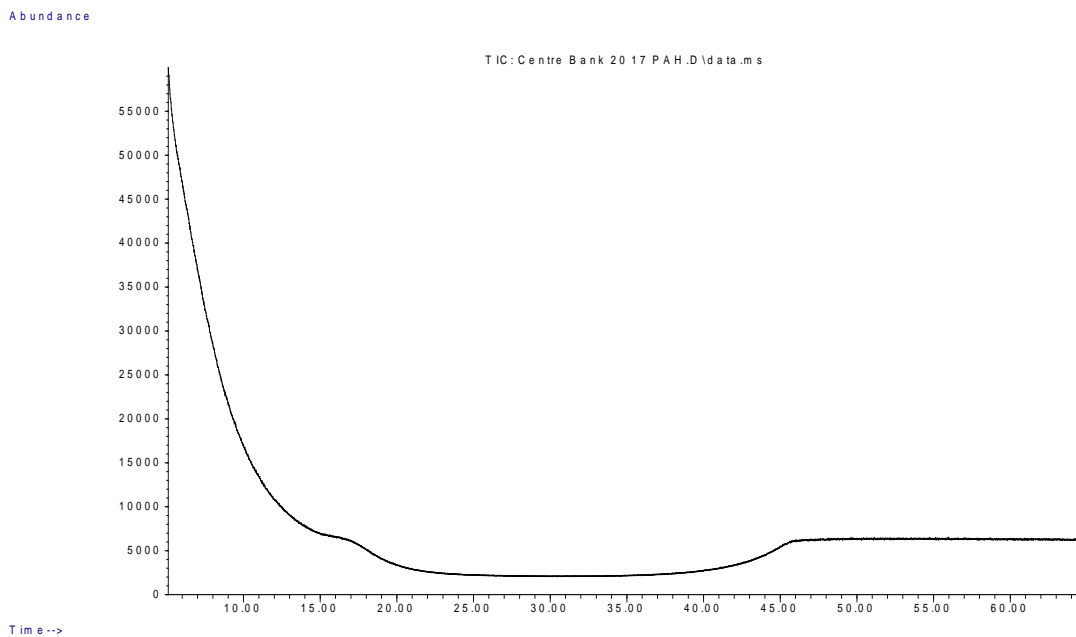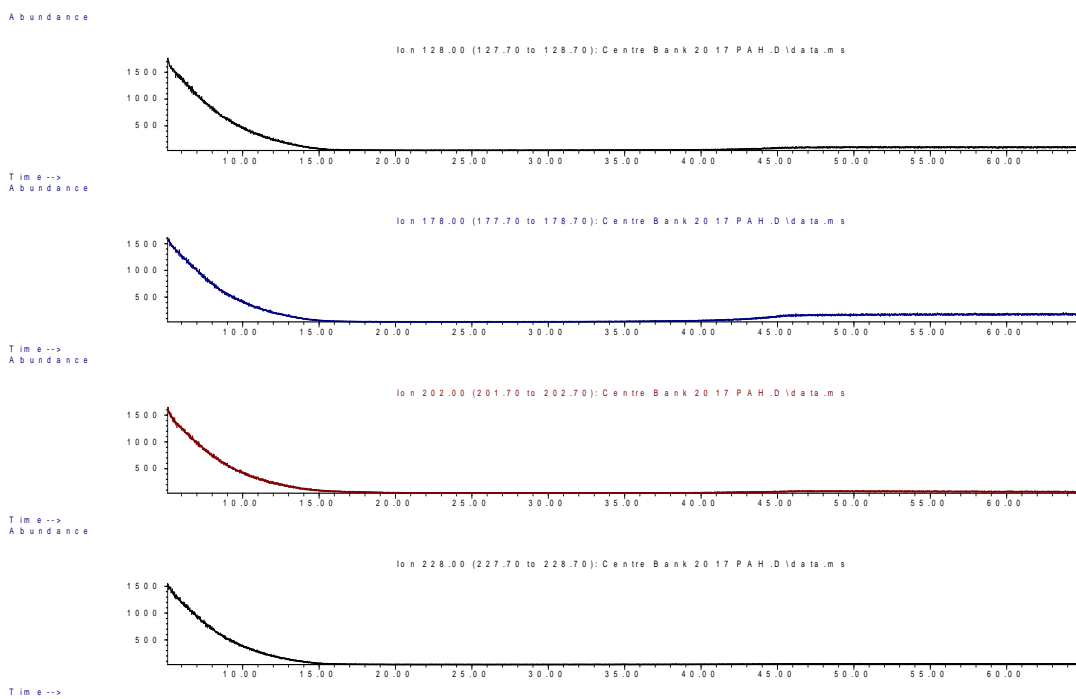
TIC: Waihi 40 16 PAH.D\data.ms

Time-->

Figure V.147: Waihi surf club high tide core for sediment, 20-40 cm deep. GC/MS total ion chromatograph results from *Rena* PAH fingerprint analysis.

Abundance

Ion 128.00 (127.70 to 128.70): Waihi 40 16 PAH.D\data.ms

Time-->
Abundance

Ion 178.00 (177.70 to 178.70): Waihi 40 16 PAH.D\data.ms

Time-->
Abundance

Ion 202.00 (201.70 to 202.70): Waihi 40 16 PAH.D\data.ms

Time-->
Abundance

Ion 228.00 (227.70 to 228.70): Waihi 40 16 PAH.D\data.ms

Time-->

Figure V.148: Waihi surf club high tide core for sediment 20-40 cm deep. GC/MS chromatograph results from *Rena* PAH fingerprint analysis for naphthalene 128 (top), phenanthrene 178 (second), pyrene 202 (third) and benzo(a)anthracene and chrysene 228 at the bottom.
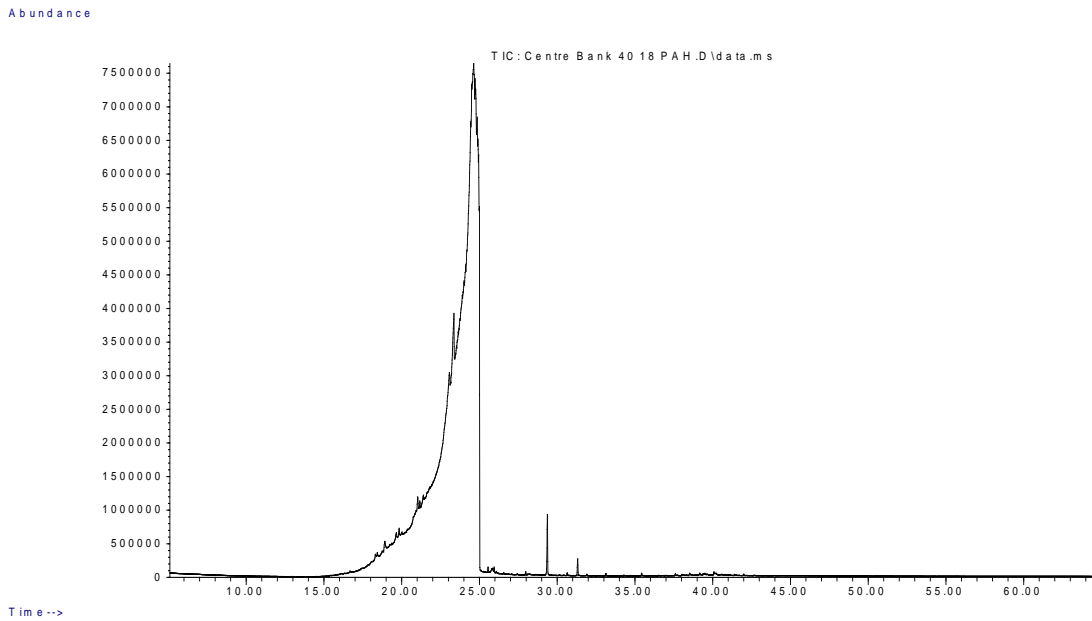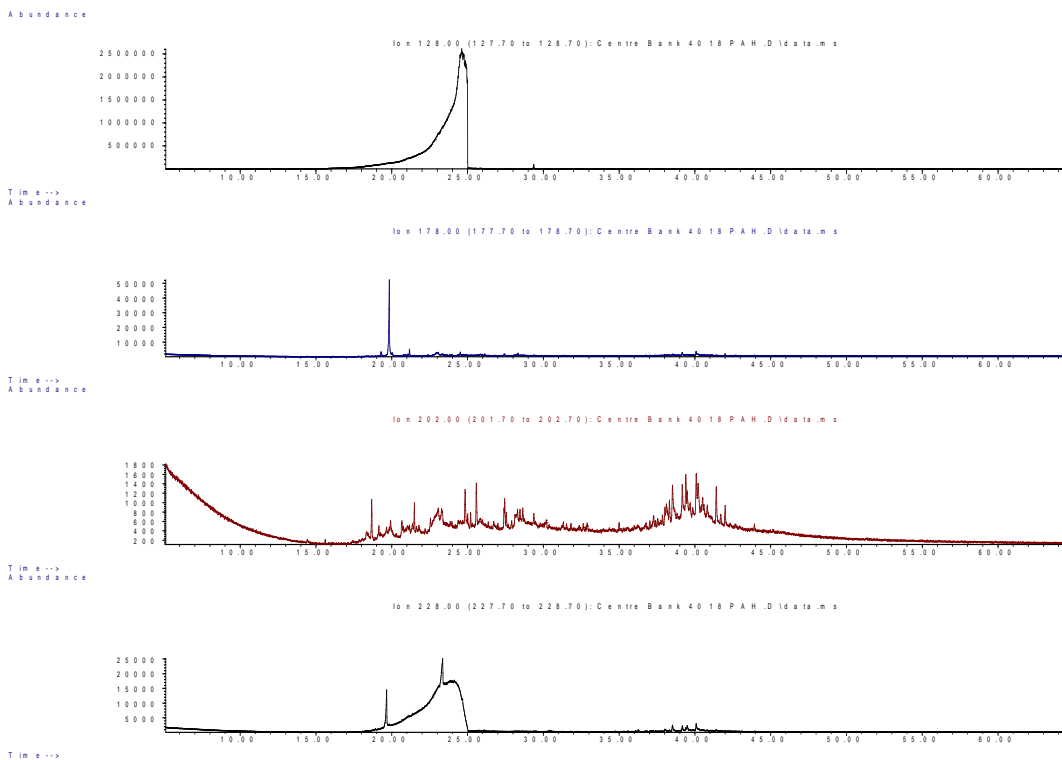
Figure V.149: Bowentown high tide core for sediment, 0-20 cm deep. GC/MS total ion chromatograph results from *Rena* PAH fingerprint analysis.

Figure V.150: Bowentown high tide core for sediment 0-20cm deep. GC/MS chromatograph results from *Rena* PAH fingerprint analysis for naphthalene 128 (top), phenanthrene 178 (second), pyrene 202 (third) and benzo(a)anthracene and chrysene 228 at the bottom.
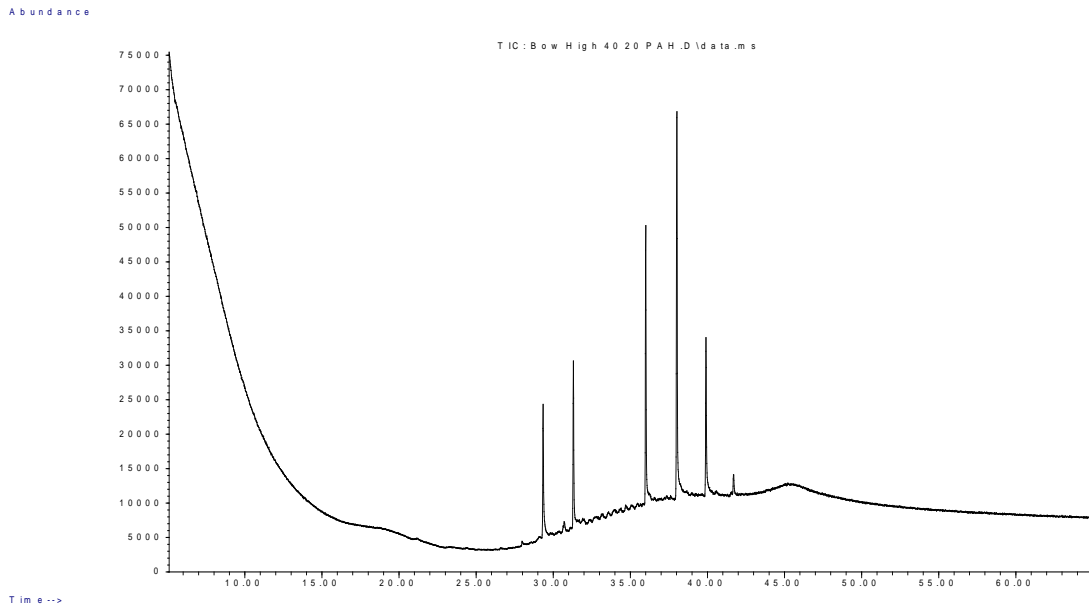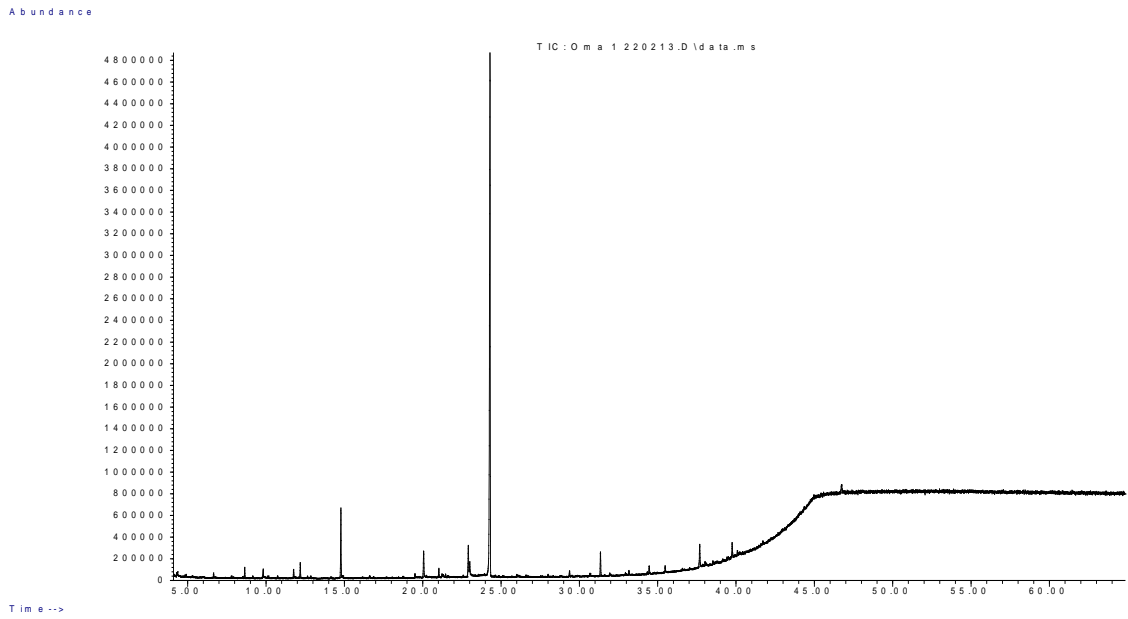
Figure V.151: Bowentown high tide core for sediment, 20-40 cm deep. GC/MS total ion chromatograph results from *Rena* PAH fingerprint analysis.
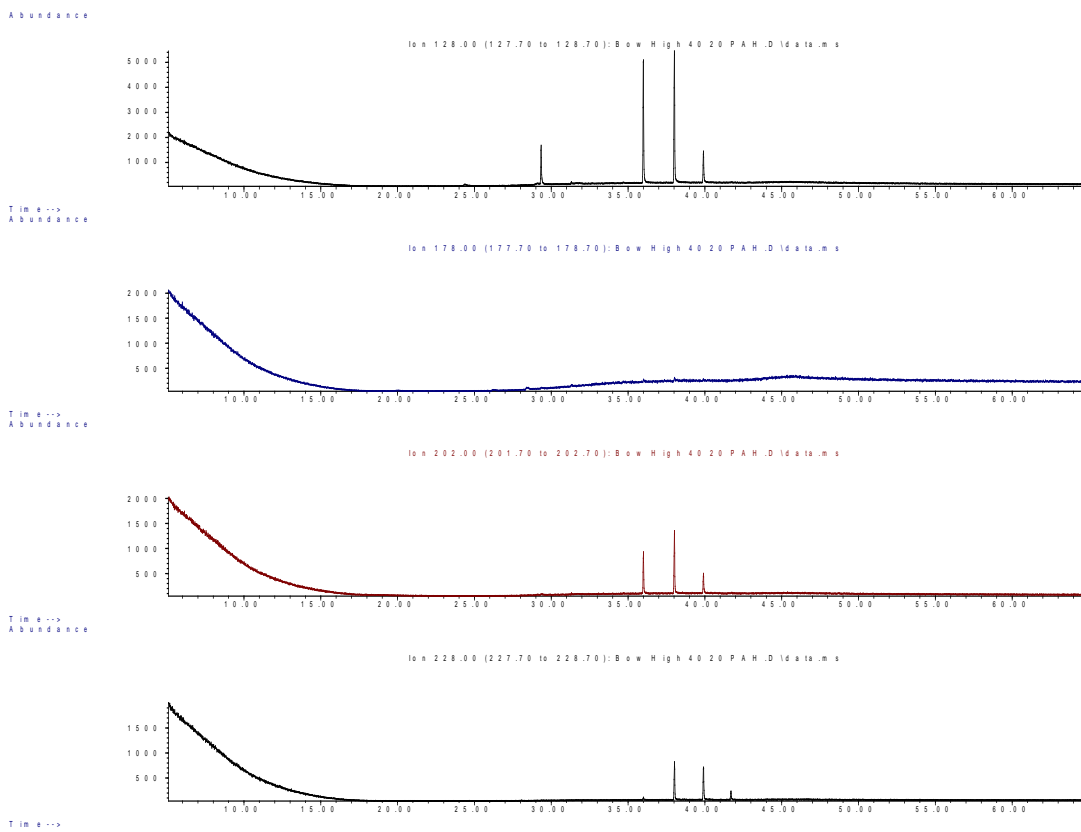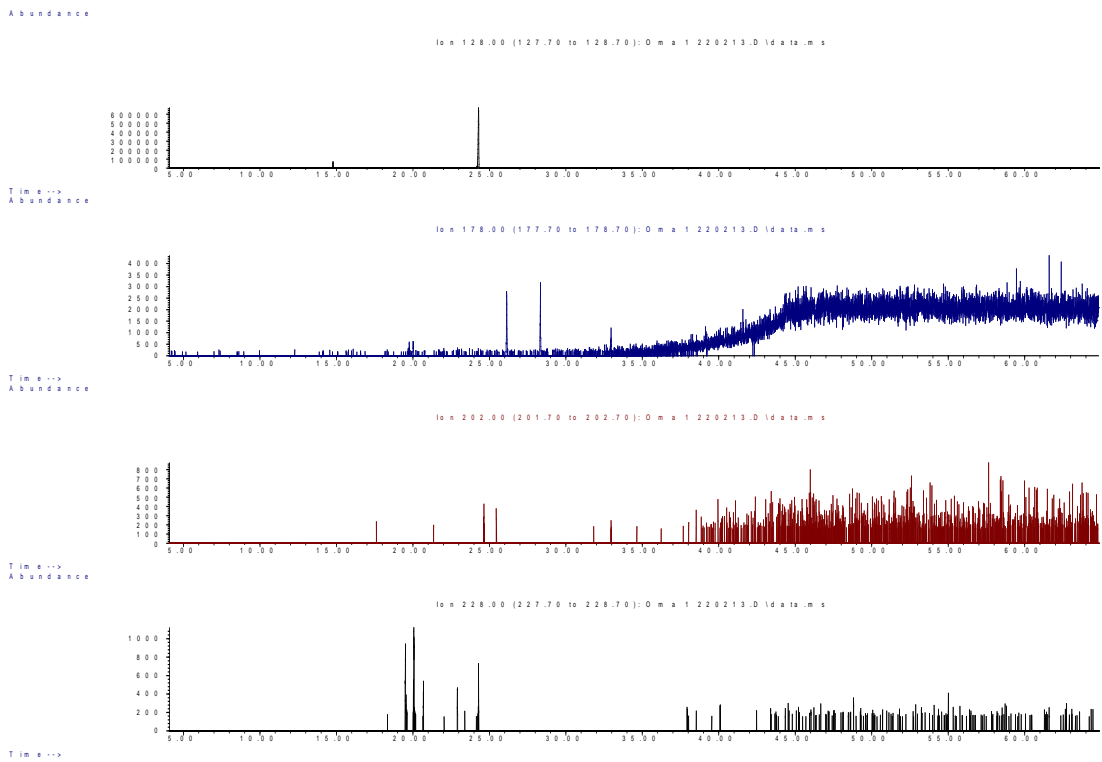

Figure V.152: Bowentown high tide core for sediment 20-40 cm deep. GC/MS chromatograph results from *Rena* PAH fingerprint analysis for naphthalene 128 (top), phenanthrene 178 (second), pyrene 202 (third) and benzo(a)anthracene and chrysene 228 at the bottom.
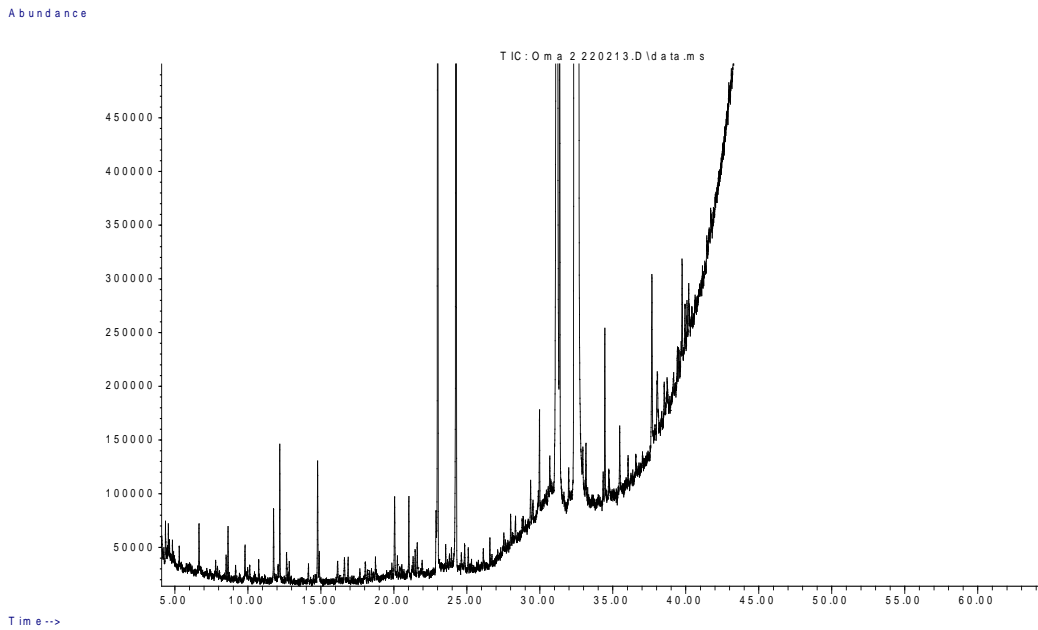
TIC: Tank Rd 40 22 PAH.D\data.ms
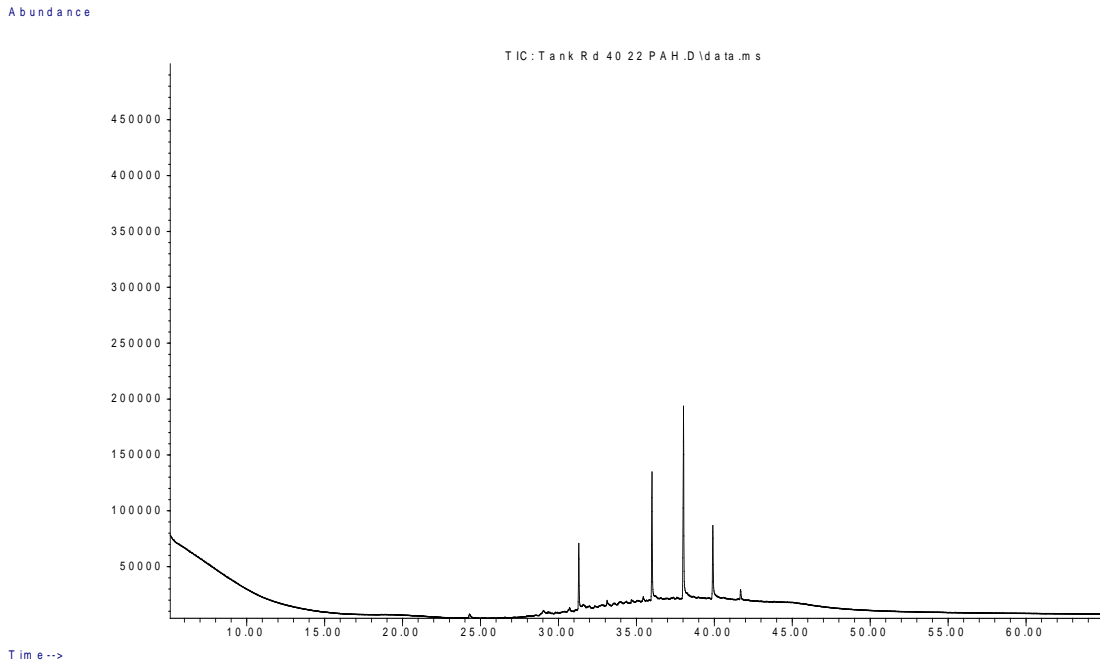
Figure V.153: Tank Road high tide core for sediment, 20-40 cm deep. GC/MS total ion chromatograph results from *Rena* PAH fingerprint analysis.
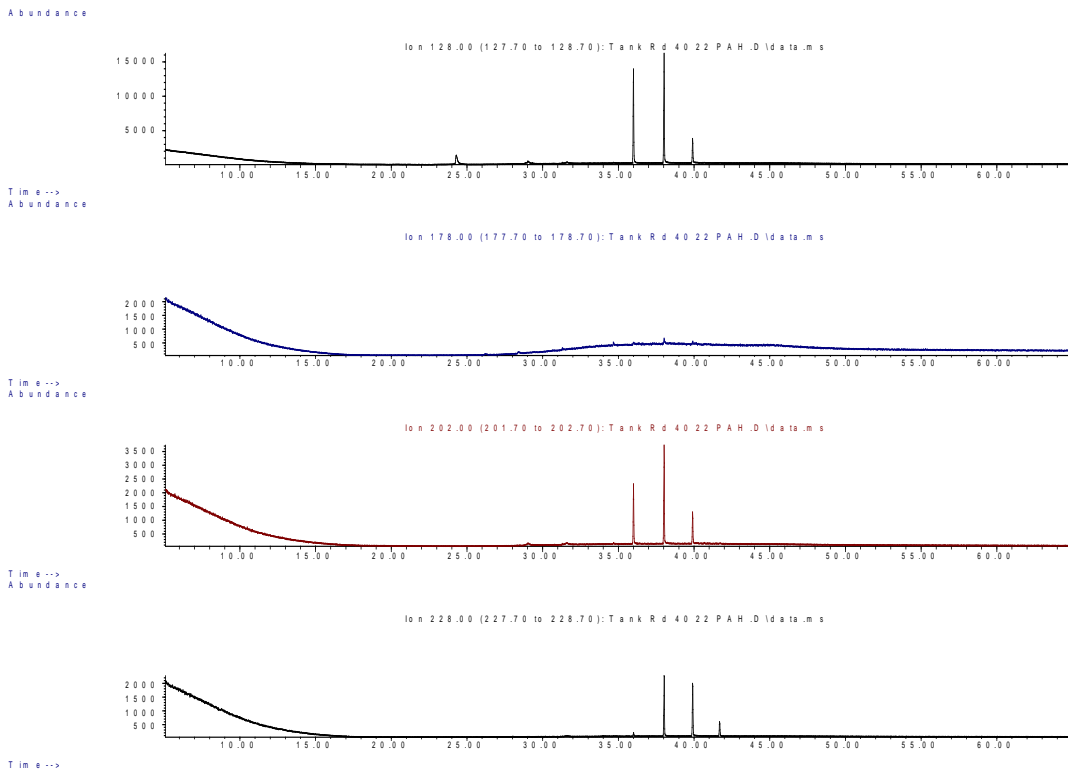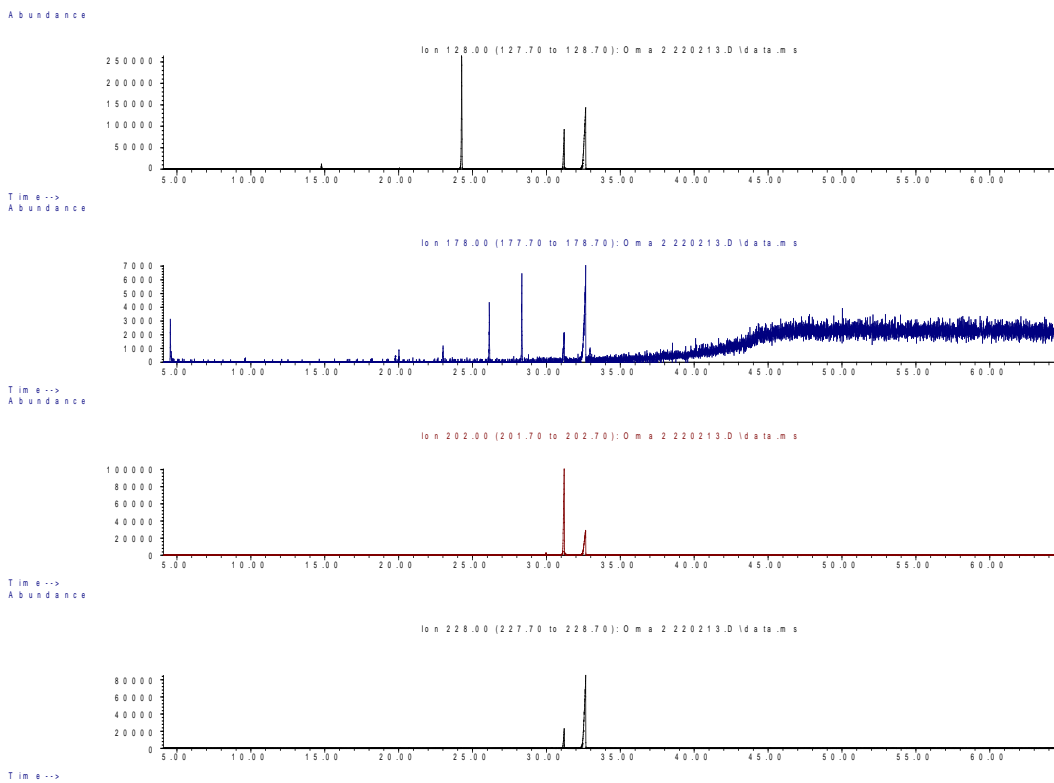

Figure V.154: Tank Road mid tide core for sediment 20-40 cm deep. GC/MS chromatograph results from *Rena* PAH fingerprint analysis for naphthalene 128 (top), phenanthrene 178 (second), pyrene 202 (third) and benzo(a)anthracene and chrysene 228 at the bottom.
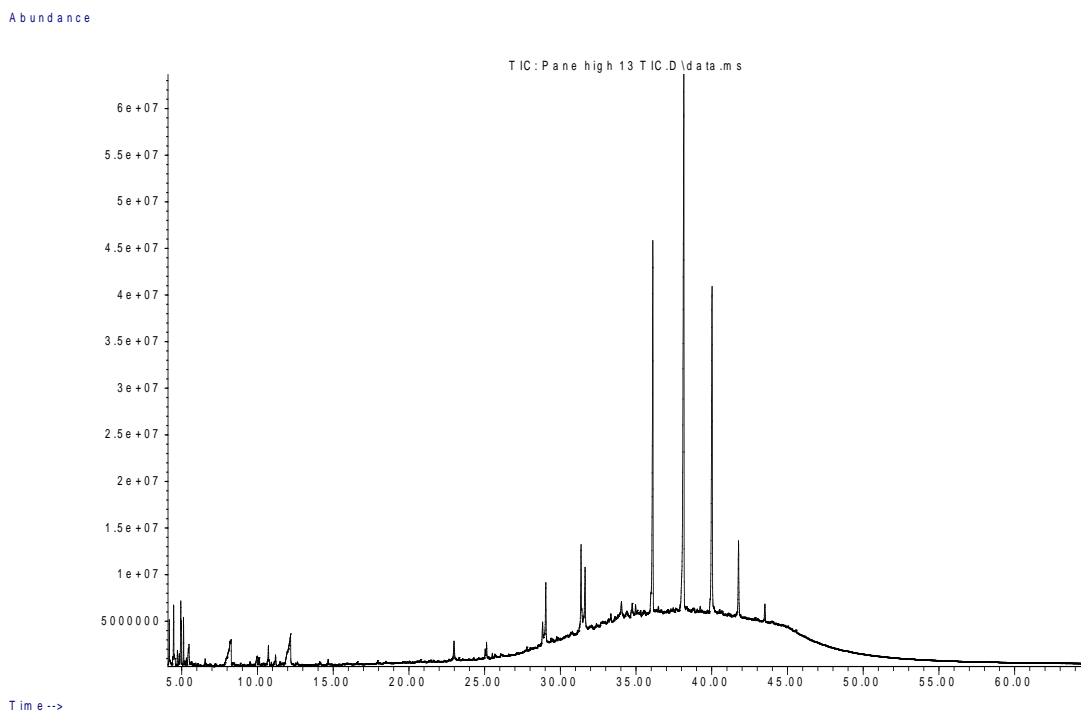
Figure V.155: Panepane Point high tide core for sediment, 0-20 cm deep. GC/MS total ion chromatograph results from *Rena* PAH fingerprint analysis.
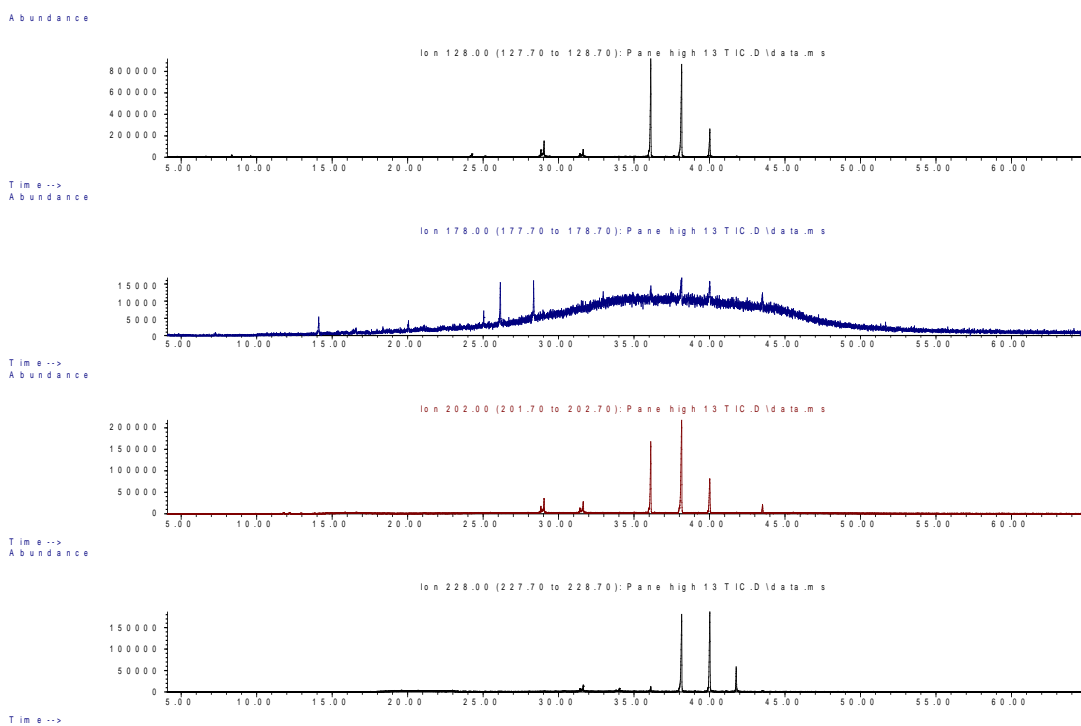
Figure V.156: Panepane Point high tide core for sediment 0-20 cm deep. GC/MS chromatograph results from *Rena* PAH fingerprint analysis for naphthalene 128 (top), phenanthrene 178 (second), pyrene 202 (third) and benzo(a)anthracene and chrysene 228 at the bottom.
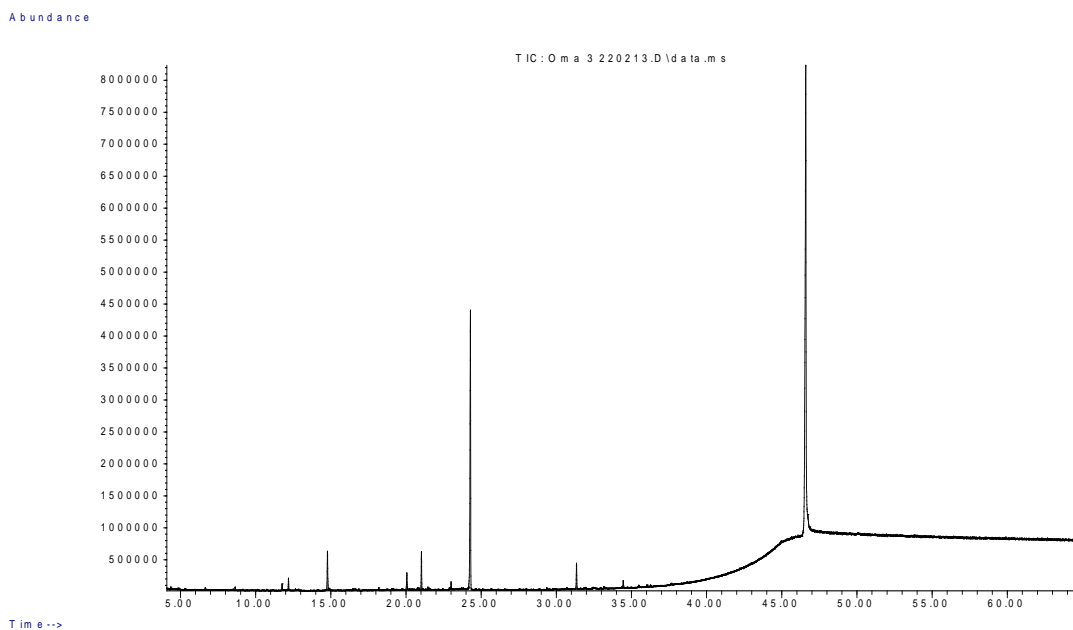
Figure V.157: Panepane Point high tide core for sediment, 20-40 cm deep. GC/MS total ion chromatograph results from *Rena* PAH fingerprint analysis.

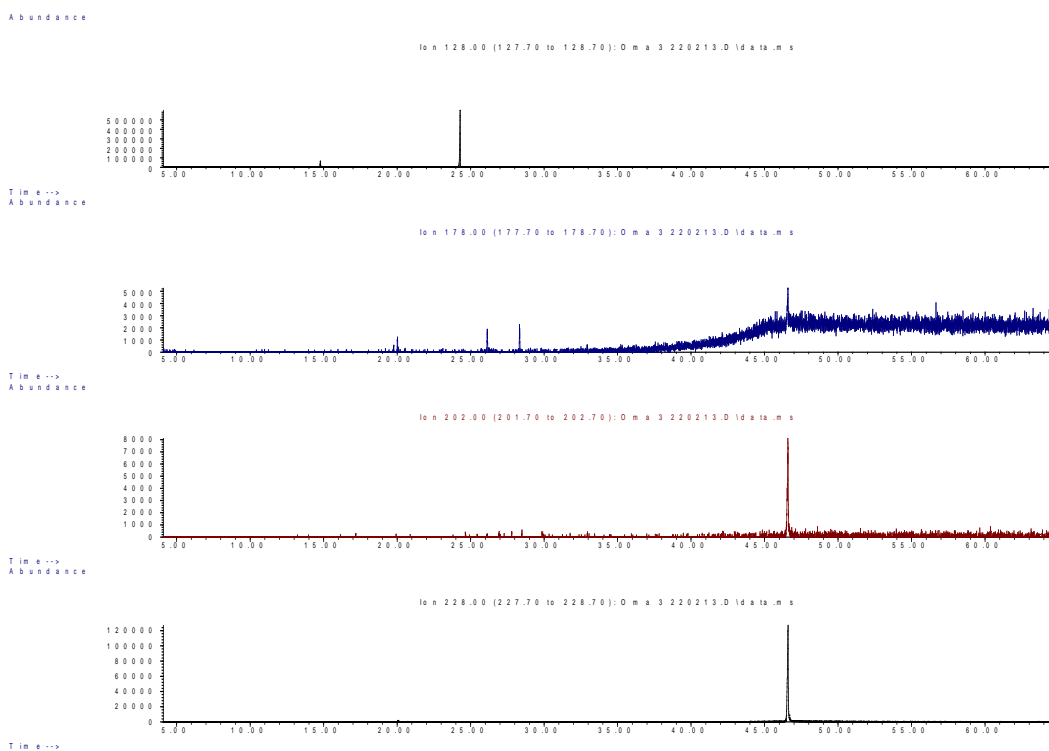Figure V.158: Panepane Point high tide core for sediment 20-40 cm deep. GC/MS chromatograph results from *Rena* PAH fingerprint analysis for naphthalene 128 (top), phenanthrene 178 (second), pyrene 202 (third) and benzo(a)anthracene and chrysene 228

at the bottom.

Figure V.159: Centre Bank core for sediment 0-20 cm deep. GC/MS total ion chromatograph results from *Rena* PAH fingerprint analysis.

Figure V.160: Centre Bank core for sediment 0-20 cm deep. GC/MS chromatograph results from *Rena* PAH fingerprint analysis for naphthalene 128 (top), phenanthrene 178 (second), pyrene 202 (third) and benzo(a)anthracene and chrysene 228 at the bottom.
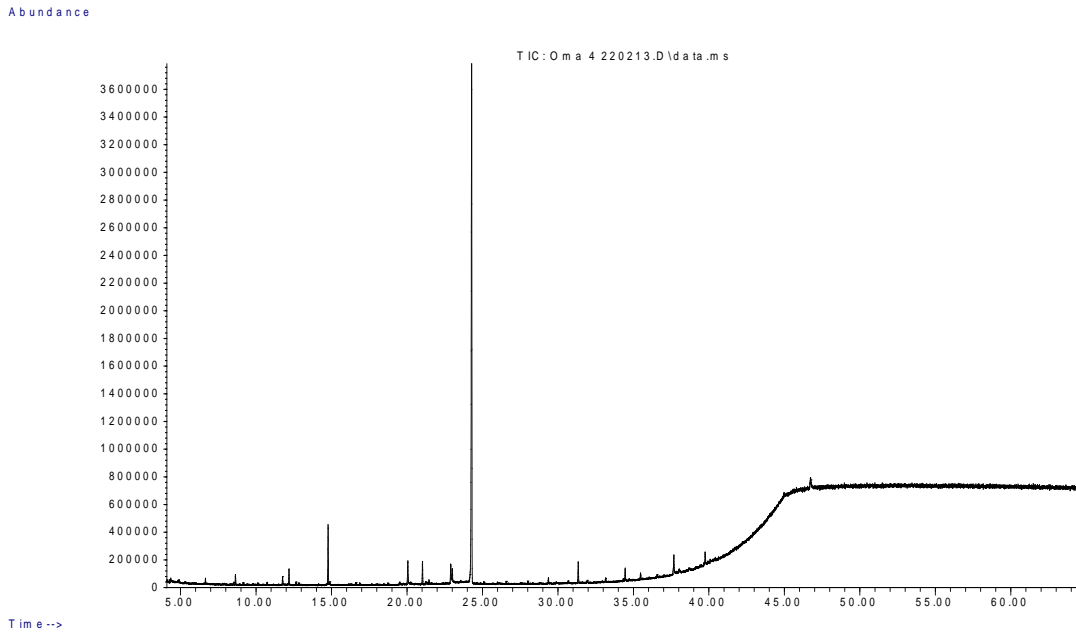
Figure V.161: Centre Bank core for sediment 20-40 cm deep. GC/MS total ion chromatograph results from *Rena* PAH fingerprint analysis.
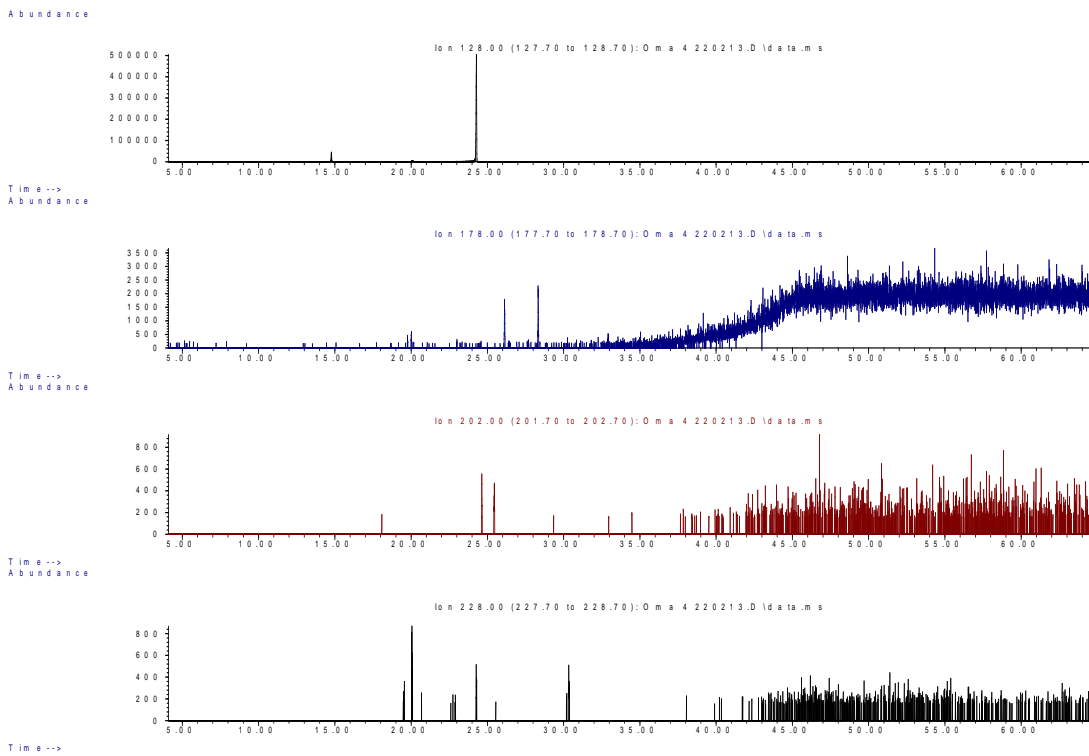

Figure V.162: Centre Bank core for sediment 20-40 cm deep. GC/MS chromatograph results from *Rena* PAH fingerprint analysis for naphthalene 128 (top), phenanthrene 178 (second), pyrene 202 (third) and benzo(a)anthracene and chrysene 228 at the bottom.
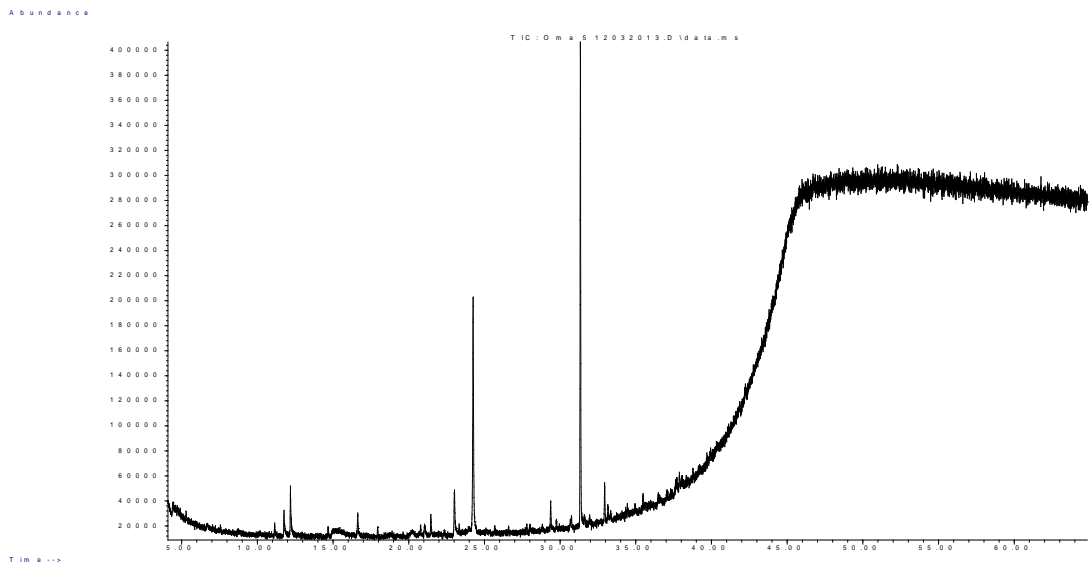
Figure V.163: Omanu high tide core for sediment, 0-5 cm deep. GC/MS total ion chromatograph results from *Rena* PAH fingerprint analysis.

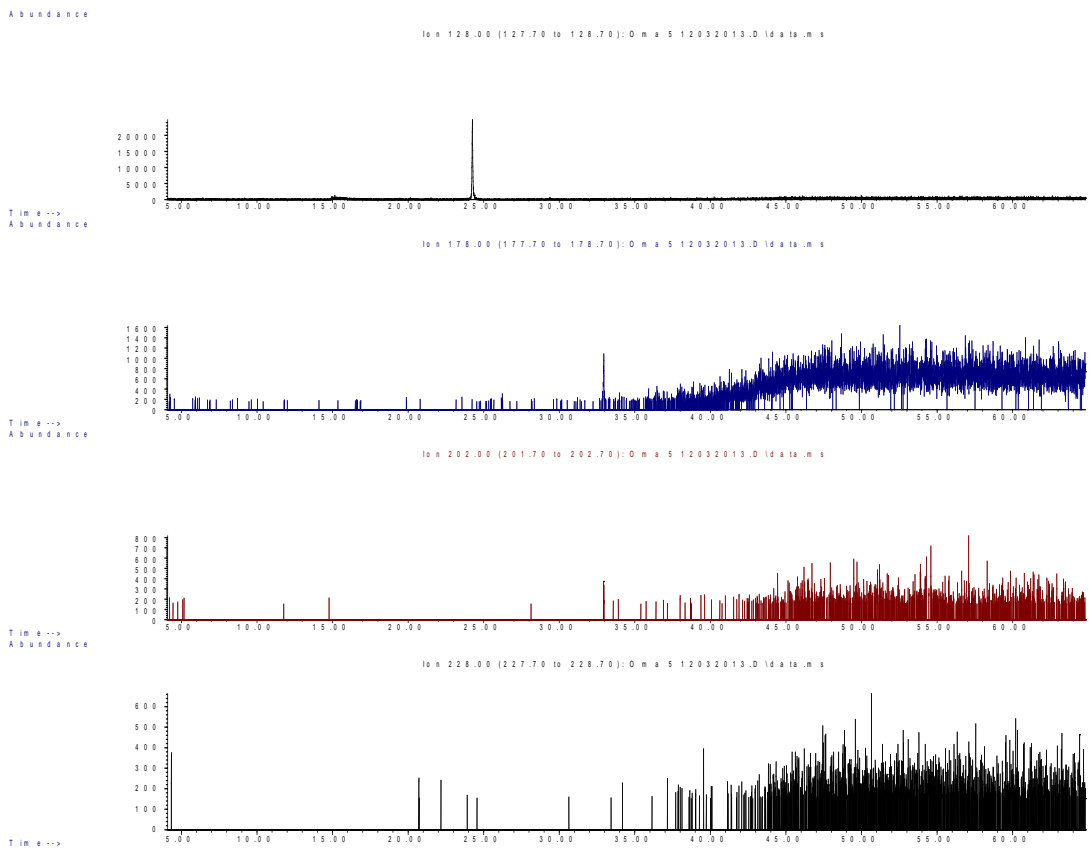Figure V.164: Omanu high tide core for sediment 0-5 cm deep. GC/MS chromatograph results from *Rena* PAH fingerprint analysis for naphthalene 128 (top), phenanthrene 178 (second), pyrene 202 (third) and benzo(a)anthracene and chrysene 228 at the bottom.

Figure V.165: Omanu high tide core for sediment, 5-10 cm deep. GC/MS total ion chromatograph results from *Rena* PAH fingerprint analysis.

Figure V.166: Omanu high tide core for sediment 5-10 cm deep. GC/MS chromatograph results from *Rena* PAH fingerprint analysis for naphthalene 128 (top), phenanthrene 178 (second), pyrene 202 (third) and benzo(a)anthracene and chrysene 228 at the bottom.
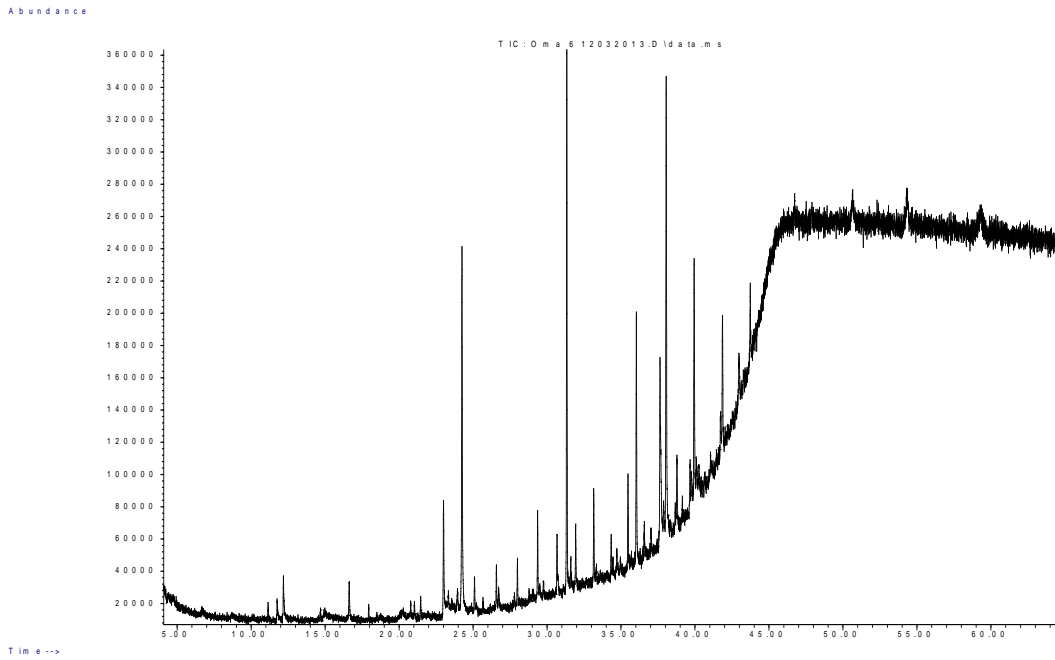
238

Figure V.167: Omanu high tide core for sediment, 10-15 cm deep. GC/MS total ion chromatograph results from *Rena* PAH fingerprint analysis.
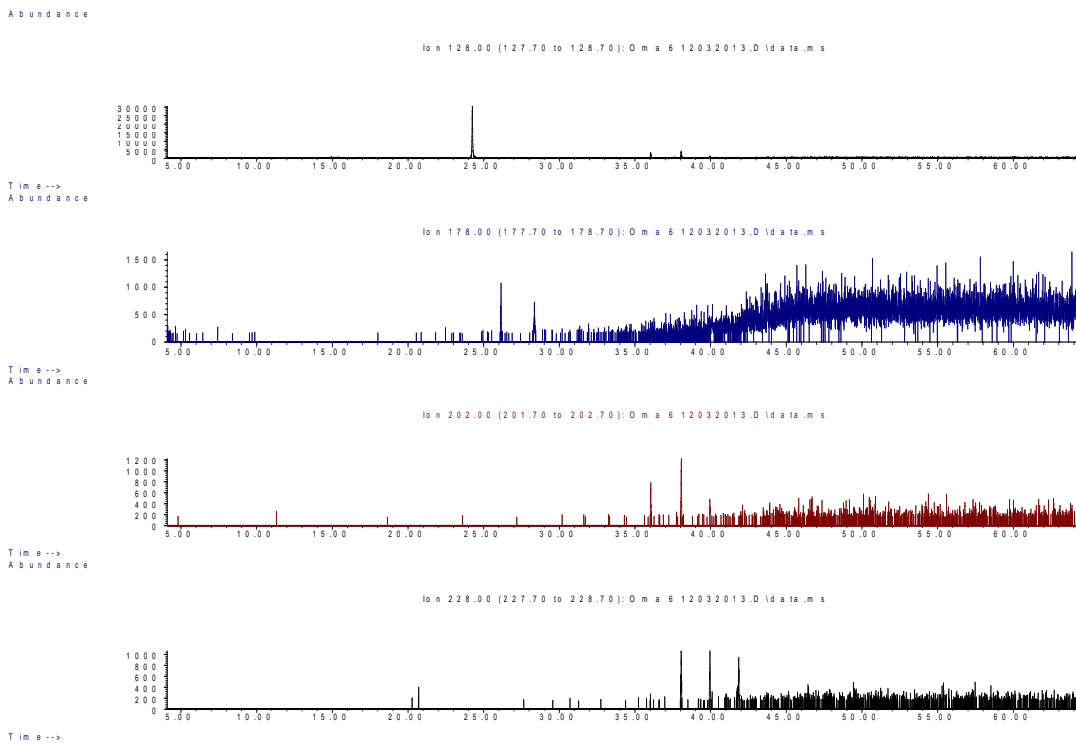

Figure V.168: Omanu high tide core for sediment 10-15 cm deep. GC/MS chromatograph results from *Rena* PAH fingerprint analysis for naphthalene 128 (top), phenanthrene 178 (second), pyrene 202 (third) and benzo(a)anthracene and chrysene 228 at the bottom.

239

Figure V.169: Omanu high tide core for sediment, 15-20 cm deep. GC/MS total ion chromatograph results from *Rena* PAH fingerprint analysis.

Figure V.170: Omanu high tide core for sediment 15-20 cm deep. GC/MS chromatograph results from *Rena* PAH fingerprint analysis for naphthalene 128 (top), phenanthrene 178 (second), pyrene 202 (third) and benzo(a)anthracene and chrysene 228 at the bottom.
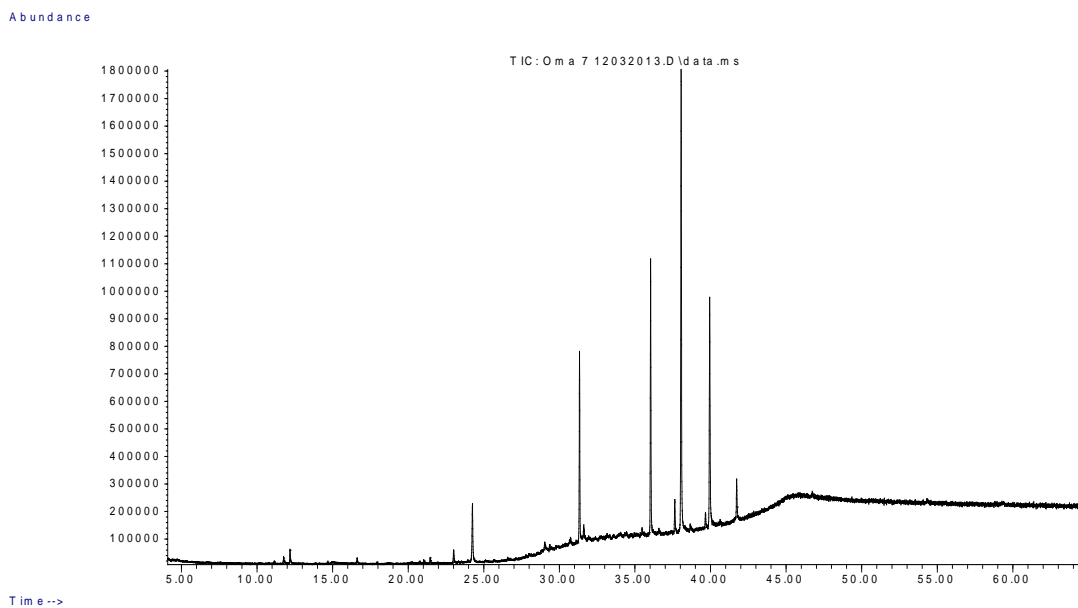
Figure V.171: Omanu high tide core for sediment, 20-25 cm deep. GC/MS total ion chromatograph results from *Rena* PAH fingerprint analysis.
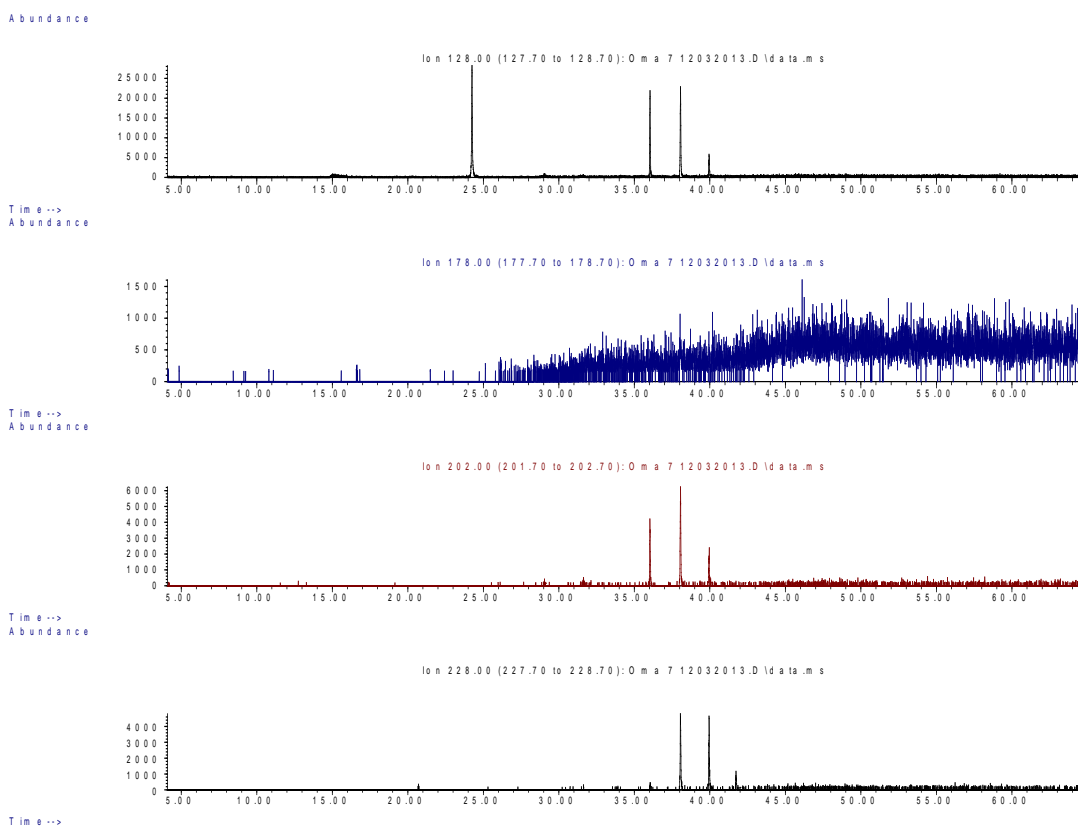

Figure V.172: Omanu high tide core for sediment 20-25 cm deep. GC/MS chromatograph results from *Rena* PAH fingerprint analysis for naphthalene 128 (top), phenanthrene 178 (second), pyrene 202 (third) and benzo(a)anthracene and chrysene 228 at the bottom.
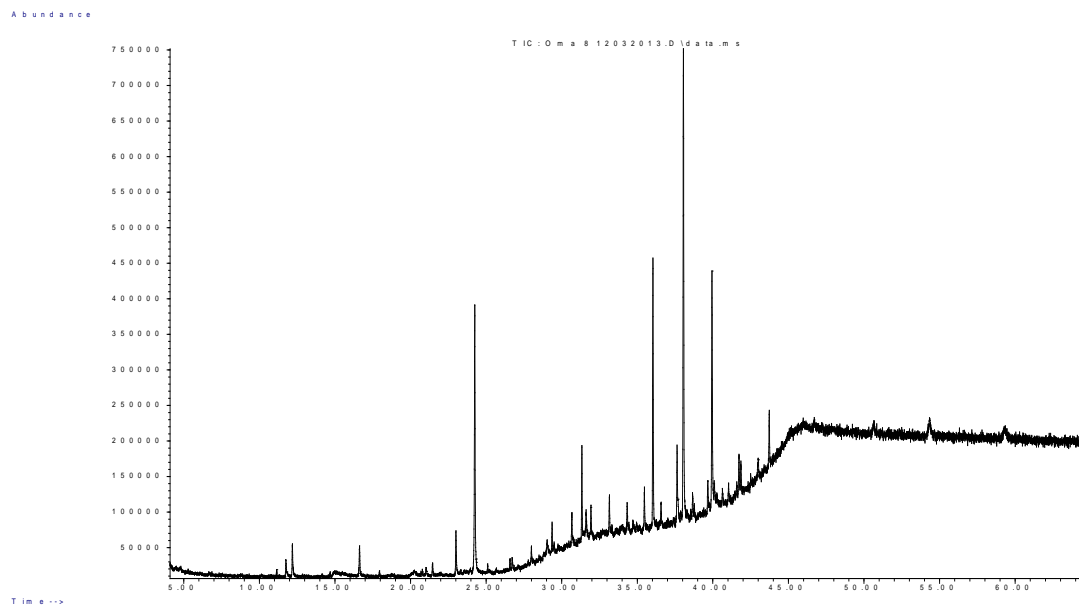
Figure V.173: Omanu high tide core for sediment, 25-30 cm deep. GC/MS total ion chromatograph results from *Rena* PAH fingerprint analysis.
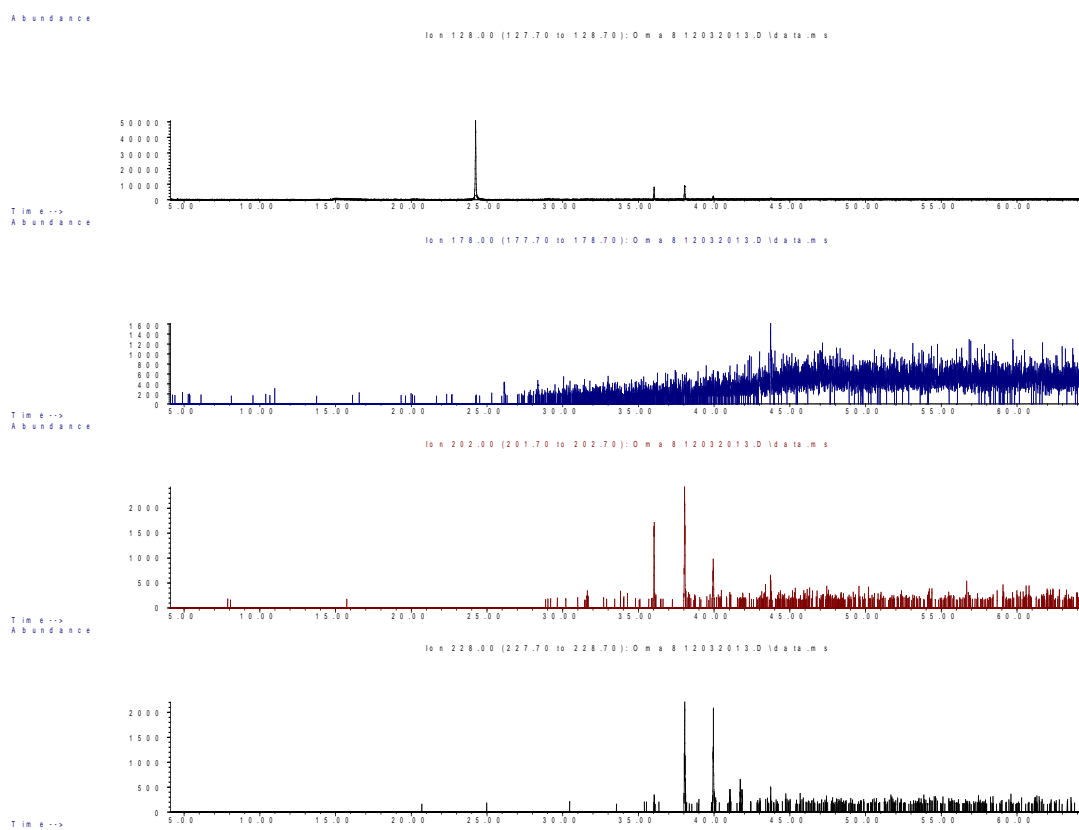

Figure V.174: Omanu high tide core for sediment 25-30 cm deep. GC/MS chromatograph results from *Rena* PAH fingerprint analysis for naphthalene 128 (top), phenanthrene 178 (second), pyrene 202 (third) and benzo(a)anthracene and chrysene 228 at the bottom.

Figure V.175: Omanu high tide core for sediment, 30-35 cm deep. GC/MS total ion chromatograph results from *Rena* PAH fingerprint analysis.

Figure V.176: Omanu high tide core for sediment 30-35 cm deep. GC/MS chromatograph results from *Rena* PAH fingerprint analysis for naphthalene 128 (top), phenanthrene 178 (second), pyrene 202 (third) and benzo(a)anthracene and chrysene 228 at the bottom.
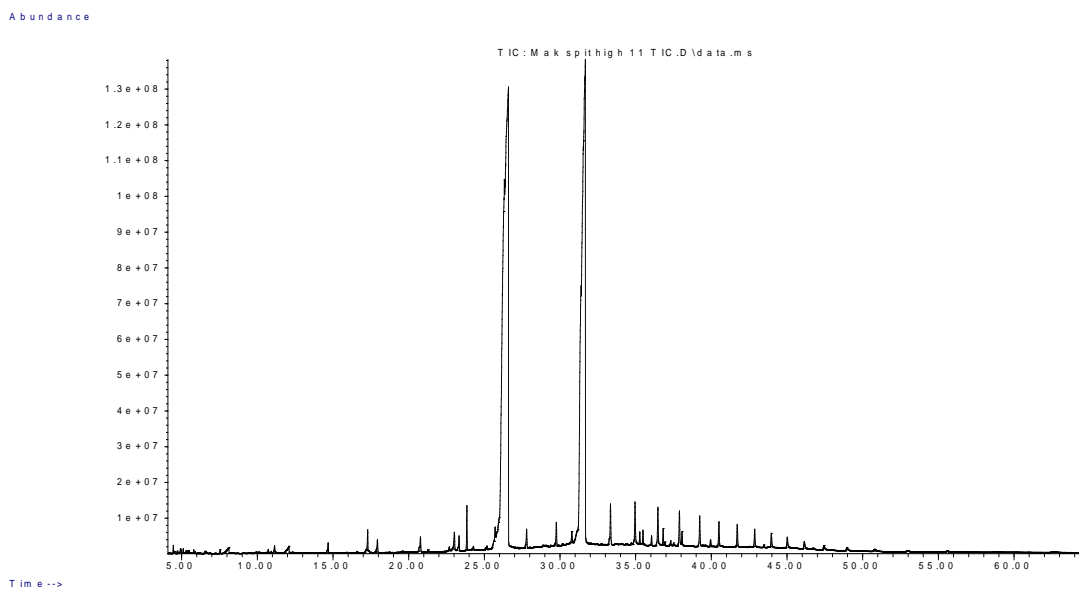
Figure V.177: Omanu high tide core for sediment, 35-40 cm deep. GC/MS total ion chromatograph results from *Rena* PAH fingerprint analysis.

Figure V.178: Omanu high tide core for sediment 35-40 cm deep. GC/MS chromatograph results from *Rena* PAH fingerprint analysis for naphthalene 128 (top), phenanthrene 178 (second), pyrene 202 (third) and benzo(a)anthracene and chrysene 228 at the bottom.

244

Figure V.179: Maketu Spit high tide core for sediment, 0-20 cm deep. GC/MS total ion chromatograph results from *Rena* PAH fingerprint analysis.
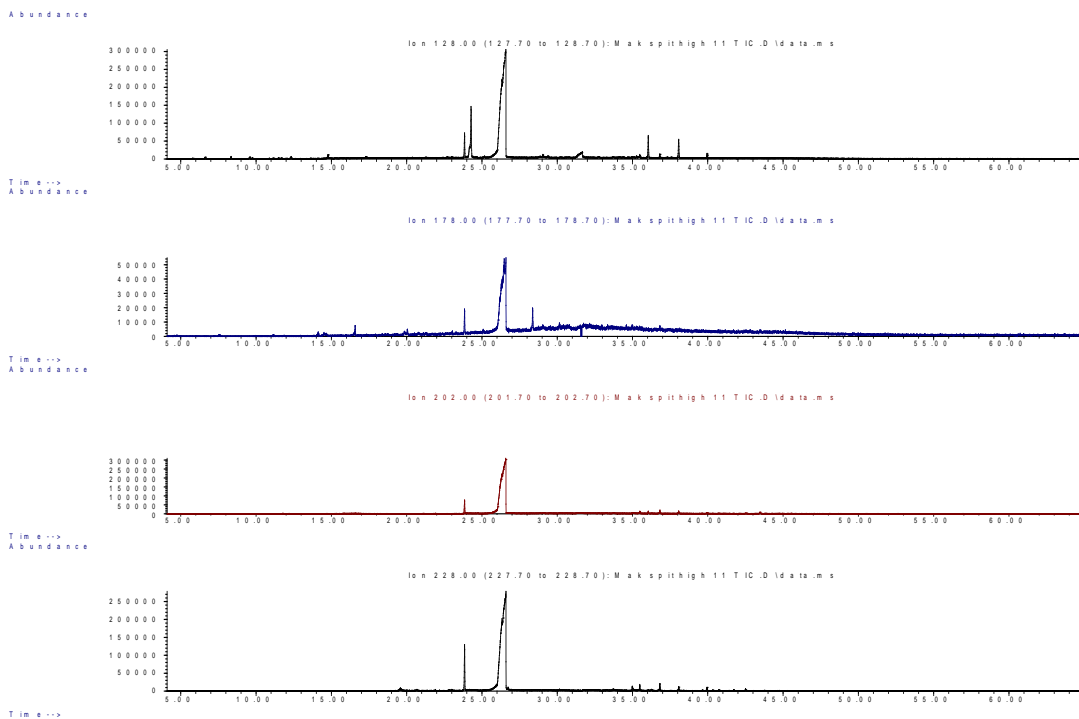

Figure V.180: Maketu Spit high tide core for sediment 0-20 cm deep. GC/MS chromatograph results from *Rena* PAH fingerprint analysis for Naphthalene 128 (top), phenanthrene 178 (second), pyrene 202 (third) and benzo(a)anthracene and chrysene 228 at the bottom.
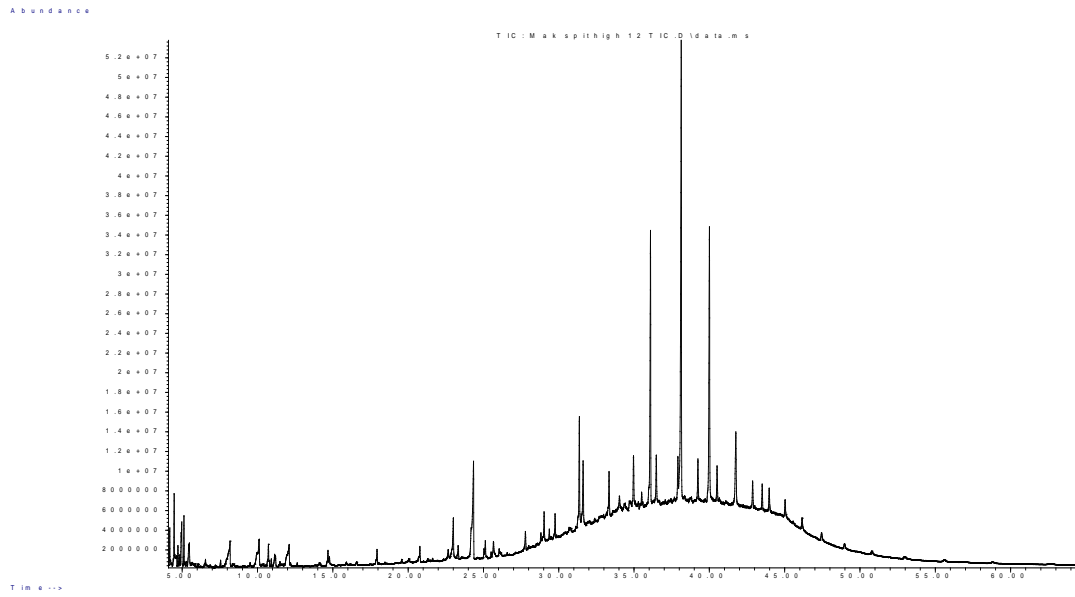
Figure V.181: Maketu Spit high tide core for sediment, 20-40 cm deep. GC/MS total ion chromatograph results from *Rena* PAH fingerprint analysis.
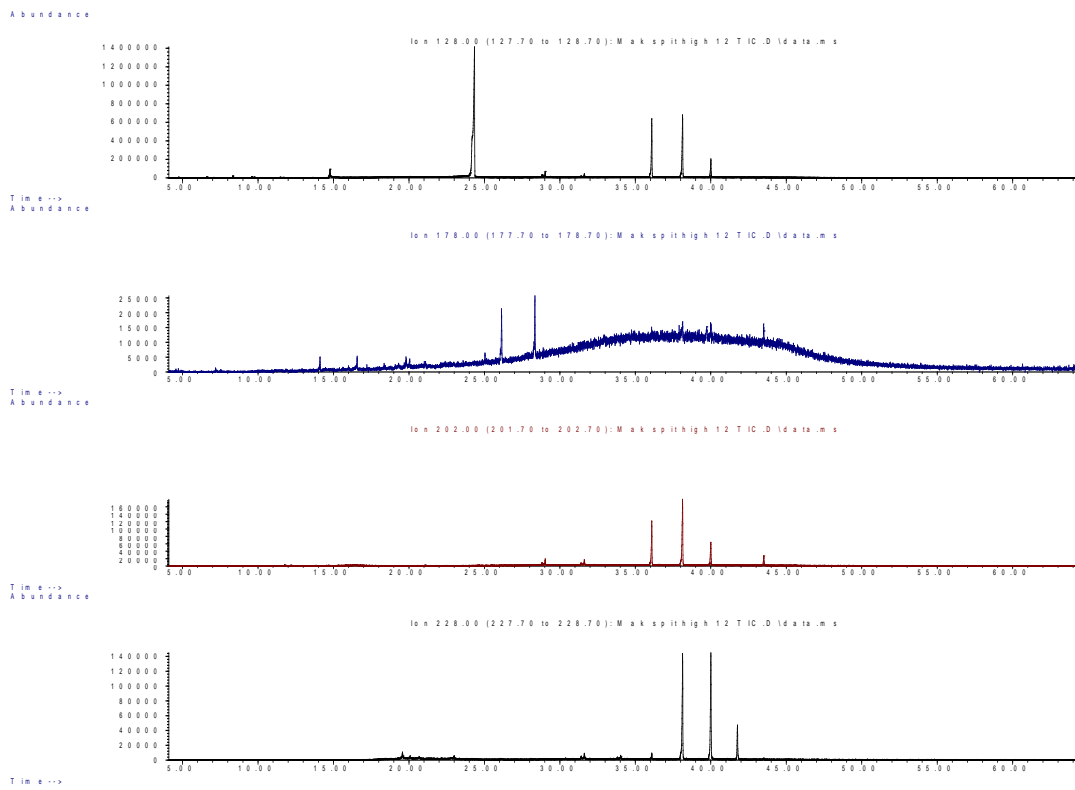

Figure V.182: Maketu Spit high tide core for sediment 20-40 cm deep. GC/MS chromatograph results from *Rena* PAH fingerprint analysis for naphthalene 128 (top), phenanthrene 178 (second), pyrene 202 (third) and benzo(a)anthracene and chrysene 228 at the bottom.